Derivative Classifier

WSRC-RP-89-815
DECEMBER 1989

REACTOR OPERATION ENVIRONMENTAL INFORMATION DOCUMENT

VOLUME I

GEOLOGY, SEISMOLOGY AND SUBSURFACE HYDROLOGY (U)

J. S. Haselow
V. Price
D. E. Stephenson
H. W. Bledsoe
B. B. Looney

Approved by: D. B. Moore, Manager
Environmental Sciences Section
Savannah River Laboratory

Westinghouse Savannah River Company
Savannah River Site
Aiken, SC 29808

Prepared for the U. S. Department of Energy under Contract No. DE-AC09-89SR18035

D Moore, Section Mgr.
Derivative Classifier

WSRC-RP-89-815
DECEMBER 1989

REACTOR OPERATION ENVIRONMENTAL INFORMATION DOCUMENT

VOLUME I

GEOLOGY, SEISMOLOGY AND SUBSURFACE HYDROLOGY (U)

J. S. Haselow
V. Price
D. E. Stephenson
H. W. Bledsoe
B. B. Looney

Approved by: D. B. Moore, Manager
Environmental Sciences Section
Savannah River Laboratory

DOES NOT CONTAIN
UNCLASSIFIED CONTROLLED
NUCLEAR INFORMATION

Reviewing Official: G. J. Barnick, Classification Officer
Date 11/29/89

Westinghouse Savannah River Company
Savannah River Site
Aiken, SC 29808

Prepared for the U. S. Department of Energy under Contract No. DE-AC09-88SR18035

TABLE OF CONTENTS

VOLUME I: GEOLOGY, SEISMOLOGY, SUBSURFACE HYDROLOGY

TABLE OF CONTENTS, Contd

VOLUME I: GEOLOGY, SEISMOLOGY, SUBSURFACE HYDROLOGY

LIST OF FIGURES

LIST OF FIGURES, Contd

LIST OF FIGURES, Contd

LIST OF FIGURES, Contd

LIST OF FIGURES, Contd

LIST OF TABLES

1.0 INTRODUCTION

The Savannah River Site (SRS) produces nuclear materials, primarily plutonium and tritium, to meet the requirements of the Department of Defense. These products have been formed in nuclear reactors that were built during 1950-1955 at the SRS. K, L, and P reactors are three of five reactors that have been used in the past to produce the nuclear materials. All three of these reactors discontinued operation in 1988. Currently, intense efforts are being extended to prepare these three reactors for restart in a manner that protects human health and the environment.

To document that restarting the reactors will have minimal impacts to human health and the environment, a three-volume Reactor Operations Environmental Impact Document (RO-EID) has been prepared. The document focuses on the impacts of restarting the K, L, and P reactors on both the SRS and surrounding areas. Volume I is a discussion of the geology, seismology, and subsurface hydrology; Volume II is a discussion of the site ecology, and Volume II is a discussion of the meteorology, surface hydrology, radiation environment, and radiological impact.

1.1 GENERAL OVERVIEW

1.1.1 Location and Description

The K, L, and P reactors are located at the Savannah River Site which is approximately 25 miles southeast and across the Savannah River from Augusta, Georgia. The site is in the Aiken, Allendale, and Barnwell counties of South Carolina. These counties are in the south-central portion of South Carolina, and about 150 miles along the Savannah River from the Atlantic Ocean.

1.2 SUMMARY

Since construction of the reactors in the 1950's, many geological, seismological, and hydrological studies have been completed. The results of these studies are thoroughly discussed in this document and summarized in the following text.

1.2.1 Geology

The SRS is located in the Upper Atlantic Coastal Plain about 20 miles southeast of the Fall Line that separates the Piedmont and Coastal Plain provinces. The SRS is on the Aiken Plateau, a comparatively flat surface that slopes southeastward but is dissected by several tributaries to the Savannah River. The SRS stratigraphy comprises about 1,000 feet of unconsolidated sands, clayey sands, which in turn are underlain by dense crystalline metamorphic rock or consolidated red mudstone. The geologic terminology (from deep to shallow) used in the SRS vicinity is as follows:

Cretaceous System: Cape Fear, Middendorf, Black Creek, and Steel Creek Member of Peedee Formation.

Paleocene Series: Rhems and Williamsburg Formations.

Lower Eocene Stage: Recently recognized sediments that are the time equivalent of the Fishbourne Formation.

Lower Middle Eocene Stage: Upper Claibornian Lisbon or Santee equivalents. Previsionally these units are assigned to the Santee Formation with a McBean sandy, micritic member, a Warley Hill sandy and often glauconitic member and the Caw-Caw glauconitic and/or lignitic shale member.

Upper Eocene Stage: The Dry Branch and Tobacco Road Formations of the Barnwell Group. In some SRS literature, the Jacksonian Dry Branch Formations has been included in the "McBean Formation."

Post Jacksonian Sediments: Gravels, clays, and arkosic sands of fluvial origin. An informal stratigraphic unit called the "Upland Unit." These gravels together with a reticulate mottled "B" soil horizon were mapped as the "Hawthorne" Formation in early SRS publications.

Flood Plain Deposits: Significant but generally this occurs along the Savannah River and its major tributaries.

1.2.2 Seismology

The Atlantic Coastal Plain tectonic province, in which the site is located, is a large area with generally low seismic activity. The general seismicity of this tectonic province is expected to remain subdued, with the high earthquake activity confined to the Charleston seismic zone. In the adjacent southern Appalachian Mountain region, the most active seismic area in the southeast, earthquakes are irregularly distributed with concentrations in northeast Georgia, western North Carolina, eastern Tennessee, and western Virginia. These areas are all more than 100 miles from the site.

The closest damaging earthquake to the site occurred on November 1, 1875. It was centered about 65 miles to the northwest and had a maximum intensity of VI near the epicenter. This earthquake may have been felt at the site at a low intensity.

The New Madrid earthquakes of 1811-1812, which were centered about 535 miles from the site, were probably felt at the site with an intensity less than VI. The Union County, South Carolina, earthquake of January 1, 1913 which had an epicentral intensity of VII-VIII may have been felt at the site at a low intensity.

The June 9, 1985 earthquake which occurred on SRS about 6 miles to the southwest of the site had an epicentral intensity of III and a local magnitude of 2.6. A local magnitude 2.0 earthquake occurred on the site on August 5, 1988, but it was not felt on the site.

The source of seismicity most affecting the site, both in terms of maximum historical intensity and number of earthquakes is the Charleston, South Carolina area. The main shock of August 31, 1886 probably produced an intensity of VI at the site. The results of recent studies of the Charleston seismic zone put the closest approach of the zone to the site at about 75 miles to the southeast. The maximum credible site intensity has been determined to be VI-VII. For conservatism, a design basis earthquake of site intensity VII-VIII is chosen. This site intensity is associated with a peak horizontal acceleration of 0.2 g.

1.2.3 Foundation Engineering

Foundation conditions were investigated prior to construction of the reactors and where necessary treatment of the subsurface soil were conducted. The investigations consisted of soil borings and sampling for bearing capacity, settlement and liquefaction potential. The major concerns in the original foundation investigations of the 1950s were the bearing capacity of the soils and the possible magnitude of settlements. The foundations of the reactors were designed on the basis of the results of these studies and have performed very well over the intervening years. In the 1960s concerns with the potential for liquefaction due to earthquake motion initiated studies which have continued into the 1980s. These studies resulted in the general conclusion that earthquake-induced liquification for ground motion corresponding to the design basis earthquake is not a potential problem for the reactors at SRS.

1.2.4 Hydrology

There are three major aquifers and aquitards that form the hydrogeologic system at the Savannah River Site. The Cape Fear formation is a heavy clay that forms the base of the system. Overlying the Cape Fear, are Cretaceous age sediments which combine to form a prolific aquifer that can easily supply up to 4 m^3/min. This aquifer has been called "Tuscaloosa" aquifer in previous reports at SRS; for this report, the unit is called the Cretaceous-age aquifer. Upper portions of the Steel Creek Member and the Ellenton combine to form a leaky aquitard that separates the Cretaceous and Tertiary-age aquifers. The Tertiary aquifer is comprised of Lower Eocene and Middle Eocene Stages and has been called the "Congaree" aquifer in past reports. In this report, it will be called the tertiary-age aquifer. The Tertiary-age aquifer can supply as much as 0.8 m^3. The Tertiary aquifer and the water table are separated by the "green clay." The green clay is fine/silty glauconitic and/or lignitic material and is part of the Santee Formation.

The direction of ground water movement at the SRS is correlated with the depth of incision of the creeks and rivers that dissect the Aiken Plateau. However, in general, water in the water table flows to surface streams, but some water flows through the "green clay" to the tertiary-age aquifer. Once in the Tertiary-age aquifer, ground water at the SRS flows to the surface at Upper Three Runs Creek or the Savannah River. Flow into the Cretaceous-age aquifer from above is impeded by the "Ellenton" aquitard, or in some portions of the plant, by an unfavorable potential gradient (head reversal). Although, at the K, L, and P areas a head reversal does not exist between the Tertiary-age and Cretaceous-age aquifers.

2.0 GEOLOGY, SEISMOLOGY, AND GEOTECHNICAL ENGINEERING

The P, L, and K reactors are located at the Savannah River Site (SRS), which is approximately 25 miles southeast of Augusta, Georgia, in Aiken, Allendale, and Barnwell counties, South Carolina (Figure 2-1 and 2-2). The SRS has, over the years, undergone numerous comprehensive geological, seismological, geophysical, and foundation engineering investigations. These studies have included thorough literature searches, aerial photographic interpretation, geologic mapping, a seismic reflection survey, drilling programs, geophysical logging, soil borings, and in situ velocity measurements by the crosshole and downhole methods.

Physiographically, the SRS and the production reactor sites are located in the upper Atlantic Coastal Plain of South Carolina (Figure 2-3). The plain slopes from 650 feet above msl* at the Fall Line to about 250 feet above msl on the southeastern boundary of SRS (Figure 2-4). The major physiographic divisions in the site region are the Aiken Plateau and the Congaree Sand Hills.

The reactor sites at SRS lie in the Coastal Plain province, which extends from the Fall Line to the edge of the Continental Shelf. Since Cretaceous time, the province has been an area of general subsidence where a thick accumulation of Cretaceous and younger age sediments have accumulated. These sediments unconformably overlie a basement complex, which consists of igneous rocks, gneisses, and shists of pre-Triassic age and fault-bounded basins of Triassic-Jurassic age.

The Coastal Plain province is a large area with low seismic activity. The only zones of concentrated seismic activity are centered near Bowman, South Carolina, and in the Charleston-Summerville area of South Carolina. The largest known earthquake to affect the site was the Charleston earthquake of 1886. On the basis of detailed reports of felt motion, the SRS probably experienced ground shaking equivalent to a modified Mercalli intensity (MMI) of VI-VII during this event. The design basis earthquake (DBE) has been conservatively established as an earthquake causing a site MMI of VII, with a corresponding zero-period peak horizontal ground acceleration of 0.20 g as discussed in Section 2.2. This DBE definition was determined on the basis of Appendix A to 10 CFR 100.

2.1 BASIC GEOLOGIC AND SEISMIC INFORMATION

2.1.1 Regional Geology

2.1.1.1 Regional Physiography

The SRS is located in the Upper Atlantic Coastal Plain, approximately 25 to 30 miles southeast of the Fall Line and the city of Augusta, Georgia (Figure 2-5). The Coastal Plain is underlain by a wedge of seaward-dipping unconsolidated and semiconsolidated sediments that increase in

* All elevations are relative to mean sea level (msl) as shown on the topographic map of the SRS prepared by the U.S. Geological Survey, 1987.

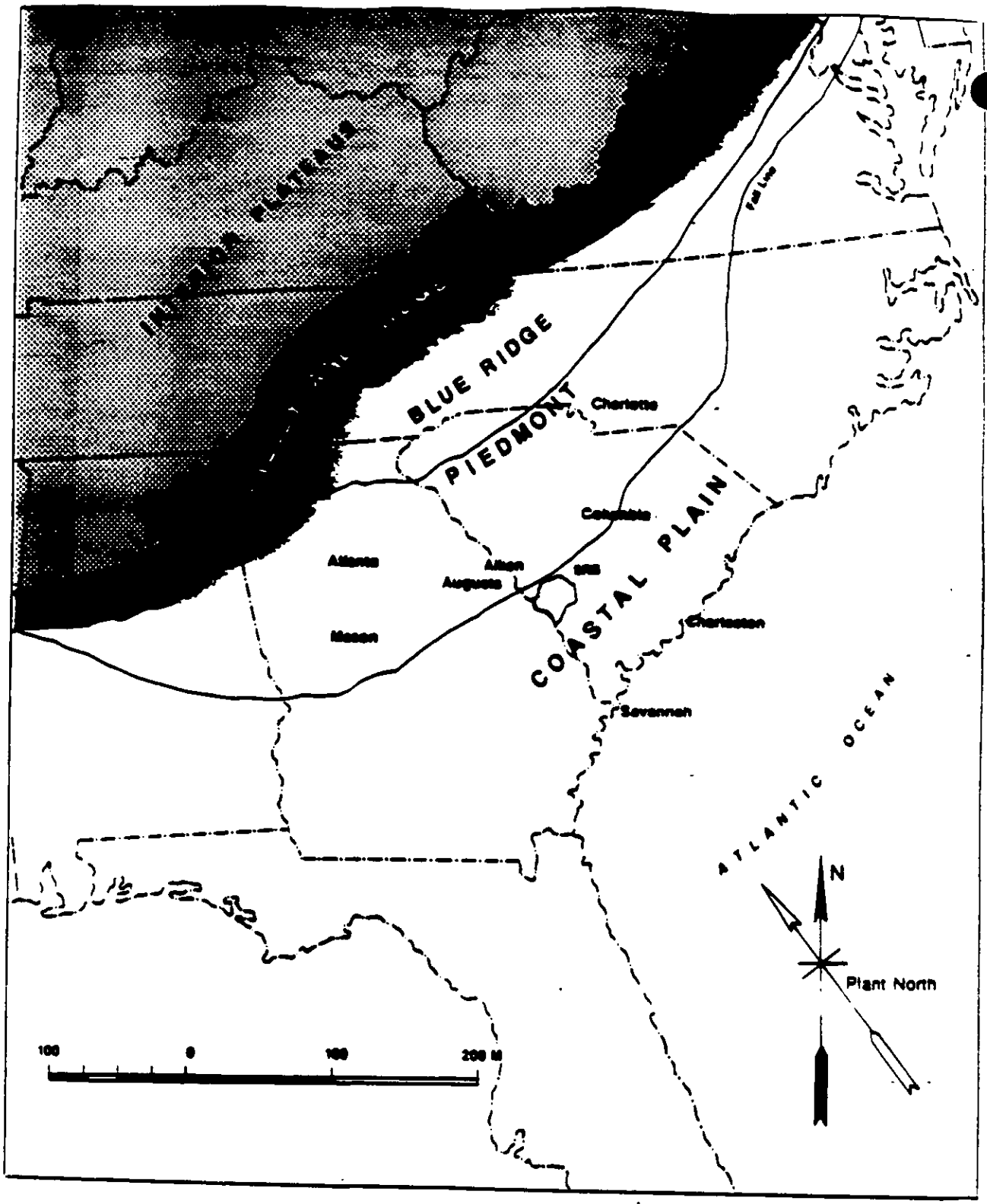

FIGURE 2-1. SRS Regional Location Map

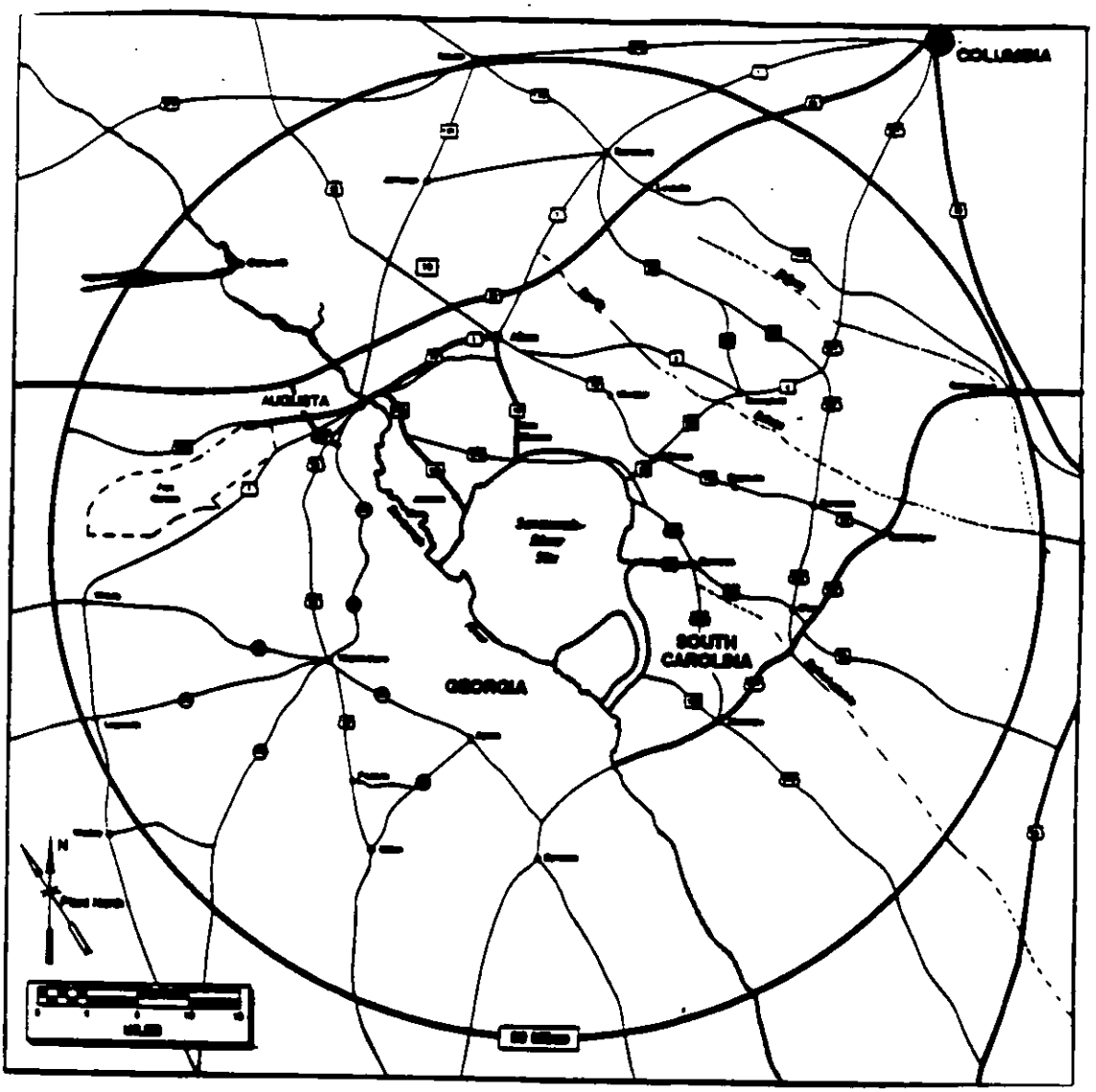

FIGURE 2-2. Fifty-Mile Radius from SRS Center

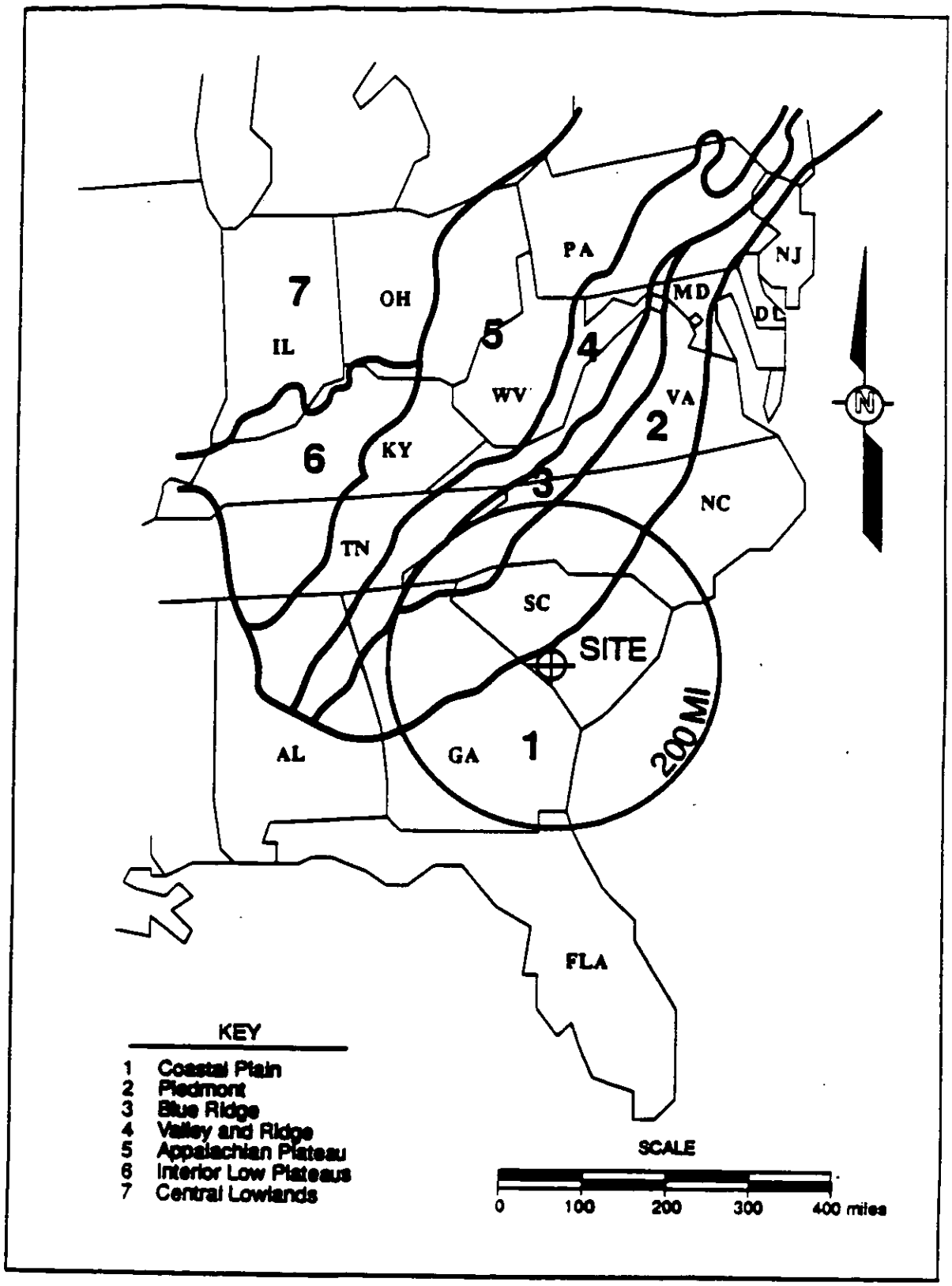

FIGURE 2-3. Physiographic Provinces of the Eastern United States

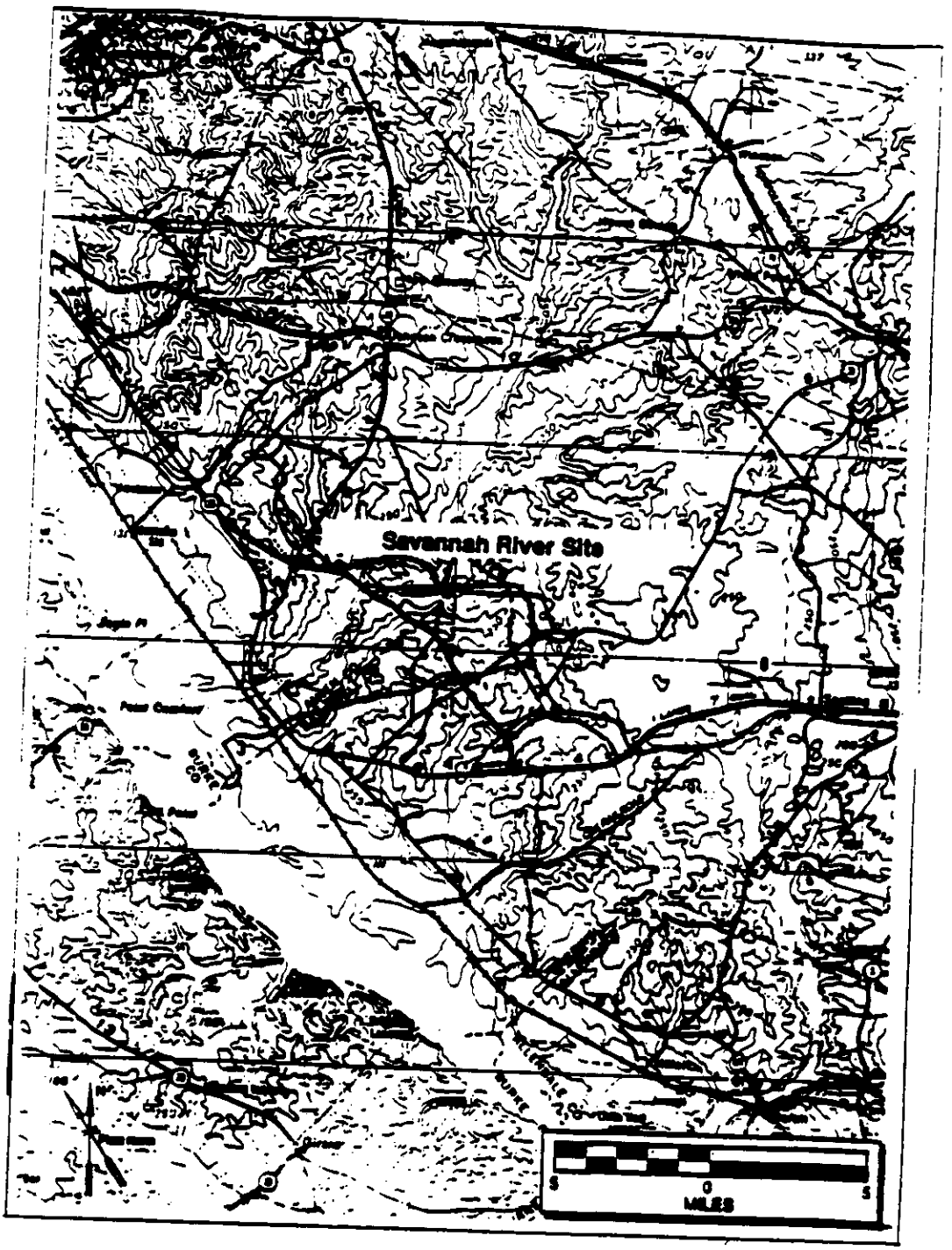

FIGURE 2-4. Topographic Map of SRS

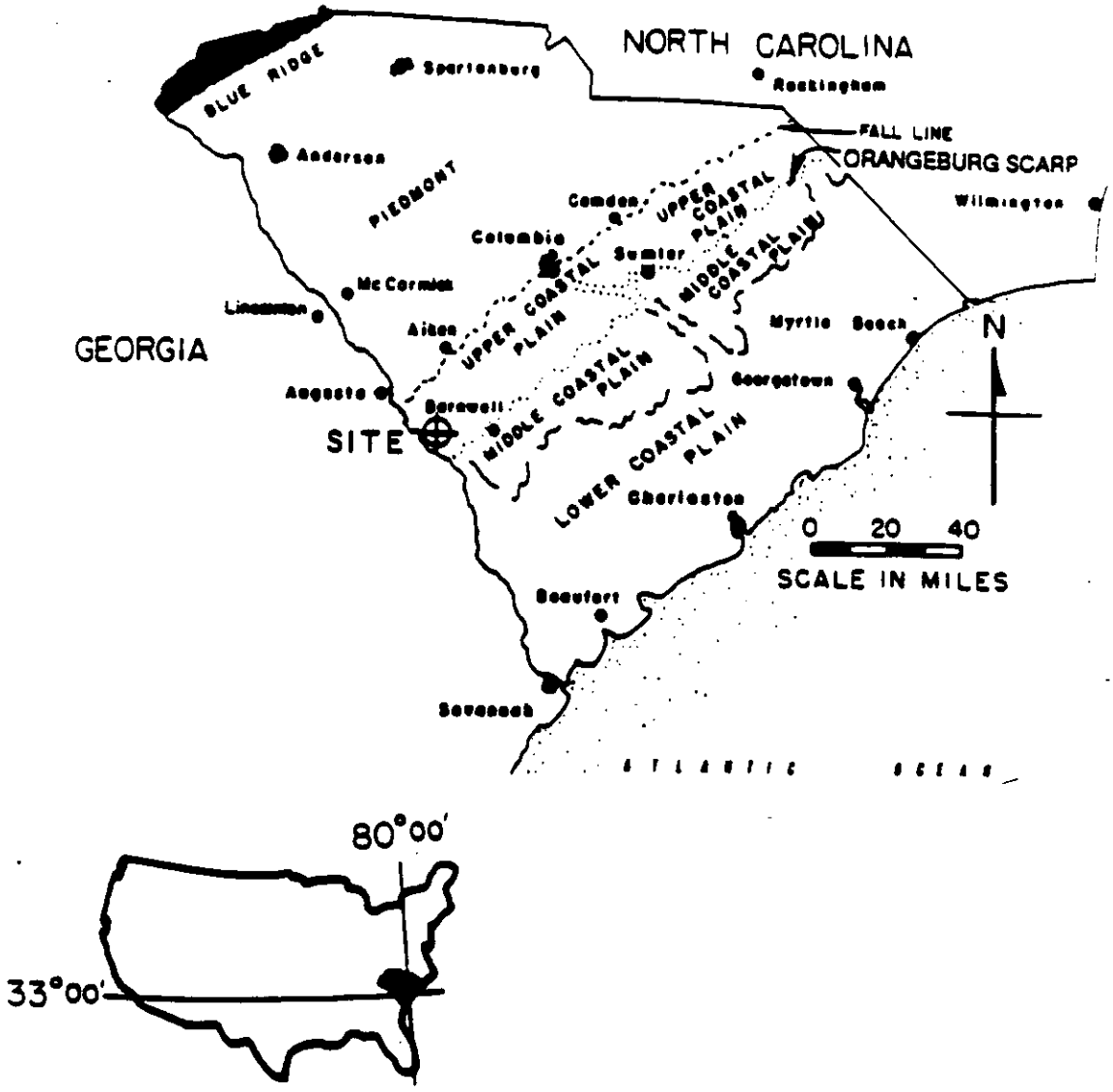

REFERENCE:
MODIFIED FROM: COLQUHOUN, D.J., HERON, S.D., JR., JOHNSON, H.S., JR., POOSER, W.K. AND SIPLE, G.E., 1969, UP-DIP PALEOCENE-EOCENE STRATIGRAPHY OF SOUTH CAROLINA REVIEWED, GEOLOGIC NOTES, DIVISION OF GEOLOGY, S.C. STATE DEVELOPMENT BOARD, V.13, P.1-25.

FIGURE 2-5. Major Physiographic Coastal Plain Subprovinces in South Carolina

thickness from zero at contact with the crystalline Piedmont at the Fall Line to more than 4,000 feet near the coast of South Carolina (Rankin, 1977). This sedimentary wedge, which ranges from early Late Cretaceous (Cenomonian) to Recent (Hazel et al., 1977), continues to the seaward edge of the Continental Shelf (Figure 2-6).

The Atlantic Coastal Plain extends southwestward from Cape Cod, Long Island, and southern New Jersey at its northern end to southern Georgia, Florida, and Alabama, where it continues as the Gulf Coastal Plain (Figure 2-7). The topographic surface of the Coastal Plain slopes gently seaward. It also slopes toward the north, as evidenced by the drowned valleys that form the Chesapeake and Delaware Bays, and the bays in the New York area.

The Coastal Plain in South Carolina is divided into three physiographic belts: the upper, middle, and lower Coastal Plains. These belts are approximately parallel to both the coast and the Fall Line (Colquhoun and Johnson, 1968), as shown in Figure 2-7. The upper Coastal Plain slopes from 650 feet above msl at the Fall Line to about 250 feet above msl on the southeastern boundary of SRS (Figure 2-6). The upper Coastal Plain is separated from the middle Coastal Plain by the Orangeburg Scarp (Figure 2-6), which has a relief of approximately 100 feet over a distance of a few miles. The Orangeburg Scarp is the locus of Eocene, Upper Miocene, and Pliocene (?) shorelines (Colquhoun and Johnson, 1968). The upper Coastal Plain is a surface of predominantly fluvial erosion, whereas the middle Coastal Plain is a surface on which "fluvial erosion has proceeded to the point where the primary depositional topography, although present, is generally not obvious" (Rankin, 1977). The lower Coastal Plain has a primary depositional topography formed during Pleistocene and Holocene times. It is distinguished from the middle Coastal Plain by a change in erosion characteristics.

The major physiographic divisions in the site region are the Aiken Plateau and the Congaree Sand Hills (Figure 2-7) (Siple, 1967; Cooke, 1936).

The Aiken Plateau is bounded by the Savannah and Congaree rivers and extends from the Fall Line to the coastal terraces. The coastal terraces correspond roughly to the lower Coastal Plain (Colquhoun and Johnson, 1968). The surface of the Aiken Plateau is highly dissected and characterized by broad interfluvial areas with narrow steep-sided valleys. Relief is locally as much as 300 feet (Siple, 1967). The plateau is generally well drained, although many poorly drained sinks and depressions exist. Depressions are fairly common as swampy areas on the topographically high (somewhat greater than 250 feet above msl) fluvial "Upland" unit, which is the youngest geologic formation at SRS (excepting recent alluvium). Some depressions are related to dissolution of calcareous sediments. These were studied extensively at the time of construction of the SRS facilities (U.S. Army Corps of Engineers, 1952). Other depressions may result from dissolution of silicate materials (Cooke, 1943).

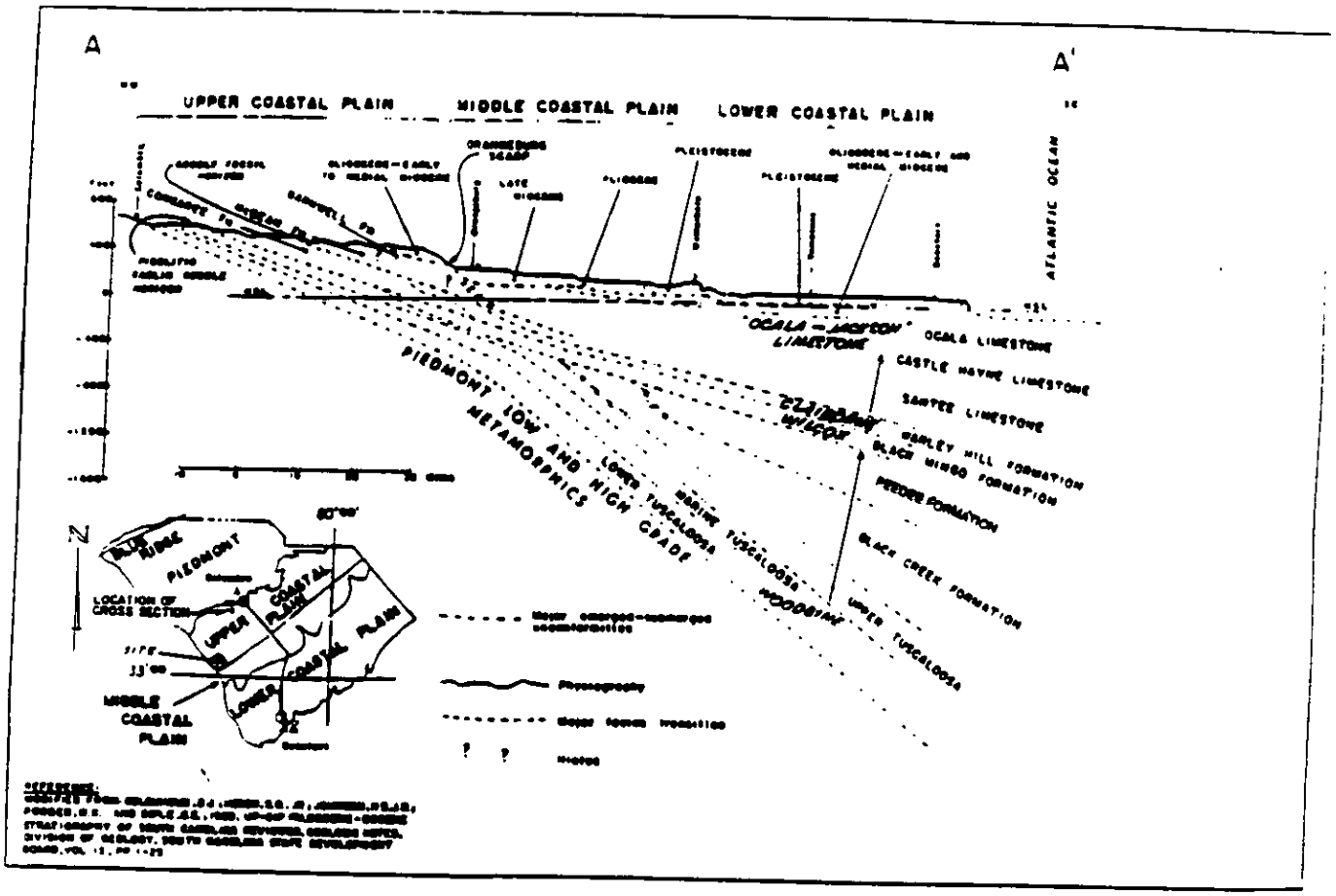

FIGURE 2-6. Generalized Cross Section of Coastal Plain in South Carolina

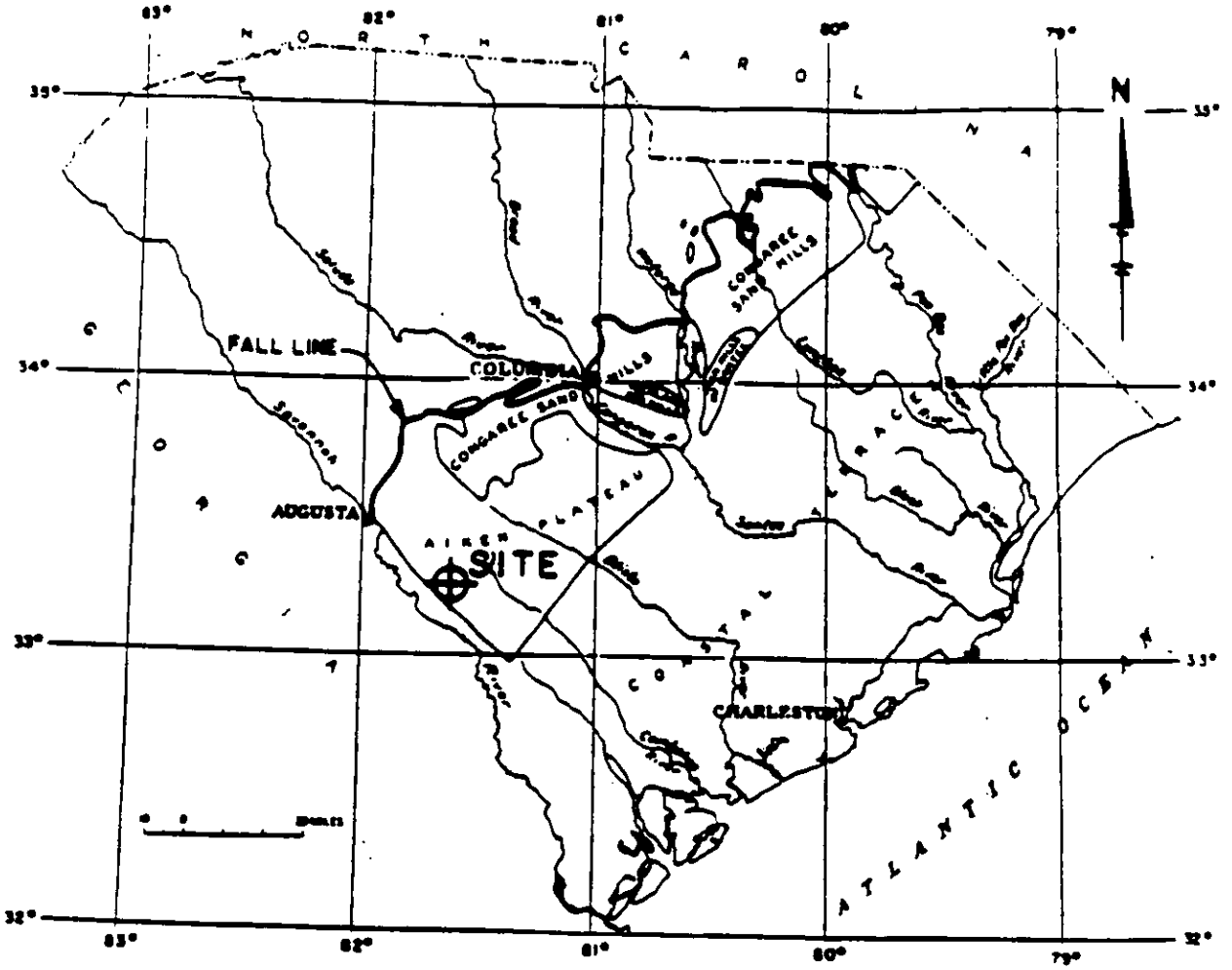

REFERENCE:
COOKE, C.W., 1936, GEOLOGY OF THE COASTAL PLAIN OF SOUTH CAROLINA, U.S. GEOLOGICAL SURVEY BULLETIN 867, 196 P.

FIGURE 2-7. Geographic Divisions of the Coastal Plain in South Carolina

The Congaree Sand Hills trend along the Fall Line northeast and north of the Aiken Plateau. The sand hills are characterized by gentle slopes and rounded summits and are interrupted by the valleys of southeast-flowing streams and their tributaries (Siple, 1967).

The site region, defined as the area within 200 miles of the site, contains elliptical depressions called Carolina Bays. These features, common throughout the Atlantic Coastal Plain, are most numerous in North and South Carolina. There are about a dozen such depressions on or near the Aiken Plateau, with major axes as long as 6,000 feet (Siple, 1967). These features are discussed in detail in Section 2.1.1.6.3.

The site region contains much of the southern Appalachians and includes portions of the Coastal Plain, Piedmont, Blue Ridge, and Valley and Ridge physiographic provinces (Figure 2-5). The Piedmont province extends from southeastern New York to Alabama in a generally northeast-southwest direction. It lies adjacent to the Atlantic Coastal Plain and is the easternmost physiographic and structural province of the Appalachian Mountains. Typically, the Piedmont Province is a broad plateau sloping gently seaward from the front of the Blue Ridge to the Coastal Plain (Figure 2-6). Its width varies from approximately 10 miles at its narrowest part in southeastern New York to about 125 miles in North Carolina. The Piedmont is the least rugged of the Appalachian Provinces; elevation of the inland boundary ranges from about 200 feet above msl in New Jersey to over 1,800 feet above msl in Georgia. Bedrock exposures are scant and poor because the bedrock is characteristically covered by deep residual soil and saprolite. The Piedmont in North Carolina, South Carolina, and Georgia consists mainly of a complex of gneisses, schists, phyllites, and slates containing granitic to ultramafic intrusives. The metamorphic grade generally increases toward the west (Popenoe and Zeitz, 1977). The Piedmont lithologies extend beneath the Coastal Plain and underlie the SRS and the three reactor facilities.

The Blue Ridge Province extends from Pennsylvania southwestward to northern Georgia. It is narrow over its northeastern half and broader in the southern part. The Blue Ridge reaches its greatest topographical expression in North Carolina and Georgia, where the mountains exceed 6,000 feet in altitude. This includes the highest point in the Appalachian Mountains, Mount Mitchell, North Carolina, which is 6,684 feet above msl. The southern Blue Ridge borders the Piedmont with an eastward-facing scarp, the Blue Ridge Front, which has a maximum altitude of 4,000 feet above msl in North Carolina. The Blue Ridge is a complexly folded and faulted metamorphic and igneous sequence, lithologically similar in many respects to the Piedmont.

The Valley and Ridge Province (Figure 2-1) is a folded and thrust-faulted section of conglomerate, sandstone, shale, and limestone. The parallel ridges and valleys, which result from differential erosion of the sedimentary layers, are most evident in the northern parts of the province. In the southern portion, however, a long zone of thrust faults

is the predominant structural feature, and the ridge-and-valley topography is less obvious. The eastern boundary with the Blue Ridge is sharp; on the west, the folds die out and the province grades into the Appalachian Plateau.

Regional drainage of the area around the SRS is provided by the Savannah, the Salkehatchie, and the Edisto rivers (Figure 2-8). The Savannah River is the largest river in the area. It flows from its point of origin at the junction of he Tugaloo and Seneca rivers, about 133 river miles upstream from the SRS, to the Atlantic Ocean, about 150 river miles downstream from the site to the southeast (Figure 2-9). It forms the boundary between South Carolina and Georgia and borders the SRS on the southwest. The river has a floodplain four to five miles wide downstream from Augusta and a stream gradient of about one foot per mile at the Savannah River Site (Siple, 1967). In addition to the Savannah River, the Salkehatchie River, and the north and south forks of the Edisto River drain areas in the vicinity of the SRS (Figure 2-8). Both the Salkehatchie and the Edisto rivers originate in the Coastal Plain and flow southeastward into the Atlantic Ocean.

2.1.1.2 Regional Stratigraphy and Lithology

2.1.1.2.1 Atlantic Coastal Plain

The sediments of the Atlantic Coastal Plain in South Carolina are stratified sand, clay, limestone, and gravel which dip gently seaward. They range in age from Late Cretaceous to Recent. The sedimentary sequence thickens from essentially zero thickness at the Fall Line to more than 4,000 feet near the mouth of the Savannah River and over 10,000 feet east of Cape Hatteras. Regional dip is to the southeast, although some beds dip and thicken locally in other directions due to the existence of locally variable depositional regimes. The beds at the base of the sequence lie on a basement complex composed of the following:

- Piedmont-type metamorphic and igneous rocks adjacent to the Fall Line
- Sedimentary and volcanic rocks of probable Triassic to Jurassic age to the east and southeast (Popenoe and Zeitz, 1977) (Section 2.1.1.4)

Interpretations of the sub-Coastal Plain basement (Figure 2-10) are based principally on magnetic, gravity, and electromagnetic data and samples recovered during the drilling of deep wells (Figure 2-11). The crystalline rocks of the Piedmont are covered by Cretaceous and Cenozoic sediments southeast of the Fall Line. The rocks crop out in stream valleys in the Upper Coastal Plain. The crystalline rocks that crop out nearest to the SRS are in the Horse Creek Valley, approximately 18 miles northwest of the production reactor sites. A stratigraphic column of the Appalachian Mountains and basins is shown in Figure 2-12.

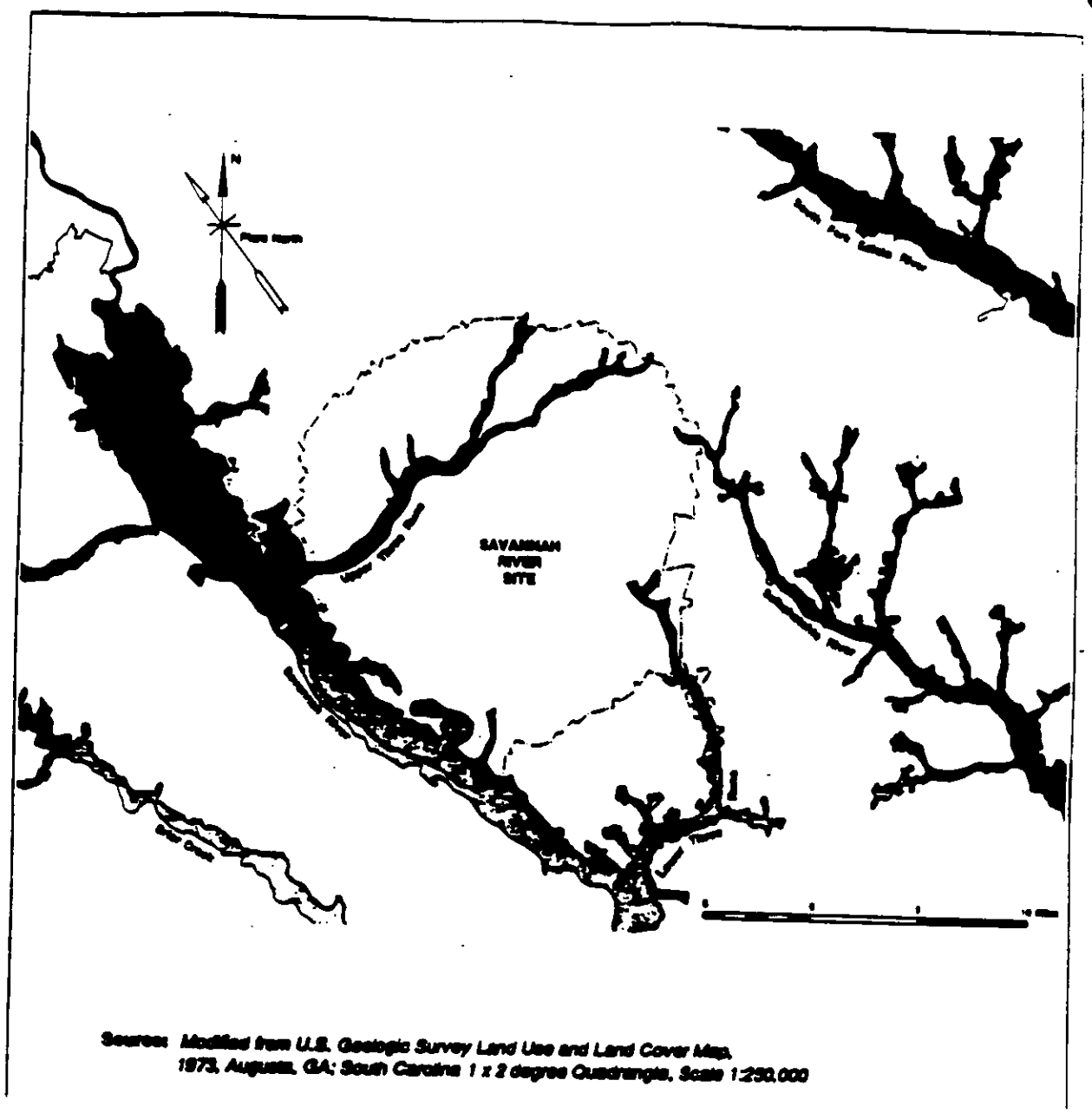

Source: Modified from U.S. Geologic Survey Land Use and Land Cover Map, 1973, Augusta, GA; South Carolina 1 x 2 degree Quadrangle, Scale 1:250,000

FIGURE 2-8. Major Rivers and Adjacent Wetland Areas Surrounding SRS

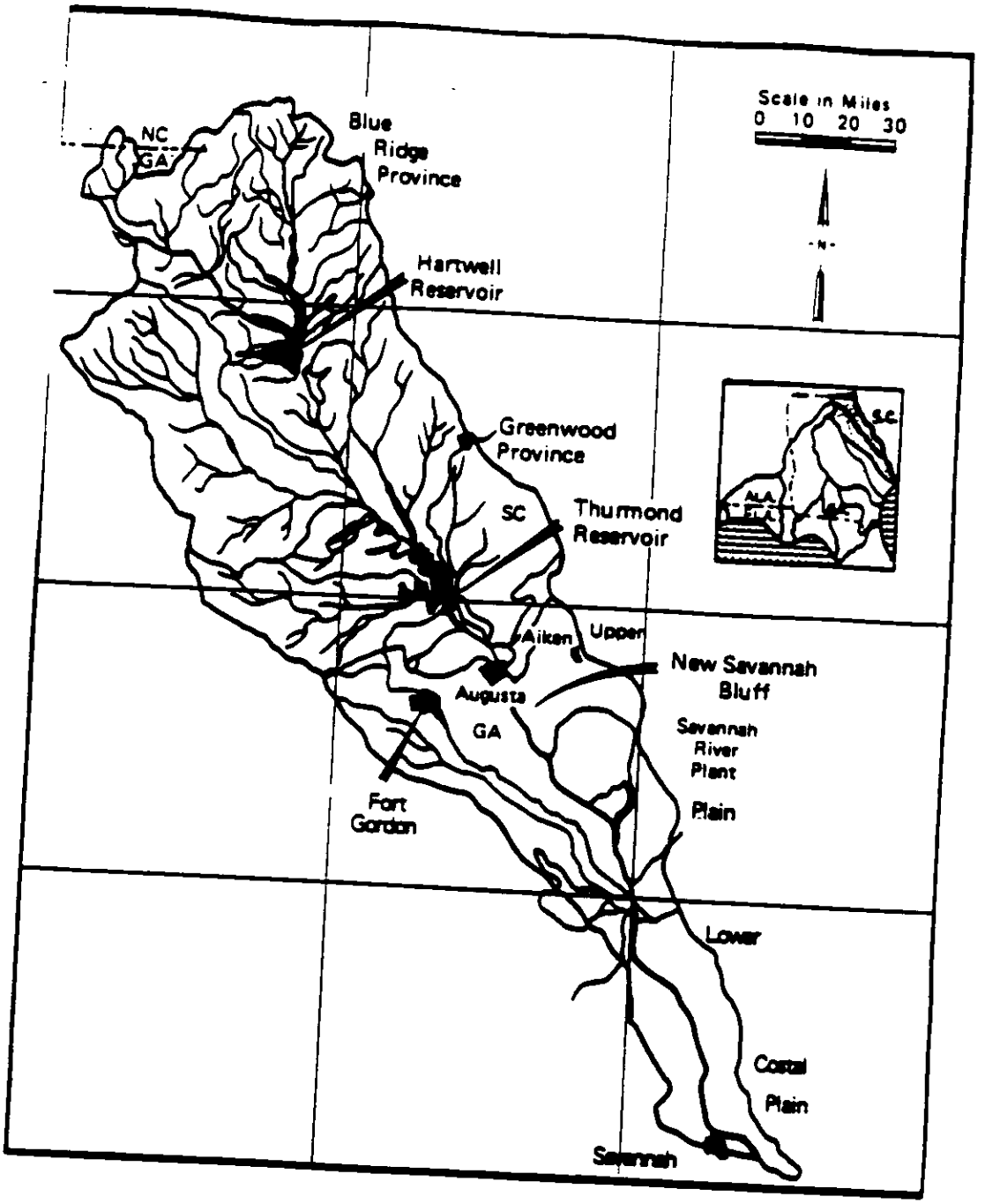

FIGURE 2-9. Savannah River Basin

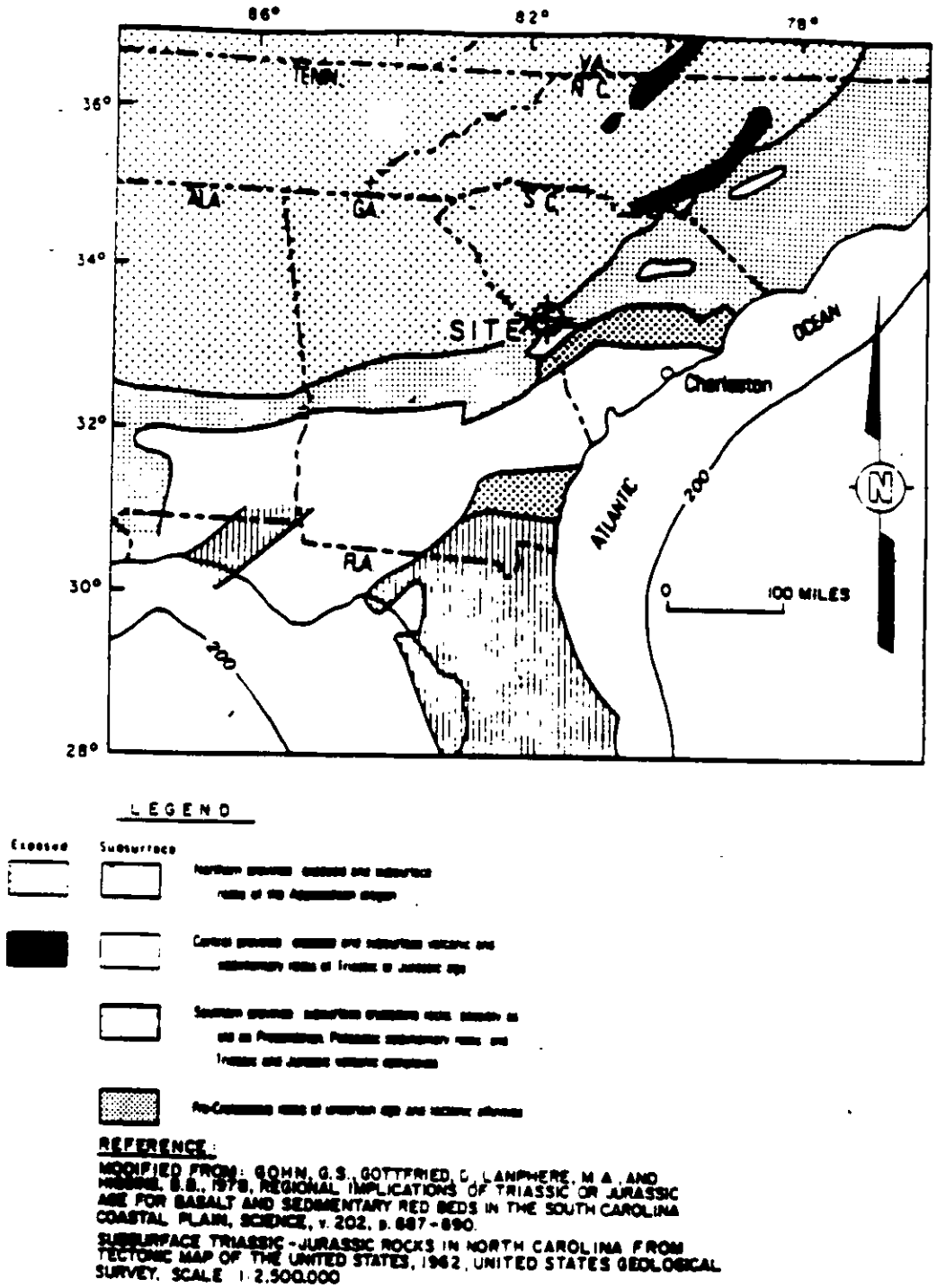

FIGURE 2-10. Major Tectonic Provinces Beneath the Coastal Plain of Southeastern United States

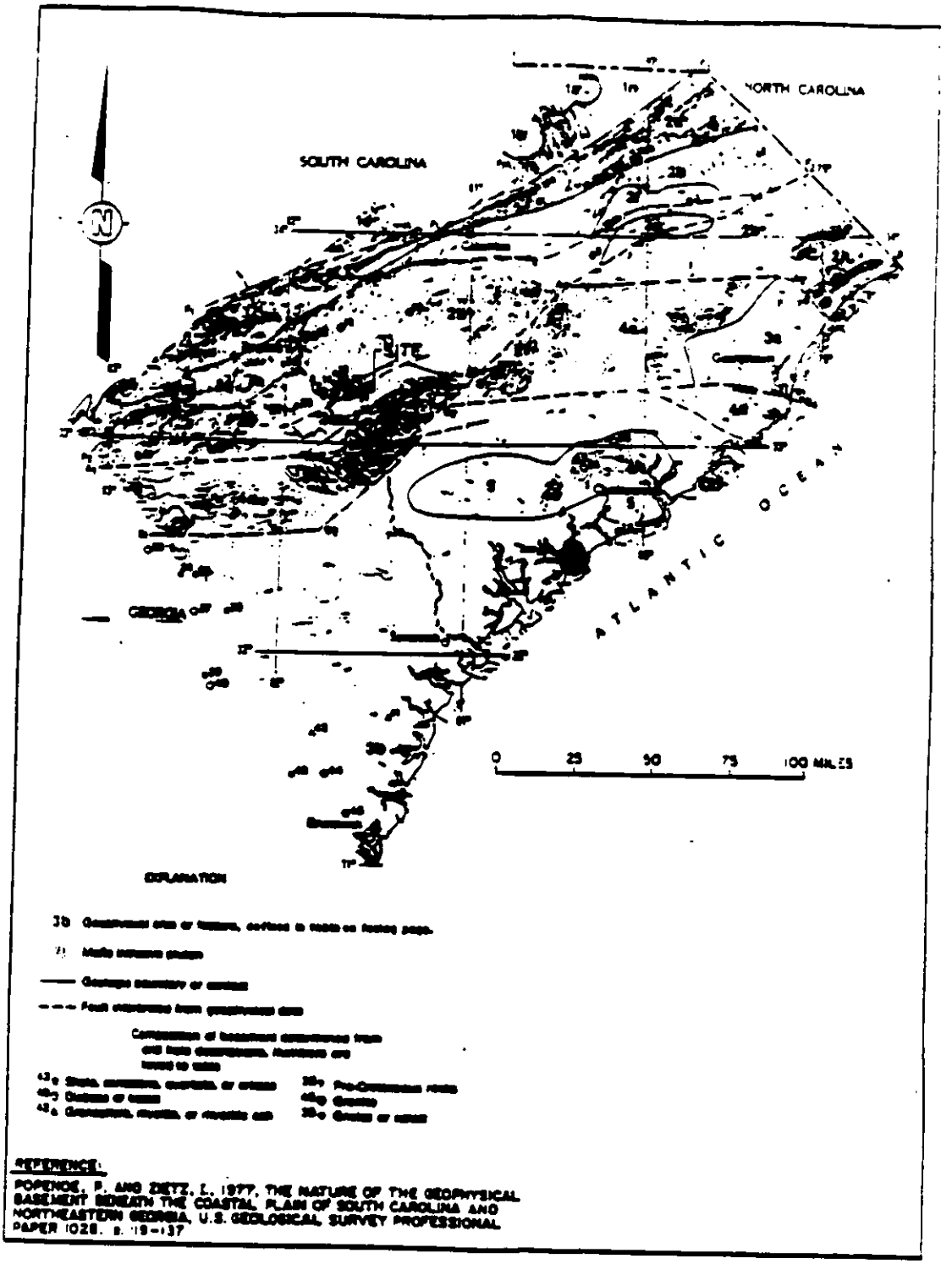

FIGURE 2-11. Aeromagnetic Map Showing Basement Units Beneath the Coastal Plain of South Carolina and Eastern Georgia

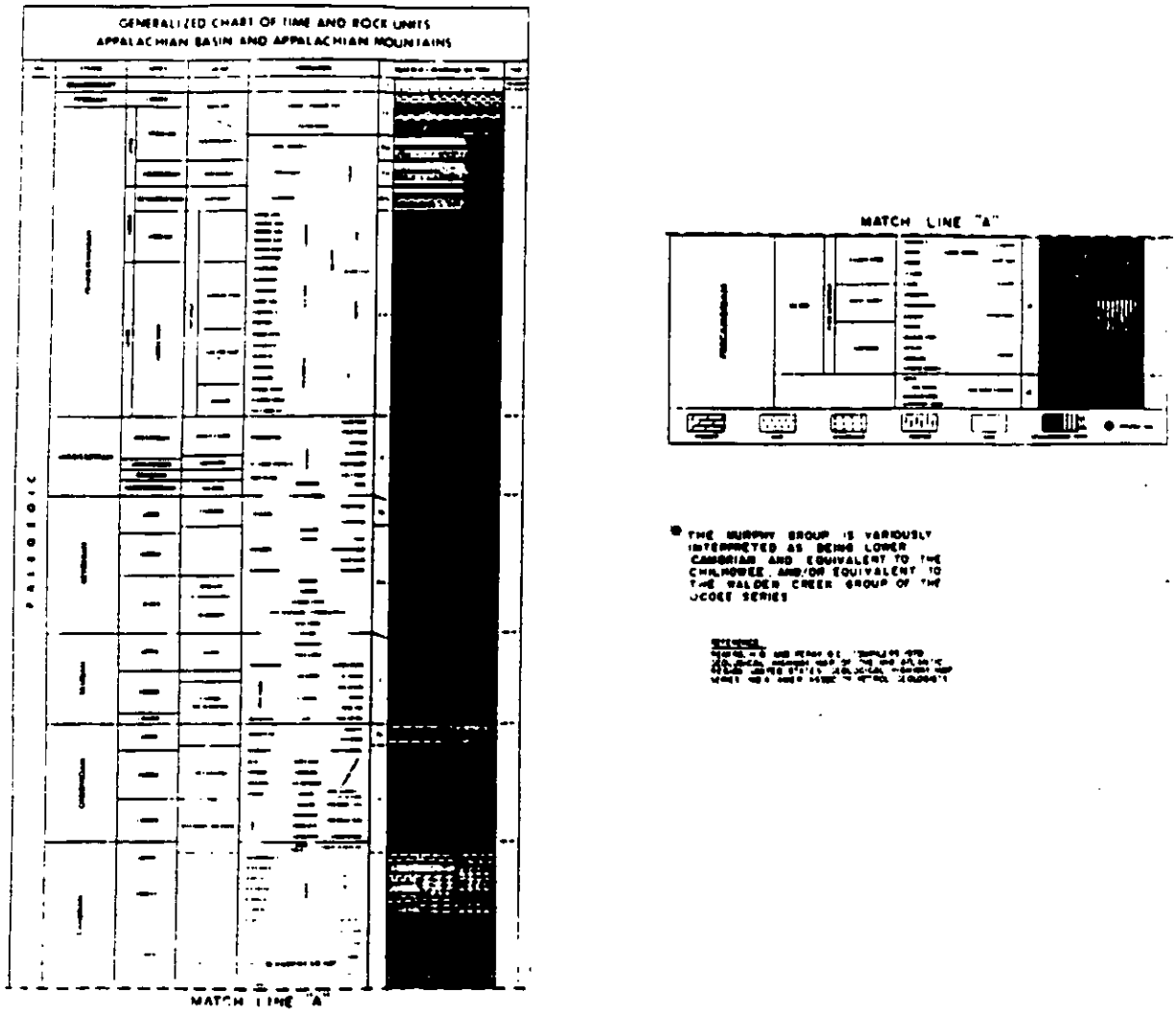

FIGURE 2-12. Generalized Columnar Log of the Appalachian Mountains and Basins

2.1.1.2.1.1 Upper Cretaceous Lumbee Group

Time equivalent units of the four formations of the Lumbee Group (Swift and Heron, 1969) are present in the vicinity of the SRS (Figure 2-13). These are, from oldest to youngest, the Cape Fear, Middendorf, Black Creek, and Pee Dee formations. The lower three units at the SRS appear to be lithologically similar to the formations at their type localities in northern South Carolina and southern North Carolina. The Pee Dee equivalent, however, is not similar and will be referred to as the "Steel Creek Member" of the Pee Dee Formation. The Cretaceous strata have in the past been referred to as the "Tuscaloosa Formation", but the type Tuscaloosa is Cenomanian (earliest Lake Cretacecus) in age. All fossil dates obtained so far from the Cretaceous in the southwestern South Carolina Coastal Plain are younger than Cenomanian. Much of what is mapped as Tuscaloosa (Siple, 1967) is now assigned to the Eocene Formations, using new paleontological data (Tschudy and Patterson, 1975; Inden and Zupan, 1975). The Lumbee strata that crop out between the Fall Line and the SRS are mostly sands and clays. It is difficult to distinguish them from the overlying Eocene units in their area of surface exposure. They are generally mapped as undifferentiated Upper Cretaceous (Nystrom and Willoughby, 1982).

The dip of the upper surface of the Lumbee Group is to the southeast at approximately 21 feet per mile across the SRS. Thickness varies across the site from 380 feet in the northwestern part of the SRS to more than 740 feet near the southeastern boundary. The Lumbee becomes calcareous downdip from the SRS, and is more than 1,500 feet thick at the coast, (Colquhoun et al., 1983).

2.1.1.2.1.1.1 Cape Fear Formation

Correlation of the basal Cretaceous at the SRS with the Cape Fear Formation is somewhat uncertain. The type locality is in southern North Carolina. The unit has not been adequately traced in the subsurface to the south. The age in the type area is reported to be Santonian which is middle Late Cretaceous (Christopher et al., 1979). The term has been applied to sediments of Cenomanian age in a deep well in eastern South Carolina (Gohn et al., 1977). The Cape Fear in North Carolina is Cenomanian, Turonian, and Coniacian (Carter, 1983). The Cape Fear has also been reported to be early Santonian in eastern Georgia and western South Carolina (Prowell et al., 1985). Pollen dated as possibly Turonian or Coniacian has been recovered from a Cape Fear sample in the SRS. Correlation studies may later reveal that the lowest Cretaceous unit at the SRS should have a different name, but the term is used provisionally herein.

The formation is highly colored, with reds, greens, tans, browns, and grays being common. The Cape Fear sediments are more indurated than the other Cretaceous formations because of their high clay content and abundance of cristobalite in the matrix (Prowell et al., 1985).

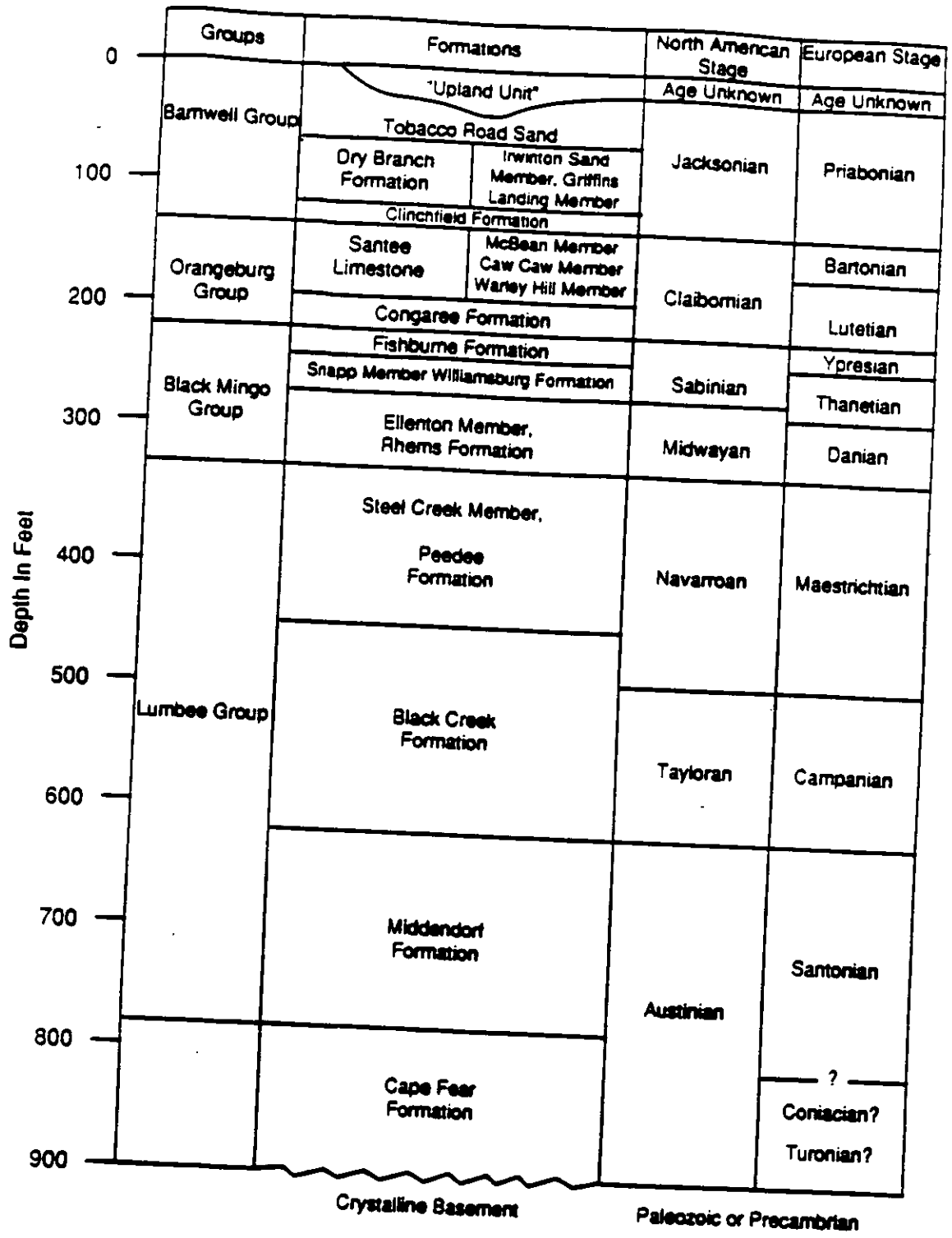

FIGURE 2-13. Tentative Correlation of Stratigraphy Terminology of Southwestern South Carolina Coastal Plain

The modal size of the quartz in the sands is variable, ranging from very fine to coarse, with medium being the most common. The sands are feldspathic in places and can be termed arkose in composition. Muscovite and iron sulfides also occur. Pebbly zones are present in many parts of the section. The environment of deposition has been interpreted as Upper Delta Plain (Prowell et al., 1985d).

The Cape Fear Formation has not been observed at the surface in the vicinity of the SRS. A facies of the formation may have been included in the undifferentiated Upper Cretaceous updip from the SRS (Nystrum and Willoughby, 1982). The Cape Fear is about 30 feet thick at the northwestern SRS boundary and thickens to more than 180 feet near the southeastern boundary.

2.1.1.2.1.1.2 Middendorf Formation

The Middendorf Formation has been correlated in outcrop from its type locality in northern South Carolina to outcrops northwest of the SRS (Nystrom and Willoughby, 1982). In the subsurface, it is approximately 130 feet thick near the northwestern boundary of the SRS and thickens to more than 180 feet near the southeastern boundary. The Middendorf has been assigned a late Santonian age in the SRS area (Prowell et al., 1985), which correlates with the UK_2 unit.

The Middendorf Formation, composed mostly of quartz sand, overlies the Cape Fear unconformably with a sharp, distinct contact. The sands of the Middendorf are tan, light gray, and yellow, much cleaner, and less indurated than the Cape Fear sediments. The Middendorf is dominantly medium and coarse sand, but sand size is quite variable. Sorting is generally moderate to good. Pebbly zones are common within the sand, and clay clasts occur in places. Some parts of the unit are feldspathic, and micaceous and lignitic zones also occur. Cross-bedding is well developed in the lower part of the section in some areas.

Kaolinitic clay lenses occur in parts of the Middendorf. Over much of the SRS, a clay zone up to 80 feet thick forms the top of the formations. In some places, the interval is a pure clay, mottled by red, yellow, orange, and gray. Interbedded sands occur in the clay in other places, some of these being fining upward bodies. In the downdip part of the SRS, this clay is micaceous and lignitic. In parts of the SRS, another clay-rich zone is developed near the middle of the formation. Near the northern part of the SRS, the formation is highly colored, being composed mostly of tan, red, and purple sands. The thick clay bodies present downdip within the SRS seem to be missing, but clay interbeds about two feet thick occur. The sediments have the characteristics of fluvial and deltaic deposits.

2.1.1.2.1.1.3 Black Creek Formation

The Black Creek has been traced in the subsurface from its type area in northeastern South Carolina into the SRS (Colquhoun et al., 1983) and it appears to be equivalent to units UK_4 and UK_5 (Prowell et al., 1985). It is difficult to identify in surface exposures northwest of the SRS but may have been included in the undifferentiated Upper Cretaceous (Nystrom and Willoughby, 1982). The Black Creek is about 110 feet thick at the northwestern boundary of the SRS and thickens to more than 250 feet near the southeastern boundary. The Black Creek is almost 500 feet thick downdip near the coast, but this includes only the Campanian part of the section (Colquhoun et al., 1983). The Black Creek in South Carolina is assigned a Campanian and early Maestrichtian age (Prowell et al., 1985a). A few samples from the SRS have yielded Maestrichtian dates from the unit called Black Creek in this document. Upper Campanian dates have recently been obtained from a well near Barnwell.

The Black Creek Formation in the SRS consists of quartz sands, silts, and clays. It is generally darker and more micaceous and lignitic than the other Cretaceous units. The lower part of the formation is mostly sand, and in much of the SRS area the upper part is clayey and silty.

The lower sandy part of the formation consists of fine, medium, and coarse grained sands. Sorting is generally moderate and poor. The sand is micaceous and becomes lignitic in the center and southwestern parts of the SRS. Pebbly layers are common, as are layers of clay clasts. Feldspathic zones also occur.

The upper clayey, silty zone of the Black Creek occurs as three facies, each trending across the site from southwest to northeast. The most updip facies is a massive clay 20 to 40 feet thick, highly colored by oxidation, and containing what appear to be traces of roots. Grays, reds, oranges, and yellows are common colors. Across the central part of the SRS, clay content is reduced, and dark gray, light gray, and tan silty micaceous sands are dominant, although thin clay layers occur. In the southeastern part, the fine-grained facies forms much of the Black Creek section. It is mostly dark gray and black clay, with interlaminated silt in much of the section. Interbedded with the clays are dark, fine, and medium grained fining upward sands. Iron sulfides are common. This is probably a lower delta plain facies. In the northwestern part of the site, the Black Creek is mostly light colored sand, probably deposited in an upper delta plain environment.

2.1.1.2.1.1.4 Peedee Formation

At its type area in northeastern South Carolina, the Peedee Formation is a fine-grained, glauconitic, dark sandstone and siltstone with marine fossils indicative of a shallow shelf environment. It has been traced in the subsurface into southwestern South Carolina (Colquhoun et al., 1983), where it is composed of light-colored sands and gray, orange, red, and

yellow clays. Because of the difference in lithology between the type Pee Dee and the sediments in southwestern South Carolina, the deposits in the vicinity of the SRS will be informally referred to as the Steel Creek Member of the Peedee Formation.

The Steel Creek Member is not known to crop out near SRS, but a facies of it may occur within the undifferentiated Upper Cretaceous northwest of the SRS (Nystrom and Willoughby, 1982). It is approximately 110 feet thick at the northwestern SRS boundary and 130 feet thick near the southeastern boundary. The Steel Creek Member is shown as being almost 400 feet thick, and calcareous downdip near the coast (Colquhoun et al., 1983), but "Peedee" in South Carolina is middle and late Maestrichtian, and the Black Creek includes early Maestrichtian deposits (Prowell et al., 1985a). Prowell et al. (1985a) referred to the Peedee in the SRS areas as the UK_6 unit. Maestrichtian dinoflagellates and pollen have been recovered from the Steel Creek Member at the SRS.

The lower part of the Steel Creek Member in and near SRS is sandy with a pebble-rich zone at its base suggesting basal unconformity. The upper part is clayey and silty with interbedded sands. The lower, sandy deposits are fine to coarse grained quartz sands and silty sands, poorly to well-sorted, and in places very micaceous. Concentrations of feldspar and lignite occur. Pebbly zones are common, as are layers with clay clasts. Tan and light-to-dark grays are the most common colors. The upper part of the Steel Creek is a clay more than 50 feet thick in places at the SRS and less than three feet thick at other places. Fining upward sands are interbedded with the clay in some areas. The clay is yellow, orange, and red in the southwestern part of the SRS and mostly various shades of gray in the northeast. The unit appears to represent both an upper delta plain environment and a lower delta plain environment. The presence of dinoflagellates indicates some marine influence in parts of the Peedee.

2.1.1.2.1.2 Paleocene-Eocene Black Mingo Group

In southwestern South Carolina, the Black Mingo Group consists of the Midwayan (early Paleocene) Rhems Formation, the early and middle Sabinian (late Paleocene) Williamsburg Formation, and the late Sabinian (early Eocene) Fishburne Formation (Colquhoun et al., 1983). These formations, with the possible exception of the Fishburne, have been traced updip in the subsurface from their type localities in the Lower Coastal Plain of South Carolina into the vicinity of the SRS. One fossil assemblage indicative of the presence of the Fishburne time equivalent has been found at the SRS, but the distribution of the unit is not known at this time, and, thus the unit is not shown on the stratigraphic column (Figure 2-13). Lower Paleocene deposits crop out in a few places northwest of the SRS. The Black Mingo Group is about 70 feet thick at the northwestern site boundary and thickens to about 150 feet near the southeastern boundary. The upper surface dips to the southeast at about 16 feet per mile across the site. The group is about 700 feet thick downdip at the coast (Colquhoun et al., 1983).

2.1.1.2.1.2.1 Rhems Formation

The Ellenton Formation was named and described from cuttings from a well at the SRS (Siple, 1967). At the time, Siple (1967) thought that the age was either Cretaceous or Paleocene. It was later dated as Midwayan and equivalent to the Rhems Formation (Prowell et al., 1985b). Because it is lithologically different from the type Rhems, the Ellenton deposits are referred to in this report as the "Ellenton Member of the Rhems Formation."

Iron sulfides are common in the darker parts of the section, as is cristobalite. Moderately sorted, glauconitic quartz sands also occur, as do yellow and tan, well-sorted, fine-grained quartz sands. Upper delta plain deposits, composed of light-colored, micaceous, moderately to poorly sorted quartz sands are common in the northwestern part of the SRS, whereas darker, more poorly sorted, micaceous and lignitic lower delta plain sediments become more dominant in the southeastern part.

The Ellenton crops out about four miles northwest of the SRS in the Hollow Creek Valley. Lighter-colored facies of the Ellenton may have been included in the Huber Formation in mapping between the Fall Line and the SRS, although most of the Huber is Eocene. The Ellenton lies unconformably on the Cretaceous sediments and consists mostly of gray, poorly sorted, micaceous, lignitic, silty, and clayey quartz sands, which are locally feldspathic, and interbedded with gray clays (Nystrom and Willoughby, 1982). The Ellenton is approximately 40 feet thick at the northwestern boundary of the SRS and thickens to about 100 feet near the southeastern boundary. The Midwayan section is about 250 feet thick and calcareous at the coast (Colquhoun et al., 1983). Unit P_1 of Prowell et al. (1985a) corresponds to the Ellenton Formation. Many dinoflagellate and pollen samples of Midwayan age have been obtained from Ellenton samples at the SRS.

2.1.1.2.1.2.2 Williamsburg Formation

The deposits in the vicinity of the SRS, which are the time equivalent of the Sabinian Williamsburg Formation, differ from the type Williamsburg and are referred to as the "Snapp Member" of the Williamsburg Formation. The unit is well developed in well P22 in the southeastern part of the SRS near Snapp Station (Figure 2-14). The sediments are typically light gray, silty, medium to coarse-grained quartz sand interbedded with gray clay. Dark, micaceous, lignitic sand also occurs. Updip on the SRS, the Snapp is orange and yellow in color, less silty and better sorted. The clay beds are thinner in this area. The Snapp appears to change from an upper delta plain facies in the northwest to a lower delta plain facies in the southeastern part of the site. The basal contact is probably unconformable.

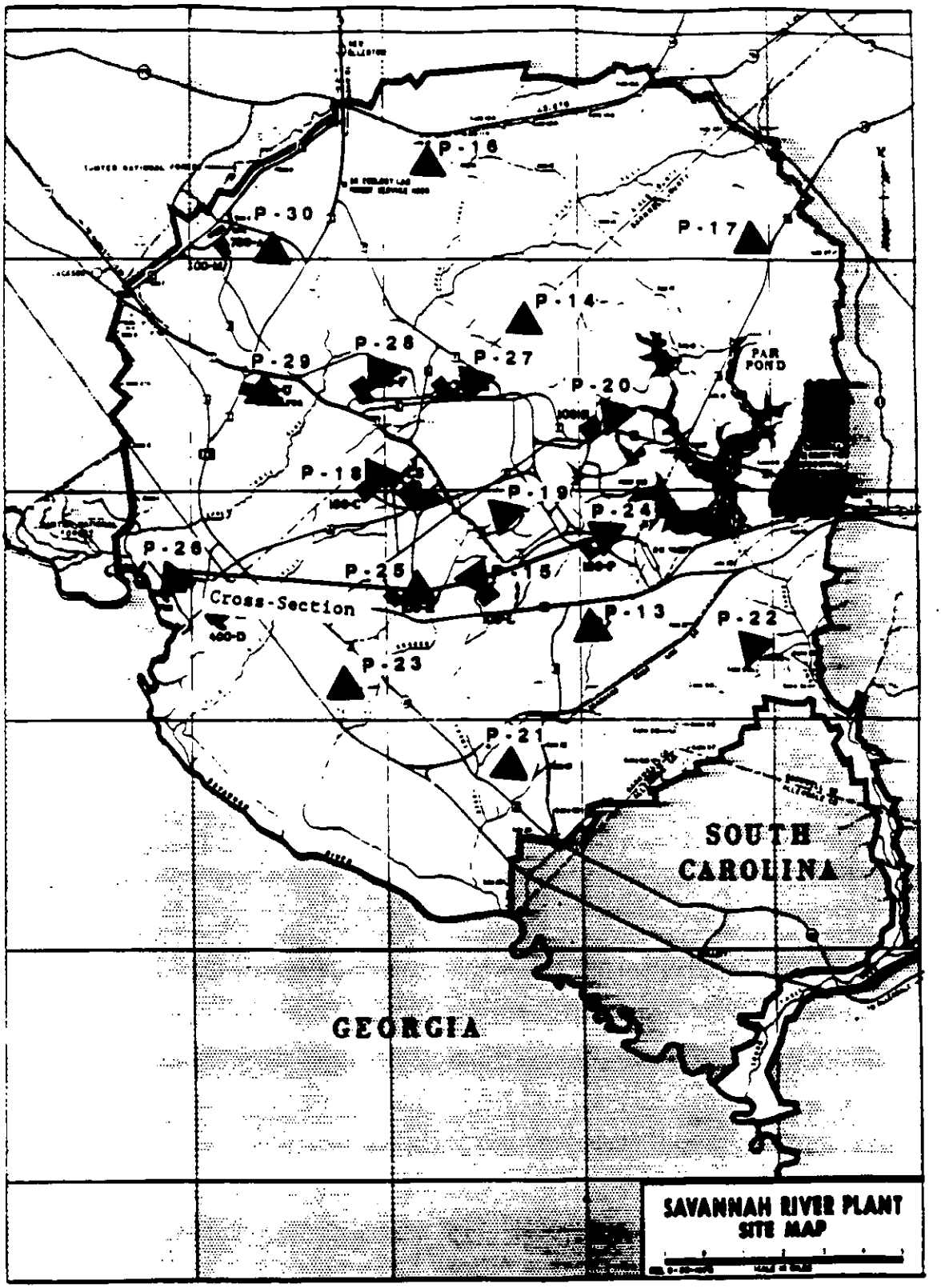

FIGURE 2-14. Well Locations on the SRS Site

Sabinian sediments have not been identified in surface exposure northwest of the SRS but may have been mapped as part of the Huber Formation. The Snapp Member is about 30 feet thick at the northwestern SRS boundary and thickens to about 50 feet near the southeastern boundary. The Williamsburg Formation is about 350 feet thick and calcareous downdip near the coast (Colquhoun et al., 1983). Unit P_2 of Prowell et al. (1985) appears to be equivalent to the Snapp Member.

A few dinoflagellate and pollen samples indicating a Sabinian age have been found at the SRS.

2.1.1.2.1.3 Middle Eocene Orangeburg Group

The Claibornian Orangeburg Group in the southwestern Coastal Plain of South Carolina consists of the lower middle Eocene Congaree Formation (Tallahatta equivalent) and the upper middle Eocene Santee Limestone (Lisbon equivalent). The group crops out in many places at lower elevations on and in the vicinity of the SRS. A pisolitic clay zone that is present at the base of the Claiborne sediments in South Carolina is similar to the clay zone at the base of the Claiborne deposits in the Gulf Coastal Plain. The sediments thicken from approximately 100 feet at the northwestern SRS boundary to about 160 feet near the southeastern boundary. Dip of the upper surface is about 12 feet per mile to the southeast across the site. Downdip at the coast, the Orangeburg section is about 325 feet thick (Colquhoun et al., 1983).

2.1.1.2.1.3.1 Congaree Formation

The early Middle Eocene Congaree deposits have been traced from the Congaree Valley in central eastern South Carolina into the SRS area. Many different stratigraphic names have been applied to the deposits in the southwestern South Carolina Coastal Plain (Colquhoun et al., 1983). At the SRS, the Congaree consists of yellow, orange, tan, gray, and greenish-gray, well-sorted, fine to coarse-grained quartz sands. Thin clay laminae occur throughout the section, and pebbly layers are present in places. Clay clasts also occur. The quartz grains tend to be better rounded than those in the rest of the stratigraphic column. The sands are glauconitic in places. A glauconitic clay encountered in some wells at SRS may be at or near the base of formation, which is unconformable with the underlying Black Mingo Group. In many places on SRS, the upper part of the Congaree is cemented with silica, and, in other places, it is slightly calcareous. The well-sorted sands, the glauconite, and a few fossils indicate that the Congaree is a shallow marine deposit.

The Congaree equivalent northwest of the SRS has been mapped as the Huber Formation, where it occurs at low elevations (Nystrom and Willoughby, 1982). It is more micaceous and poorly sorted there, and is more fluvial and deltaic than at the SRS. The Congaree is about 60 feet thick at the northwestern boundary of the SRS and about 85 feet near the southwestern

boundary. The Tallahattan deposits become much more calcareous between the SRS and the coast (Colquhoun et al., 1983). Units E_3 and E_4 of Gohn et al. (1977) may correlate with the Congaree at the SRS.

A few fossils of Tallahattan age have been recovered from samples at the SRS.

2.1.1.2.1.3.2 Santee Limestone

The late Middle Eocene deposits in the vicinity of the SRS, consisting of carbonates, calcareous quartz sands, quartz sands, glauconitic sands, and clays, are assigned to the Santee Limestone in this chapter. In the past, "McBean Formation" and "Lisbon Formation" have been applied to these sediments. The McBean Formation at its type locality occurs across the Savannah River from the SRS near McBean, Georgia. It consists of a limestone overlain by quartz sand. Most of the overlying sand is apparently of Late Eocene age (Huddlestun and Hetrick, 1985). The typical McBean carbonate lithology is limited to a small area near the type locality. The practice has developed to use McBean as a member of the Santee Limestone Formation rather than a formation.

The Georgia Power Company Plant Vogtle Final Safety Analysis report uses "McBean" as a member of the Lisbon Formation (Carter, 1983). "McBean Member of the Santee Limestone" is used herein because the type locality of the Santee in South Carolina is closer than the type Lisbon in Alabama and because "Santee" has priority. Furthermore, the lithofacies described by Sloan (1908) all seem to be present in the SRS cores, and Sloan applied the Santee, Warley Hill, Caw Caw nomenclature at the SRS (Sloan, 1908; localities 41, 42, 43, 220, McBean Creek) before the McBean Formation was proposed by Veatch and Stevenson in 1911. The "McBean Formation" of previous SRS reports consists largely of sediments which are now known to be Late Eocene (Dry Branch Formation).

A fine-grained, often glauconitic, sandstone occurs in many places within the SRS at the base of the Santee. Surface exposures of this sandstone along Tinker Creek have been assigned to the "Warley Hill phase," correlating with the type locality in Calhoun County in the central eastern South Carolina Coastal Plain (Sloan, 1908). These sediments are referred to as the "Warley Hill Member of the Santee Limestone" herein. Sloan also referred to exposures of green clay along Tinker Creek as belonging to the Caw Caw "phase," the type locality also being found in central eastern South Carolina. These deposits are assigned to the "Caw Caw Member of the Santee Limestone" herein. Both the Warley Hill and the Caw Caw lithologies occur at or near the base of the Santee Limestone at the SRS and are the "green clay" of many SRS reports. The remainder of the Santee is made up of micritic, calcarenitic, and shelly limestone, of calcareous quartz sand, and of noncalcareous, generally fine-grained quartz sand, and is assigned to the "McBean Member of the Santee." This facies is the dominant one. The calcareous parts are rare in the northwestern part of the SRS, more abundant but still sporadic in the central part, and become widespread and thick in the southeastern part.

All three members of the Santee occur on the surface within the site. The Santee Limestone Formation is approximately 40 feet thick at the northwestern boundary and thickens to more than 80 feet near the southeastern boundary. The Santee may be equivalent to unit E_5 of Gohn et al. (1977).

Many fossils of Middle Eocene age have been recovered from the Santee within the SRS.

Siple (1967) speculates that calcareous material has undergone dissolution, causing subsidence of the overlying beds and formation of depressions. Siple (1967) mentions encounters with voids or loosely compacted sediments during the drilling of wells, and notes that large amounts of cement grout were used to stabilize the subsurface before construction of heavy structures.

2.1.1.2.1.4 Late Eocene Barnwell Group

Upper Eocene deposits lie unconformably on the Santee Limestone Formation. The Upper Eocene stratigraphy of the Georgia Coastal Plain has been revised (Huddlestun and Hetrick, 1985), and this approach has been extended into South Carolina (Nystrom and Willoughby, 1982; Nystrom et al., 1986). These authors elevated the Eocene (Jacksonian) "Barnwell Formation" to the "Barnwell Group." In Burke County, Georgia, this group includes (from oldest to youngest) the Clinchfield, Dry Branch, and Tobacco Road formations. The Clinchfield Formation is sandy in Georgia and contains some clay and siliceous sponge spicules. It grades into sandy limestone downdip and eastward, and thins markedly to the east. The Dry Branch Formation includes the Twiggs Clay Member, which predominates west of the Ocmulgee River in Georgia; the Irwinton Sand Member, which predominates from the Savannah River eastward; and the Griffins Landing Member, which contains carbonate. The Tobacco Road Sand, the youngest unit of the Barnwell, is probably typical "Barnwell" of older literature.

2.1.1.2.1.4.1 Clinchfield Formation

The quartz sand of the Clinchfield Formation is difficult to identify unless the Griffins Landing carbonate and the McBean carbonate are both present, with the sand sandwiched between them. It has been identified at several localities within the SRS, but is not mappable with the available data, and, therefore, the unit is not included on the stratigraphic section.

2.1.1.2.1.4.2 Dry Branch Formation

The carbonate of the Griffins Landing Member of the Dry Branch Formation is up to 45 feet thick in the southeastern part of the SRS. Previous reports of the SRS geology have assigned all carbonate to the Middle Eocene "McBean Member Santee Limestone Formation." The large oyster,

Crassostrea gigantissima, which occurs in the Griffins Landing at its type locality, appears to be restricted to the Upper Eocene within the SRS. The Griffins Landing carbonate occurs sporadically at SRS and is not known to be present northwest of Tinker Creek and Upper Three Runs within the site. The occurrence of Crassostrea gigantissima on Tinker Creek above Middle Eocene deposits has been reported (Sloan, 1908). The Griffins Landing appears to have formed in a shallow marine or lagoonal environment.

The remainder of the Dry Branch Formation within the SRS is made up of the Irwinton Sand Member. The Irwinton is composed of tan, yellow, and orange, moderately sorted quartz sand, with interlaminated clays in places. Pebbly layers occur, as do clay clast-rich zones. The Twiggs Clay Member is present in the central part of SRS but has not been mapped over the entire site, and is not shown on the stratigraphic section. It has not been mapped at SRS, but clay which is similar lithologically to the Twiggs is present at various stratigraphic horizons within the Dry Branch. This clay facies, which is tan, light gray, and brown, is up to 12 feet thick in SRS wells, but the layers are not continuous over long distances.

The Dry Branch crops out in many places around and within the SRS. It is about 50 feet thick near the northwestern boundary and about 80 feet thick near the southeastern boundary. Most of the upper, noncalcareous part of the "McBean Formation" of previous SRS reports is the Irwinton Sand Member. The Late Eocene age of the Dry Branch has been established in Georgia (Huddlestun and Hetrick, 1985). Several fossil samples of Late Eocene age have been taken from the Griffins Landing Member at the SRS.

2.1.1.2.1.4.3 Tobacco Road Sand

The Upper Eocene Tobacco Road Sand conformably overlies the Dry Branch. The base of the unit is marked by a coarse layer which contains flat quartz pebbles in places. The formation consists of moderately to poorly sorted, red, brown, tan, purple, and orange quartz sands. Pebble layers are fairly common. Ophiomorpha burrows are abundant in parts of the formation. The sediments are characteristic of shallow marine deposition and environments.

The Tobacco Road crops out over much of the southwestern South Carolina Coastal Plain and is widely exposed at the SRS. Its upper surface is irregular. The thickness varies and ranges up to 50 feet in places. Colquhoun et al. (1983) show the combined thickness of Dry Branch and Tobacco Road formations at the coast to be almost 400 feet. These two formations correspond to the E_g unit of Prowell et al. (1985).

The Late Eocene age of the Tobacco Road has been established in Georgia (Huddlestun and Hetrick, 1985), but parts of the formation may be younger (Colquhoun et al., 1983; Prowell et al., 1985).

2.1.1.2.1.5 "Upland" Unit

The "Upland" unit is an informal stratigraphic term applied to deposits which occur at higher elevations in some places in the southwestern South Carolina Coastal Plain (Nystrom and Willoughby, 1982; Nystrom et al., 1986). The sediments are poorly sorted, clayey, silty sands, with lenses and layers of conglomerates, pebbly sands, and clays. Clay clasts are abundant. Flecks of weathered feldspar are common in the sandy facies in places. Cross-bedding occurs in parts of the unit. The lower surface is irregular because of erosion of the underlying deposits which occurred as the "Upland" unit was deposited.

The "Upland" unit occurs at the surface at higher elevations in many places around and within the SRS, but is not present at all higher elevations. It may be up to 70 feet thick in parts of the SRS. It extends downdip as far as the Orangeburg scarp (Figure 2-5) (Coloquhoun et al., 1983).

The age of the "Upland" unit is not precisely known, but a Miocene age has been suggested (Prowell et al., 1985a). Nystrom et al. (1982) also suggested a Miocene age, correlating it with the Altamaha Formation in Georgia. Much of the "Upland" unit corresponds to the Hawthorn Formation (Prowell et al., 1985b), but the Miocene Hawthorn in the type area is a carbonate formation. The Hawthorn of Siple (1967) probably is mostly "Upland" unit. The pebbly zones of the "Upland" have also been assigned to the Citronelle Formation (Doering, 1960). Foraminifera of Pliocene age have been reported in this "Hawthorn" Formation (Siple, 1967).

2.1.1.2.1.6 Quaternary Marine Terrace Deposits

Cooke (1936) identified seven marine terraces in the site region, although the remnants do not lend themselves to ready interpretation (Siple, 1967). The terrace deposits are a few tens of feet thick, and their origin is problematical.

2.1.1.2.1.7 Quaternary Alluvium

Recent alluvium occurs in the valleys of the Savannah River and other streams in the site vicinity.

2.1.1.2.2 Appalachian Mountains

The Appalachian Orogen was constructed along the ancient Precambrian continental margin of eastern North America by a series of compressional events that began in the Ordovician and episodically spanned much of the Paleozoic Era (Hatcher, 1987). The southern and central Appalachians may best be described using subdivisions based on the stratigraphic and

lithotectonic characteristics of the rocks. These tectonostratigraphic subdivisions primarily include the Valley and Ridge, Blue Ridge, and Piedmont provinces, and are separated from one another by long-inactive fault zones.

2.1.1.2.2.1 Geology of the Valley and Ridge Province

The Valley and Ridge Province is characterized by a thick sequence of sedimentary rocks ranging from Cambrian through Pennsylvanian age. The Rome Formation (Lower Cambrian) of the Valley and Ridge Province is a complex of variegated shales, sandstones, and carbonates grading from a western clastic facies to an eastern carbonate-rich facies. The Conasauga Group (Middle-Upper Cambrian) also has a northwestward or westward clastic source and grades from west to east like the Rome Formation.

The Knox Group (Upper Cambrian-Lower Ordovician) is predominantly a carbonate sequence with several sandstone sequences whose sediments were derived from the northwest. The absence of a major influx of clastic sediments indicates that the deposition of the Knox Group occurred during a time of relative tectonic quiescence (Hatcher, 1987). From west to east, the sequence changes from dolomite to predominantly limestone in composition. The group is bounded above by a regional unconformity that developed when the region was uplifted at the end of the Early Ordovician. This unconformity between Early and Middle Ordovician rocks is observed over the Valley and Ridge and Cumberland Plateau area. Carbonate deposition continued at the beginning of the middle Ordovician; but shortly thereafter, an extensive clastic wedge with an eastern source began to develop on the eastern side of the Valley and Ridge. Sedimentation continued intermittently throughout the remainder of the Paleozoic era.

On the west, relatively thin units of Silurian, Devonian, and Mississippian rocks are deposited. The relatively thin units of Pre-Pennsylvanian rocks are most limestones and shales, with occasional dolomites, sandstones, and cherts. The Pennsylvanian System consists primarily of shales and sandstones, with occasional limestone and numerous coal beds.

2.1.1.2.2.2 Geology of the Blue Ridge Province

The Precambrian basement complex of the Blue Ridge Province is overlain (Figure 2-15) by the Late Precambrian Ocoee Supergroup, which extends from southwestern Virginia to northern Georgia. The Ocoee Supergroup consists primarily of metamorphic volcanic rocks, slates, metaquartzites, and metamorphosed sandstones. In Virginia, the Mount Rogers Formation has been considered to be separate from the Ocoee; however, excellent evidence has been provided for the inclusion of the Mount Rogers Formation as an upper member of the Ocoee Supergroup, as done herein (Rankin, 1970). This group is succeeded by the Chilhowee and Murphy groups (Early Cambrian).

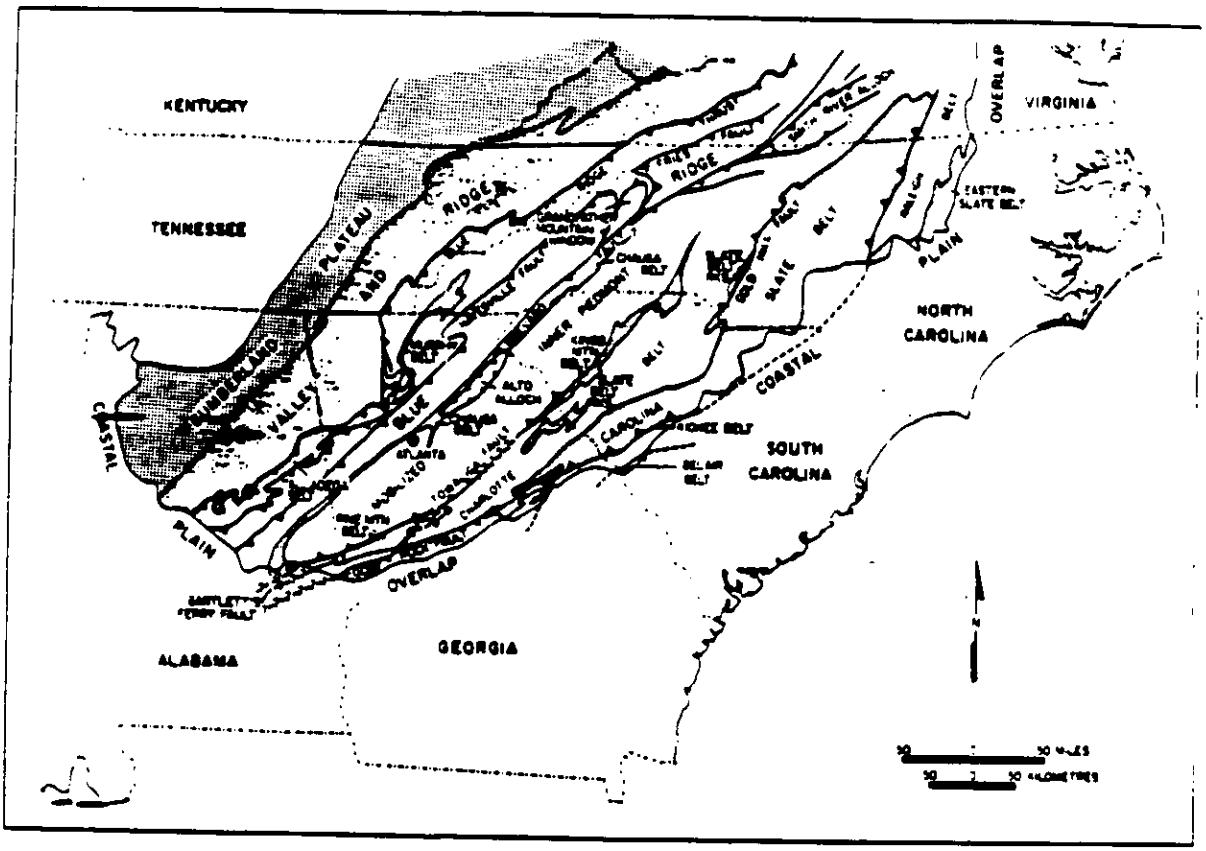

FIGURE 2-15. Regional Physiographic Map of the Southern Appalachians (Hatcher, 1987)

Several geologists, including the originators of Figure 2-15, have indicated that the Murphy Group is also Lower Cambrian and equivalent to the Chilhowee. Other geologists suggest that the Murphy Group may be equivalent to the Walden Creek Group of the Ocoee Supergroup (Hatcher, 1987). Lithologic similarities are closer to the Walden Creek Group than to the higher Chilhowee, Shady, and Rome formations. Since these last three formations occur in the Blue Ridge thrust sheet, very significant facies changes would be required if the Murphy Group were equivalent to the younger units. In northeast Tennessee and portions of Virginia, the Ocoee Supergroup is absent and the Chilhowee directly overlies basement. In the Blue Ridge Province, northeast of Alabama, the Shady Dolomite and Rome formations (Early Cambrian) are the youngest units that are preserved.

Lithologic relations on the southeast side of the Blue Ridge are more obscure because the higher metamorphic grade makes it difficult to recognize the differences between basement and nonbasement rocks. Mapping in southwestern North Carolina has included rocks previously supposed to be basement in the Ocoee Supergroup (Hatcher, 1987). The Ash Formation, believed to be equivalent to part of the Ocoee, has been found north of the Grandfather Mountain Window, the location of which is shown in Figure 2-15. Various units in the Ocoee have been delineated in the southeast side of the Blue Ridge in the Black Mountain area of North Carolina.

Late Precambrian metasedimentary rocks have been recognized in northwestern South Carolina and northeastern Georgia adjacent to the Brevard Zone. These metasedimentary sequences have also been recognized near Brevard, North Carolina, in the Brevard Zone in west Georgia, Alabama, and near Atlanta.

2.1.1.2.2.3 Geology of the Piedmont Province

The Piedmont Province, extending from New Jersey to Alabama, consists of northeast-trending belts defined on the basis of tectonic history, metamorphic grade, and structural relationships. The province consists of variably deformed and metamorphosed igneous and sedimentary rocks ranging in age from Middle Proterozoic to Late Permian. The Piedmont Province in South Carolina and Georgia can be subdivided into seven distinctive tectonostratigraphic belts: the Chauga, Inner Piedmont, Kings Mountain, Charlotte, Carolina Slate, Kiokee, and Belair (Figure 2-15 and 2-16).

The Chauga belt (Hatcher, 1987), which extends from Alabama to North Carolina, is located between the Blue Ridge and Inner Piedmont provinces. The rocks within the Chauga belt are stratified, low- to medium-grade, nonmigmatitic metasediments and metamafic rocks assigned to the stratigraphically equivalent, Precambrian to Early-Cambrian Chauga River and Poor Mountain Formations (Hatcher, 1970). The Chauga River Formation, located on the northwest flank of the Chauga belt, consists of graphitic phyllite, chlorite-muscovite phyllite, and impure marble. The Poor Mountain Formation consists of chlorite-muscovite phyllitic metasilt

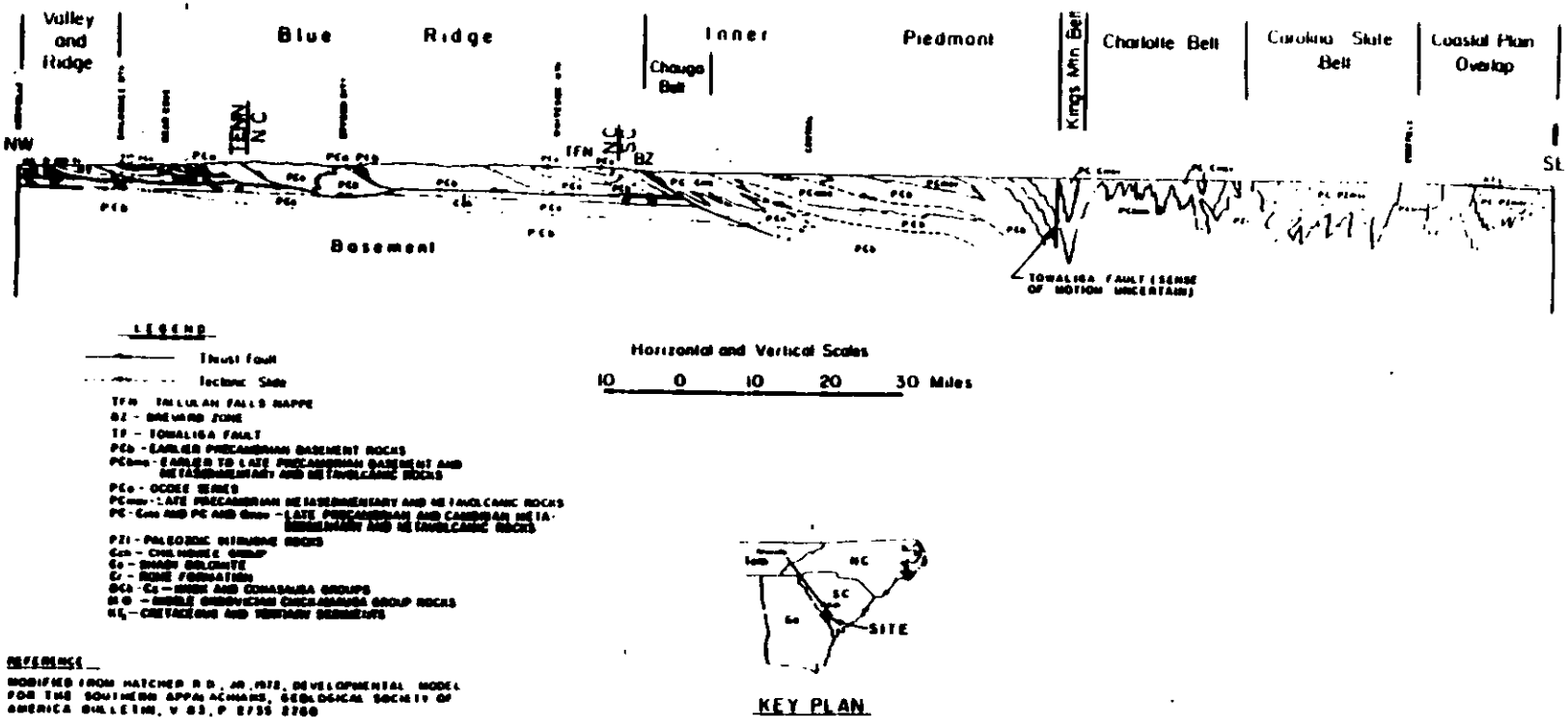

FIGURE 2-16. Regional Geologic Cross-Section of the Southern Appalachian Mountains and Coastal Plain

stone, fine-grained amphibolites, marble, and quartzite. This succession of Chauga River-Poor Mountain formations is overlain by the Henderson Gneiss and Alto allochthon (Hatcher, 1987; Edleman et al., 1987). The Henderson Gneiss is a granitic augen gneiss with U-Pb zircon crystallization ages of 535 Ma (Hatcher, 1987) and 500 Ma (Odom and Fullagar, 1973). The Alto allochthon consists of migmatitic amphibolite facies rocks which were transported northwest from the Inner Piedmont (Hatcher, 1987).

The Inner Piedmont belt contains rocks of the highest metamorphic grade found in the southern Appalachian Piedmont. These include volcanic and sedimentary rocks metamorphosed to the Staurolite-Kyanite and Sillimanite-Almandine subfacies of the Almandine-Amphibolite facies. These rocks consist of amphibolite, granitic gneiss, paragneiss, metasandstone, and schist. The rocks in the core of the Inner Piedmont are of a higher metamorphic grade than rocks on either the northwest or southeast flanks (Griffin, 1971). Structures generally verge towards the northwest (Hatcher, 1987). Folds are overturned to the northwest and are recumbent to reclined, forming large thrust nappes in the northwestern Inner Piedmont that overlie the Chauga belt (e.g., Six-Mile thrust nappe in South Carolina) (Hatcher, 1987; Griffin, 1974). In the southeastern flank in the vicinity of the Kings Mountain belt, the structures steepen, becoming nearly vertical (Hatcher, 1987). The Blue Ridge and Inner Piedmont are believed to contain stratigraphically equivalent rocks (Hatcher et al., 1986).

The Kings Mountain belt extends southwestward from central North Carolina into northeast Georgia where it includes the Lowndesville belt (Griffin, 1969; Horton et al., 1981). The Kings Mountain belt separates the Inner Piedmont from the Charlotte belt and is itself separated from the Inner Piedmont by the Kings Mountain shear zone (Horton, 1981) (Figures 2-15 and 2-16).

The oldest unit in the Kings Mountain belt is a volcanic-intrusive complex. It consists of felsic metavolcanic rocks interlayered with quartz-sericite schist and intruded by metatonalite of Late Proterozoic age (Horton, 1981). This complex grades upward into a sequence that is primarily sedimentary in origin. The complex is composed of quartz-sericite schist with beds of quartzite, quartz pebble metaconglomerate, and manganiferous schist. The western part of the belt consists of a metasedimentary sequence containing units of marble, amphibolite, and calc-silicate rocks (Horton et al., 1981).

The green schist facies metamorphic grade of the Kings Mountain belt is generally lower than that of the adjacent Inner Piedmont and Charlotte belts. However, parts of the Kings Mountain belt are in the Sillimanite zone of the Upper Amphibolite facies (Horton et al., 1981). Major structures within the Kings Mountain belt are gently plunging folds and faults.

Recent evidence of Alleghenian age events within the Kings Mountain belt have been documented (Horton, 1987). A U-Pb Zircon concordant age of 317 Ma was obtained for the High Shoals megacrystic biotite granite in the North Carolina segment. The Ar-40/Ar-39 plateau ages of 318 to 323 MYA were obtained from hornblende from the amphibolite facies metamorphic rocks adjacent to the High Shoals granite (Horton, 1987).

The Charlotte belt (Figures 2-15 and 2-16), which extends from western Georgia to Virginia, is a belt of numerous intrusions and moderate- to high-grade metamorphism. Much of the belt has been metamorphosed to amphibolite grade. The highest grade was attached during the Taconic Orogeny (Butler, 1979), but retrograde metamorphism is widespread. The oldest rocks are amphibolite, biotite gneiss, hornblende gneiss, and schist. All these rocks are thought to be derived from volcanic, volcaniclastic, or sedimentary protoliths.

The rocks of the Charlotte belt were intruded by several premetamorphic and postmetamorphic plutons of diverse compositions. Plutons of the oldest group (530 to 550 MYA) are generally highly deformed and have been genetically related to the volcanic rocks of the Carolina Slate belt (Fullagar, 1971; Gilbert et al., 1982; Weisenfluh and Snoke, 1978).

A younger group of late synkinematic intrusions was emplaced in the Charlotte belt in the period from 430 to 335 MYA. The composition of this group varies from gabbro to leucocratic granite (Butler and Ragland, 1969; Butler and Fullagar, 1978).

A final group of postkinematic granite plutons was emplaced in the Charlotte belt in the period from 325 to 265 MYA (Fullagar, 1971; Secor and Snoke, 1978; Dallmeyer et al., 1986).

The Charlotte belt is also characterized by numerous prekinematic-to-postkinematic, concordant and discordant sheets and dikes of granitoid intrusive rocks (Secor et al., 1982). These appear to be the intrusive equivalent of some of the volcanic rocks of the Carolina Slate belt (Overstreet and Bell, 1965).

The Carolina Slate belt (Figures 2-15 and 2-16), which extends from Virginia to Georgia, is characterized by felsic to mafic matavolcanic rocks and thick sequences of metasedimentary rocks derived from volcanic source terrains. These rocks have been subjected to low- to medium-grade regional metamorphism during the period from 500 to 300 Ma and subsequently intruded by granitic and gabbroic plutons about 300 MYA (Carpenter, 1978).

The oldest stratigraphic unit recognized in the Carolina Slate belt is a sequence of intermediate to felsic ashflow tuff and other associated volcaniclastic rocks. These rocks are identified as the two-mile-thick Persimmon Fork Formation in South Carolina (Secor and Snoke, 1978; Secor and Wagener, 1968), the six-mile-thick Uwharrie Formation in North

Carolina (Conley and Bain, 1965; Seiders, 1978) and the three-mile-thick Lincolnton Metadacite in Georgia (Whitney et al., 1978; Carpenter, 1982). Geochronological studies of the rocks indicate deposition occurred during 530 to 580 MYA (Dallmeyer et al., 1986; Carpenter, 1982; Wright and Seides, 1980). A U-Pb whole rock isochron age for volcaniclastic rocks in the Haile-Brewer area near Kershaw, South Carolina, show an age of 466 ±40 MYA (LeHuray, 1987).

These rocks are overlain by a sequence of mudstones, siltstones, greenstones, greywackes, and sandstone with some interbedded volcanic tuffs and flows. Sedimentary structures suggest turbidite deposition below wave base (Kearns et al., 1981).

In the North Carolina segment of the Carolina Slate belt, this sequence is called the Albemarle Group and is approximately nine miles thick (Conley and Bain, 1965; Stromquist and Sundelius, 1969). The Rb/Sr whole rock ages from these rocks range from 502 to 562 MYA (Fullager, 1971; Hills and Butler, 1969). Paleomagnetic results from the Cid Formation of the Albemarle Group suggest a Late Ordovician pole for these rocks which is in agreement with other Late Ordovician poles from the stable craton of North America (Vick et al., 1987). This is also in agreement with a K-Ar whole rock age of 483 Ma from slate from the Albemarle Group (Kish et al., 1979) and a Ar-40/Ar-39 plateau age of 455 MYA (Late Ordovician) for the Tillery Formation which underlies the Cid Formation (Noel et al., 1988). However, Ediacarian-like fauna of metazoan fossils of supposed Eo-Cambrian age have been found in the Upper Albermarle Group (Gibson et al., 1984). Also, the Slate belt may not have been attached to the stable craton and has rotated since Eo-Cambrian time.

The correlative sequence of rocks in South Carolina is named the Richtex Formation, with a thickness estimated to be greater than two miles (Secor and Wagener, 1968). Sponge spicules found in the Richtex Formation have been identified as Middle Cambrian (Bourland and Rigby, 1982).

Furthermore, in South Carolina, the Richtex Formation is overlain by the Asbill Pond Formation (Secor et al., 1982). The formation consists of an estimated thickness of greater than three miles of metasediments interbedded with mafic to felsic metavolcanic rocks, quartz siltstones, and sandstones displaying sedimentary structures suggestive of deposition on a tidal shelf (Secor and Snoke, 1978).

Middle Cambrian age, Acado-Baltic trilobites (Paradoxides) have been identified from the upper Asbill Pond Formation (Secor et al., 1983). This identification indicates that the South Carolina Slate belt was faunally isolated from Laurentia (North America). This factor has been interpreted to indicate that the Carolina Slate belt comprises an exotic terrain (the Carolina terrain) that was accreted to North America subsequent to the Middle Cambrian (Secor et al., 1983; Secor, 1987).

Structural relationships in the Carolina Slate belt in central South Carolina indicate that the Richtex Formation overlies the Persimmon Fork Formation. However, it is uncertain if the contact is stratigraphic or tectonic (Secor, 1987). In some places it is interlayered with the underlying Persimmon Fork Formation, suggesting that the Asbill Pond Formation is conformable with the Persimmon Fork Formation (Secor, 1987). The Richtex Formation also appears to be in fault contact with the Persimmon Fork and Asbill Pond formations. The Richtex Formation has been suggested to be part of a regional allochthon emplaced before, or during, the initial deformation event (Secor, 1987).

The oldest recognizable deformation phase (D_1) in the Carolina Slate belt was an Early to Middle Paleozoic episode consisting of tight to isoclinal folding under conditions of greenschist facies regional metamorphism. The same event affected the Charlotte belt under conditions of amphibolite facies regional metamorphism. The deformational event postdates Cambrian strata in the Carolina Slate belt and occurred before intrusion of Silurian- to Devonian-age plutons in the Charlotte belt, which do not record the D_1 fabric (Fullagar, 1981). Furthermore, the Charlotte belt has been interpreted as a tectonic infrastructure of the Carolina Slate belt (Secor et al., 1982).

The Precambrian to Cambrian volcanic and sedimentary rocks that constitute the Carolina Slate belt have been interpreted as representing a subduction-related volcanic arc. It is believed that this arc developed an oceanic crust in response to the closing of a small ocean basin in Middle Proterozoic to Middle Cambrian time (Seiders, 1978; Secor et al., 1983; Hatcher and Zietz, 1980). Rogers (1982) suggests that it formed in a continental margin setting, whereas, Glover et al. (1978) suggest that the Carolina Slate belt developed as a volcanically active continental margin on Greenville-age crust.

During the Late Paleozoic period, several large granitic plutons intruded into the Carolina Slate belt in South Carolina. These plutons are undeformed and have associated with them contact metamorphic aureoles which overprint the elements formed by the earlier greenschist facies metamorphism. However, along the Fall Line and adjacent to the Kiokee belt in South Carolina, plutons contain a moderate to strong post-emplacement, locally mylonitic deformation foliation which is a manifestation of the Late Paleozoic Alleghenian orogeny (Secor and Snoke, 1978; Dallmeyer et al., 1986; Secor et al., 1982; Secor, 1987).

The Kiokee belt (Figures 2-15 through 2-17) is located between the Carolina Slate belt and the Atlantic Coastal Plain in central Georgia and South Carolina. The interior of the Kiokee belt is a migmatitic complex of biotite amphibole paragneiss, leucocratic paragneiss, sillimanite schist, amphibolite, ultramafic schist, serpentinite, and feldspathic metaquartzite, and contains granitic intrusion of Late Paleozoic age (Secor, 1987). The high-grade (amphibolite facies) Kiokee belt is interpreted as mid-crustal rocks of an Alleghenian infrastructure exposed in regional antiforms produced by the ramping of underlying thrust faults

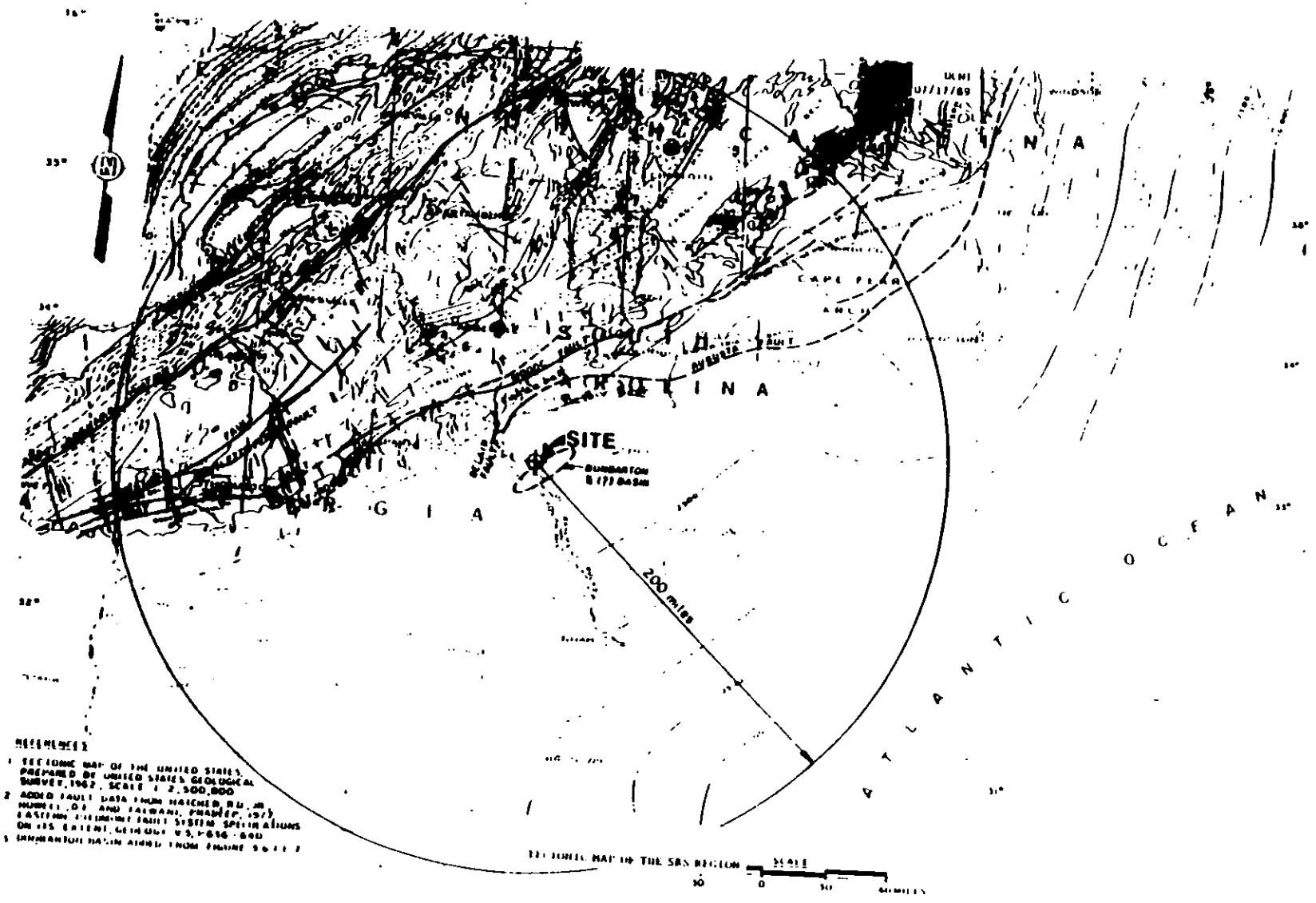

FIGURE 2-17. Tectonic Map of the SRS Region

(Secor et al., 1982; Secor, 1987). Structural evidence suggests that the migmatitic rocks in the interior of the Kiokee belt were located, relative to the Carolina Slate belt, at least six miles north-northeast of their present position prior to the Alleghenian Orogeny (Sacks and Dennis, 1987). The migmatitic rocks may be stratigraphic equivalents to similar units in the Charlotte belt or even a separate terrain, exotic with respect to both North America and the volcanic arc rocks (Secor, 1987).

The northwest boundary of the Kiokee belt is interpreted to be a cryptic fault embedded in the Modoc shear zone (Figure 2-17), which juxtaposes deformed equivalents of the migmatitic complex against the rocks of the Asbill Pond Formation (Sacks and Dennis, 1987). Continuity of rock units from the Carolina Slate belt across the Modoc shear zone into the Kiokee belt has been suggested (Bramlett, 1980; Snoke et al., 1980). The Augusta Fault forms the southeast flank of the Kiokee belt. It exhibits polyphase, ductile, and brittle deformation, and it juxtaposes the migmatitic rocks of the Kiokee belt against the low grade metamorphic rocks of the Belair belt (Maher, 1987).

The Belair belt located near Augusta, Georgia, is a small belt of greenschist-grade metasediment and metavolcanic rocks and is separated from the Kiokee belt by the Augusta Fault zone (Maher, 1987; Prowell and O'Conner, 1978). As determined from geophysical and well data, the Belair belt extends beneath the Atlantic Coastal Plain (Daniels, 1974). The age of the main metamorphism and deformational event is uncertain but appears to be analogous to that in the Carolina Slate belt which is 385 to 580 MYA (Dallmeyer et al., 1986; Secor et al., 1982).

Immediately south of the Fall Line in South Carolina and Georgia, medium- to high-grade metamorphic rocks and granitic plutons are interpreted from gravity, aeromagnetic, and well data. These rocks are interpreted as the subsurface continuation of the Piedmont province beneath the Atlantic Coastal Plain (Popenoe and Zeitz, 1977; Daniels, 1974; Chowns and Williams, 1983).

In addition to the aforementioned lithostratigraphic belts within the Piedmont province, there are several down-faulted basins containing rocks of Triassic-Jurassic age. These fault-bounded basins, which contain Mesozoic sedimentary rocks, are exposed in eastern North America from Nova Scotia to South Carolina (Figures 2-17 and 2-18) (Rogers, 1970). Rocks in these discontinuous basins consist mostly of continental-derived clastic sediments (sandstones, conglomerates, siltstones, shale, and coal). Igneous rocks of basaltic composition occur as flows, sills, and stocks within the basins and as extensive dike swarms within and outside the basins (King, 1971). The basins are usually elongated NE-SW and are bordered on at least one side by a normal fault, suggesting crustal extension and the formation of grabens and/or half grabens. The basins were produced as a result of incipient rifting in the Early Mesozoic that preceded the eventual Jurassic opening of the Atlantic Ocean (Ratcliffe, 1971). Several of these basins have been interpreted as being localized along reactivated Paleozoic ductile or brittle fault zones (Ratcliffe, 1971; Lindholm, 1978; Glover et al., 1983; Peterson et al., 1984).

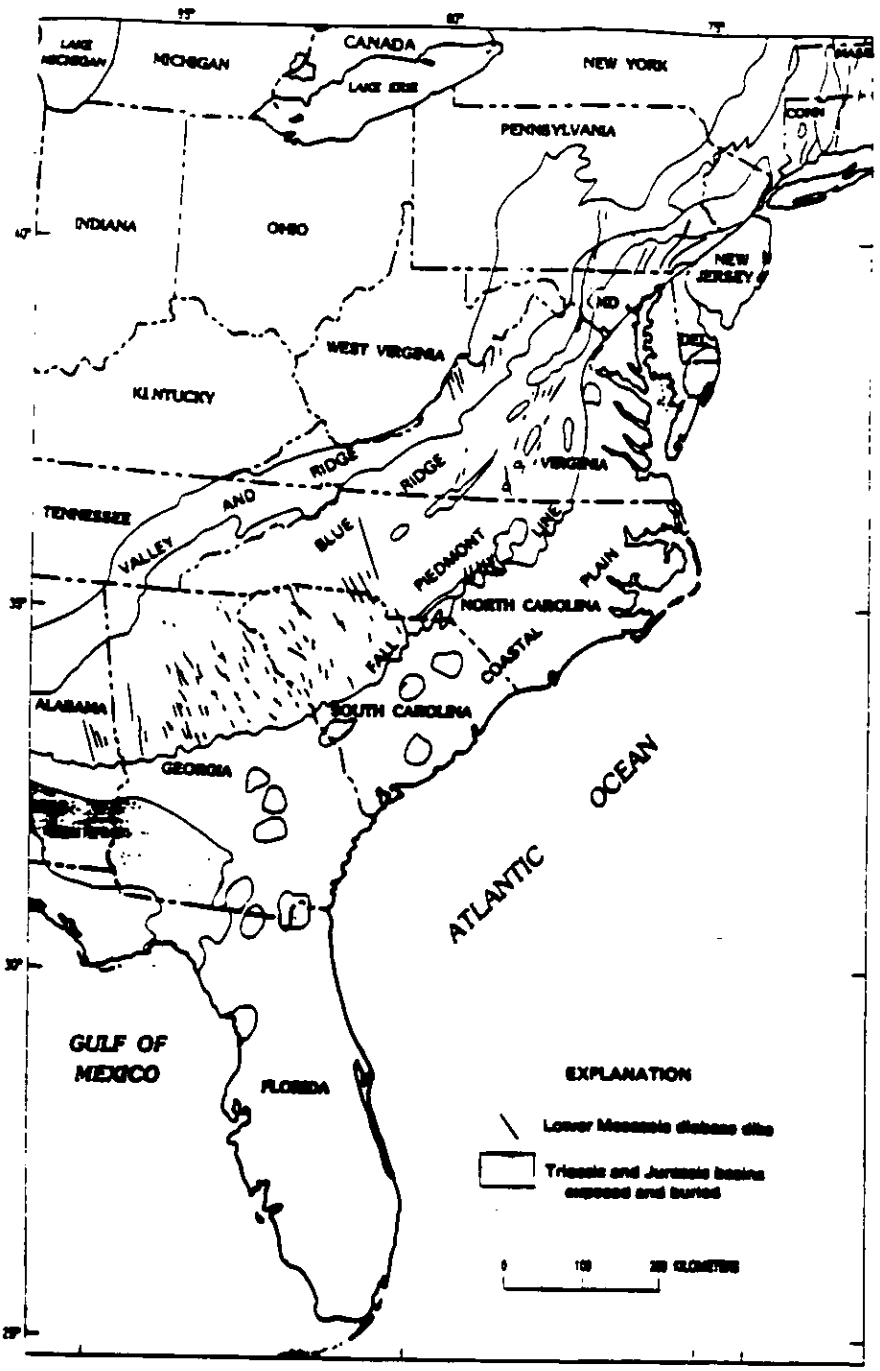

FIGURE 2-18. Geologic Map of the Eastern United States (King, 1971; Marine and Siple, 1974; Dooley and Wampler, 1983)

In addition to the Triassic-Jurassic basins exposed in the Piedmont province, several more basins have been identified beneath the Atlantic Coastal Plain and offshore regions. This new information is based on the interpretation of geophysical and well data. These basins appear to be more widespread and more extensive than the exposed basins (Rogers, 1970; Manspeizer et al., 1978; Klitgord and Behrendt, 1979; Steel and Colquhoun, 1985).

Recent geophysical and geological studies to determine the cause of the 1886 earthquake, in the Charleston, South Carolina, area have revealed further information on the buried Triassic basins in the area (Rankin, 1977; Gohn, 1983). Three basement test wells drilled near Charleston encountered Jurassic-age basalts and redbed sediments. Refraction studies revealed that lateral velocities vary beneath the Atlantic Coastal Plain and are interpreted to be indicative of structure within the basement (Ackerman, 1983).

Seismic reflection studies throughout the Coastal Plain region have revealed that the basement contains numerous fault-bounded basins (Peterson et al., 1984; Behrendt, 1985; McBride et al., 1988). These studies recognized a strong horizontal reflector at the base of the Coastal Plain sediments. This reflector, which has been correlated with basalt flows encountered in the Clubhouse Crossroad wells near Charleston, South Carolina, is interpreted as representing an extensive and widespread basalt flow extending throughout southern Georgia and South Carolina and the offshore regions.

This horizon was initially interpreted as basement, based on several refraction surveys throughout the region (Bonini and Woolard, 1960). However, recent refraction studies suggest that the basement is much deeper than was previously recognized (Smith and Talwani, 1987; and Smith et al., 1988). They suggest that the basalt is intercalated with Mesozoic sediments and represents episodic basalt flows or intrusions as sills associated with the Mesozoic extension of the crust. These studies, in conjunction with other geophysical and geological data, also suggest that the basement beneath the middle and lower Coastal Plain sediments represents a complex system of basins and subbasins. These basins formed during the Mesozoic extensional event and utilized older zones or structural weaknesses produced by the Alleghenian (or older) orogenic event.

Interpretation of the regional COCORP seismic reflection data in Georgia reveals that the Mesozoic Riddleville Basin is a half graben with a major south-dipping normal fault on the northern boundary which goes into the Augusta fault to the south (Peterson et al., 1984).

The South Georgia Rift Basins comprises a vast area beneath the Coastal Plain in Georgia. Based on the interpretation of drill hole, seismic reflection, and other geophysical data, the rift consists of a complex system of interconnecting basins with variable depths to basement and thickness of Mesozoic sediments (Chowns and Williams, 1983; McBride et al., 1988; Daniels et al., 1983; and Hatcher, 1972).

2.1.1.3 Geochronology

This section describes the geochronology events at the SRS.

2.1.1.3.1 Metamorphic Events

Hatcher has summarized much of the recent work to establish an absolute chronology of metamorphic events in the southern Appalachians (Nelson et al., 1985). Prior to thermal events (periods of elevated temperature) associated with the Appalachian orogeny, there was a Middle Precambrian event 1300 or 1050 million years ago (Davis et al., 1962 and Dietrich et al., 1969). Corbin Gneiss in the Blue Ridge in Georgia and the Woodland Gneiss and intrusive charnokitic rocks from the Pine Mountain belt in the Georgia Piedmont have yielded U-Pb ages greater than one million years (Odom et al., 1973).

The thermal peak of the last regional metamorphic event in the Piedmont occurred 380 to 420 million years ago (Fullagar, 1971). Movement on the Brevard, Towaliga, and Goat Rock faults occurred after this thermal peak (Figure 2-17). A Rb-Sr, whole-rock age of 360 million years was measured for mylonite in the Brevard Zone near Rosman, North Carolina (Odom and Fullagar, 1970). This may be the age of the fault's earliest movement (Nelson et al., 1985). Ages of about 300 million years have been reported for the three faults (Wampler et al., 1970).

Several investigators support a metamorphic event 250 million years ago, based principally on K-Ar mica ages. However, Rb-Sr data do not support an event more recent than 300 million years ago (Fullagar, 1971). Furthermore, measurements of Ar-40/Ar-39 incremental-release ages for 12 biotites and eight hornblendes across the 250-million-year-old mica belt in the Georgia Inner Piedmont from the Brevard Zone to the Towaliga Fault showed that the age spectra were undisturbed (Hatcher, 1971). This finding is inconsistent with a regional metamorphic event 250 million years ago. Biotite total-gas ages ranged from 236 to 317 million years, while hornblende ages ranged from 300 to 355 million years. The older ages were from the northwest part of the mica age belt, and they decreased to the southeast. At each locality where both hornblende and biotite were collected and dated, the hornblende age exceeded the biotite age by 25 million years. Thus, the total-gas ages were interpreted as times of postmetamorphic cooling. The Ar-40/Ar-39 age spectra of biotite and muscovite from the postmetamorphic Stone Mountain granite also were found to be undisturbed. The total-gas age of biotite is 281 million years, and that of muscovite is 283 million years. These ages are younger than those of the biotite and hornblende of the adjacent Inner Piedmont Gneisses. This information suggests that cooling of the country rock (pre-existing mother rock) below the argon retention temperatures preceded emplacement of the Stone Mountain pluton 291 million years ago.

Comparison of Ar-40/Ar-39 data with estimates of metamorphic conditions suggests that 15 miles of uplift occurred between regional metamorphism 365 million years ago and establishment of the Early Mesozoic erosion surface, which is close to the present erosional surface. The 15 miles of uplift corresponds to an average uplift of 0.006 inch per year (Hatcher, 1971).

2.1.1.3.2 Igneous Activity

The oldest known igneous rocks in the southern Appalachians are plutonic bodies about 1100-million years old (Nelson et al., 1985). Volcanism and plutonism occurred during the late Precambrian and Early Paleozoic in both the Blue Ridge and Piedmont (Dallmeyer, 1977; Rankin et al., 1969). Rb-Sr whole-rock dates of 525 to 656 million years have been reported for rhyolites in the Carolina Slate belt of North Carolina (Hills and Butler, 1969). Late Precambrian intrusives have been found in the Virginia Piedmont (Fullager, 1971; Glover et al., 1971). Intrusion may have occurred before, during, and after the Paleozoic regional metamorphism (Butler and Ragland, 1969). Rb-Sr, whole-rock ages of 14 Piedmont plutons fell into three groups---592 to 520, 415 to 385, and approximately 300 million years (Fullagar, 1971). These age groups correspond roughly to the above pre-, syn-, and post-metamorphic categories (Butler and Ragland, 1969).

Mafic dikes intruding into the sediments of Triassic basins were once thought to be Triassic in age, based on their association. But paleomagnetic data indicate that the dikes intruded during the Jurassic Period (De Boer, 1967).

The $^{207}Pb/^{206}Pb$ ages of detrital zircons in some undeformed, unmetamorphosed Lower Paleozoic sediments beneath the Coastal Plain in Florida were measured. The age of a split of zircon sample was 685 million years. Dark, well-rounded zircons handpicked from the sample were found to be older than 1850 million years. The older zircons may have been derived from the west African or Guinean shield. This would suggest that Florida was originally a part of another continent (Odom and Brown, 1976).

2.1.1.4 Regional Geologic History

The eastern North American Continental margin has developed to its present state over geologic time through a series of continental collision and rifting events. The collision events generally correlate with an older concept of mountain building because they may give rise to folded mountain ranges such as the Alps or the Appalachians.

The rifting events produce fault-bounded basins in which sediments accumulate. Thinning of the upper mantle (mantle lid) allows increased heat flow from deeper within the earth, and consequent thermal expansion of the continental crust produces local uplift due to isostatic adjustment. Subsequently, erosion may result in thinning of the continental

crust. Sediments deposited in the basins may be preserved. With time a more normal geothermal gradient will be re-established, and a new mantle lid will form. Isostatic readjustment results in subsidence over a period of 100 million years or more.

During the period of passive cooling-induced subsidence, coastal sediments may accumulate to great thickness depending on their availability.

Figure 2-19 shows the subsidence of several passive continental margins with time. The Atlantic continental margin has been a site of coastal sediment accumulation since middle Jurassic time, about 175 million years ago.

Collision events occur when continental masses collide. For continents to approach one another, oceanic crust is destroyed, and continental margin sediments are either compressed and folded, or may be carried downward beneath the edge of a continental mass. The collision finally results in thickening of the continental crust which produces isostatically supported mountain chains. The Appalachians, Alps, and Himalayas are examples of such folded mountain chains.

Isostatic support (or thick crust) is evidenced by negative Bouguer gravity anomalies. Because collisions are accompanied by metamorphism and production of igneous intrusive rocks, they are easily dated.

The oldest dated rocks that are routinely encountered in the southern Appalachian area are approximately 1,100 million years old. These are attributed to the Grenville Orogeny. Perhaps 800 million years ago, a rifting event occurred and rocks now known as the Ocoee Supergroup were deposited in the rift basins. Figure 2-20 is a proposed reconstruction of the paleogeography at the time of Ocoee deposition.

Six hundred million years ago continental margin sediments were accumulating and are recognized today as the Chilhowie Group, named for exposures of Chilhowie Mountain in eastern Tennessee. Figure 2-21 shows a plausible reconstruction of the paleogeography at this time.

Sediments of Early Cambrian age, 600 to 550 million years before present (mybp), indicate a western sediment source. By Early Ordovician time approximately 475 mybp, the source of sediments now preserved in east Tennessee was clearly from the east.

Much of the material now in the Piedmont (Inner Piedmont, Charlotte belt, Slate belt) may have been part of a micro-continent called the Avalon platform (Figure 2-22). Rocks in this area participated in a collisional event about 600 million years ago which is similar in time to ages recorded from igneous rocks in Africa (so-called pan-African dates). At the time of the 600 mybp event, the Avalonian or Carolina terrain was probably not connected to the North American continent.

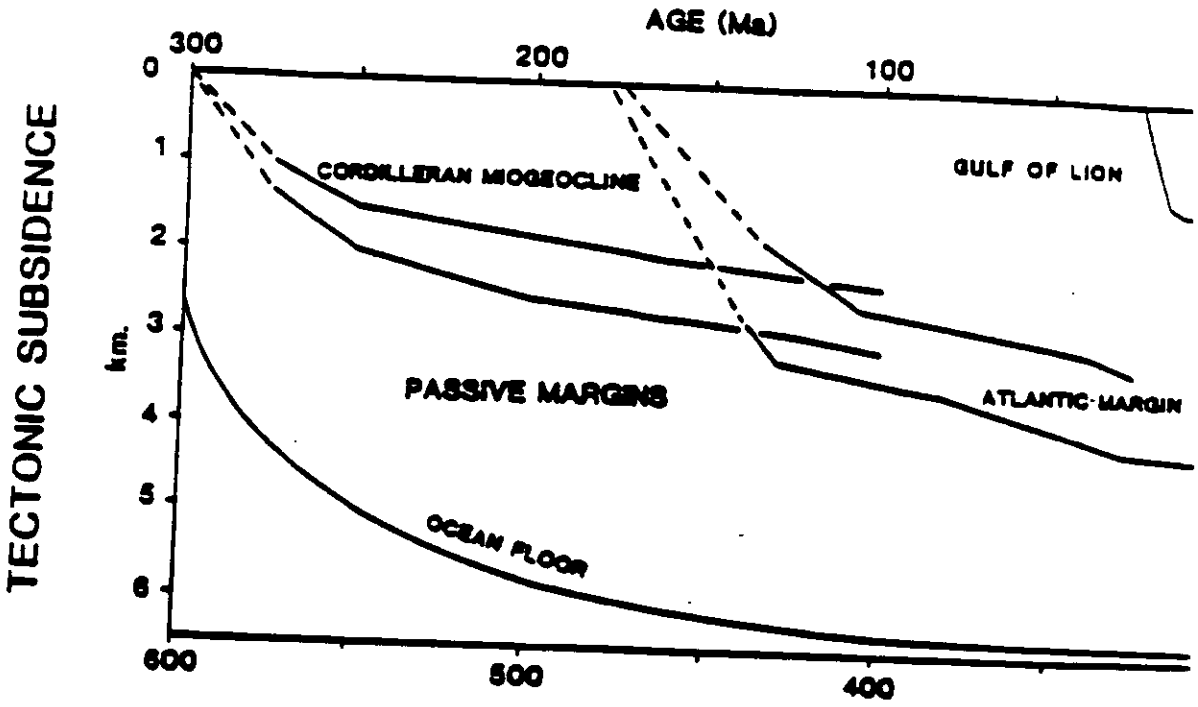

FIGURE 2-19. Tectonic Subsidence

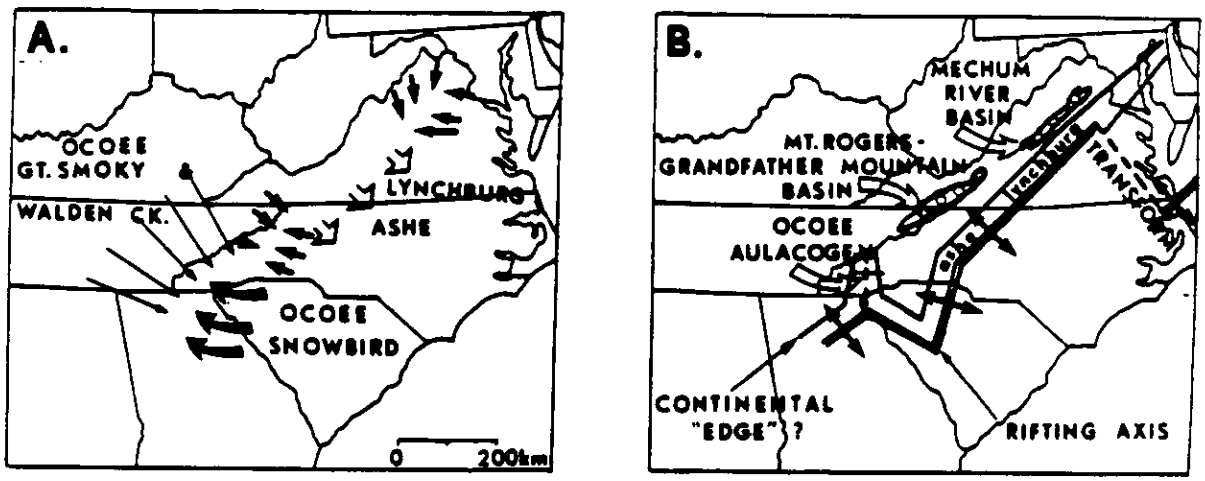

Late Precambrian dispersal and paleogeography. (3-A) Dispersal patterns for late Precambrian stratified assemblages: long straight arrows, Great Smoky and Walden Creek Groups of the Ocoee Series or Supergroup (directional structures and facies); long curved arrows, Snowbird Group of the Ocoee Series or Supergroup (directional structures and facies); open arrows, Ashe and Lynchburg Formations (facies); short solid arrows, "centripetal" interior drainage of Mechum River and Grandfather Mountain-Mount Rogers basins (cross-bedding; lithofacies). (3-B) Speculative paleogeographic reconstruction showing late Precambrian stratified assemblages accumulating within (open circles) interior rift basins (Grandfather Mountain-Mount Rogers-Mechum River Formations), within an Ocoee "aulacogen", and along a zig-zagging continental edge offset by transform faulting (Ashe and Lynchburg Formations).

FIGURE 2-20. Late Precambrian Dispersal and Paleogeography
(Schwab, 1986)

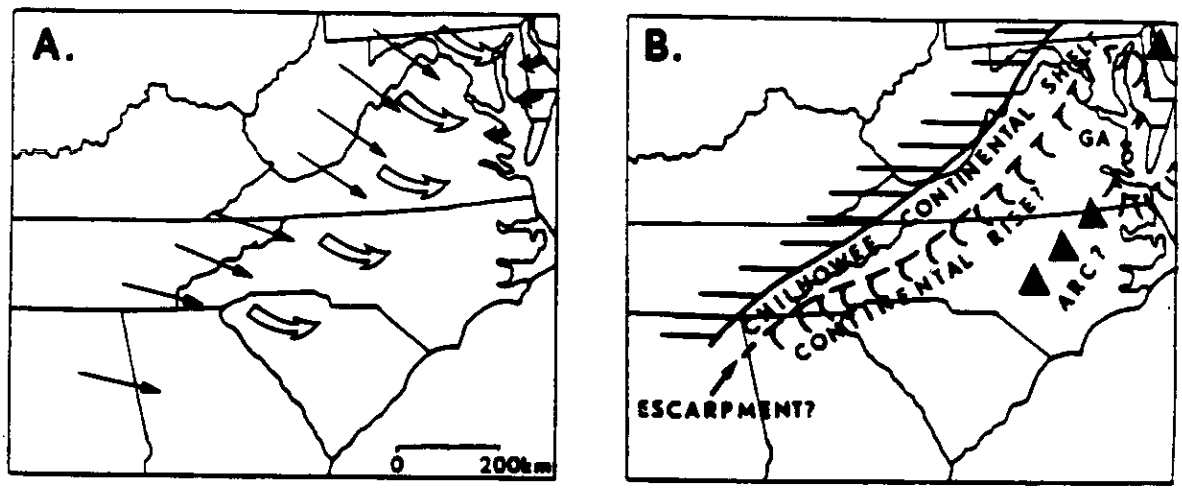

Fig. 5. Early Cambrian dispersal and paleogeography. (5-A) Dispersal patterns for the Early Cambrian stratified sequences: long straight arrows, Chilhowee Group (based on cross-bedding azimuths with longshore component not shown); open curved arrows, Alligator Back Formation, basal portion of Evington Group, and Frederick, Maryland carbonates (based on lithofacies and very limited directional structures); short, solid, curved arrows, Glenarm Series or Supergroup (based on lithofacies). (5-B) Very speculative paleogeographic reconstruction showing an Early Paleozoic passive, Atlantic-type continental margin with sediments accumulating across a shallow water continental shelf (Chilhowee Group with overlying Cambro-Ordovician carbonate bank) and as an adjacent, deeper water continental rise wedge (Alligator Back Formation and Evington Group). The Glenarm Series or Supergroup basin (GA) is shown as an embayment into the continental margin, much like the present-day Sea of Okhotsk west of the Kamchatka Peninsula in the Western Pacific. Solid triangles represent an incipient island arc (James Run Formation, Chopawamsic Formation, and Hatcher Complex) analogous to the Kuril Islands.

FIGURE 2-21. Early Cambrian Dispersal and Paleogeography
(Schwab, 1986)

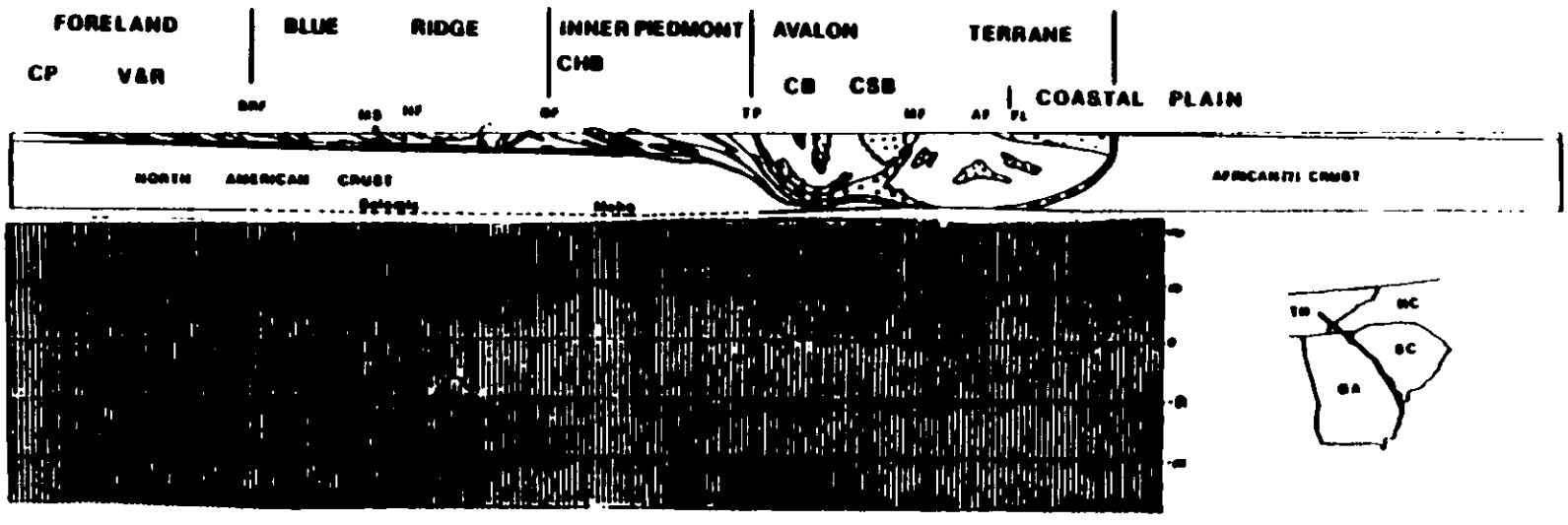

FIGURE 2-22. Appalachian Cross Section (Hatcher, 1986)

By Middle Ordovician time (475 mybp), a collisional event called the Taconic orogeny was well under way. Figure 2-23 illustrates a probable Appalachian cross-section from Tennessee across South Carolina at this time (Hatcher, 1972). North American continental and Atlantic (proto-Atlantic or Iapetan) oceanic crusts were converging, and the oceanic crust was being subducted beneath the continental margin. Thickening and heating of sediments at the locus of subduction resulted in uplift of a tectonic land called Appalachia. This uplifted land provided an eastern sediment source for the sea still existing along the continental margin.

The convergence of North American and African masses continued until the African plate overrode the edge of the North American plate. Granites dated at about 275 to 300 mybp may record melting of the lower edge of the North American crustal plate.

The overriding of one continental mass by another produces a thickened crust which, by isostatic adjustment, produces a mountain range. The Alps provide an example of one such range which has been studied in considerable detail. Figure 2-24 shows a schematic section across the Alps showing the Bouguer gravity anomaly and associated geological model.

Figure 2-22 compares the Alpine model to a generalized tectonic section across the Appalachians (Hatcher et al., 1986). The Appalachian gravity profile is subdued relative to that of the Alps, but the latter range is much younger and has not had sufficient time to erode.

The youngest sediments deposited in the Appalachian Basin are Carboniferous and Permian in age. By mid-Permian time, some 250 million years ago, isostatic uplift of the Appalachian Mountain chain eliminated the sea in which sediments had been accumulating.

Early in the Mesozoic Era, some 240 million years ago, the supercontinent called Pangea, which resulted from Paleozoic collisions, began to break up. The present Atlantic Ocean was created by rifting which began in the north and progressed to the south.

In eastern North America, rift basins accumulated sediments in Late Triassic time. Figure 2-25 shows the occurrence of these basins. Across Virginia and into North Carolina there seem to be western and eastern belts of basins. The western belt ends in Davie County, North Carolina. The eastern belt extends into South Carolina and is in approximate alignment with the buried Dunbarton Basin beneath the SRS.

Two types of models have been proposed for the origin of rift basins. The pure shear model is perhaps the best known. This model would produce two parallel belts of basins which, if rifting continue, would eventually become separated by a belt of new oceanic crust. The steps in this process are illustrated in Figure 2-26.

A simple shear model suggests that a low angle shear zone may traverse the entire crust and mantle lithosphere. Figure 2-27 illustrates this concept. Figure 2-28 shows the application of the simple shear model to western North American tectonics.

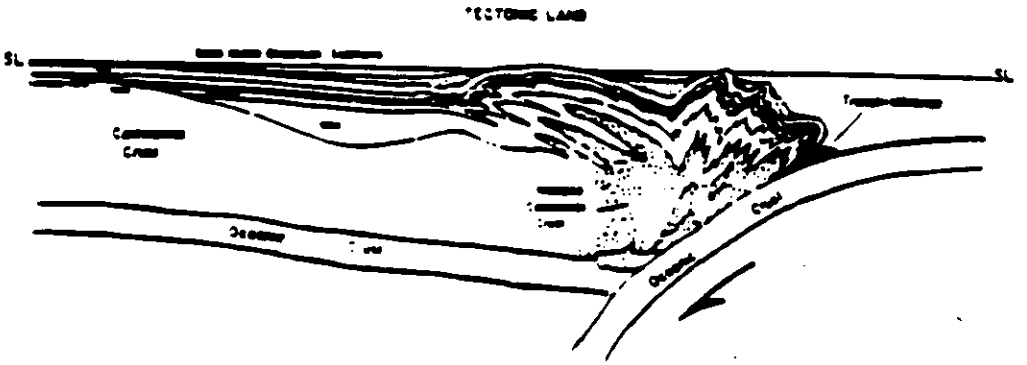

E. EARLY - MIDDLE ORDOVICIAN

FIGURE 2-23. Early-Middle Ordovician

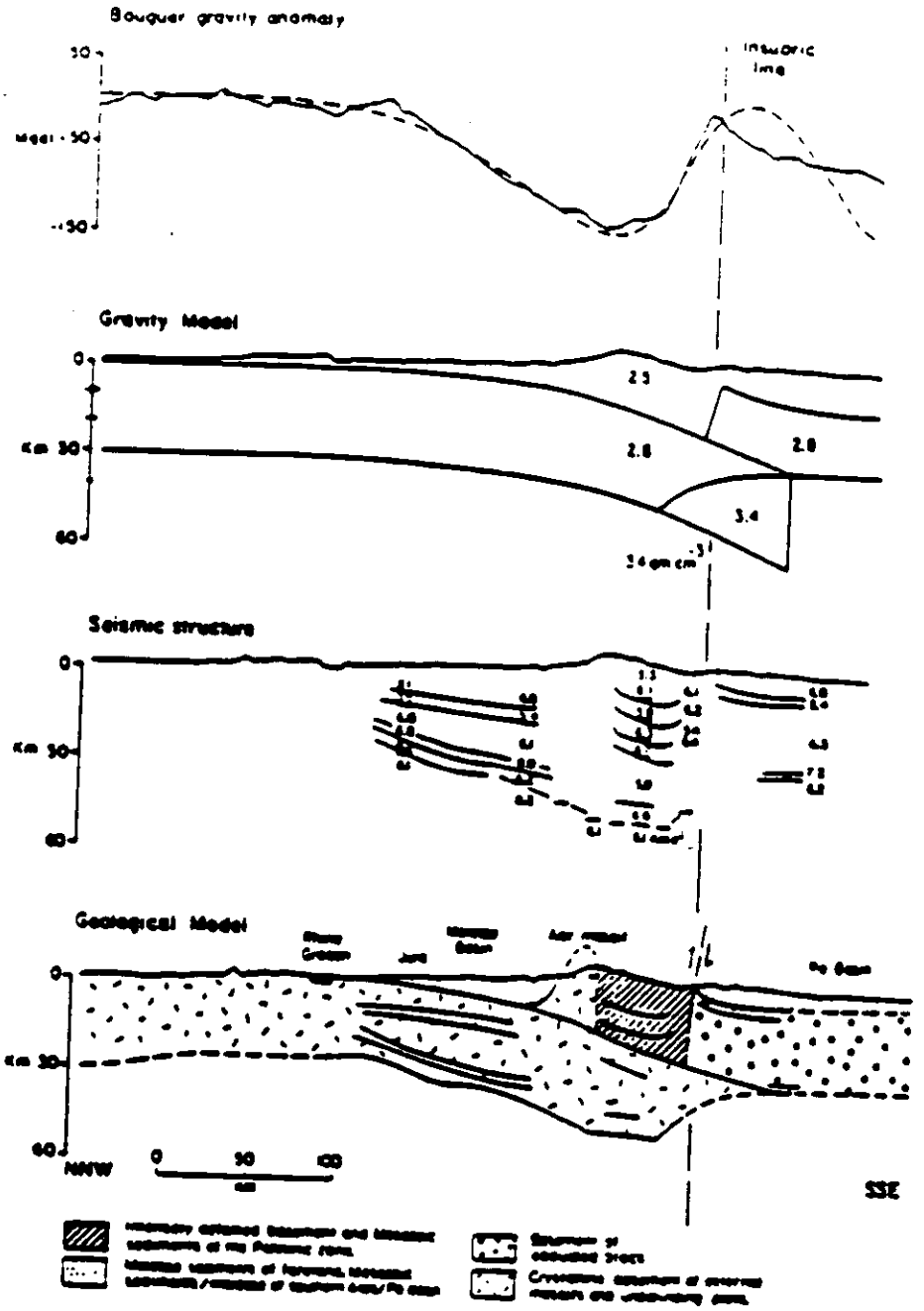

FIGURE 2-24. Bouguer Gravity Anomaly, Gravity Model, Seismic Structure, and Geological Model Along the Swiss Geotraverse (Karner and Watts, 1983)

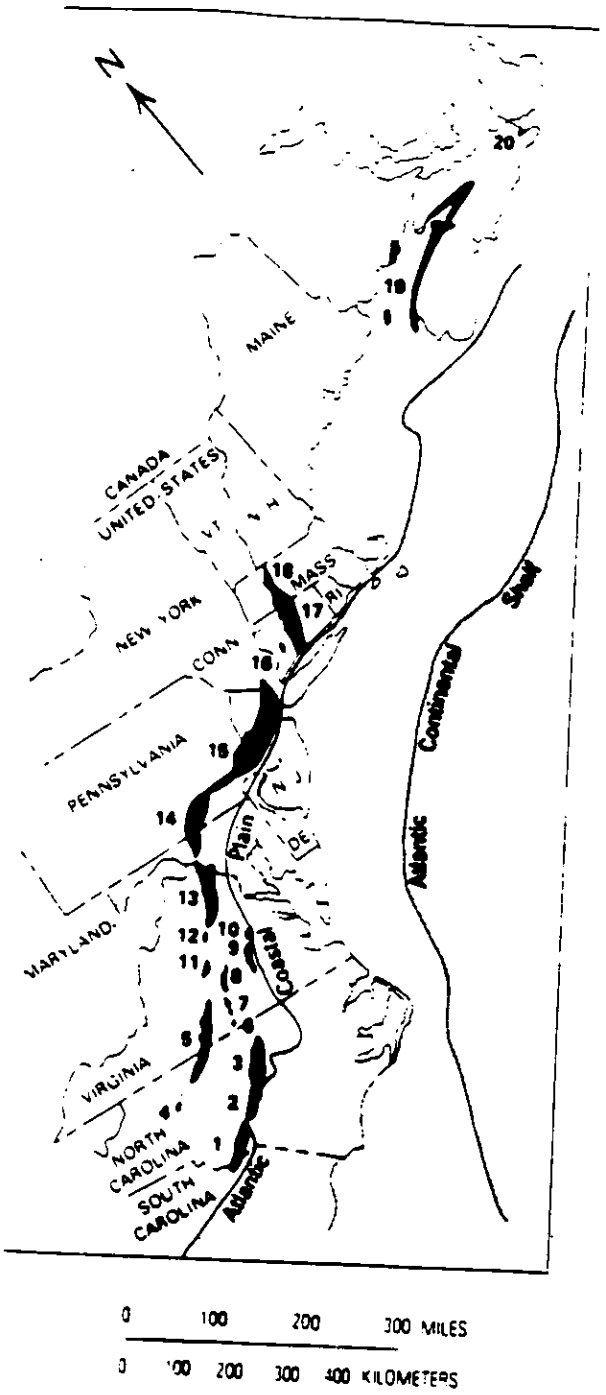

EXPLANATION

1. Wadesboro (N.C.-S.C.)
2. Sanford (N.C.)
3. Durham (N.C.)
4. Davie County (N.C.)
5. Dan River and Danville (N.C.-Va.)
6. Scottsburg (Va.)
7. Basins north of Scottsburg (Va.)
8. Farmville (Va.)
9. Richmond (Va.)
10. Taylorsville (Va.)
11. Scottsville (Va.)
12. Barboursville (Va.)
13. Culpeper (Va.-Md.)
14. Gettysburg (Md.-Pa.)
15. Newark (N.J.-Pa.-N.Y.)
16. Pomperaug (Conn.)
17. Hartford (Conn.-Mass.)
18. Deerfield (Mass.)
19. Fundy or Minas (Nova Scotia, Canada)
20. Chedabucto (Nova Scotia, Canada)

FIGURE 2-25. Exposed Basins of Newark Supergroup in Eastern North America (Froelich and Olsen, 1984)

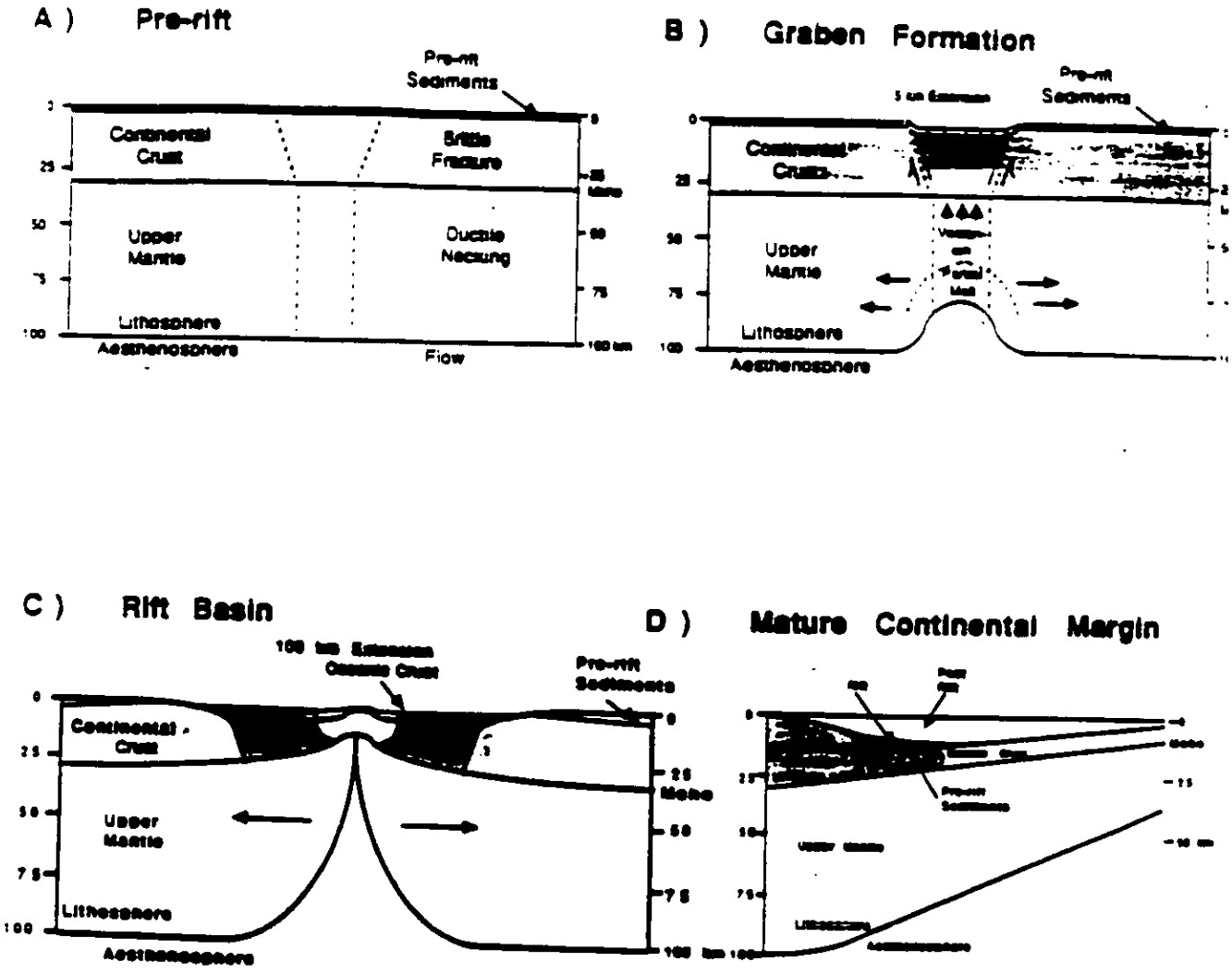

FIGURE 2-26. Pre-Rift and Graben Formation

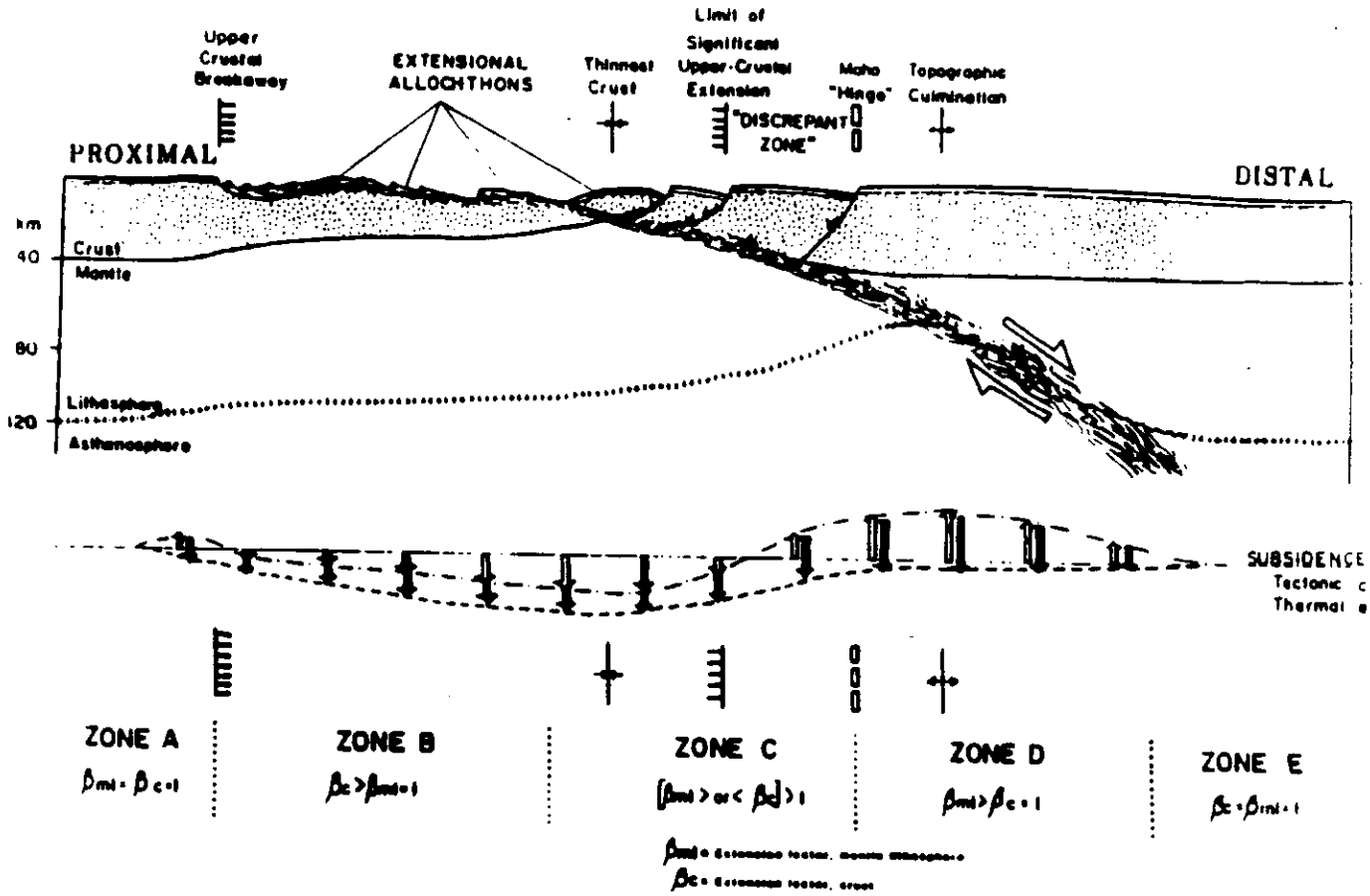

FIGURE 2-27. Simple Shear Model for Rifting Hypothetical Simple Shear of the Entire Lithosphere

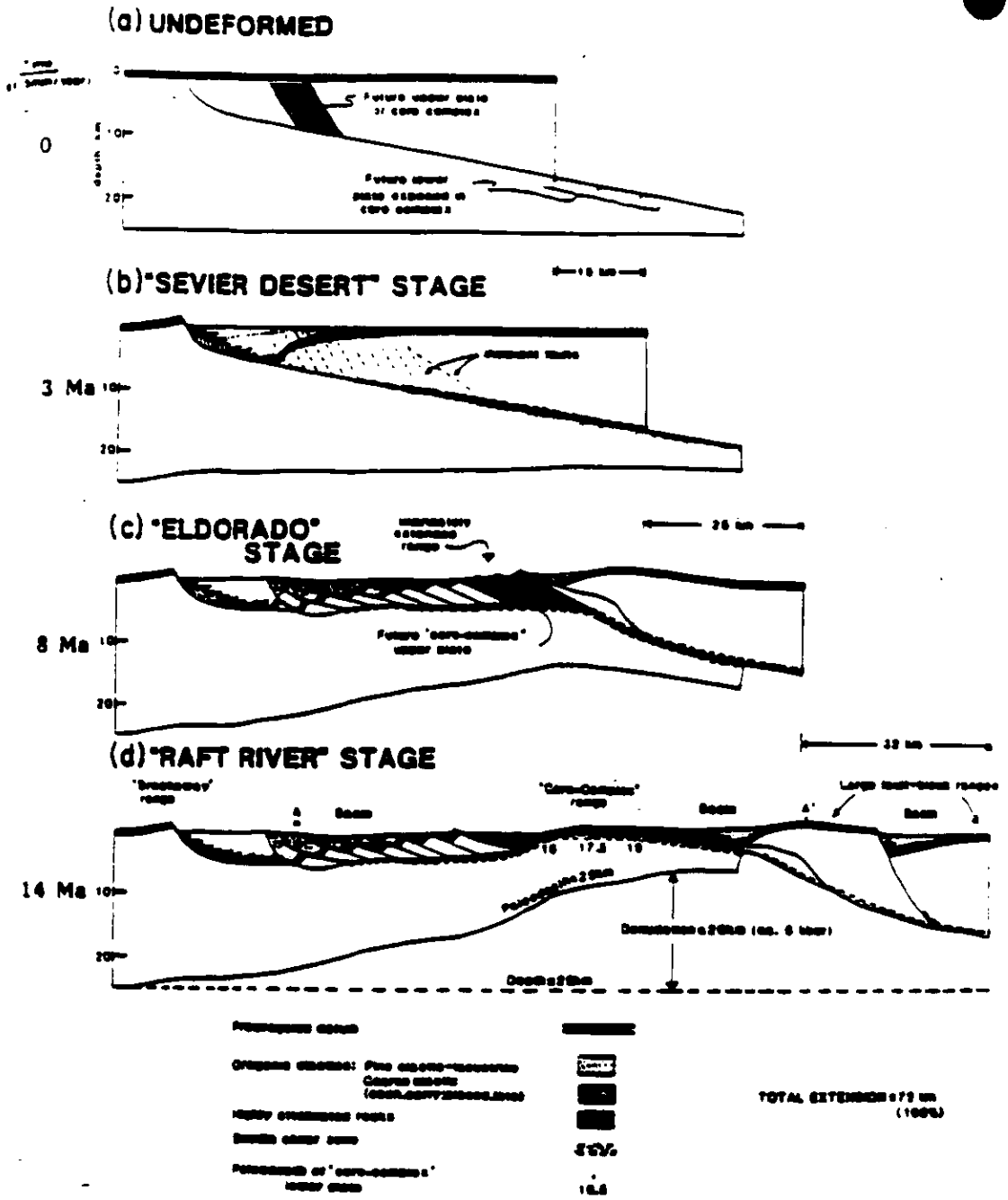

FIGURE 2-28. Developmental Model of Extensional Shear System in the Upper and Middle Continental Crust

A COCORP seismic profile was prepared across the Piedmont and Coastal Plain of Georgia, with the transect line passing about 50 miles west of the SRS (Peterson et al., 1984). The authors data suggest that the Riddleville Basin was formed on tensionally reactivated Appalachian thrust faults. An alternative interpretation is that the seismic features believed to be old thrust faults may be tensional shear faults as suggested in the simple shear model.

2.1.1.4.1 Present Tectonic Setting

Since Triassic/Jurassic time, the Atlantic Coast of North America has been a passive continental margin with little activity other than subsidence and sediment accumulation. Some differential subsidence or uplift has occurred giving rise to broad features, such as the Cape Fear arch or the South Georgia embayment (Figure 2-28).

Even though the region has been tectonically passive, evidence is occasionally encountered for small-scale faulting through Middle Eocene time. One such example is the Graingers, North Carolina wrench zone (Brown et al., 1982).

Normal faulting is associated with a small graben in the Barnwell Group (Eocene) near Langley, South Carolina (Inden and Zupan, 1975). The faults bounding this graben are oriented north 30° west, with a dip of 68° to the east, and north 40° west, dipping 75° to the west. Displacement is about 4 feet, as measured at a faulted section of interbedded kaolin and sand within the Barnwell Group. Numerous smaller faults within the graben have approximately the same orientations. Fractures in associated massive kaolin have strikes ranging between north 25° west and north 35° west, and dips between 68° east and 75° east. The graben in the Barnwell Group is minor and is located approximately 17 miles northwest of the DWPF site (studies in this section were conducted for the Defense Waste Processing Facility and are applicable to other facilities at the SRS). This graben has no adverse effect on site safety or seismic risk.

Folding and faulting near Cheraw, South Carolina, over 94 miles away, involve Paleozoic Carolina Slate belt argillites and sediments of the Middendorf Formation (Late Cretaceous) (Howell and Zupan, 1974). A large anticline at one location involves both Slate belt rocks and Middendorf sediments. Its wavelength is about 100 feet and its plunge is 9° in a north, 77° east direction. The axial plane dips 70° north. One hundred feet south of this anticline are smaller folds, with wavelengths of 6 feet and with axial plane orientations of north 80° east, dips of 80° north, and plunges of 10° in a north 80° east direction. Middendorf sediments unconformably truncate the folds; however, clastic dikes present in the sediments contain argillitic material similar to the Paleozoic Carolina Slate belt argillite. The orientations of the clastic dikes are approximately the same as those of the fold axial planes. This evidence suggests that the origin of the folding is tectonic activity that begun before erosion of the argillite and continued during or after deposition of the Middendorf sediments (Howell and Zupan, 1974).

A reverse fault, about two miles from the exposed folds near Cheraw, shows Paleozoic Carolina slate belt argillite in juxtaposition with Middendorf sediments (Late Cretaceous). The fault plane strikes north 82° west and dips 42° north. Sediments in the football block have been overturned, and a 0.25- to 0.5-inch-gouge zone is developed. Vertical offset is estimated at four feet, although it is probably oblique, and no estimate of actual offset was possible at the time of the investigation (Howell and Zupan, 1974). Both the fold described in the previous paragraph and this reverse fault are located approximately 140 miles to the northeast and, consequently, have no impact on either site safety or seismic risk.

2.1.1.4.2 Subsurface Faulting in the Coastal Plain

Higgins et al. (1978) postulated faulting in the subsurface Coastal Plain sediments in the vicinity of Charleston, South Carolina, on the basis of structure-contour mapping of the Eocene-Oligocene unconformity, which lies between about 100 and 200 feet beneath the surface. Near Clubhouse Crossroads, about 15 miles west-northwest of Charleston, relief of over 130 feet occurs on the unconformity between wells spaced as closely as one mile apart. A fault was intersected by a deep test hole, as indicated by a dip-slip slickensides and a compressed stratigraphic section. According to Higgins et al. (1978) the structure is either a northwest-trending, northeast-dipping normal fault with 130 feet of throw, or a 0.5-mile-wide graben trending northwest. Another probable fault, which occurs about eight miles west of Charleston, exhibits about 40 feet of relief on the unconformity. Whether the faults offset sediments older or younger than Eocene and Oligocene is not known ; therefore, it is not reasonable to argue a genetic relationship between these shallow faults and modern earthquakes that occur at depths greater than about 1.2 miles. These faults are all located more than 70 miles from the production reactor sites and do not affect site safety or seismic risk.

Studies of isopach and structure-contour maps of Oligocene rocks in the Georgia Coastal Plain led Cramer and Arden (1978) to postulate the following faults:

- A prominent normal fault, east side downthrown several tens of feet, trending southeastward from the Macon area, near the Fall Line in central Georgia, through Coffee County into and probably through Charleston County

- Less prominent faults parallel to the one cited above, in the northern part of the Georgia Coastal Plain, forming horsts and grabens

- A pronounced graben, up to 10 miles wide, trending northeastward from Decatur and Grady counties, in southwesternmost Georgia through northern Coffee County to probably the Savannah River and beyond, and with several hundred feet of throw; it transects the faults cited above; Oligocene and Miocene rocks in the graben are thicker than elsewhere; it is postulated to cross beneath the Savannah River approximately 50 miles southwest of the production reactor sites

- Faults parallel to the graben, some with southeast side downthrown, with Oligocene rocks thin or absent on the upthrown sides of some; one is postulated to exist approximately 32 miles southeast of the production reactor sites

- Smaller faults with a north-south orientation

Some of these faults, if verified, would suggest tectonic movement during the early Tertiary. There is no evidence at present, however, that rocks younger than Miocene have been affected and as a result, these faults do not affect site safety or seismic risk.

2.1.1.5 Buried Triassic-Jurassic Basin, Charleston, South Carolina

An extensive program of geological and geophysical investigations is being conducted in the Charleston area to determine the cause of the Charleston earthquake of 1886. Aeromagnetic surveys indicate the presence of a sharp magnetic anomaly approximately nine miles west of Middleton Place, the epicentral area of the 1886 earthquake (Figure 2-15). A drilling program to investigate this anomaly revealed a Triassic-Jurassic basin in the crystalline rocks beneath the Coastal Plain sediments. Mafic plutons associated with the Triassic-Jurassic basin are assumed to cause the magnetic anomaly. The upper part of the basin consists primarily of an 840-foot-thick unit of basalt, with some thin interbeds of sedimentary rock which overlie at least 400 feet of red sandstone and shale (Rankin, 1977). Several potassium-argon determinations of the age of the altered basalt show scatter but support a Triassic or Jurassic age (Pojecta et al., 1976). The sedimentary rocks are similar to sedimentary rock found in other Triassic age basins in the southeast. No fossils have been found in these rocks. The presence of diabase was reported at a depth of 2,400 feet in a well near Summerville (Cooke, 1936).

Since recent seismic activity in the Charleston area has originated largely or entirely in the basement beneath the Coastal Plain sediments (Rankin, 1977), the cause of the Charleston earthquake of 1886 may be related to the Triassic-Jurassic basin beneath these sediments. It is significant, as discussed in Section 2.2.6.3, that the tops of the mafic plutons associated with the basin are at a depth of 1.5 to 2.2 miles and extend to depths of 2.8 miles. Since the top of the basement surface is 0.4 to 0.9 mile beneath the surface, the mafic plutons are also within the crystalline rock framework (Phillips, 1977).

2.1.1.5.1 Other Basement Structures Beneath the Atlantic Coastal Plain

In general, the basement surface beneath the Coastal Plain dips gently seaward. In addition to the Triassic-Jurassic basins found within the basement, several other structures are present which are transverse to the normal structural pattern. The most prominent of these transversely-oriented structures are the Cape Fear Arch, near the North Carolina-South

Carolina border, and the Peninsular Arch (Ocala Arch) of Florida (Figures 2-17 and 2-18). The Cape Fear Arch may have a history as a sedimentary divide, because glauconite-rich clastic sediments are characteristic north of the arch, and carbonate rocks become more important to the south. In addition, lower Cretaceous rocks are common in the Coastal Plain north of the arch, but none of these have been identified to the south (Rankin, 1977).

Deformation of the Coastal Plain may have continued into the Pleistocene due to uplift on the Pennisular and Cape Fear arches (Winker and Howard, 1977).

As indicated earlier, aeromagnetic data suggest that the Coastal Plain sediments are not wholly underlain by Piedmont-type metamorphic rocks (Butler, 1979; Daniels, 1974). A Piedmont-type magnetic signature exists from the Fall Line approximately to the Orangeburg Scarp, suggesting that Piedmont rocks extend that far. Southeast of the Orangeburg Scarp, however, the magnetic pattern is quite different (Figure 2-11). The basement here may be made up of undeformed tuffaceous clastic rocks, basalt and rhyolite flows, and ash-fall deposits (Popenoe and Zeitz, 1977). Wells that penetrated the basement encountered these rock types (Popenoe and Zeitz, 1977; Milton and Grasty, 1969; Milton and Hurst, 1965).

Mafic or ultramafic intrusives have been suggested as the cause of high-amplitude, steep-gradient, generally circular magnetic anomalies and positive gravity anomalies known to be present (Rankin, 1977).

Beneath the Coastal Plain in southwestern Georgia and northern Florida are unfolded, unmetamorphosed clastic rocks which contain fossils ranging in age from Early Ordovician to Middle Devonian (Rankin, 1977; Daniels, 1974). They were not deformed by the Appalachian orogenic event, and they contain pelecypod fauna quite similar to those of central Bohemia and Poland. They are also similar to those of Nova Scotia, North Africa, and South America (Rankin, 1977; Pojecta et al., 1976). It has therefore been suggested that Florida may once have been part of Africa, and that it was attached to North America during the Early Paleozoic closing of the Iapetus (proto-Atlantic) Ocean (Odom and Brown, 1976). Later, Florida was separated from Africa and was left with North America during the opening of the Atlantic Ocean. It has been suggested that the basement of the Charleston Block may have formed as a broad zone of Mesozoic crustal extension in a manner similar to the formation of Triassic-Jurassic basins (Section 2.1.1.3) but on a much grander scale (Popenoe and Zeitz, 1977; Long and Lowell, 1973). This zone of extension may be as wide as 62 to 125 miles and is presumably related to the initial rifting of the Atlantic Ocean basin (Rankin, 1977).

2.1.1.6 Geomorphology and Potential Hazards

Physiographic and geomorphic features of the area in the vicinity of the SRS are discussed in Section 2.1.1.1. Geomorphic processes or terrains that might result in hazardous conditions for a large structure are discussed in this section.

2.1.1.6.1 Subsidence

Subsidence is the downward settling of material due to slow removal of material from beneath the subsiding mass (Thornberry, 1954). Wherever water is drawn from a confined aquifer, enough to lower the piezometric surface, the aquifer is compressed and the land surface may subside (Siple, 1967).

During an investigation of subsidence as it relates to the SRS, several first-order vertical control profiles within the site area were determined by the U.S. Coast and Geodetic Survey in 1961. The survey areas were those associated with the heaviest withdrawal of ground water from the Cretaceous sands. Comparison of nine altitudes obtained from first-order leveling with second- and third-order altitudes obtained at an earlier time showed a maximum decrease of 0.141 feet in H Area. Measurements in M Area showed a decrease of only 0.064 feet. However, these calculated values are subject to considerable error. This situation was discovered when data with significantly different accuracies and precisions were compared. Nevertheless, it was concluded that "whereas there is a definite possibility that the predominantly lower altitudes obtained in 1961 indicate some amount of subsidence, the evidence is insufficient to establish this amount conclusively on the basis of the present data" (Siple, 1967). Thus, it appears that although a small amount of subsidence may have occurred, it is negligible and should not be considered a hazard to site development.

There are no mine or quarry operations within the SRS, nor are oil and gas produced from the subsurface; consequently, subsidence due to the removal of subsurface materials is not a concern.

2.1.1.6.2 Cavernous or Karst Terrain

No well-developed karst terrain exists in the vicinity of the SRS, although there are numerous poorly drained sinks or depressions, particularly in areas "underlain by calcareous beds" (Siple, 1967). These sinks may have been caused by leaching of calcareous material within the Santee and Griffins Landing units, and this process may have caused localized subsidence (Bechtel Corp., 1968).

The subsurface support for heavy structures has been successfully stabilized by filling cavities in calcareous beds with large volumes of cement grout (Siple, 1967).

2.1.1.6.3 Carolina Bays

Carolina Bays are common geomorphic features, and some occur at SRS on the coastal plain. Carolina Bays are oval depressions with a sandy rim. Their interiors may be water filled, with or without an accumulation of peat, or may simply be an area of poorly drained soils. The long axes of these depressions are oriented northwest-southeast. They are numerous in

the southeastern Coastal Plain, especially in North and South Carolina. An estimated 500,000 bays exist, 140,000 of which are more than 500 feet in length (Prouty, 1952). The largest bay is about seven miles (11 km) long. Their oriented oval shape makes them such prominent features that they have raised considerable interest and speculation as to their origin.

Theories of origin include meteorite impact, sinks, and wind and water current interactions (Prouty, 1952; Thom, 1970). Any mechanism for developing Carolina Bays must account for their large numbers, oval shape, presence on Coastal Plain surfaces of several ages, large variation in size, bays within bays, and bays with multiple rims.

The rims of many bays appear to be accumulations of sand that stand slightly above the surrounding area. In air photos, the rims are narrow, light-colored arcuate areas outlining the darker bay interior and are most prominent along the east and southeast sides. The literature was reviewed on the features and proposed origins of Carolina Bays and the results and interpretations of investigations of three bays in the North Carolina Coastal Plain.

Carolina Bays are surface features that apparently have no effect on subsurface materials. Figure 2-29 shows a longitudinal section and a cross section of the Goldsboro Ridge, located just east of Goldsboro, North Carolina. The characteristics and possible origin of this ridge have been discussed by Daniels and Wheeler (1971). Figure 2-30 shows the mapped extent of the ridge and the outlines of the associated bays, including two bays that are actually within or on the ridge proper. The larger of the two bays on the ridge is shown in Sections 2-1 through 2-3 on the long axis in Figure 2-29.

The larger bay is formed on the sand body of the Goldsboro Ridge. The sand is about 14 feet thick at the rims and 8.5 feet thick in the bay. The sand has an abrupt contact with the underlying Sunderland clay in all drill holes. The Sunderland clay bed continues under the bay without disturbance or interruption. The relief on this clay surface is no greater under the bay than along the other parts of the section. Whatever processes formed this bay apparently operated at the surface and/or within the ridge sand and had no detectable effect below the sand.

Dark-colored, poorly and very-poorly drained, moderately fine-textured mineral silts now occupy the floor of the bay. In the eastern end there is one to four feet of silty clay to silty clay loam at the surface. The eastern rim is sand to a depth of 7.5 feet and sandy loam to a depth of 14 feet base of the ridge sand. The soil consists of one foot of yellowish-brown, loamy sand, A_1 horizon, and two feet of reddish-yellow B horizon over three feet of very pale brown C or A'_2 horizon. This is a normal sort of pedogenic sequence to be expected in sands in this area.

Further evidence of the surficial character of Carolina Bays is given by Bryant and Reed (1970), who studied the soils of bay and interbay areas in Scotland County, North Carolina. They reported that the bays are in surficial sediments 20 feet or less thick, with a basal sand to sandy

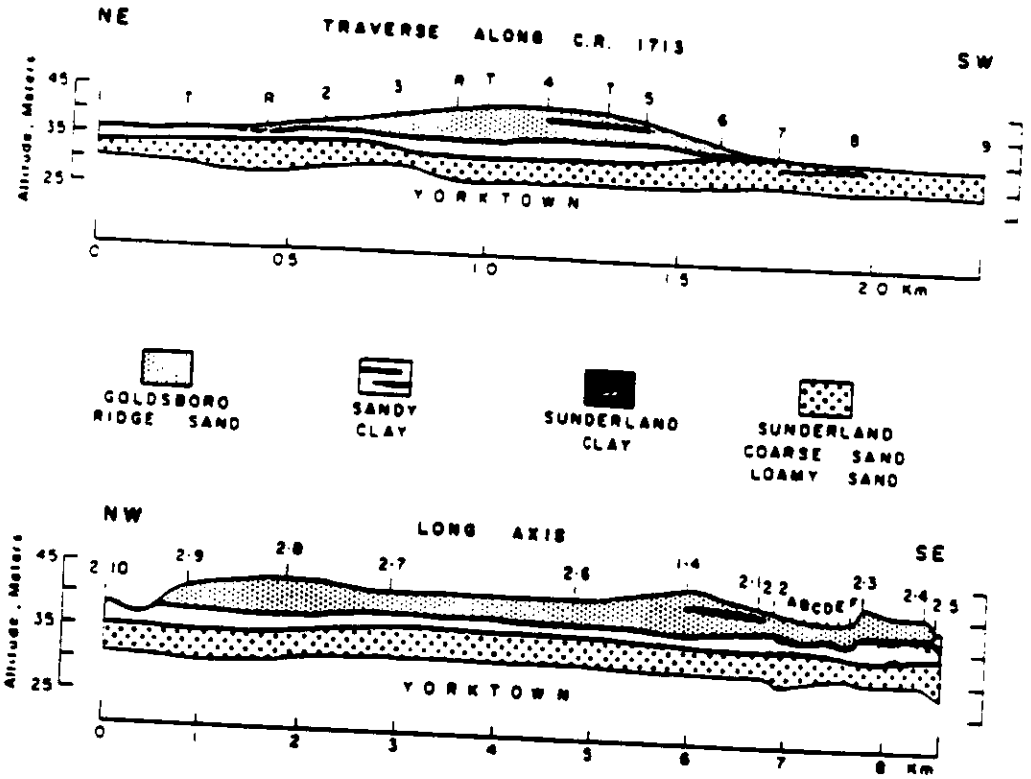

FIGURE 2-29. Goldsboro Ridge Cross Section (Gamble, Daniel and Wheeler, 1977)

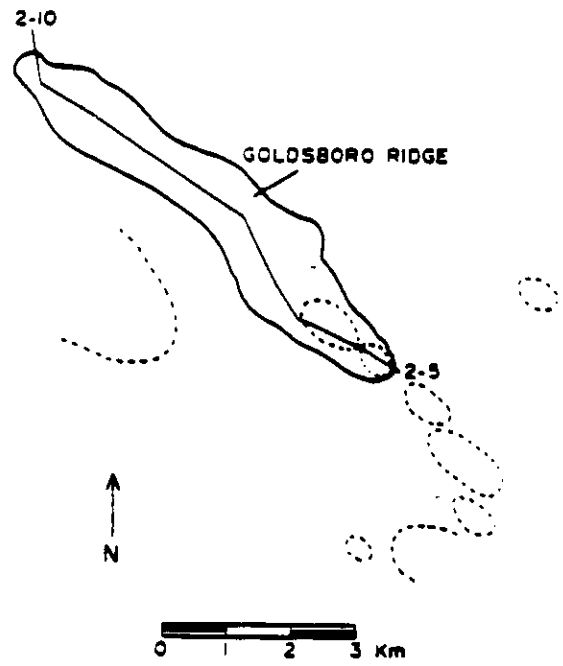

FIGURE 2-30. Goldsboro Ridge and the Carolina Bays

loam that is continuous beneath bay and interbay areas, with no evidence of disruption of material beneath the bays. Preston and Brown (1964) reached the same general conclusion on the basis of a series of power auger drill holes across a bay in Sumter County, South Carolina. The conclusion was that the bay-forming mechanism must produce the bay without deforming the underlying strata and that a surficial mechanism is most consistent with observed data. Drill traverses contain additional evidence of the surficial character of bays (Thom, 1970). In Horry and Marion counties, South Carolina, no evidence exists of solution-related subsidence of Carolina Bays in spite of the presence of carbonate-rich strata in the subsurface and some localized sink holes of irregular shapes with depths on the order of 20 feet.

Field studies suggest that there are two types of bay rims. One is the primary rim that is simply the edge of the original oval depression formed as part of the deposition of the surficial sediment. The other is a secondary rim, deposited at some later time. The secondary rims have a characteristic aarcuate shape. Bays may have only a primary rim, or they may have some combination of primary and secondary rim.

The concept of secondary bay rims, while not clearly stated, is alluded to by Melton (1934). It also appears that the secondary rims appeared to be developed by modification of the primary rim by eolian (wind erosion) or aqueous activity, or both. This requires the original depression to have been water filled throughout the greater part of the development of the secondary rim. The secondary rim would be a shore feature of a bay lake. The source of sand for modifying and adding to the primary rim is from the lakeshore beach. This is essentially the same sort of mechanism as that suggested for the development of bay rims in South Carolina and is also part of the suggested "artesian-solution-lacustrine-aeolian hypothesis" (Thom, 1970; Johnson, 1942).

Formation of secondary bay rims as a consequence of wind and water action along the shores of a shallow body of water can account for the development of multiple bay rims and bays within bays. Receding water levels could alter the shape of the shoreline and cause one or more subsequent secondary rims to develop inside the confines of the first one. The altered shape of the water body could cause the new secondary rim to truncate and obliterate part of the old secondary rim.

A secondary rim can develop some time after the original depression and its primary rim are formed. The buried soil under the secondary rim in one bay studied shows that the depression did not have a secondary rim for some time after it was formed. Thus, in this bay, the primary rim and the secondary rim are significantly different in age. In a second bay, there is no buried soil beneath the secondary portion of the rim. This suggests only a short interval between the origin of the primary rim, and the deposition of the secondary rim sand. The two may be nearly contemporaneous. It would seem possible for the present form of the bays and rims on any one Coastal Plain surface to have considerable variation in age, depending on the time between the formation of the primary depression and the development of a secondary rim.

The origin of bays appears, in part, to be related to the textural characteristics of the sediment. In general, bays are common where the surficial Coastal Plain sediments are sandy (sandy loams, sandy clay loams) and are absent or few in number in areas of silty or clayey materials. Similar relationships exist in South Carolina and in North Carolina (Thom, 1970; Mixon and Pilkey, 1976). Bays do not occur north and west of the Goldsboro Ridge where silty and silty clay soils developed in a clay bed that forms the top of the Sunderland "formation" (Daniels and Wheeler, 1971). There are many bays in sandy materials on the Sunderland surface to the southeast of the Goldsboro Ridge. There are few or no bays where silty soils are dominant.

Development of the secondary rims of Carolina Bays requires a depression deep enough or in a wet enough site for it to be partially water filled. Therefore, the basic problem in the study of Carolina Bays is the origin of this primary depression. There is a range in shape of depressions on the depositional surfaces of the Coastal Plain from irregular to circular to well-shaped elliptical. Usually the large depressions are more or less elliptical and small ones are not. The present form of many bays (i.e., those with secondary rims or multiple rims) appears to result from a modification of an original depression by the eolian lake shore process. It would seem in these cases that the original shape of the depression and its mode of origin (fluvial, marine, or eolian) would be immaterial. The modification would seem to have been responsible for the final oval-oriented shape. However, not all bays have an identifiable secondary rim and yet they have the characteristic oval shape. This suggests that some primary depressions were originally formed with an oval-oriented shape.

Bays examined in several studies are clearly surficial features without subsurface expressions (Thom, 1970; Bryant and Reed, 1970; Preston and Brown, 1964). This suggests that the primary depression, regardless of its original shape, was probably formed as a part of the final phase of the process of deposition of the surficial sediments. But the fact remains that the exact mechanism of the origin of primary depressions is not known.

Carolina Bays are surface features formed when the surficial sediments of the Coastal Plain were deposited. These primary depressions have, in some cases, been modified by the development of secondary rims that may bury the original rim or edge of the depression. The secondary rim is apparently a product of wind and water action around the shore of a water-filled bay. Rims within rims and other kinds of bay morphology resulted as water levels changed. The sandy character of many primary bay rims is simply a consequence of the development of a slightly thicker soil A_2 horizon, caused by the better drainage on the edge of the primary bay depression. The rims of some bays are a combination of primary and secondary rims with the secondary accumulation of sand occurring on the southeast end.

2.1.1.6.4 Landslides

Landslides and other slope stability problems are not a hazard at or near the SRS. Landslides generally include earthflows, sheet floods, mudflows, and creep. They result from the accumulation of debris in such quantities and at such angles of repose that a slight triggering mechanism causes massive slope failure. The topography on the SRS site is relatively flat, generally <50 ft/0.25 miles. Therefore, landslides at most SRS facilities should not be considered a hazard. Properly designed excavations likewise will not result in slope failure.

2.1.1.6.5 Tectonic Movements

The region is tectonically quiet, and there is no evidence of historic surface fault movements. Therefore, no tectonic movements are anticipated.

2.1.2 Site Geology

Stratigraphic terminology, the geology of the SRS, and the regional stratigraphic relationships are discussed more fully in Section 2.1.1.

The site topography is discussed in Section 2.4, along with the excavation and backfill performed at each of the production reactors. Ground water conditions at the site are discussed in Section 3. Geophysical studies conducted at the SRS are discussed in Section 2.4.

2.1.2.1 Site Physiography

The reactor sites are located in the South Carolina Atlantic Coastal Plain approximately 30 to 35 miles southeast of Augusta, Georgia. In South Carolina, the Coastal Plain sediments thicken southeastward from the Fall Line near Augusta, Georgia, to the coast where their thickness exceeds 4000 feet (Rankin, 1977). In the vicinity of the production reactor sites, these sediments are approximately 1000 feet thick and range in age from Late Cretaceous to Recent.

The Atlantic Coastal Plain province in South Carolina is divided into the northeast-trending Upper, Middle, and Lower Coastal Plain subprovinces, (Colquhoun and Johnson, 1968) as shown in Figure 2-5. The Aiken Plateau, in which the reactor sites are located, extends from the Savannah River to the Congaree River and southeastward from the Fall Line to the Coastal Terraces. The Aiken Plateau slopes gently to the southeast at approximately eight feet per mile and ranges in elevation from 650 feet above msl in the northwest to approximately 350 feet above msl in the SRS area, which includes most of Aiken and portions of Barnwell counties (Siple, 1967). The Aiken Plateau is bordered by the Piedmont on the west and the Congaree Sandhills on the north and northwest.

The Coastal Terraces extend from the southeastern margin of the Aiken Plateau to the Atlantic Coast, a distance of 80 to 90 miles. This subprovince is bounded by the Orangeburg Scarp on the northwest. The Orangeburg Scarp is also called the Citronelle Escarpment and the Coharie Terrace (Cooke, 1936; Doering, 1960). The Orangeburg Scarp marks the boundary between the Upper and Middle Coastal Plain subprovinces and is characterized by a break in slope between the Upper Coastal Plain at approximately 250 feet above msl and the Middle Coastal Plain at approximately 100 to 150 feet above msl. The regional physiography is discussed in Section 2.1.1. The SRS, located in the Aiken Plateau, has elevations ranging from about 350 feet above msl on the crests of the interstream divides to 70 to 80 feet above msl in the Savannah River floodplain. The Savannah River is an extended consequent stream that cuts southeastward through the Aiken Plateau six to 12 miles southwest of the reactor sites. A consequent stream is a stream that originates on a newly exposed or recently formed surface and that flows along a course determined entirely by the initial slope and configuration of that surface. The Savannah River flows southeastward from its point of origin, at the confluence of the Tugaloo and Seneca rivers, to the Atlantic Ocean, 150 river miles southeast of the site. Downstream from Augusta, Georgia, it is in a stage of early-to-middle maturity and is characterized by well-developed meanders and a floodplain one to two miles wide. In the vicinity of the SRS between Lower and Upper Three Runs Creek, the Savannah River has a gradient of approximately 0.5 feet per mile.

The interfluvial areas in the SRS vicinity are relatively narrow and well drained and are flanked by steep-sided subsequent stream valleys that form relief of as much as 300 feet in some areas (Siple, 1967). A subsequent stream is a tributary that has developed its valley (mainly by headward erosion) along a belt of underlying weak material and is therefore adjusted to the regional structure. In the reactor sites area, elevations range from approximately 135 feet above msl in the floodplain of Lower Three Runs Creek to approximately 330 feet above msl on a small knoll west of the P-Reactor Area near the junction of Roads 9 and B, a relief of approximately 195 feet.

Topographic maps for the areas around the reactors are taken from the U.S. Geological Survey 7.5 minute topographic maps (Figures 2-31 through 2-33). Figure 2-34 shows the streams at the SRS.

The large subsequent streams in the SRS area generally have symmetrical cross-valley profiles, with the exception of Upper Three Runs Creek, the largest of the subsequent streams in the site vicinity. The northwest valley slope of Upper Three Runs Creek is less steep than the southeast valley slope. Furthermore, the stream has an unusually wide floodplain, nearly 4000 feet wide in some areas. This asymmetry may be related to both structure and lithology. Siple (1967) indicates that the flow direction of Upper Three Runs Creek is approximately parallel to the regional northeast strike of the underlying beds, which dip to the southeast. This suggests that the valley may be a strike valley which, upon downcutting of the creek, has shifted its position downdip to the southeast, following the surface of a relatively resistant bed. This

process is referred to as homoclinal shifting (Glenn, 1895). Subsurface sampling information in the DWPF area, and profiles constructed from geophysical logs obtained in borings on both sides of Upper Three Runs Creek, substantiate this possibility. A stiff clay and sandy silt unit found at depth in the subsurface at the site, extend northwestward and intersect the surface near Upper Three Runs Creek.

In the vicinity of the reactor sites, other conditions exist that produce anomalous drainage patterns. Generally, the stream divides are well drained, although some undrained depressions exist on the interfluvial crests, as well as on valley slopes and valley floors. These depressions may be either solution sinks or possibly Carolina Bays and represent locally developed internal drainage. The origin and characteristics of Carolina Bays are discussed in Section 2.1.1.6.3. Drainage patterns associated with these depressions and the subsurface conditions associated with their formation are discussed in detail in Section 2.1.2.2.1.

2.1.2.2 Geomorphology

2.1.2.2.1 Depression Features

There are numerous shallow depressions in the vicinity of the SRS which vary in size from a few tens of feet to over 6,000 feet across their greatest dimension. A depression near Dunbarton at the intersection of SRS Roads B and F is one of the largest in the vicinity of the reactor sites. Most of the depressions, however, have maximum dimensions of several hundred feet or less. Depressions found throughout the area investigated may be associated with solution of underlying materials.

A great deal of relevant information is available from wells recently drilled and cored in support of waste management programs at the SRS. The Santee Limestone Formation is present in all of the wells examined. The thickness of the formation shows very little variation, even though there is tremendous variation in the carbonate content and though some wells have no carbonate in them. Some wells in the K-, L-, P-Areas penetrated carbonate of Griffins Landing Member, and other wells encountered no carbonate.

The preponderance of evidence suggests that there is no demonstratable subsidence associated with variation in carbonate content.

An investigation of a large depression near R Area, 3 miles north of P Reactor, was conducted by the U.S. Army Corps of Engineers. A series of test borings were drilled along the major and minor axes of this depression, which Siple (1967) calls a typical Carolina Bay. The original U.S. Army Corps of Engineers' report summarizes results of the sink studies at R Area and other nearby areas. These results are discussed in the following paragraphs.

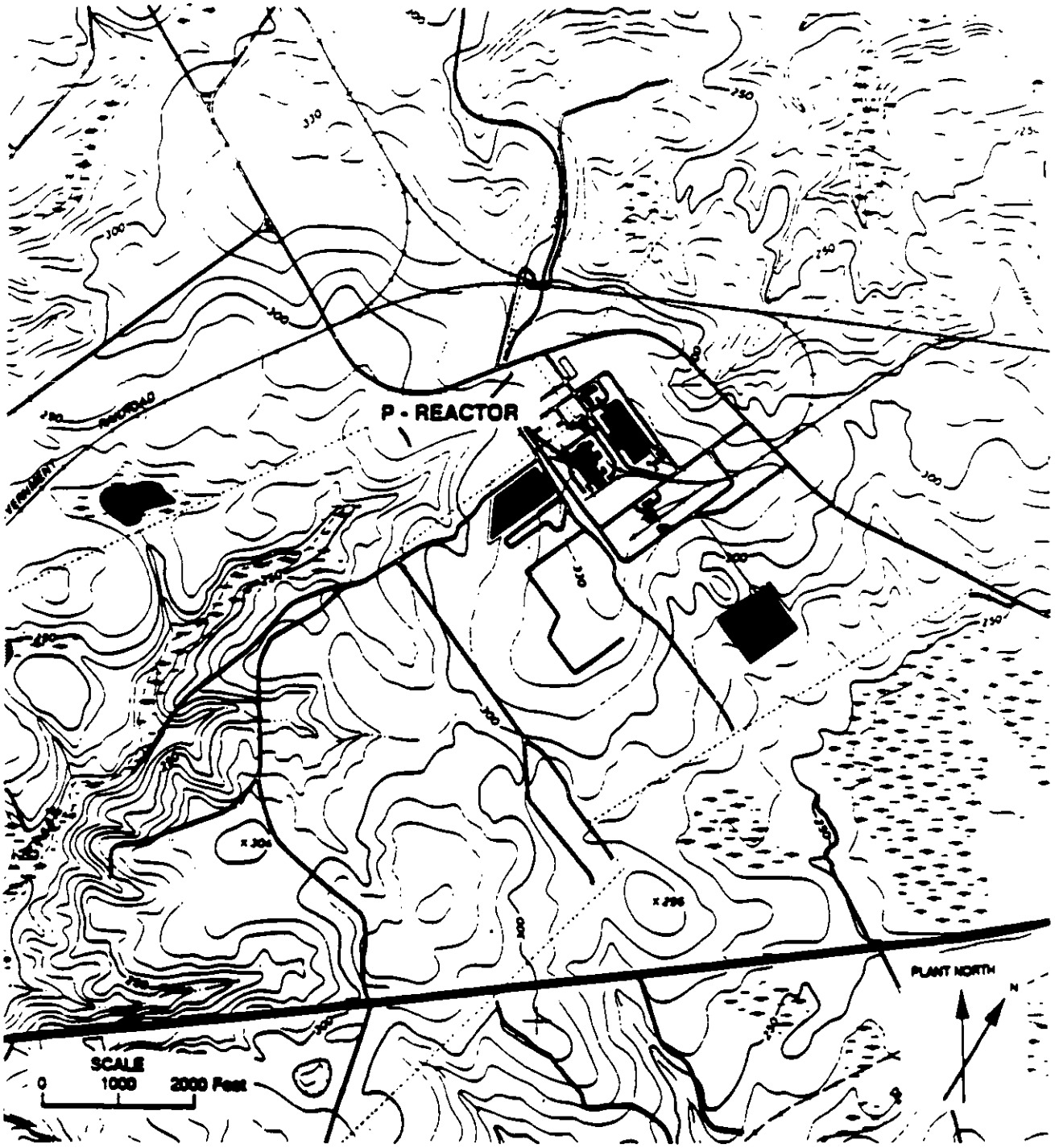

FIGURE 2-31. Topographic Map of P Area

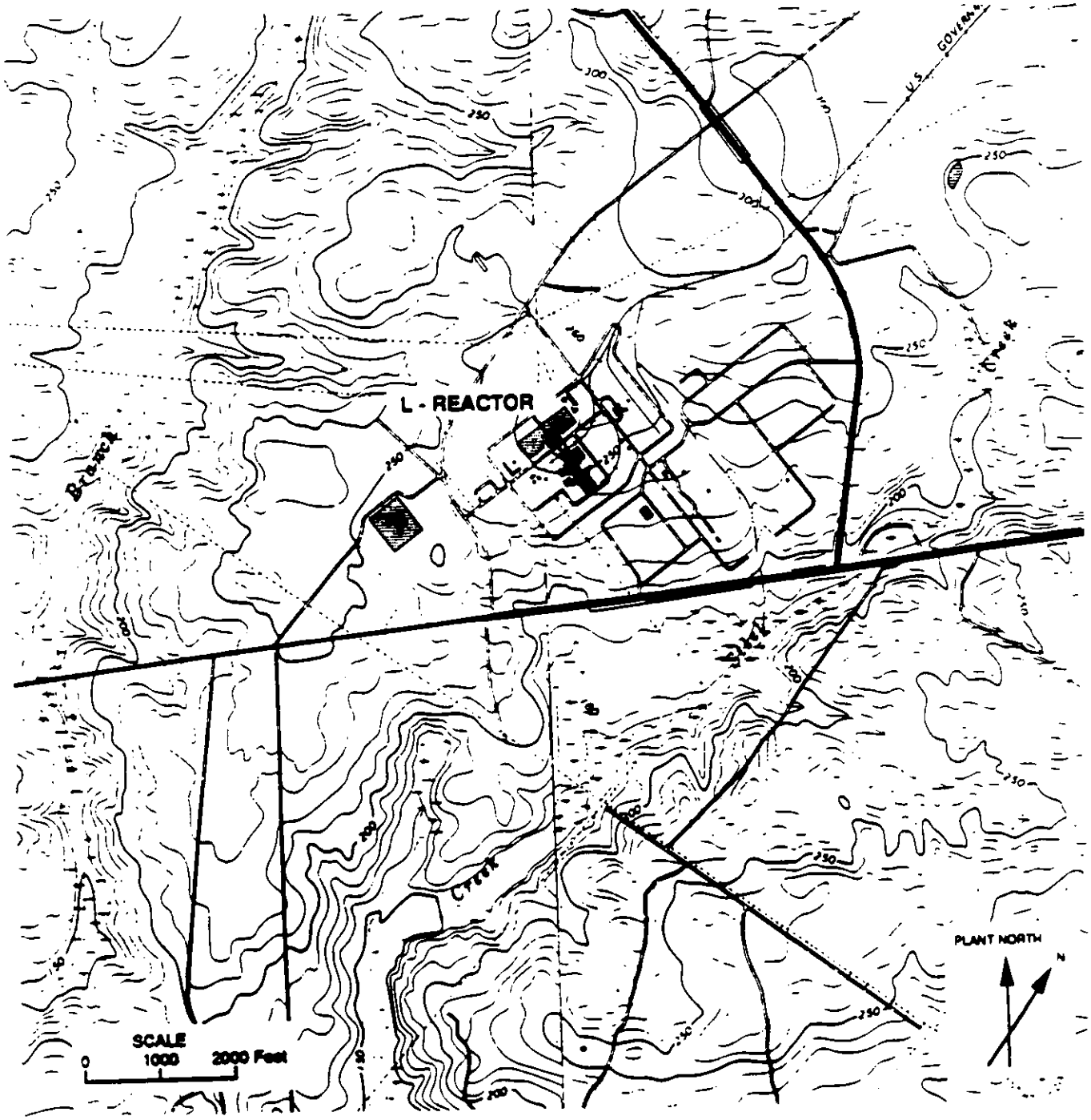

FIGURE 2-32. Topographic Map of L Area

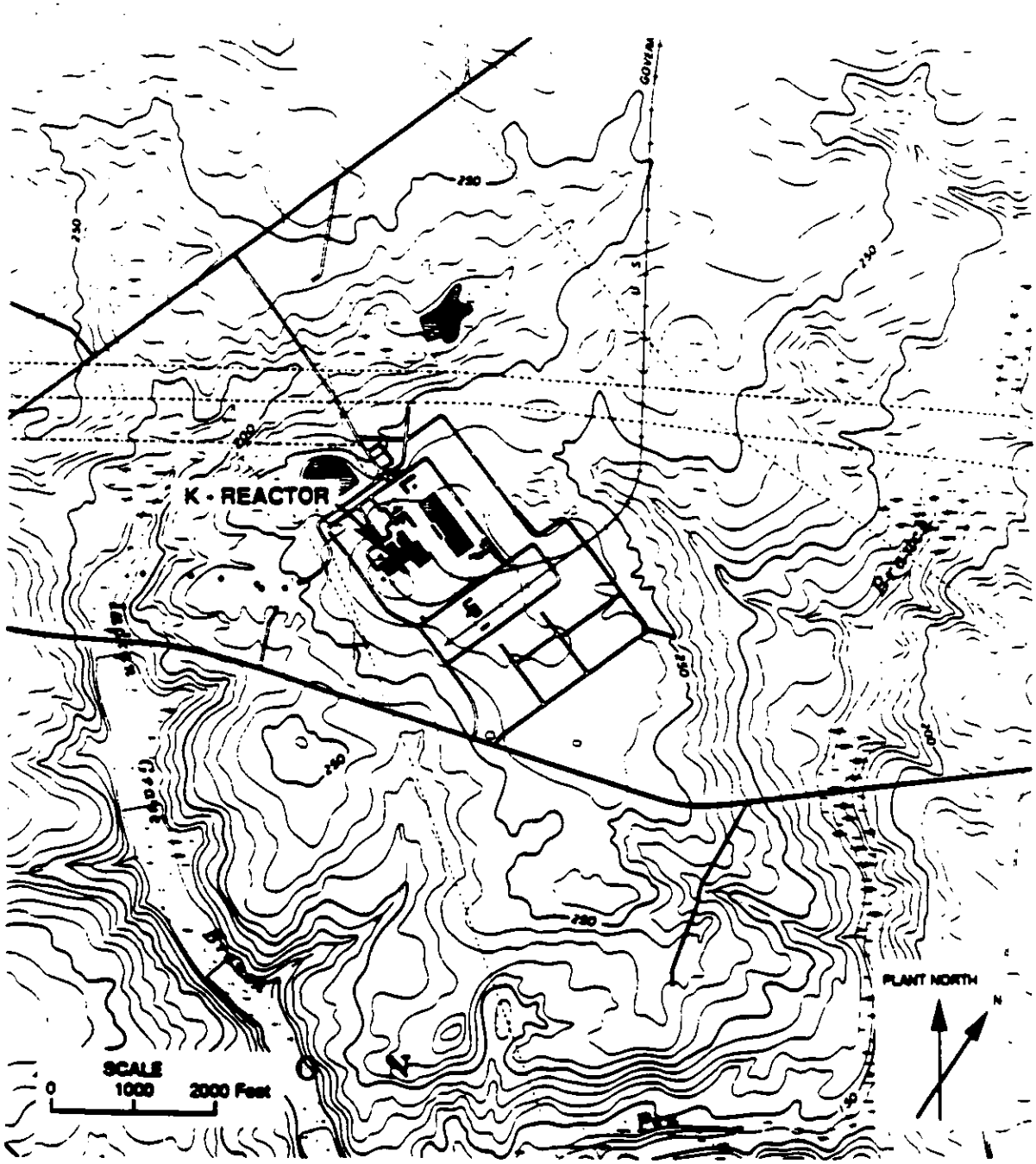

FIGURE 2-33. Topographic Map of K Area

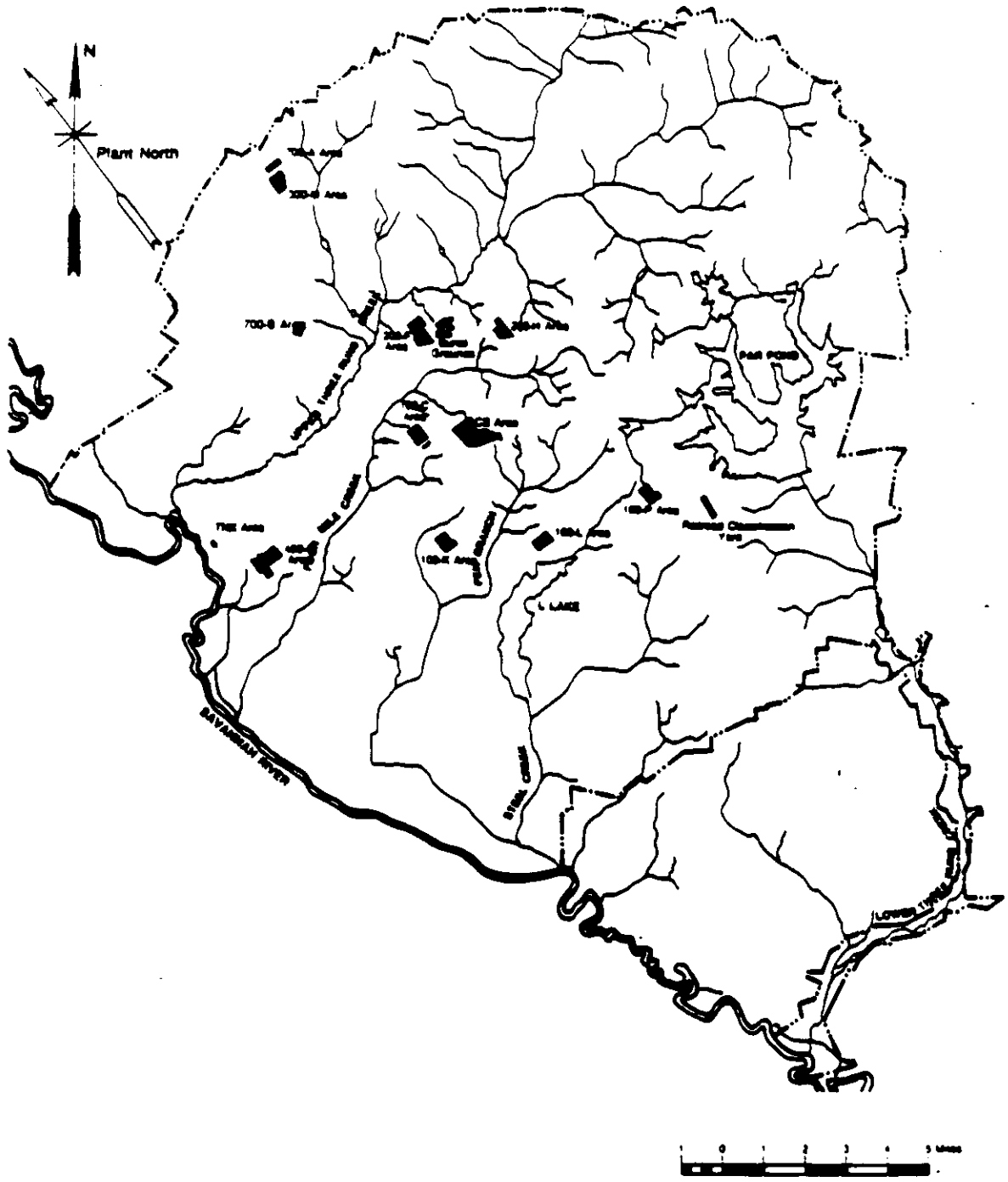

FIGURE 2-34. Surface Drainage Map of SRS

"Borings in or near sinks indicate that they are generally associated with the presence of calcareous material above which the strata show apparent evidence of subsidence. Zones of low-penetration resistance and mud losses generally are limited to the interval immediately above or in the upper portion of the calcareous materials and occur more frequently on the peripheries than in the centers of the sinks. The seat of the subsidence is a zone of calcareous material that occurs in the upper-middle portion of the McBean formation. This suggests that the sinks have been formed by solution of calcareous material."

The data collected in the study by the Corps of Engineers were, in fact, inconclusive as to a causal relationship between the solution cavity and the Carolina Bay. It is possible that these features may be sinks related to consolidation, or differential compaction distributed over large sediment thicknesses. This would explain a collapse origin for these depressions and also explain the fact that sedimentary warping and other features characteristic of large-scale collapse were not observed. Siple (1967) tended to call all depressions Carolina Bays.

It can be concluded that at least some of the larger depressions, referred to as Carolina Bays, may, in fact, be wide, shallow sinks. There are a number of characteristics peculiar to Carolina Bays, which are not possessed by the depressions that were observed in the SRS area.

Many of the nonelliptical closed-surface depressions occur in the "Upland" unit which is the youngest high-level stratigraphic unit in the area. Also, structural control of drainage patterns is not pronounced on this unit; the drainage is dominantly deranged to incipiently dendritic above about 250 feet above msl. These facts suggest that: (1) the bays could be related to original depositional topography, and (2) any tectonism which produced drainage-controlling fractures antedates deposition of the Upland unit.

Siple (1967) recognized that many of the features called Carolina Bays at the SRS had characteristics different from features identified as Carolina Bays farther east on the Coastal Plain (Salisbury, 1898; Melton, 1898; and Schriever, 1933). Carolina Bays located in eastern South Carolina (Dillon, Marion, and Horry counties) are oriented approximately north 45° west, as compared to north 14 to south 18 degrees west for the depressions in the SRS area. Some of the larger depressions in the SRS area exhibit flattening on the north rim and, thus, have a pear-shaped or triangular perimeter (Smith, 1931). Smith (1931) suggests that the Carolina Bays were formed by dissolution of limestone, marl, or calcareous sand, which ultimately resulted in subsidence. He also suggests that the removal of fine sand could cause collapse, due to the subsequent readjustment of residual coarse grains. It was demonstrated that dissolution of silicate minerals could explain some bays in the Aiken area (Smith, 1931).

A comparison of the undrained depressions found at the SRS with the characteristics of Carolina Bays reveals the following differences (Prouty, 1952). The Carolina Bay-like depressions that are seen at the SRS trend in a more northerly direction than typical Carolina Bays

(Siple, 1967). There are some elongated depressions found in the SRS area which trend northeast-southwest, inconsistent with the general trend of most Carolina Bays. The presence of a sand rim is a feature of most Carolina Bays, and it is best developed on the southeast side; however, in the Carolina Bay-like structures that are seen in the SRS area, this rim is not present. Generally, Carolina Bays are filled with peat varying in thickness from 15 to 30 feet. Based on the investigations performed near R Area, the Carolina Bay-like structures at the SRS do not contain accumulations of peat. There was no mention of appreciable accumulations of organics, nor was there any indication that the southeast end of the bay was deeper than the northwest end. Many of the closed surface depressions at SRS are not Carolina Bays.

2.1.2.2.2 Terraces

Seven marine terraces of Pleistocene age occur in the Atlantic Coastal Plain of South Carolina (Cooke, 1936). The highest terraces are present in the Savannah River valley. From oldest to youngest, they are the Hazlehurst Terraces, at approximately 270 feet above msl; the Coharie Terrace, at 215 feet above msl; the Sunderland Terrace, at approximately 170 feet above msl; and the Okefenokee Terrace, at approximately 145 feet above msl.

2.1.2.3. Stratigraphy

The reactors are in the Upper Coastal Plain subprovince and are underlain by a sedimentary wedge approximately 1100 feet thick. The Coastal Plain wedge consists of unindurated and semi-indurated fluvial, deltaic, and marine sediments that dip gently to the southeast and range in age from Late Cretaceous to Holocene (Figure 2-35). (The planar view of the well locations is given in Figure 2-14.) The sedimentary sequence is underlain by a Precambrian/Paleozoic basement complex composed of folded and faulted metamorphic rocks similar to those exposed in the Piedmont. Within the basement complex is a Newark-type basin which contains sedimentary rock of Triassic age.

2.1.2.3.1 Basement

Under K-L-P area, the basement surface is at an elevation of about 750 to 850 feet below msl, strikes approximately north 60 degrees east and dips approximately 40 feet per mile to the southeast (Siple, 1967). The crystalline Piedmont rocks beneath the SRS consist of granitic intrusives and associated hornblende gneisses and chlorite hornblende schists similar to the lithologies found in the Charlotte belt (Siple, 1967).

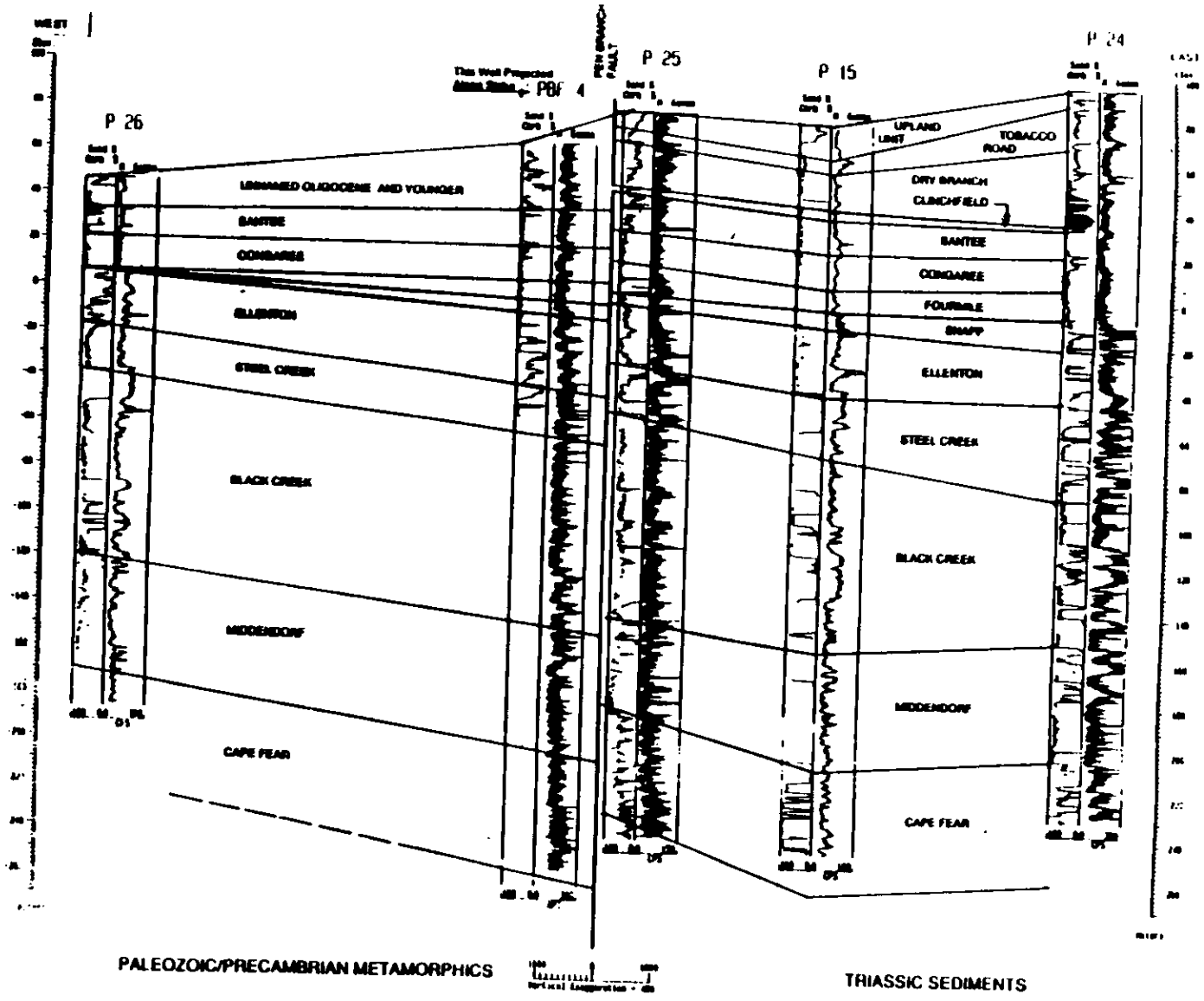

FIGURE 2-35. Geologic Cross-Section at K, L and P Area

An aeromagnetic survey of the area in 1958 by the U.S. Geological Survey indicated the presence of a magnetic low. Based on these data and cored wells, a basin, the Dunbarton Triassic Basin, was defined as being approximately 30 miles long. The strike of the basin axis is approximately north 63° east and parallels the regional strike of the underlying crystalline rock surface (Siple, 1967). Several wells in the southeastern part of SRS have penetrated maroon siltstones, feldspathic sandstones, and fanglomerates which are similar to the Triassic deposits of the Newark Supergroup. The maximum thickness of the Triassic sediments in unknown. A well drilled in 1969 penetrated 1953 feet of these sediments before encountering metamorphic rock. The northwestern border of the basin has recently been defined by wells drilled as part of the Pen Branch Fault Project (Figure 2-36). All or almost all of the K-L-P area is within the limits of the basin.

2.1.2.3.2 Late Cretaceous Cape Fear Formation and Lumbee Group

Quartz sands and clays which are assigned to the Cape Fear Formation and the three formations of the overlying Lumbee Group appear to be present beneath the K-L-P area. The formations of the Lumbee are the Middendorf, the Black Creek, and the Steel Creek Member of the Peedee Formation. The upper surface of the Lumbee is about 100 to 160 feet below msl in the K-L-P area and the unit is approximately 670 feet thick.

2.1.2.3.2.1 Cape Fear Formation

In the vicinity of the reactor sites, the Cape Fear is composed of brown, red, gray, and tan, poorly-sorted, pebbly, silty, clayey quartz sands interbedded with clays. Grain size of sands is dominantly fine-to coarse and they are slightly to well-indurated. Feldspar and muscovite are abundant in places. Many of them fine upward and bedding thickness is from about 10 to 40 feet. The interbedded clays are from less than 1 foot to about 20 feet thick. The Cape Fear in the SRS area has been interpreted as an upper delta plain deposit (Christopher et al., 1979). The top of the Cape Fear Formation is approximately 600-800 below msl and the unit is about 200 feet thick. The high clay content of the Cape Fear gives it a low permeability. Pollen dated as possibly Turonian or Coniacian (late Cretaceous) has been obtained from Cape Fear samples at SRS.

2.1.2.3.2.2 Middendorf Formation

The Middendorf Formation lies with a sharp unconformable contact on the Cape Fear, the contact marked in most SRS wells by a coarse, pebbly zone and a distinct change in the lithology. Deep wells in the K-L-P area indicate that the Middendorf is made up of a lower sandy zone about 100 feet thick, overlain by a clayey zone about 30 feet thick. The lower quartz sand is loose to slightly indurated, fine to coarse, and moderately sorted. Pebbly zones and micaceous zones occur. Clay clasts and small pieces of lignite are present in some places. Some of the sandy section

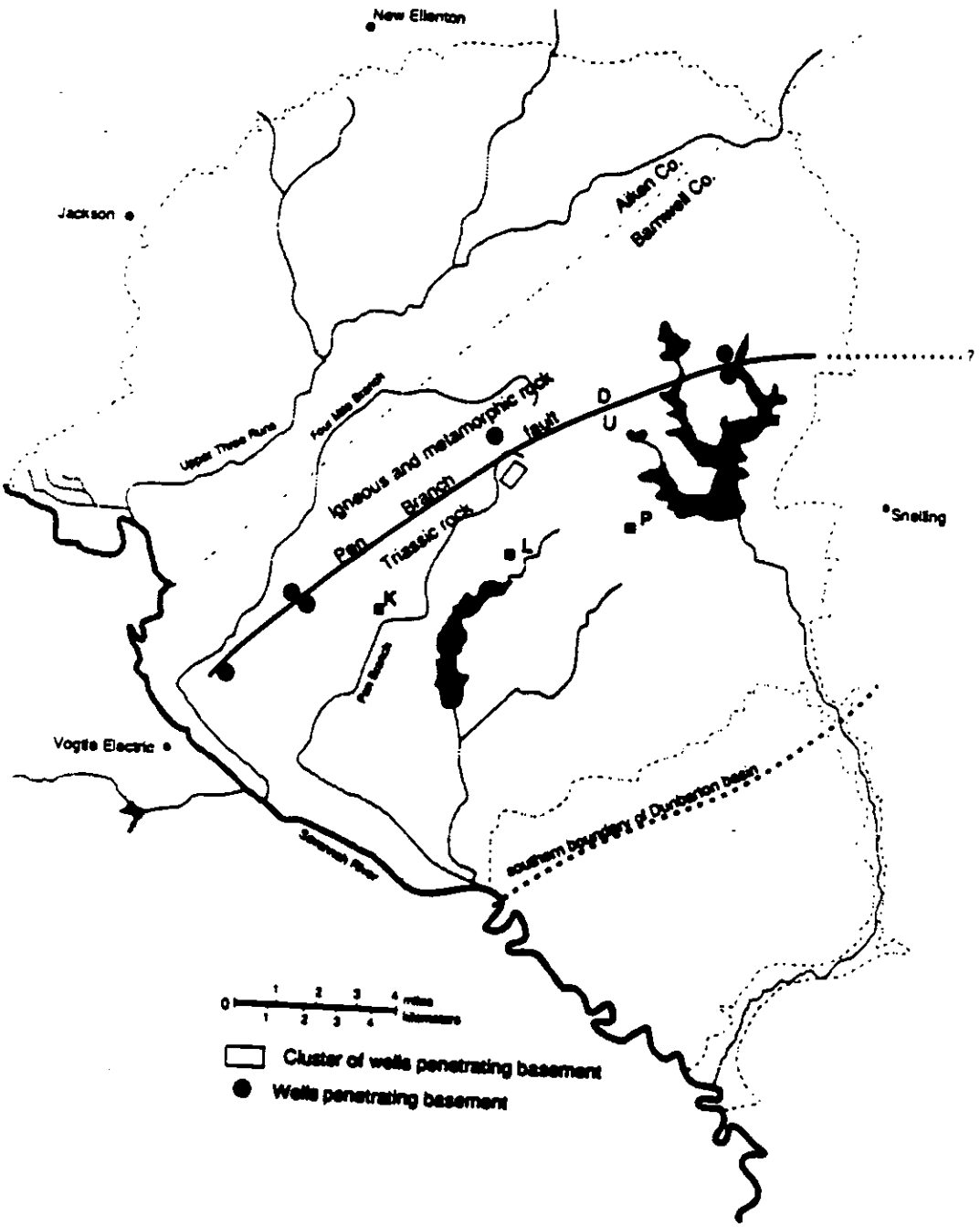

FIGURE 2-36. Northwest Border of Dunbarton Basin as Determined by Drilling

is composed of stacked, fining upward packages. Light gray and tan are the dominant colors. In L Area, a clayey zone about 70 feet thick occurs with the lower part of the formation. The upper clayey zone is light to dark gray and orangeish-gray. The middendorf has the characteristics of an upper delta plain deposit.

The lower part probably has moderate to high permeability. The upper clayey zone should be an aquitard, although it may not be continuous. The top of the Middendorf is about 470 to 500 feet below msl, and the unit is about 130 feet thick. The Middendorf is thought to be late Santonian (late Cretaceous) in age (Christopher et al., 1979).

2.1.2.3.2.3 Black Creek Formation

The basal sands of the Black Creek Formation lie in sharp, probably unconformable, contact on the upper clay of the Middendorf. The unit is composed of quartz sand with thin clay laminae in places. The sands are loose to sightly indurated, fine to very coarse, and mostly medium grained. They are poorly to well sorted, and some of the section is composed of stacked, fining upward packages. Pebbly zones occur and clay clasts are common in some parts of the formation. Dark, clayey, silty, lignitic, micaceous zones with iron sulfide are fairly common, especially, in the middle of the unit. Above the dark, clayey part of the Black, Creek, tan and light gray sands are dominant. At the top of the unit is a massive clay about 20 feet thick. The formation has the characteristics of a deltaic deposit.

The lower part of the formation probably has moderate to high permeability, the middle clayey zone has low permeability, the upper sands have moderate to high permeability, and the upper massive clay should be an effective aquitard. The top of the Black Creek is approximately 170 to 250 feet below msl and the formation is about 250 to 300 feet thick at the site Campanian and early Maestrichtian fossils occur in the Black Creek Formation.

2.1.2.3.2.4 Steel Creek Member of the Peedee Formation

The Steel Creek is composed of a lower tan and gray quartz sand, loose to slightly indurated, and light to dark gray, tan, yellow, and orange upper clay. The lower sand in the vicinity of the reactor sites is very fine to very coarse and poorly to well sorted. It is pebbly in places and micaceous zones and clay clast-rich zones occur. Thin clay laminae are present in parts of the section. The upper clay is from 25 to 55 feet thick. The lower sandy part was probably deposited in an upper delta plain environment, and the upper clay probably formed in a lower delta plain setting.

The lower sand probably has a moderate to high permability. The overlying clay should form an effective aquitard. The top of the Steel Creek in the area has an elevation of 100 to 150 feet below msl, and the formation is about 70 to 90 feet thick. The Steel Creek is Maestrichtian in age.

2.1.2.3.3 Paleocene-Eocene Black Mingo Group

The Black Mingo Group at SRS consists of the early and late Paleocene Ellenton Member of the Rhems Formation, the late Paleocene Snapp Member of the Williamsburg Formation, and the early Eocene Four Mile Member of the Fishburne Formation. Quartz sands and clays are the dominant lithologies. In the K-L-P area, the top of the group is about 0 to 50 feet above sea level, and the group is about 160 feet thick.

2.1.2.3.3.1 Ellenton Member of the Rhems Formation

The Ellenton unconformably overlies the Steel Creek. In the K-L-P area, it is mostly composed of dark gray and black poorly sorted, clayey, silty sand and moderately sorted sand, with interbedded dark, laminated clay. The clay content increases to the east, and clay beds are up to 25 feet thick. Grain size in the sands, which fine upward in places, is generally fine to coarse. Induration is slight to moderate. Muscovite, lignite, and iron sulfide are common throughout the unit, and glauconite occurs in places. The Ellenton has the characteristics of a deltaic deposit.

Some of the sands have moderate permeability, but the clayier ones are probably aquitards, and the unit as a whole is probably an effective aquitard. The Ellenton top is about 10 to 70 below msl in the K-L-P area and is about 90 feet thick. Both Midwayan (early Paleocene) and early Sabinian (late Paleocene) fossils have been found in the Ellenton.

2.1.2.3.3.2 Snapp Member of the Williamsburg Formation

The Snapp overlies the Ellenton, perhaps unconformably. It is made up of dark gray, light gray, yellow and orange, pebbly, silty sands with interbedded clays. Clay beds are up to 10 feet thick. The sands, which fine upward, contain lignite, muscovite, iron sulfide, and clay clasts in places, and they are loose to slightly indurated. The environment of deposition was probably fluvial and deltaic.

The Snapp sands have low to moderate permeability, and the clays should be effective aquitards. The top of the Snapp is from 0 to 30 feet below sea level at the K-L-P area where the sands are from 10 to 50 feet thick. The age is middle Sabinian (late Paleocene).

2.1.2.3.3.3 Fourmile Member of the Fishburne Formation

The Fourmile unconformably overlies the Ellenton and is composed almost entirely of loose, moderately and well-sorted quartz sands. In places, clay layers up to about 3 feet thick occur near the base and at the top of the unit. Small amounts of glauconite occur in both the sand and clay facies. Dominant colors are yellow, orange, tan green and gray. The Four Mile was deposited in shallow marine and lagoonal environments.

The unit has high permeability, the clays having a sporadic distribution. In the K-L-P area, the top of the Fourmile is about 0 to 50 feet above msl and is from 35 to 50 feet thick. The age is late Sabinian (early Eocene).

2.1.2.3.4 Orangeburg Group

The Orangeburg Group contains sands, clays, and limestones of the early middle Eocene Congaree Formation and the late middle Eocene Santee Limestone. The top of the group is from 100 to 130 feet above msl and its thickness is approximately 80 to 90 feet.

2.1.2.3.4.1 Congaree Formation

The Congaree overlies the Fourmile, probably unconformably. It is composed of loose, moderately and well-sorted sand, fining upward from coarse to very fine. Clay is rare and is limited to a few thin laminae. The environment of deposition was shallow marine.

The Congaree has high permeability. In the K-L-P area, the top of the Congaree is about 55 to 70 feet above sea level and is about 45 to 60 feet thick. The age early Claibornian (early middle Eocene).

2.1.2.3.4.2 Santee Limestone

In the K-L-P Area, the Santee is an extremely variable unit which contains quartz sand, glauconitic sand and clay, limestone and calcareous clay, and thin yellow, tan, and green clay beds. The basal part is a poorly to moderately sorted, medium and coarse sand resting unconformably on the Congaree. In places the basal sand is glauconitic. Tan, yellow, and brown interbedded sands and clays overlie the basal sands. The clays are up to 10 feet thick and are both glauconitic and nonglauconitic. In other places, limestone occurs in much of this part of the section. The occurrence of the limestone, the McBean Member, is sporadic and its thickness is quite variable. Some wells in the area have not encountered carbonate. Lithology of the calcareous unit varies from moderately indurated micritic limestone to highly indurated moldic limestone. The upper part of the Santee is composed of sands and clays in varying proportions. The Santee was deposited in a shallow marine environment.

The sediments of the Santee have highly variable permeabilities, but the formation as a whole is probably an aquitard. In the K-L-P area, the top of the Santee is about 100 to 130 feet above sea level and is about 30 to 40 feet thick. The age is late Claibornian (late middle Eocene).

2.1.2.3.5 Barnwell Group

The Barnwell Group of Jacksonian age is composed of sands, clays and limestones of the Clinchfield, Dry Branch, and Tobacco Road formations. The group probably crops out at lower elevations in the K-L-P area. Its thickness is highly variable and probably is as much as 200 feet in places.

2.1.2.3.5.1 Clinchfield Formation

The basal unit of the Barnwell, the Clinchfield, lies unconformably on the Santee. In the K-L-P Area, it consists of loose to slightly indurated, brown, tan, and yellow, medium grained, poorly to moderately sorted quartz sand. The environment of deposition was probably shallow marine.

The top of the Clinchfield is about 80 to 135 feet above sea level and its thickness varies from about 5 to 15 feet. Its age is probably early Jacksonian.

2.1.2.3.5.2 Dry Branch Formation

The Dry Branch consists of several facies: the Griffins Landing Member, a carbonate, the Irwinton Sand member, and clays lithologically similar to the Twiggs Clay Member of Georgia. The clays, which tend to be tan and yellow and most abundant in the lower part of the formation are up to 15 feet thick in parts of the K-L-P Area. The clayey zone as a whole is up to 30 feet thick in places. The carbonate, which is both calcilutite and calcarenite, is sporadic in distribution, and is up to at least 45 feet thick in places. Oyster shells are abundant in places.

Wells logs from the Corps of Engineer borings (U.S. Army Corps of Engineers, 1951) indicate the presence of carbonate of either the Griffins Landing Member of the McBean Member, or both, directly beneath the K, L, and P areas. During the boring operations, circulation was lost in this part of the section, and large quantities of grout were pumped into the subsurface. The grout moved horizontally in the subsurface over distances of at least 150 feet in K Area, 50 feet in L Area, and 100 feet in P Area. (U.S. Army Corps of Engineers, 1952), indicating zones of high permeability.

The Irwinton Sand constitutes the upper part of the Dry Branch. Most of this member consists of yellow, orange, and red, poorly to moderately sorted medium sand, loose to slightly indurated. In places in the K-L-P

areas, interbedded clays up to 6 feet thick are present in the middle of the unit. Pebbly zones occur in places especially in the lower part of the member.

The environment of deposition of the Dry Branch was shallow marine and lagoonal.

The clays and the lutitic carbonate are local aquitards. The Irwinton Sand probably has moderate to high permeability. The top of the Dry Branch is from about 160 to 130 feet above msl and is approximately 80 to 130 feet thick. Its age is middle Jacksonian.

2.1.2.3.5.3 Tobacco Road Sand

The Tobacco Road sand overlies the Irwinton, probably conformably. It consists of red, purple, orange, and yellow, poorly to moderately sorted coarse and medium quartz sand. Pebbly zones occur in places. Clay layers a few thick occur in various parts of the unit but do not appear to be laterally continuous. Induration is slight to moderate. The formation was probably deposited in a shallow marine and lagoonal environments.

The top of the Tobacco Road may coincide with the ground surface in the lower elevations within the K-L-P areas. It appears to be missing in at least one place where erosion preceding the deposition of the overlying unit removed it. Tobacco Road probably has low to moderate permeability. The formation is late Jacksonian in age.

2.1.2.3.5.4 "Upland Unit"

The K-L-P areas are capped in most places by a deposit of Miocene(?) age which is informally referred to as the "Upland" unit. It is quite variable in lithology, containing poorly sorted sands, pebbly sands, conglomerates, and clays. Observed thicknesses are up to 42 feet, and clay bodies over 20 feet thick occur. The beds within the "Upland" do not have great lateral continuity and the environment of deposition was fluvial. The sediments have low permeability.

2.1.2.3.5.5 Floodplain Alluvium

Alluvium of Recent age occurs in the floodplains of the Savannah River and along the minor tributaries that drain the area surrounding the reactor sites. The deposits are poorly-sorted sands, clays, and gravels, which vary in thickness from a fraction of an inch in the higher elevations of the headwaters of the tributaries to nearly 30 feet in the river flood-plain south of the sites (Siple, 1967).

2.1.2.4 Geologic Structures

The reactors are situated on the western margin of the Atlantic Coastal Plain province, approximately 30 to 35 miles southeast of the Fall Line. The Coastal Plain consists of a wedge of interstratified and interfingering beds and lenses of semiconsolidated and unconsolidated sediments, which dip to the southeast and range in age from Late Cretaceous to Recent. Most evidence indicates that the Atlantic Coastal Plain has been tectonically quiet since Late Cretaceous time . Recently, a number of tectonic structures have been studied in several localities throughout the plain. In the site region, similar structures have been identified and are discussed in the following sections.

2.1.2.4.1 Soil Fractures

Roadcuts and excavations on interfluve areas near the SRS commonly expose a deeply developed soil profile. The A horizon may be up to 10 feet thick and typically consists of buff to nearly white structureless medium to fine-grained quartz sand. The B horizon may be from 2 to 10 feet thick and shows the effect of chemical deposition of iron and aluminum compounds leached from the overlying material. Reticulate mottling of this plinthic horizon is a salient feature.

Weathering effects extend to depths of at least 25 feet because feldspars in the originally arkosic "Upland" unit are completely disintegrated to that depth and some quartz cobbles are soft enough to crush in the hands.

Volume reduction resulting from the demonstrably intense chemical weathering produced tension which is expressed in some areas as soil fractures. In shallow exposures, such as roadsides and drainage ditches, these fractures may seem to be a dominant feature of the landscape. It is easy to presume that they extend to great depth. In deeper exposures the fractures are seen to lose the appearance of being caused by physical displacement. They typically terminate as colored bands in the less-weathered parent sedimentary material.

These soil fractures have been called "clastic dikes" for want of a better name. This is an unfortunate misnomer because true clastic dikes are the result of liquefaction and upward injection of water-saturated sand through a more brittle overlying stratum. Thus, true clastic dikes imply episodic earth movements sufficient to cause liquefaction. No true clastic dikes have been observed at the SRS.

A 25-foot (8 meters) deep trench at the SRS provided a recent opportunity in late 1987 to observe the soil fractures. This exposure was entirely in the "Upland" unit. Plinthic mottled zones extend downward as extensions of the B soil horizon to depths of 10 to 13 feet below ground level. From 13 to 19 feet, iron has migrated laterally from the fractures, leaving secondary alumino-silicates (clay) as the dominant constituents and cementing the laterally adjacent material with iron oxides. Silica

is presumed to be more mobile than iron or aluminum but is continually available because it is the most abundant constituent in the sediment/soil system.

The lower terminus of most of the observed fractures seems to be a bleached zone from which iron has been removed and in which silicate minerals are being replaced by clay. The appearance of physical disruption of pre-existing material does not continue to the lower meter or so of the fractures.

True clastic dikes are apparently found in the South Carolina Coastal Plain. Clastic dikes have been found in possible Eocene and Miocene sediments in Calhoun County, South Carolina (Johnson and Heron, 1965). Clastic dikes also cut possible Miocene and Pleistocene sediments in the west-central part of the plain (Heron et al., 1965). Howell and Zupan (Howell and Zupan, 1974) note the presence of clastic dikes cutting possible Cretaceous sediments north of Cheraw, South Carolina. At that site, clastic dikes are associated with folds and faults in semiconsolidated Coastal Plain sediments. Nearly vertical clastic dikes cross-cutting sedimentary bedding extend from a Paleozoic argillite to the surface, and that the infilling clay from the argillite closely resembles that of the Paleozoic argillites stratigraphically below the soil horizon. The orientations of the clastic dikes approximate the axial plane orientation of an anticline, which strikes north 77° east and dips north 70°. Axial plane cleavage within the argillite core of the anticline shows as a step-like series of normal faults in the argillite bed, with a maximum observed offset of approximately 4 inches. Zupan and Abbot (1975) describe the presence of clastic dikes northwest of Columbia, South Carolina, where the dikes are associated with low-angle reverse faults, suggesting that southeast-northwest compressional forces affected the Paleozoic basement and overlying post-Miocene sediments at the time of faulting. The reverse faults strike between north 35° east and north 115° east, and dip north to northwest at 17 and 87°, with a measured displacement of approximately 5 feet. Large numbers of clastic dikes along the exposure originate in the Paleozoic argillites of the Carolina Slate belt and transecting the overlying post-Eocene sediments, with no apparent offset of bedding on either side of the clastic dikes.

Clastic dikes that formed in fractures created by volume changes associated with weathering have also been described (Johnson and Heron, 1965). The dike formation was a result of soil forming involving movement of soil horizon clays into the fractures.

In their study of structures near Cheraw, Howell and Zupan (1974) indicate that tension fractures developed in overlying Cretaceous sediments at the time of anticlinal folding. Compressional forces are thought to have forced the underlying argillaceous saprolite into the fractures, forming the clastic dikes.

2.1.2.4.2 Folds

Areas near the reactors were investigated, with particular emphasis placed on structure and stratigraphy. During a field reconnaissance at Chem-Nuclear Systems, Inc., east of the SRS, a low-amplitude anticline was found. The fold is symmetrical with a vertical axial plane striking northeast. The limbs dip northwest and southeast approximately 10°, and the wavelength is estimated to be at least several hundred feet. In the vicinity of the fold, small-scale gravity faults, thrust faults, and clay-filled fissures were found in shallow sediments.

A similar structure was reported at the Georgia Power Company's VEGP along the Savannah River in Burke County, Georgia. The structure, described as a "dip reversal", is an asymmetrical flexure that trends northeast-southwest. Structure contours derived from outcrop and subsurface information indicate that the southeast dip is about 30 to 40 feet per mile, whereas the maximum northwest dip is approximately 265 feet per mile. The marker bed drops approximately 50 feet toward the northwest. The results of the slope reversal investigation were summarized as follows:

- The trend of the feature is approximately northeast-southwest.
- No indication that it is fault-controlled was found during the investigation.
- It does not appear to be an erosional feature on top of the bearing stratum because both the top and bottom of that stratum have similar dips.
- It does not dip in a direction consistent with a possible near-surface expression of the underlying Dunbarton Basin boundary.
- No relationship to the assumed boundary fault contact at the northwestern edge of the Dunbarton Basin could be found.
- It appears to have been formed previous to or during the deposition of the thick deposits affected by the reversal.
- Striated bedding planes were found on the southwestern part of the reversal.
- Water losses related to jointing in the upper 15 feet of a marl were observed during exploratory drilling.

The reversal is believed to parallel an irregular erosional surface formed on the underlying sands, and differential compaction possibly occurred during and shortly after deposition of the bearing stratum. According to subsurface cross sections in the Vogtle FSAR, expression of this dip reversal can be seen in sediments over 100 feet thick.

Flexures have been found in Coastal Plain sediments near the Westfield Creek, north of Cheraw where folding occurred in Carolina Slate belt argillites and late Cretaceous sediments of the Middendorf Formation (Howell and Zupan , 1974). The post-Cretaceous structure includes an anticline that trends north 77° east and plunges 9°, and has a wavelength of approximately 100 feet. The axial plane strikes north 77° east and dips 70° north; axial plane cleavage within the argillite core of the anticline shows a step-like series of normal faults in the argillite bedding, with maximum offset of approximately 4 inches.

During subsurface engineering investigations near the reactors, no fold structures were observed. The only evidence of a flexure near the sites is a radial drainage pattern that is developed 2 to 3 miles north near the intersection of Roads F and 6. The center of this radial drainage pattern lies near the projected boundary of the Dunbarton Basin, in proximity to two fault locations within the boundaries. Seismic reflection data and geophysical data from within borings show no indication of a flexure or dome, which is characteristically associated with a radial drainage pattern. Thus, it is probable that the radial drainage pattern formed from erosion along joints which are oriented in different directions.

2.1.2.4.3 Faults

The Pen Branch fault cuts Coastal Plain strata of Cretaceous, Paleocene, and Eocene age. Its position has recently been determined by drilling and it overlies and appears to be directly related the northwestern border of the Dunbarton Basin (Figure 2-37). The fault is within about 1/2 mile of the K Area and may underlie it. It is approximately 2 miles northwest of the L and P areas. The fault strikes northeast-southwest dips almost vertically and is down thrown on the northwestern side. Preliminary investigations indicate that the fault is not capable, but extensive further study is planned.

Subsurface mapping on the fault indicates displacement of approximately 100 feet on the basement surface, 50 feet on the top of the Cretaceous Steel Creek Member, and about 30 feet on the top of the middle Eocene Santee Limestone. There is no subsurface evidence that movement on the fault has occurred since Eocene time. The Eocene epoch ended approximately 36 million years ago. The fault appears to have offset aquitards within the Coastal Plain section allowing lateral communication between the aquifers.

A reflection seismic line suggests another fault approximately 1/2 mile northwest of P Area (Chapman and DiStefano, 1989), but because it seems to have been detected by only one seismic line, its strike cannot be determined. Its upward extent also cannot be determined.

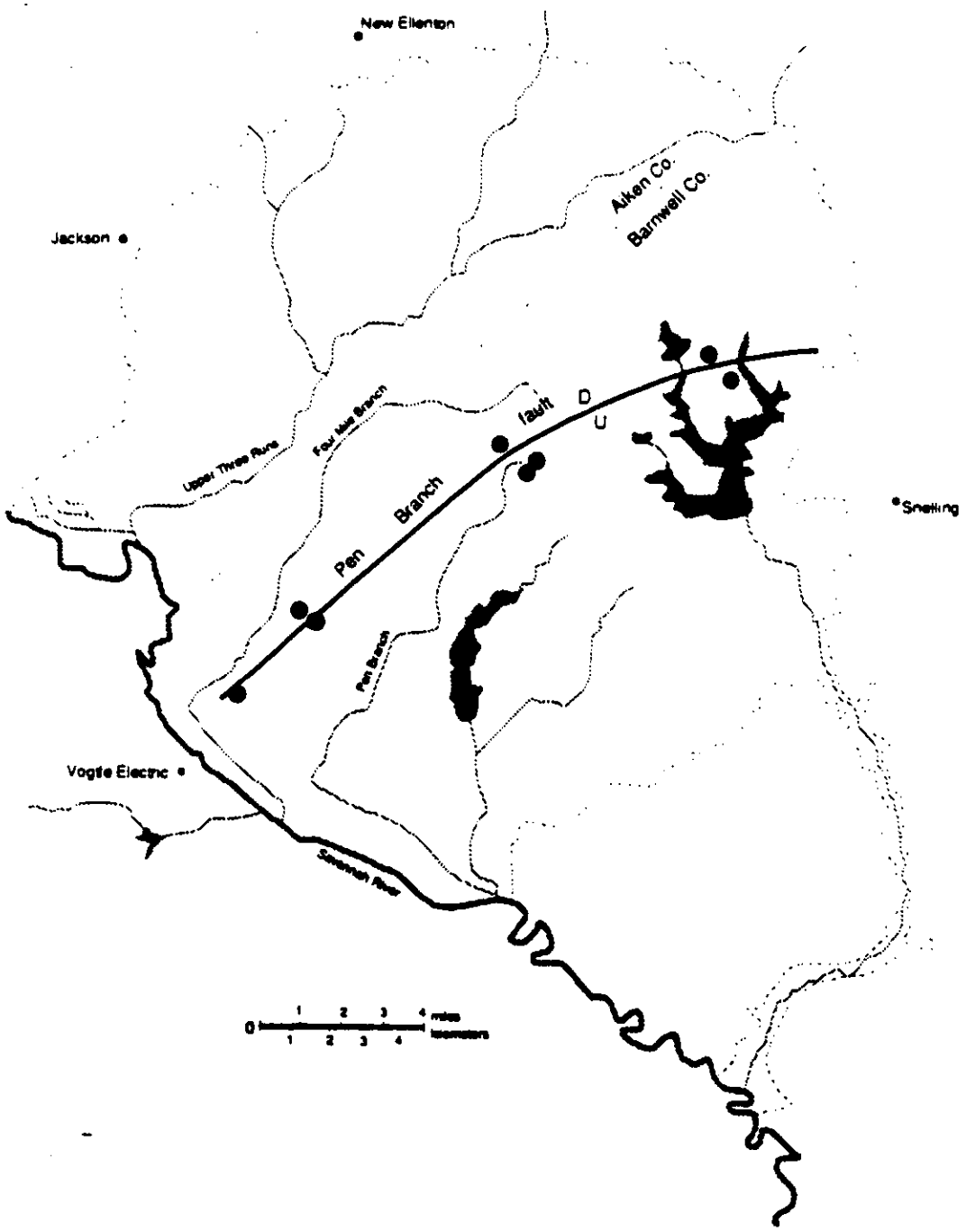

FIGURE 2-37. Pen Branch Fault at SRS

W8907038

2.1.2.5 Geologic History

Igneous and sedimentary rocks originating in pre-Triassic time have been subjected to several periods of deformation and metamorphism. The last period culminated in the formation of the Blue Ridge and Appalachian structures, approximately 300 million years ago, at the close of the Paleozoic Era. During the Triassic, fault bounded structural basins were developed in portions of the crystalline basement. During their development these basins were filled with thick terrestrial sedimentary sequences, which were intruded by diabase sills and dikes. A gently undulating erosional surface subsequently formed over the basement complex and Mesozoic sediments.

The crystalline rocks and Triassic sediments were gently downwarped to the southeast. Fluvial and deltaic sediments began accumulating during late Cretaceous time and the formation of the Coastal Plain began.

Deposition was interrupted several times during this epoch because of drops in sea level. At some time following deposition of the oldest Cretaceous sediments, but before the end of Cretaceous, reverse faulting occurred, causing about 50 feet or less displacement.

During the Paleocene Epoch, fluvial and deltaic environments were again present in the site area, with at least one episode of erosion.

In Eocene time, SRS was occupied by shallow marine environments in which sands, clays, and calcareous sediments were deposited. There were at least two erosional interruptions. Some of the carbonate was later removed by solution.

At some time after deposition of the Eocene sediments, sea level fell and streams cut down into the strata. The valleys were later filled with conglomerates, pebbly sands, and clays.

Erosion has prevailed since then, with deposition occurring mainly in floodplains or incised valleys formed at times of exceptionally low sea levels.

2.1.2.6 Evaluation of Potential Geologic Hazards

Small faults are seen in some soil exposures at the SRS. Most have offsets of only a few inches but offsets up to 23 to 30 inches have been noted. These faults may be related to volume reduction attendant upon lateritic weathering. Interpretation of subsurface profiles, geophysical borehole logs, and the high resolution seismic reflection profiles indicate no geologic structures near the reactor sites that could be interpreted as providing conditions adverse to the construction of any major facility. Within the 5-mile radius of the sites, mining efforts are restricted to borrow areas used in construction. The borrow areas are usually local and shallow, and create no adverse effects on the

subsurface foundation material by the removal of solid material. Irregular weathering profiles have not been observed in the SRS vicinity. Soil horizons are generally uniform and relatively shallow, on the order of several feet. No structures have been identified which would result in adverse effects upon the reactors.

Based on preliminary studies, the Pen Branch Fault does not appear to be active. Extensive further study is planned.

2.1.2.6.1 Carbonate Dissolution

Evaluation of the potential for dissolution and subsequent collapse of subsurface materials is necessary for the Dry Branch and Santee formations. Only the Santee was reported to have contained calcareous material near the reactor sites. This material came from the interval between 140 and 150 feet above msl.

Low penetration values were obtained in nearly every sampling interval during the subsurface investigation of the DWPF site, which is near the reactors. There are five zones where loosely compacted material exists: from 268 to 290 feet above msl, 216 to 263 feet above msl, 190 to 200 feet above msl, 167 to 171 above msl, and 140 to 156 feet above msl. These zones in individual borings generally do not exceed 10 feet in thickness.

As part of the ground preparation for construction at SRS, cement grout was injected into boreholes in all construction areas where tests indicated the presence of porous limestone or loosley compacted material (Corps of Engineers and U.S. Army, 1952).

2.1.2.6.2 Subsidence

Wherever water is drawn from a confined aquifer and a lowering of piezometric surface results, there is a compression of the aquifer and a consequent subsidence of the land surface (Siple, 1967). In the SRS area, the principal aquifer is in Upper Cretaceous strata. In March 1961, several first-order vertical controlled profiles were made across selected areas within the SRS by the U.S. Coast and Geodetic Survey. The purpose of the leveling was two-fold:

- To determine if ground-water withdrawal would cause ground surface subsidence of any measurable amount
- To establish first-order bench marks as a basis for future measurement of subsidence

A comparison of elevations was made between this survey and previous surveys. This comparison did not indicate any significant subsidence due to the withdrawal of fluids from the subsurface. As a result, it is not anticipated that withdrawal of ground water at the reactor sites will result in subsidence. In addition, because the area surrounding the

reactor sites is in a restricted, government-owned area, drilling and mining will be prohibited. As a result, subsidence due to man's activities is not a consideration at this site. In addition to the above-referenced leveling studies, checks have been made for settlement of existing SRS facilities, which are built on materials similar to those at the reactors. No significant settlement has ever been noted.

2.1.2.7 Ground Water

Ground water conditions at the K, L, and P Area are discussed in Section 3, Subsurface Hydrology.

2.2 VIBRATORY GROUND MOTION

The Atlantic Coastal Plain tectonic province, where the SRS is located, is a large area with generally low seismic activity that is expected to remain subdued. High earthquake activity will be confined to the Charleston seismic zone. Currently, the most active seismic zone in the southeast is the southern Appalachian seismic zone. Seismicity in this zone is distributed irregularly in northeast Georgia, western North Carolina, eastern Tennessee, and western Virginia. These areas are all more than 100 miles from the site.

2.2.1 Seismicity

The most damaging earthquake closest to the SRS occurred near Lincolnton, Georgia on November 8, 1875. It was centered about 65 miles to the northwest of the site and had a maximum intensity of VI near the epicenter. A weak tremor from this earthquake may have been felt at the SRS.

The New Madrid, Missouri earthquakes of 1811-1812, centered about 535 miles away, were probably felt at the site with an intensity of less than VI. The Union County, South Carolina earthquake of January 1, 1913 which had an epicentral intensity of VII-VIII, was felt at Aiken with an intensity of II-III (Taber, 1913).

The June 9, 1985 earthquake, centered on the DWPF site, had an epicentral intensity of III and a duration magnitude of 2.6. It was very close to the K Reactor site but was not felt at the P Reactor site.

The source of seismicity most affecting the SRS site, both in terms of intensity and number, is the Charleston, South Carolina area. The main shock of August 31, 1886, probably produced an intensity of VI-VII at the site. Recent studies of the Charleston seismic zone put the closest approach of the zone to the site at about 75 miles to the southeast.

The maximum credible site intensity has been determined to be VI-VII. Conservatively, a design basis earthquake (DBE) of site intensity VII-VIII is chosen. This site intensity is associated with a peak horizontal acceleration of 0.2 g (URS/Blume and Assoc. Engineers, 1982).

2.2.1.1 Geologic Structures and Tectonic Activity

The Dunbarton Triassic Basin is approximately 30 miles south of the Fall Line in the Aiken Plateau subregion of the Atlantic Coastal Plain. Like Mesozoic basins that formed in Piedmont rocks to the north it has a north-east trend, as opposed to the east-west trend of the Mesozoic basins to the southwest. The Dunbarton Basin is recognized as a broad aeromagnetic low, roughly 31-mile-long and 6-mile-wide basin. Marine (1974) and, more recently, Smith and Talwani (1987) have proposed that the basin may be linked to the larger Southeast Georgia Embayment to the southeast, partially separated by an upthrown block of Piedmont affinity to the southwest.

The Dunbarton Basin is overlain by approximately 1100 feet of Coastal Plain sediments (Marine, 1974). At the center of the aeromagnetic low, 3050 feet of Triassic sediments were penetrated (Marine and Sipple, 1974). Although local changes in basement depth and orientation can be observed, the general dip of magnetic basement is to the southeast. The northern border fault of the Dunbarton basin is defined by a low aeromagnetic gradient and correlated with the northern side of a closed magnetic depression (Marine and Sipple, 1974). Well DRB 9 penetrated the northern border fault, represented by a zone of alteration, at a depth of about 2627 feet and passed into crystalline rocks beneath (Marine and Sipple, 1974). A newly delineated subsurface fault, the Pen Branch Fault, runs almost parallel to and may, in part, coincide with the northern border fault of the Dunbarton Basin (Snipes, Fallaw, and Price, 1988). The data used to document the existence of this fault were obtained from cores and geophysical data from 45 wells drilled at SRS and from a seismic reflection survey completed in mid-1988 (Stephenson and Chapman, 1988).

A post-triassic fault postulated at the southern border of the Dunbarton basin, known as the Millett fault (Faye and Prowell, 1982), was subject of recent controversy. The Millett fault was thought to offset Coastal Plain sediments of Triassic, Cretaceous, and Lower Tertiary age, based upon interpretation of stratigraphic and hydraulic anomalies (Faye and Prowell, 1982). The apparent offset along this northeast-trending fault was inferred to be 700 feet at the base of the Cretaceous and 20 feet in strata of late Eocene age (Faye and Prowell, 1982). The lateral extent of the postulated Millett fault within Coastal Plain sediments was thought to coincide with the Ogeechee River in east-central Georgia and the Edisto River in west-central South Carolina. Re-evaluation of this and related geological and geophysical data by the Bechtel Corporation (1982) resulted in a different conclusion. The 1982 report described a possible offset of 50 feet on the top of the Triassic and continuity of all overlying subsurface reflectors across the trace of the postulated Millett fault. Re-evaluation of the well-cuttings in AL 66 supports a Cretaceous rather than a Triassic age as was previously assumed, negating upthrown Triassic rocks as a basis for the fault as was proposed by Faye and Prowell (1982).

2.2.1.2 Behavior During Prior Earthquakes

Using published attenuation relationships and an epicentral intensity of X for the 1886 Charleston earthquake, the calculated site intensity is VI-VII (Heron et al., 1965). This calculated value correlates well with observed values of VI which were assigned to two locations within the SRS boundary.

2.2.1.4 Earthquake History

All significant, reported earthquakes that could have reasonably affected the site region were reviewed and are considered. The site region is defined as that area within 200 miles of the center of the site. All reported earthquakes of Modified Mercalli Index (MMI) IV or greater or magnitude 3.0 or larger within the site region were considered. Earthquakes outside the region but probably felt at the site were also included in the evaluation.

All significant site region earthquakes are listed in Table 2-1. These same data are shown on Figures 2-38 through 2-40, except for the Charleston area, where only those of MMI VI or larger are plotted because of the large number reported.

Most of the information on earthquakes, before the early 1970s, was derived from intensity data, or chronicles of the effects of earthquakes on people, structures, and landforms. Different intensity scales have been used; however, throughout this subsection, the Modified Mercalli Scale of 1931 is used for the descriptive ranking of earthquake effects (a version of this scale is shown in Table 2-2). Epicenters of earlier earthquakes were set at near the center of the maximum shaking as determined by the observed effects (I_o), which depended upon the population distribution. By the mid-twentieth century, instrumental recordings from a few regional seismographic stations improved epicentral locations. Earthquakes listed in Table 2-1 have an uncertainty in epicenter location of about 15 miles. This is estimated to be representative of the uncertainty in earthquake locations for the site region events averaged over the chronological range of their occurrence. This uncertainty is an average. For some of the events, the actual uncertainty is probably several times greater.

The detection and location of earthquakes in the region greatly improved in the 1970s with the installation of seismic networks in the eastern United States. A seismic network was established on the SRS in 1976. Recent events, recorded with the new instruments, are listed in Table 2-3. These locations have an uncertainty in epicentral position on the order of three miles. This precision has also been given for events before the early 1970s that were relocated in Snipes et al. (1988).

Few focal depths have been determined for events before the early 1970s. In the relocation of earthquakes, Dewey (Dewey, 1985) notes that few of the calculated focal depths are estimated to be precise to about six

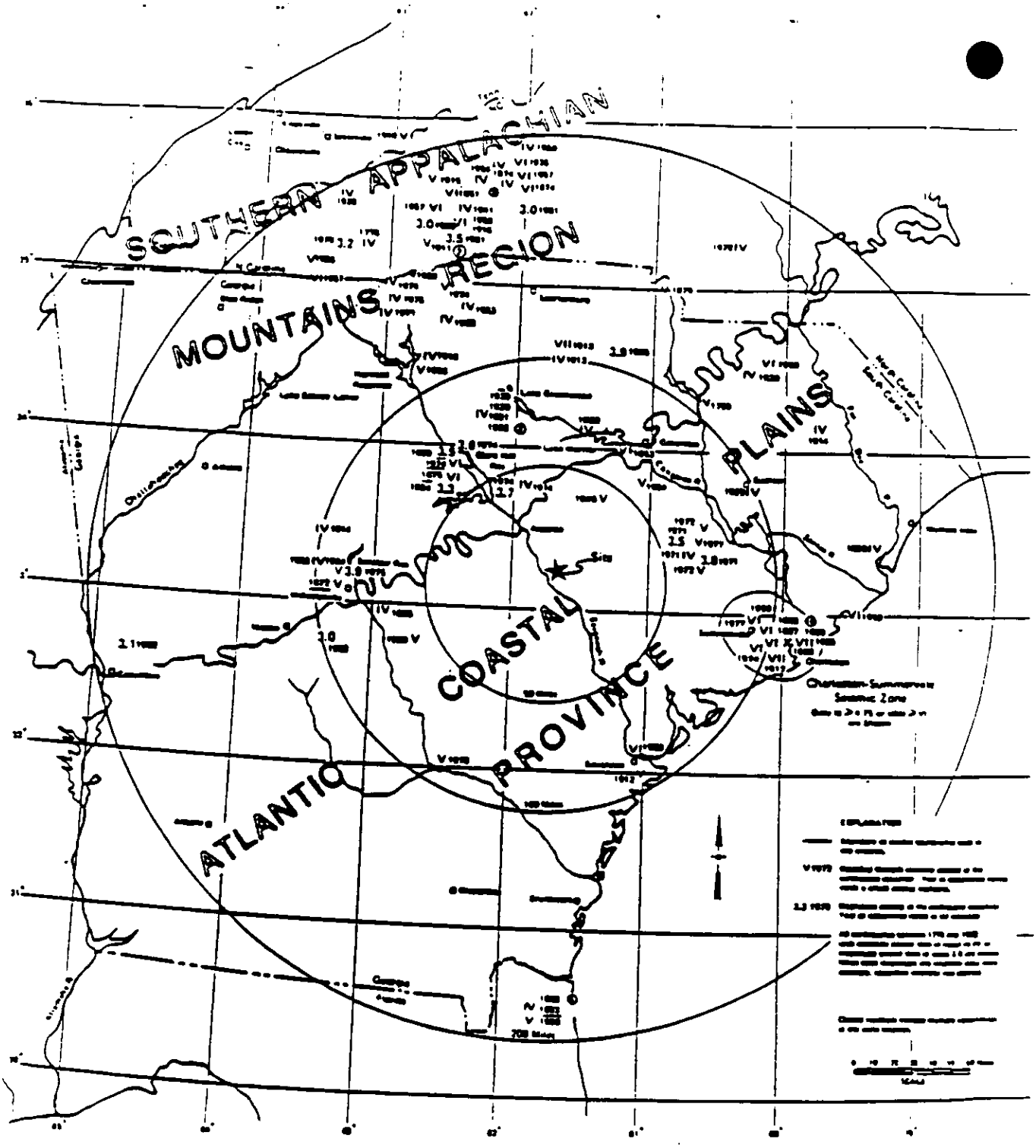

FIGURE 2-38. Seismic Map of Eastern United States

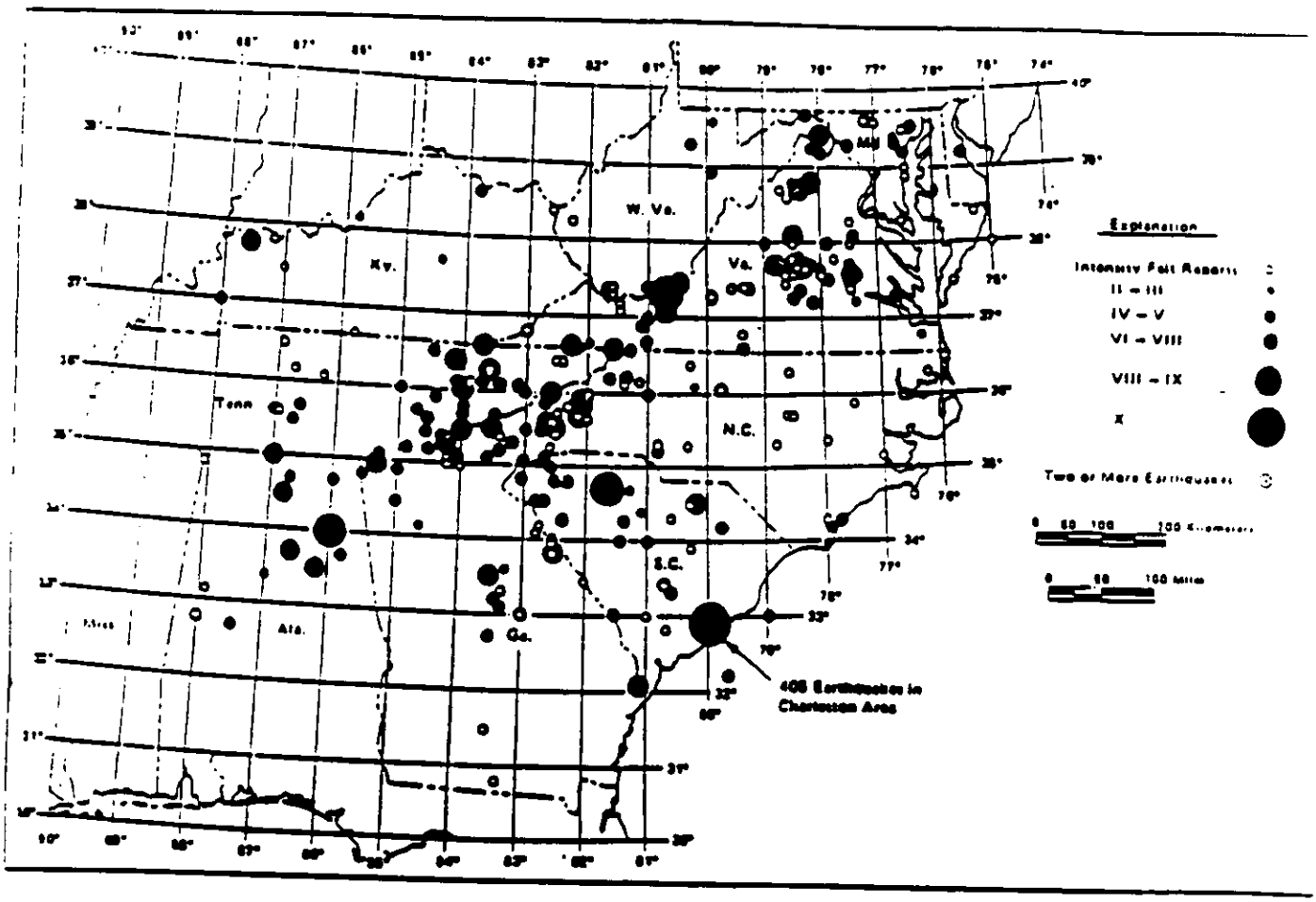

FIGURE 2-39. Distribution of Seismic Events, 1754 Through 1971 (Bollinger, 1975)

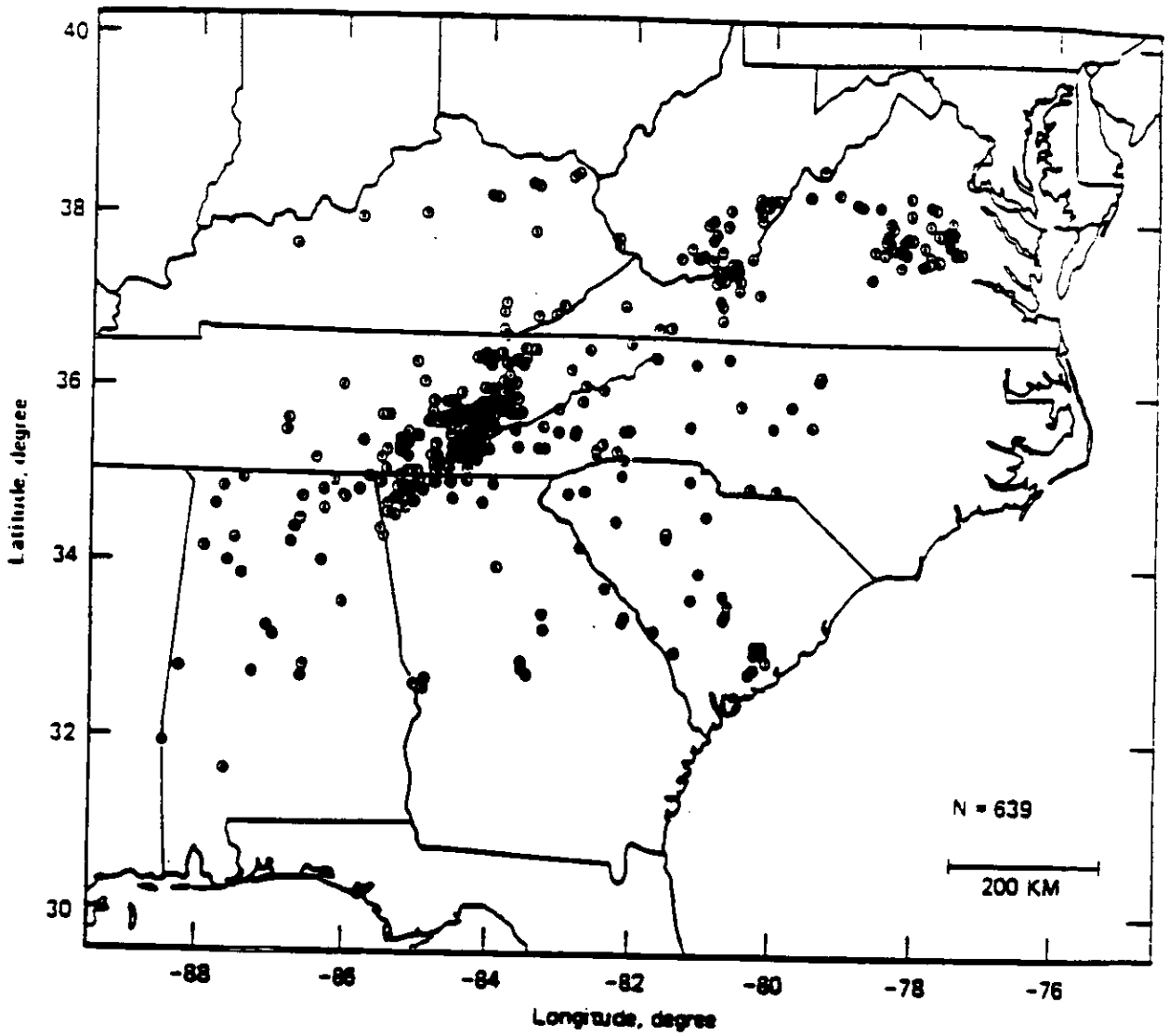

Instrumental Seismicity in the
Southeastern United States
(July 1977-June 1987)
from Bollinger et al. (1987)

FIGURE 2-40. Instrumental Seismicity in the Southeastern United States (July 1977 through June 1987) (Bollinger et al., 1987)

TABLE 2-1

Significant Earthquakes Within 200 Miles of the SRS (Intensity ≥IV or Magnitude ≥2)

Date Year	GMT Mo	Day	Hour	Min	Sec	Location °N	°W	Depth[a] Mile	MMI	Mag.[b]	Dist. Mile	Data Source
1776	11	5	-	-	-	35.3	83.2	-	IV	-	170	BOL
1799	4	4	-	-	-	32.9	80.0	-	V	-	105	STR
1799	4	11	8	20	-	32.9	80.0	-	V	-	105	STR
1799	4	11	14	55	-	34.3	80.6	-	V	-	105	BOL
1817	1	8	4	1	1	32.8	79.8	-	V	-	115	BOL
1820	9	3	8	30	-	33.4	79.3	-	IV	-	145	STR
1851	8	11	1	55	-	35.6	82.6	-	V	-	175	STR
1853	5	20	-	-	-	34.0	81.2	-	VI	-	70	STR
1857	12	19	9	4	-	32.8	79.8	-	V	-	115	BOL
1860	1	16	18	-	-	32.8	79.8	-	V	-	115	BOL
1869	0	0	-	-	-	32.9	80.0	-	IV	-	105	STR
1872	6	17	20	-	-	33.1	83.3	-	V	-	90	EQH
1874	2	10	-	-	-	35.7	82.1	-	VI	-	175	BOL
1874	2	22	-	-	-	35.7	82.1	-	IV	-	175	EUS
1874	3	17	-	-	-	35.7	82.1	-	IV	-	175	EUS
1874	3	26	-	-	-	35.7	82.1	-	VI	-	175	EUS
1874	4	14	-	-	-	35.7	82.1	-	IV	-	175	EUS
1874	4	17	-	-	-	35.7	82.1	-	IV	-	175	EUS
1875	11	2	2	55	-	33.8	82.5	-	VI	-	60	EUS
1876	12	12	-	-	-	32.9	80.0	-	IV	-	105	STR
1879	12	13	-	-	-	35.0	80.9	-	V	-	140	EUS
1885	10	17	17	30	-	33.0	83.0	-	IV	-	70	BOL
1886	8	27	8	30	-	33.0	80.2	-	V	-	90	BOL
1886	8	28	8	45	-	32.9	80.0	-	VI	-	105	STR
1886	8	28	9	40	-	32.9	80.0	-	IV	-	105	STR
1886	8	28	18	20	-	32.9	80.0	-	IV	-	105	STR
1886	9	1	2	51	-	32.9	80.0	-	X	-	105	EQH
1886	9	1	6	5	-	32.9	80.0	-	VI	-	105	STR
1886	9	2	4	55	-	32.9	80.0	-	V	-	105	STR
1886	9	3	21	-	-	30.4	81.7	-	IV	-	190	STR
1886	9	4	4	1	-	32.9	80.0	-	VI	-	105	STR
1886	9	4	9	-	-	30.4	81.7	-	IV	-	190	STR
1886	9	5	-	-	-	30.4	81.7	-	IV	-	190	STR
1886	9	6	4	6	-	32.9	80.0	-	VI	-	105	STR
1886	9	6	16	35	-	32.9	80.0	-	IV	-	105	STR
1886	9	8	-	-	-	30.4	81.7	-	IV	-	190	STR
1886	9	9	18	47	-	30.4	81.7	-	IV	-	190	STR
1886	9	17	6	29	-	32.9	80.0	-	VI	-	105	STR
1886	9	21	10	15	-	32.9	80.0	-	VI	-	105	STR
1886	9	21	10	30	-	32.9	80.0	-	V	-	105	STR
1886	9	27	19	2	-	32.9	80.0	-	VI	-	105	STR
1886	9	27	22	2	-	32.9	80.0	-	V	-	105	STR

TABLE 2-1. Contd

Date Year	GMT Mo	Day	Hour	Min	Sec	Location °N	°W	Depth[a] Mile	MMI	Mag.[b]	Dist. Mile	Data Source
1886	10	9	3	40	-	32.9	80.0	-	IV	-	105	STR
1886	10	9	5	40	-	32.9	80.0	-	IV	-	105	STR
1886	10	9	6	48	-	32.9	80.0	-	VI	-	105	STR
1886	10	22	10	20	-	32.9	80.0	-	VI	-	105	EQH
1886	10	22	19	45	-	32.9	80.0	-	VII	-	105	EQH
1886	10	23	1	7	-	32.9	80.0	-	IV	-	105	STR
1886	11	5	17	20	-	32.9	80.0	-	VI	-	105	EQH
1886	11	28	20	13	-	32.9	80.0	-	IV	-	105	STR
1887	1	4	11	44	-	32.9	80.0	-	VI	-	105	STR
1887	3	4	7	-	-	32.9	80.0	-	IV	-	105	STR
1887	3	17	14	9	-	32.9	80.0	-	V	-	105	STR
1887	3	18	23	10	-	32.9	80.0	-	IV	-	105	STR
1887	3	19	-	-	-	32.9	80.0	-	IV	-	105	STR
1887	3	24	-	-	-	32.9	80.0	-	IV	-	105	EQH
1887	3	24	4	5	-	32.9	80.0	-	IV	-	105	STR
1887	3	28	-	-	-	32.9	80.0	-	IV	-	105	STR
1887	4	7	4	-	-	32.9	80.0	-	IV	-	105	STR
1887	4	8	8	-	-	32.9	80.0	-	IV	-	105	STR
1887	4	10	11	30	-	32.9	80.0	-	IV	-	105	STR
1887	4	14	7	25	-	32.9	80.0	-	IV	-	105	STR
1887	4	26	10	-	-	32.9	80.0	-	IV	-	105	STR
1887	4	28	8	-	-	32.9	80.0	-	V	-	105	STR
1887	5	6	-	-	-	32.9	80.0	-	IV	-	105	STR
1887	6	3	12	-	-	32.9	80.0	-	IV	-	105	STR
1887	7	10	18	-	-	21.9	80.0	-	IV	-	105	STR
1887	8	27	4	30	-	32.9	80.0	-	V	-	105	STR
1887	8	27	9	20	-	32.9	80.0	-	IV	-	105	STR
1888	1	12	15	54	-	32.9	80.0	-	VI	-	105	STR
1888	1	16	17	52	-	32.9	80.0	-	IV	-	105	STR
1888	2	29	11	-	-	32.9	80.0	-	V	-	105	STR
1888	3	3	-	-	-	32.9	80.0	-	IV	-	105	STR
1888	3	3	4	30	-	32.9	80.0	-	IV	-	105	STR
1888	3	4	-	-	-	32.9	80.0	-	IV	-	105	STR
1888	3	14	5	-	-	32.9	80.0	-	V	-	105	STR
1888	3	20	5	-	-	32.9	80.0	-	IV	-	105	STR
1888	3	25	-	-	-	32.9	80.0	-	VI	-	105	STR
1888	4	16	-	-	-	32.9	80.0	-	IV	-	105	STR
1888	4	16	-	-	-	32.9	80.0	-	IV	-	105	STR
1888	4	16	-	-	-	32.9	80.0	-	IV	-	105	STR
1888	5	2	-	-	-	32.9	80.0	-	IV	-	105	STR
1889	2	10	-	31	-	32.9	80.0	-	IV	-	105	STR
1889	7	12	2	54	-	32.9	80.0	-	IV	-	105	STR
1891	10	13	5	55	-	32.9	80.0	-	IV	-	105	STR
1893	6	21	4	5	-	32.9	80.0	-	V	-	105	STR
1893	6	21	7	7	-	32.9	80.0	-	IV	-	105	STR

TABLE 2-1, Contd

Date Year	GMT Mo	Day	Hour	Min	Sec	Location °N	°W	Depth[a] Mile	MMI	Mag.[b]	Dist. Mile	Data Source
1893	7	5	8	10	-	32.9	80.0	-	IV	-	105	STR
1893	7	6	9	5	-	32.9	80.0	-	IV	-	105	STR
1893	7	8	7	48	-	32.9	80.0	-	IV	-	105	STR
1893	7	8	15	25	-	32.9	80.0	-	IV	-	105	STR
1893	9	19	7	5	-	32.9	80.0	-	IV	-	105	STR
1893	9	19	7	40	-	32.9	80.0	-	IV	-	105	STR
1893	9	19	8	55	-	32.9	80.0	-	IV	-	105	STR
1893	11	8	4	40	-	32.9	80.0	-	IV	-	105	STR
1893	11	8	6	5	-	32.9	80.0	-	IV	-	105	STR
1893	12	27	6	51	-	32.9	80.0	-	IV	-	105	STR
1893	12	27	7	17	-	32.9	80.0	-	IV	-	105	STR
1893	12	27	9	9	-	32.9	80.0	-	IV	-	105	STR
1893	12	27	9	56	-	32.9	80.0	-	IV	-	105	STR
1893	12	28	9	20	-	32.9	80.0	-	IV	-	105	STR
1894	1	10	8	5	-	32.9	80.0	-	IV	-	105	STR
1894	1	10	8	49	-	32.9	80.0	-	IV	-	105	STR
1894	1	10	9	15	-	32.9	80.0	-	IV	-	105	STR
1894	1	30	4	5	-	32.9	80.0	-	IV	-	105	STR
1894	2	1	5	21	-	32.9	80.0	-	IV	-	105	STR
1894	6	16	2	16	-	32.9	80.0	-	IV	-	105	STR
1894	12	11	5	27	-	32.9	80.0	-	IV	-	105	STR
1895	1	8	5	40	-	32.9	80.0	-	IV	-	105	STR
1895	1	8	5	58	-	32.9	80.0	-	IV	-	105	STR
1895	1	8	7	29	-	32.9	80.0	-	IV	-	105	STR
1895	4	27	7	40	-	32.9	80.0	-	IV	-	105	STR
1895	7	25	4	1	-	32.9	80.0	-	IV	-	105	STR
1895	10	6	6	25	-	32.9	80.0	-	IV	-	105	STR
1895	10	20	17	8	-	32.9	80.0	-	IV	-	105	STR
1895	11	12	23	33	-	32.9	80.0	-	IV	-	105	STR
1896	3	19	8	22	-	32.9	80.0	-	IV	-	105	STR
1896	8	11	5	58	-	32.9	80.0	-	IV	-	105	STR
1896	8	11	6	14	-	32.9	80.0	-	IV	-	105	STR
1896	8	11	8	15	-	32.9	80.0	-	IV	-	105	STR
1896	8	11	9	24	-	32.9	80.0	-	IV	-	105	STR
1896	8	12	7	42	-	32.9	80.0	-	IV	-	105	STR
1896	8	14	5	45	-	32.9	80.0	-	IV	-	105	STR
1896	8	30	3	24	-	32.9	80.0	-	IV	-	105	STR
1896	9	8	18	16	-	32.9	80.0	-	IV	-	105	STR
1896	11	14	8	15	-	32.9	80.0	-	IV	-	105	STR
1899	3	10	5	45	-	32.9	80.0	-	IV	-	105	STR
1899	12	4	12	48	-	32.9	80.0	-	IV	-	105	STR
1900	10	31	16	15	-	30.4	81.7	-	V	-	190	EQH
1901	12	2	0	26	-	32.9	80.0	-	IV	-	105	STR
1903	1	24	1	-	-	32.9	80.0	-	IV	-	105	STR
1903	1	24	1	15	-	32.1	81.1	-	VI	-	80	EQH

TABLE 2-1. Contd

Date - Year	GMT Mo	Day	Hour	Min	Sec	Location °N	°W	Depth[a] Mile	MMI	Mag.[b]	Dist. Mile	Data Source
1903	1	31	10	54	-	32.9	80.0	-	IV	-	105	STR
1903	2	3	10	6	-	32.9	80.0	-	IV	-	105	STR
1907	4	19	8	30	-	32.9	80.0	-	V	-	105	EUS
1911	4	20	22	-	-	35.2	82.7	-	V	-	150	BOL
1911	4	21	3	-	-	35.2	82.7	-	V	-	150	EUS
1912	6	12	10	30	-	32.9	80.0	-	VII	-	105	EUS
1912	6	20	-	-	-	32.0	81.0	-	V	-	90	EUS
1912	9	29	8	6	-	32.9	80.0	-	IV	-	105	STR
1912	10	23	1	15	-	32.7	83.5	-	IV	-	105	STR
1913	1	1	18	28	-	34.7	81.7	-	IV	-	105	STR
1914	3	5	20	5	-	34.7	81.7	-	VII	-	105	EQH
1914	3	7	1	20	-	33.5	83.5	-	VI	-	100	EQH
1914	7	13	20	53	-	34.2	79.8	-	IV	-	135	STR
1914	9	22	2	4	-	33.0	80.2	-	IV	-	90	BOL
1915	10	29	6	-	-	33.0	80.2	-	V	-	90	BOL
1916	2	21	17	39	-	35.8	82.7	-	V	-	190	EQH
1916	3	2	5	2	-	35.5	82.5	-	VII	-	170	BOL
1923	12	31	20	6	-	34.5	82.7	-	IV	-	105	EUS
1924	10	20	8	20	-	34.8	82.5	-	IV	-	120	BOL
1926	7	8	9	50	-	35.0	82.6	-	V	-	135	EQH
1928	11	20	3	45	-	35.9	82.1	-	VI	-	190	EQH
1928	12	23	2	30	-	35.8	82.3	-	IV	-	185	STR
1929	1	3	12	5	-	35.3	80.3	-	IV	-	170	STR
1929	10	28	2	15	-	33.9	80.3	-	IV	-	100	STR
1930	12	10	0	2	-	34.3	82.4	-	IV	-	85	STR
1930	12	26	3	-	-	34.3	82.4	-	IV	-	85	STR
1931	5	6	12	18	-	34.5	80.3	-	IV	-	125	STR
1933	6	9	11	30	-	34.3	82.4	-	IV	-	85	STR
1933	12	19	14	12	-	33.3	83.5	-	IV	-	100	STR
1933	12	23	9	40	-	33.0	80.2	-	IV	-	90	EUS
1933	12	23	9	55	-	32.9	80.0	-	V	-	105	BOL
1934	12	9	5	-	-	32.9	80.0	-	IV	-	105	STR
1935	1	1	3	15	-	33.0	80.2	-	IV	-	90	BOL
1938	3	31	10	10	-	35.1	83.6	-	V	-	170	BOL
1940	12	25	-	-	-	35.6	83.5	-	IV	3.8	195	NUT
1941	5	10	11	12	-	35.9	82.9	-	V	-	200	USE
1943	12	28	10	25	-	35.6	82.6	-	IV	-	175	STR
1944	1	28	17	30	-	33.0	80.2	-	IV	-	90	BOL
1945	1	30	20	20	-	32.9	80.0	-	IV	-	105	STR
1945	7	26	10	32	16	32.9	80.0	-	IV	-	105	STR
1947	11	2	4	30	-	33.8	81.4	-	V	4.4	48	D&G
1949	2	2	10	52	-	32.9	80.0	-	IV	-	105	STR
1949	6	27	6	53	-	32.9	80.0	-	IV	-	105	STR
1951	3	4	2	55	-	32.9	80.0	-	V	-	105	STR
									IV	-	105	STR

TABLE 2-1, Contd

Date Year	GMT Mo	Day	Hour	Min	Sec	Location °N	°W	Depth[a] Mile	MMI	Mag.[b]	Dist. Mile	Data Source
1951	12	30	7	55	-	32.9	80.0	-	IV	-	105	STR
1952	11	19	-	-	-	32.8	80.0	-	V	-	105	BOL
1956	1	5	3	-	-	34.3	82.4	-	IV	-	85	BOL
1956	5	19	14	-	-	34.3	82.4	-	IV	-	85	BOL
1956	5	27	18	25	-	34.3	82.4	-	IV	-	85	BOL
1957	5	13	14	24	51	35.8	82.1	3*	IV	4.1	185	D&G
1957	7	2	9	33	1	35.6	82.6	-	IV	4.6	175	EUS
1957	11	24	20	6	17	35.0	83.5	-	IV	-	160	BOL
1958	5	16	22	30	-	35.6	82.6	-	V	-	110	BOL
1959	8	3	6	8	37	33.1	80.1	1*	VI	4.4	96	D&G
1959	8	8	6	8	30	33.0	79.5	-	VI	-	135	BOL
1959	10	27	2	7	28	34.5	80.2	-	VI	-	130	EUS
1960	1	3	7	30	-	35.9	82.1	-	IV	-	190	STR
1960	3	12	4	47	44	33.07	80.12	6	V	4.0	96	D&G
1960	7	23	-	-	-	33.0	80.0	-	V	-	105	USE
1960	7	28	3	37	30	32.8	82.7	-	V	-	60	EUS
1963	4	11	17	45	-	34.9	82.4	-	IV	-	125	EUS
1963	5	4	21	1	50	32.97	80.19	3*	IV	3.3	93	D&G
1964	1	20	13	37	52	35.9	82.3	-	IV	-	190	EUS
1964	3	7	18	2	59	33.72	82.39	3	-	3.3	53	D&G
1964	3	13	1	20	18	33.19	82.31	1*	V	3.9	89	D&G
1964	4	20	19	4	44	33.84	81.10	2	V	3.5	62	D&G
1965	9	9	14	42	20	34.7	81.2	-	-	3.9	110	STR
1967	10	23	9	4	3	32.80	80.22	12	V	3.4	94	D&G
1968	7	12	1	12	1	32.8	79.7	-	IV	-	125	STR
1968	9	22	21	41	18	34.11	81.48	1*	IV	3.5	69	D&G
1969	5	18	-	-	-	34.0	82.6	-	V	3.5M1	75	STR
1969	12	13	10	19	30	35.04	82.85	4	IV	4.4	145	D&G
1971	5	19	12	54	4	33.36	80.65	1*	VI	3.7	67	D&G
1971	7	13	6	42	26	34.8	83.0	-	IV	3.8	135	BOL
1971	7	31	20	16	55	33.34	80.63	2	III	3.8	68	D&G
1971	8	11	3	50	-	33.4	80.7	-	-	3.5	65	BOL
1972	2	3	23	11	10	33.31	80.58	1	V	4.5	71	D&G
1973	12	19	10	16	9	32.97	80.27	4	-	3.0	88	D&G
1974	8	2	8	52	11	33.91	82.53	2	VI	4.1	68	D&G
1974	10	28	11	33	-	33.79	81.92	-	IV	3.0	45	CSC
1974	11	5	3	-	-	33.73	82.22	-	III	3.7	48	CSC
1974	11	22	5	25	56	32.92	80.14	5	VI	4.3	96	D&G/BOL
1974	12	3	8	25	-	33.95	82.50	-	III	3.6	69	CSC
1975	4	1	21	9	-	33.20	83.20	-	-	3.9M1	82	STR
1975	4	28	5	46	53	33.00	80.22	6	IV	3.0M1	91	STR
1975	10	18	4	31	-	34.90	83.00	-	IV	-	140	STR
1975	11	25	15	17	35	34.93	82.93	1	IV	3.2	140	D&G/GS
1976	12	27	6	57	15	32.06	82.50	9	V	3.7	86	D&G/GS
1977	1	18	18	29	14	33.04	80.21	7	VI	3.0M1	91	STR

TABLE 2-1. Contd

Date Year	GMT Mo	Day	Hour	Min	Sec	Location °N	°W	Depth[a] Mile	MMI	Mag.[b]	Dist. Mile	Data Source
1977	3	30	8	27	48	32.95	80.18	5	V	2.9Ms	94	STR
1977	8	25	4	20	7	33.39	80.69	-	V	3.1	65	GS
1977	12	15	19	16	43	32.92	80.22	-	V	3.0	92	GS
1979	9	6	20	38	16	35.30	83.24	6	-	3.2Ml	171	VPI
1980	6	10	23	47	32	35.46	82.81	1*	-	3.0	170	VPI
1981	4	9	7	10	31	35.51	82.05	-	-	3.0	164	VPI
1981	5	5	21	21	57	35.33	82.42	6	-	3.5	155	VPI
1982	3	1	3	33	13	32.94	80.14	-	-	2.8	78	BOL
1982	10	31	3	7	37	32.67	84.87	0*	-	3.0	192	BOL
1982	10	31	3	12	12	32.64	84.89	0*	-	3.1	194	BOL
1982	12	11	0	25	-	32.85	83.53	0	-	3.0Ml	113	BOL
1983	1	26	14	7	47	32.85	83.56	-	-	3.5	115	BOL
1983	3	25	2	47	11	35.33	82.46	-	V	3.3	154	BOL
1983	11	6	9	2	20	32.94	80.16	-	V	3.3	87	BOL
1984	3	7	20	47	7	34.32	81.32	-	-	2.0	78	RIS
1984	4	18	5	41	1	33.86	82.53	-	-	2.5	69	RIS
1984	4	19	2	53	53	33.87	82.44	-	-	2.1	66	RIS
1984	4	19	2	58	44	33.87	82.43	-	-	2.0	66	RIS
1984	6	13	9	4	35	33.92	82.43	-	-	2.1	68	RIS
1984	9	2	22	46	44	32.94	80.21	-	-	2.0	84	-
1984	10	1	18	24	22	35.31	83.61	-	-	2.0	186	-
1984	12	23	20	12	53	35.55	83.26	-	-	2.2	188	-
1985	1	15	17	48	38	34.33	81.30	-	-	2.0	80	RIS
1985	1	29	1	56	58	33.98	82.50	-	-	2.0	74	-
1985	3	19	0	2	6	35.30	82.52	-	-	2.1	154	FELT
1985	4	20	5	33	35	34.32	81.33	-	-	2.0	79	RIS
1985	5	19	23	29	14	33.01	80.16	-	-	2.1	86	-
1985	6	9	0	38	43	33.22	81.70	-	III	2.7	4	-
1985	12	22	0	56	5	35.70	83.72	8.4	-	3.3	206	TEIC
1986	2	13	11	35	46	34.76	82.94	-	V	3.5	132	-
1986	3	9	23	49	15	32.97	80.17	-	III	2.2	86	-
1986	3	13	2	29	31	33.23	83.23	-	IV	2.4	93	-
1986	9	17	9	33	49	32.93	80.15	-	IV	2.6	88	-
1987	3	16	13	9	-	34.55	80.95	8.0	-	3.2	95	TEIC
1987	12	12	3	53	29	34.24	82.63	-	IV	3.0	93	-
1988	1	23	1	57	16	32.95	80.18	-	V	3.3	85	-
1988	2	17	17	33	33	33.61	81.72	-	-	2.5	28	FELT
1988	2	18	0	37	46	35.37	83.85	-	IV	3.5	198	-

[a] Asterisk (*) indicates that the depth has been constrained to enable stable earthquake location solution.

[b] Magnitude is given as body wave magnitude (mb), unless otherwise specified as local magnitude (Ml) or surface wave magnitude (Ms).

TABLE 2-2

Modified Mercalli Intensity Scale

I. Not felt except by a very few under especially favorable circumstances (I Rossi-Forel Scale).

II. Felt only by a few persons at rest, especially on upper floors of buildings. Delicately suspended objects may swing (I to II, Rossi-Forel Scale).

III. Felt quite noticeably indoors, especially on upper floors of buildings, but many people do not recognize it as an earthquake. Standing motor cars may rock slightly. Vibration like passing truck. Duration estimated (III Rossi-Forel Scale).

IV. During the day felt indoors by many; outdoors by few. At night some awakened. Dishes, windows, doors disturbed; walls made cracking sound. Sensation like heavy truck striking building. Standing motor cars rocked noticeably (IV to V Rossi-Forel Scale).

V. Felt by nearly everyone; many awakened. Some dishes, windows, etc., broken, a few instances of cracked plaster, unstable objects overturned. Disturbance of trees, poles, and other tall objects sometimes noticed. Pendulum clocks may stop (V to VI Rossi-Forel Scale).

VI. Felt by all; many are frightened and run outdoors. Some heavy furniture moved; a few instances of fallen plaster or damaged chimneys. Damage slight (Vi to VII Rossi-Forel Scale).

VII. Everybody runs outdoors. Damage negligible in buildings of good structures; considerable in poorly built or badly designed structures; some chimneys are broken. Noticed by persons driving motor cars (VIII Rossi-Forel Scale).

VIII. Damage slight in specially designed structures; considerable in ordinary substantial buildings with partial collapse; great in poorly built structures. Panel walls thrown out of frame structures. Fall of chimneys, factory stacks, columns, monuments, walls. Heavy furniture overturned. Sand and mud ejected in small amounts. Changes in well water. Disturbs persons driving motor cars (VIII+ to IX Rossi-Forel Scale).

IX. Damage considerable in specially designed structures; well designed frame structures thrown out of plumb; great in substantial buildings, with partial collapse. Buildings shifted off foundations. Ground cracked conspicuously. Underground pipes broken (IX+ Rossi-Forel Scale).

TABLE 2-2, Contd

X. Some well-built wooden structures destroyed; most masonry and frame structures destroyed, with foundations and ground badly cracked. Rails bent. Landslides considerable from river banks and steep slopes. Shifted sand and mud. Water splashed (slopped) over banks (X Rossi-Forel Scale).

XI. Few, if any, masonry structures remain standing. Bridges destroyed. Broad fissures in ground. Underground pipe lines completely out of service. Earth slumps and land slides in soft ground. Rails bent greatly.

XII. Damage total. Waves seen on ground surfaces. Lines of sight and level distorted. Objects thrown upward into the air.

TABLE 2-3

Recent Recorded Earthquakes Near the SRS

Date	Origin Time (UTC)	Latitude (°N)	Longitude (°W)	Magnitude M(M_L)
08-14-72	15:05:60	33.2	81.4	3.0 (USGS)
09-15-76	05:15:35.44	33.14	81.41	2.5 (SRS)
06-05-77	00:42:29.73	33.05	81.41	2.7 (USGS)
01-28-82	05:52:52.10	32.98	81.39	3.4 (USGS)
06-09-85	00:38:42.93	33.22	81.69	2.6 (SRS)
08-05-88	03:59:21.80	33.13	81.40	2.0 (SRS)

miles, although data do indicate that most small to moderate earthquakes in the eastern United States typically occur in the upper part of the earth's crust (about 20 miles in the region). Since the mid-1970s, earthquakes for which focal depth has been determined generally have a precision of about one mile.

The magnitude of an earthquake depends upon the amplitude of the motion on a standard instrument normalized to take into account the separation of the earthquake location from the instrumental recording site. In the site region, several magnitude scales are commonly employed which are not exactly equivalent; however, the magnitudes reported are approximately equivalent to body wave magnitude. The uncertainty in instrumentally determined magnitudes is about ±0.3 magnitude units. For magnitudes estimated from intensity information, intensity falls off with distance and extent of felt area provides uncertainty values of ±0.4 to 0.6.

The highest estimated intensity at the site is MMI VI-VII, which is associated with the August 31, 1886, Charleston, South Carolina earthquake. A detailed isoseismal map of the State of South Carolina for the 1886 earthquake is shown on Figure 2-41. On June 9, 1985, an intensity III earthquake with a local magnitude of 2.6 occurred on the SRS. The isoseismal map of this event is shown on Figure 2-42. Two other earthquakes with intensities of IV or greater have been reported within about 50 miles of the site; the July 26, 1945, intensity V event to the northeast, and the October 28, 1974, intensity IV earthquake to the north. There are no specific felt reports at the site for these events. A SRS survey following the 1974 event indicates that it was felt by a few individuals.

Most recently, on August 5, 1988, an earthquake of local magnitude 2.0 and intensity of I-II (MMI) occurred. The focal depth was estimated as 2.86 kkm. The event was not felt on site and the seismic alarms in plant facilities were not activated. Also, the earthquake was only detected by seismometers within about 100 km of SRS.

An earthquake of epicentral intensity greater than or equal to VII occurred near the Charleston area on January 1, 1913, in Union County. This earthquake, which occurred about 100 miles north-northeast of the site, had an epicentral intensity of VII-VIII. This earthquake was felt at Aiken with an MMI II-III (Taber, 1913).

Several other earthquakes, including some of the aftershocks from the 1886 Charleston event, are estimated to have been felt at the site with an intensity equal to or less than MMI IV.

Several large earthquakes more than 200 miles away are significant in evaluating the site. The New Madrid earthquake sequence of 1811-1812 occurred about 550 miles west-northwest of the site, but was probably felt at the site.

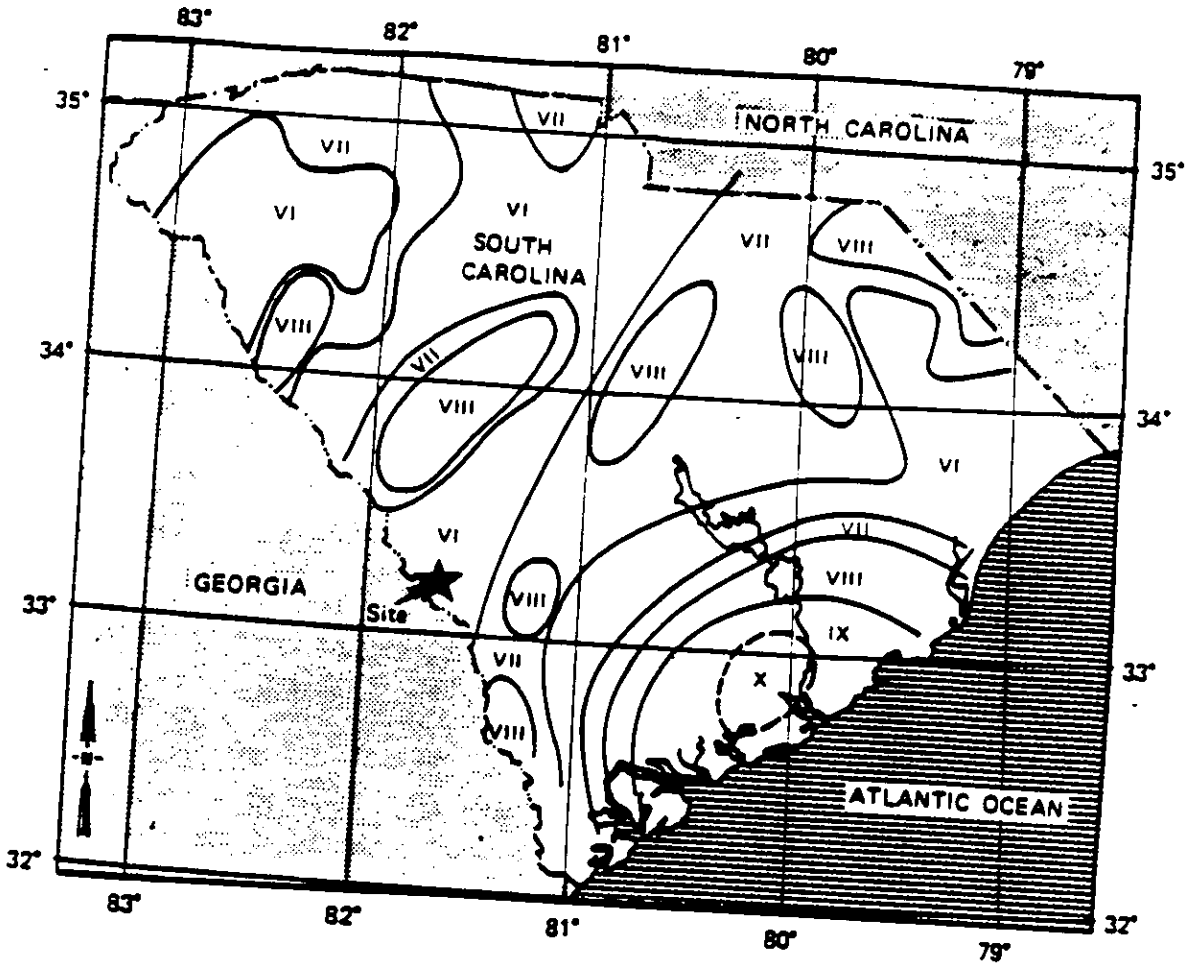

EXPLANATION

Detailed isoseismal map for the State of South Carolina for the 1886 Charleston earthquake.

REFERENCE:

G. A. Bollinger, 1977.

FIGURE 2-41. Isoseismal Map of South Carolina for 1988 Charleston Earthquake (Bollinger, 1977)

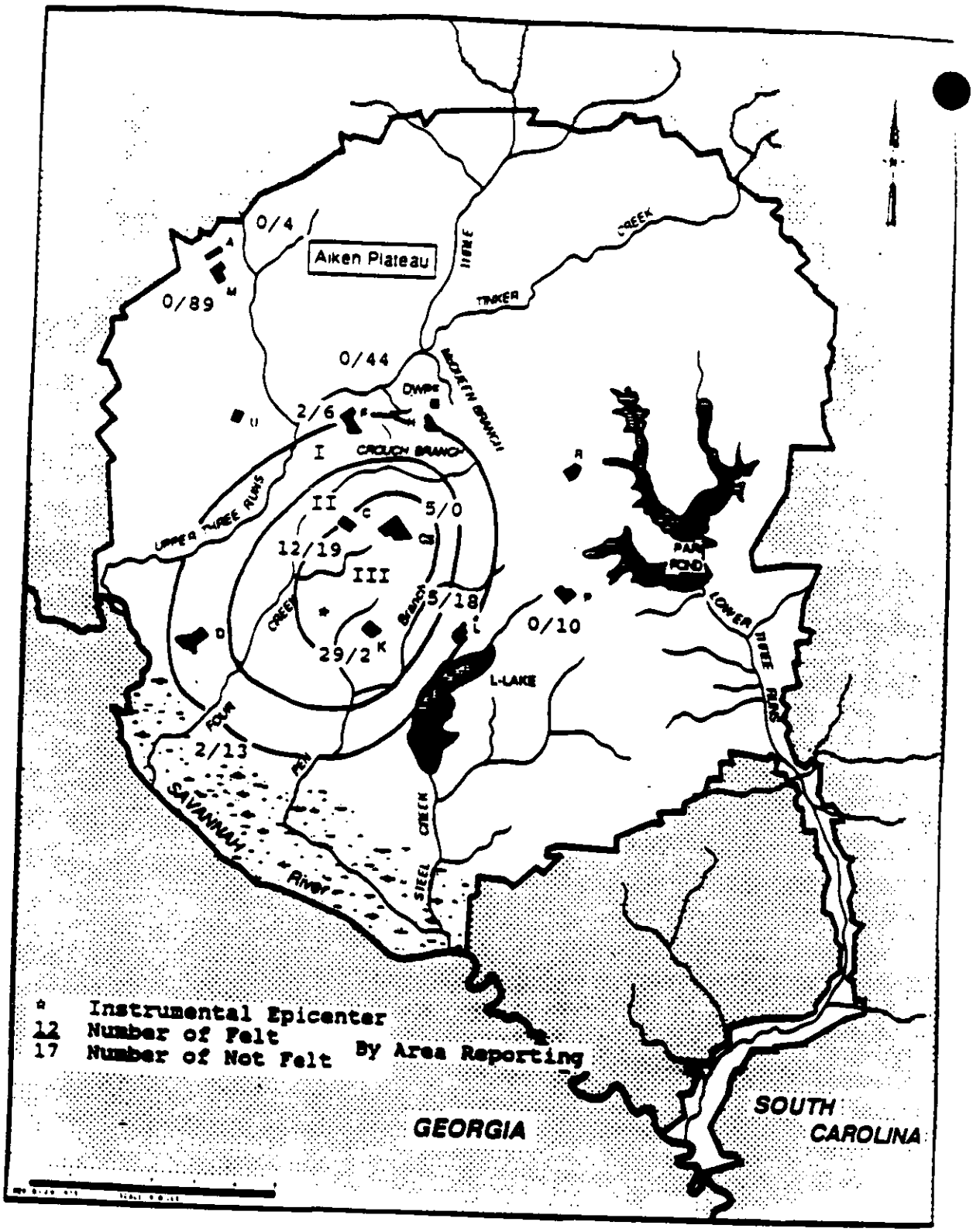

FIGURE 2-42. Isoseismal Map Showing Reported Intensities for June 1985 Earthquake (SRS)

The epicentral intensities of the largest earthquakes of this sequence have been estimated as MMI X-XI or XII. A generalized isoseismal map of the December 16, 1811, earthquake developed by Nuttli indicates that the site may have felt an intensity of V to VI.

The Giles County, Virginia earthquake of May 31, 1897 had an estimated intensity at the epicenter of VIII and occurred about 280 miles north. It may have had an intensity of MMI III at the site.

From the data in Table 2-1, Figures 2-38 through 2-41, and the discussion above, it is evident that the Charleston area is the source of seismicity most affecting the SRS site. This is true in terms of both the number of earthquakes felt at the site and the site intensity.

2.2.1.4.1 Modern Stress Regime

Seismicity can result from anomalous local stress concentrations, from a tectonic stress field acting on pre-existing zones of weakness, or both. Hence, it is of great importance to determine the state of ambient in-situ stress. The orientation of S_{Hmax} can be determined from a variety of data, including earthquake focal mechanisms, in-situ stress measurements by a hydrofracture, by overcoring techniques, and by geologic evidence of recent deformation (McGarr and Gay, 1978; Zoback and Zoback, 1980). In recent years, analysis of stress-induced wellbore elongation (or breakouts) has been increasingly used to determine the direction of S_{Hmax} (Shar and Sylees, 1977).

In the southeastern United States, several studies have described the direction of S_{Hmax}. Based on results of earthquake focal mechanisms, S_{Hmax} trends east to northeast and is nearly horizontal for the area extending west of the Appalachian Mountains to central North America (Zoback et al., 1987). The results of shallow hydrofracture in-situ stress measurements in unconsolidated sediments at Clubhouse Crossroads near Charleston suggested a northwest to southeast orientation for S_{Hmax} (Tarr, 1977). In their compilation of the stress map of the United States, Zoback and Zoback (1980) cited local effect in arguing against the use of in-situ overcoring measurements for inferring the state of tectonic stress. In view of the sparse in-situ stress data and many northeast-trending Cenozoic faults in the Atlantic Coastal Plain, the orientation of S_{Hmax} in the southeast was northwest to southeast. However, based on four composite fault plane solutions of microearthquakes in the Charleston area, and the agreement of the inferred P-axes that were derived for the M 3.8 November 22, 1974 event, the orientation of S_{Hmax} is east northeast to west southwest (Tarr, 1977; Talwani, 1982). However, in-situ measurement at a depth of 1100 feet in unconsolidated sediments may not be representative of S_{Hmax} of the tectonic stress field (Zoback et al., 1987).

Zoback (1983) reevaluated that existing data and using televiewer data to map well breakouts at the Clubhouse Crossroads and Monticello Reservoir wells, concluded that the orientation of S_{Hmax} is northeast to southwest.

A compilation of available fault-plane solutions, in-situ hydrofracture measurements, and one overcoring stress measurement in a tunnel led Talwani to suggest that the orientation of S_{Hmax} in the Southeast was uniform and lies between east northeast to west southwest and east to west, a direction similar to that in the central United States.

At Charleston, the stress orientation was based on four composite fault-plane solutions (Talwani, 1982), one single event solution (November 22, 1974, M 3.8) (Tarr, 1977), and well breakout data of Zoback (1983). At Monticello Reservoir, the stress orientation was based on an average of the P-axes of 22 fault-plane solutions and some well breakout data. At Lake Jocassee, the orientation was based on four fault plane solutions (Rastogi and Talwani, 1981), hydrofracture measurements (Haimson, 1975), and overcoring in a pilot tunnel at a depth of about 1000 feet (Schaeffer et al., 1979). All three data points show clearly consistent orientation of stress.

In Giles County, Virginia, again, the data are based on revised fault-plane solutions in Bell and Gough (1979) as well as some hydrofracture data (Munsey and Bollinger, 1985; Bollinger and Wheeler, 1982).

Munsey and Bollinger (1985) using some single event and composite focal mechanisms for earthquakes in central Virginia, suggested that the orientation of S_{Hmax} was NE-SW above 5 miles and northwest to southeast below that depth. No satisfactory explanation was given for this suggestion. Nelson and Talwani (1985), however, re-evaluated Munsey and Bollinger's (1985) data, and by using a different way of compositing events, argued that all data were consistent with a northeast to southwest orientation of S_{Hmax}.

The stress orientation in Kentucky was based on fault-plane solutions for the 1980 Sharpsburg earthquake (Mauk et al., 1982). The fault plane solutions in eastern Tennessee are from Bollinger et al. (1976).

Focal mechanism solutions for recent earthquakes in Georgia also support a NE-SW orientation for the P-axes (Long et al., 1986). All these stress data have been presented by Talwani (1985).

The current observations for the northeastern United States are in substantial agreement with those in the southeast and central states, suggesting a uniform regional-stress orientation for the entire eastern United States (Gephart and Forsyth, 1985). (Some sparse, isolated data, especially from the Northeastern states, are in disagreement.)

The consensus appears now to be that the S_{Hmax} in the Southeast and Central states, and perhaps also in the northeast, is oriented east northeast to west southwest to east to west. This conclusion, if found to be valid, has significant implications in defining what structures are

likely to be seismogenic and understanding the cause of seismicity in the region. Many of the hypotheses that were postulated to explain the cause of seismicity near Charleston were based on interpretation of S_{Hmax} in a northwest to southeast direction (Behrendt et al., 1983; Seever and Armbruster, 1981) in agreement with the results of Zoback et al. (1987). Now, however, current understanding is that S_{Hmax} in oriented east northeast to west southwest. Thus, a careful re-evaluation of these models is in order.

The latest compilation of stress data for the conterminous United States is for the forthcoming DNAG volume (Bollinger et al., 1987). In that compilation, questionable data were eliminated and additional data incorporated (especially from wellbore breakouts) (Zoback et al., 1987). The geological, seismological, and in-situ stress data all suggest a northeast to southwest to east northeast to west southwest compressive stress regime (characterized by strike slip or reverse faulting) in the southeast. This direction is consistent with plate tectonic ridge push forces for the North American plate (Zoback et al., 1987). One implication of this observation is that the probable cause of most of the observed seismicity in the region is due to the action of tectonic stress on zones of locally weak structures, rather than due to inherently local stress concentrations. Zoback et al. (1987) has, however, noted a few anomalously high stress locations.

Thus, we may conclude that in areas of ongoing seismicity the stress regime is primarily governed by plate tectonic sources. But at locations of infrequent or rare seismicity (e.g., near granite plutons in South Carolina), the source may be local stress concentrations.

2.2.2 Correlation of Earthquake Activity with Geological Structures

A comparison of historical seismicity (with a higher magnitude threshold) and epicenters recorded by network monitoring (lower detection threshold and more accurate locations), shows that they both display the same spatial pattern. That is, in a time frame of a few hundred years, the seismicity shows spatial stationaries. The seismicity occurs in local clusters in the Piedmont and the Coastal Plain, and in an elongated trend along the Appalachian highlands. Thus, for considering seismic hazard in the lifetime of critical facilities, the seismicity sources can be taken to be fixed and not floating.

The seismic sources of concern are the Charleston and Bowman seismic zones, and isolated episodes of microearthquake activity at other locations. The most important is the Charleston-Summerville seismic zone. This has been subjected to multidisciplinary studies by the U.S. Geological Survey (USGS) (Gohn, et al., 1983; Rankin, 1977), and by the University of South Carolina. The various data and postulated models, were reviewed by Talwani (1985). Dewey (1985) reviewed the various hypotheses. Both authors described a general absence of consensus on the cause.

Paleoseismic studies suggested that earthquakes such as the 1886 Charleston event occurred every 1200 to 1800 years (Talwani and Cox, 1985). Recurrence rates were also estimated statistically, using historical data and yielded a return period of about 1600 years (Amick and Talwani, 1986).

These observations were reconciled in a seismo-tectonic model wherein the seismicity in the Summerville-Charleston area occurs at the intersection of the Ashley River fault and Woodstock fault in response to a compressional stress regime with S_{Hmax} oriented east-northeast; where large events occur every 1500 years, and where the episodic seismicity, which began about 48 million years ago, has affected the shallow stratigraphy. Evidence of the Ashley River fault is also found in potential field and seismic reflection and refraction data (Talwani, 1985).

The Bowman seismic zone was studied by Smith et al. (1988) and the seismicity was found to occurr at the intersection of a northwest trending feature with the border fault of a buried Triassic basin. The seismicity is shallow and trends northeast-southwest. The seismogenic structure was delineated with detailed gravity and seismic refraction data (Smith et al., 1988). These were compared with available seismic reflection, shallow stratigraphic, and other geological data. The northwest basin discovered in the shallow stratigraphic data (Muthanna et al., 1987) altered the regional east-west-trending contours of the 48-million-year-old Unconformity 8 at the base of the Santee Limestone (Colquhoun et al., 1983). A similar change in the orientation was also observed in the detailed gravity contours, suggesting that the 48-million-year-old sediments had been affected by activity on deeper features. The isopach map of Cretaceous-age sediments revealed the presence of a northeast-trending Bamberg warp, which was not affected by the northwest feature (Colquhoun et al., 1983). These observations suggested possible seismic activity since about 48 million years ago. These results are a part of an ongoing study.

The June 1985 event at SRS appears to be located at the intersection of a northwest feature and the northeast-trending border fault of the Dunbarton Triassic Basin (Talwani et al., 1985). Unlike the seismicity at Charleston, which extends to nine miles, and Bowman where it extends to four miles, this event was in the top mile. The northwest feature appears to have helped to define its location. The exact nature of this northwest feature, which was first observed on the aeromagnetic maps is not well understood. It is currently being studied by detailed transient electromagnetic, gravity, and seismic reflections methods, and drilling.

In summary, the seismic structures responsible for the seismicity at Charleston are locally buried intersections of faults or similar structures. The largest shaking at the SRS would come from a repeat of a Charleston event, and URS/Blume (1982) estimates that it would be MMI VI. The seismic intensity due to a magnitude 4.5 (the larger event at Bowman) would be less than MMI VI at the site. The shaking intensity due to Piedmont events (MMI VII-VIII at Union County, MMI V-VI along the

eastern Piedmont fault system such as the Columbia 1945 event), or clusters of activity near plutons (such as intensity V near Newberry pluton) are all likely to produce lower intensities than the Charleston event (Rawlins, 1986).

2.2.2.1 Identification of Active Faults

There are no known active faults within 200 miles of the site.

2.2.2.2 Description of Capable Faults

No capable faults are known to exist in the region [of the site] (URS/Blume and Assoc. Engineers, 1982).

2.2.3 Maximum Earthquake Potential

Maximum earthquake intensities were considered by URS/Blume and Assoc. Engineers (1982) for three seismic source regions: (1) the Appalachian Mountains; (2) the Atlantic Coastal Plain; and (3) the Charleston seismic zone. The maximum historical earthquake in the Appalachian Mountains was the 1897 Giles County event with an MMI of VIII. The maximum historical earthquakes in the Atlantic Coastal Plain (excluding the Charleston zone) were of MMI VII. The Charleston seismic zone contains the 1886 event of MMI X.

The maximum postulated earthquakes would be:

- An MMI VII event in the Atlantic Coastal Plain near the SRS
- An MMI VIII event along the Fall Line nearest to the site, a distance of 25 to 30 miles
- An MMI X event at Middleton Place, a distance of 90 miles, the postulated epicenter of the 1887 Charleston event
- An MMI X event at Bowman along the northwest trend of the Charleston seismic zone, a distance of 60 miles

2.2.4 Design Basis Earthquake

The URS/Blume (1982) report defines the Design Basis Earthquake (DBE) as the maximum postulated earthquake producing the greatest peak ground acceleration. Using Bollinger's (1977) attenuation relation and the Murphy and O'Brien (1977) mean intensity-acceleration relation, the following results were obtained for the SRS intensities and peak ground acceleration, respectively:

- Local event (M = 5.1): VII, 0.10 g
- Fall Line event (M = 4.1): VI 0.06 g
- Middleton Place event (M = 7.1): VII, 0.075 g
- Bowman event (M = 7.1): VII, 0.10 g

To account for uncertainties in the acceleration intensity relationship, the 80th percentile values from the Murphy and O'Brien study have a resulting free-field horizontal peak ground acceleration of 0.20 g. This corresponds to the SRS site DBE. The free-field peak ground acceleration in the vertical direction is two-thirds the horizontal or 0.13 g.

2.2.5 Probabilistic Assessment of Peak Ground Acceleration

A probabilistic analysis was performed to assess the recurrence of peak ground acceleration at the SRS (URS/Blume and Assoc. Engineers, 1982). This analysis was performed using the geographic distribution of earthquakes and their recurrence rates as a function of epicentral intensity, the variation of intensity with epicentral distance, and the peak ground acceleration as a function of intensity. Three source regions, following the tectonic province definition above, were used with the Charleston seismic zone having two separate configurations. The mean annual rates of equal or exceeding peak free-field accelerations of 0.10 g and 0.20 g are 2×10^{-3} and 2×10^{-4}, respectively. Probabilities of exceeding acceleration of 0.10 g and 0.20 g in any 50-years period are 10% and 1%, respectively.

2.2.6 Design Response Spectra

Response spectra were derived from statistical analyses of selected sets of strong-motion accelerograph data recorded in California and related to the SRS as resulting from a Charleston-type and a local event (URS/Blume and Assoc. Engineers, 1982). The DBE response spectra envelop both of these controlling events.

The shapes of the DBE response spectra are given on Figure 2-43 and are normalized to a zero period acceleration of 1.0 g. For design purposes, these spectra are to be appropriately scaled, i.e., to 0.20 g in the horizontal direction and 0.13 g in the vertical direction.

2.3 SURFACE FAULTING

Faulting within the SRS region can be considered as belonging to one of three different categories, each associated with a distinctive geologic time period and stress regime. The first and oldest of these categories is the Paleozoic-age faulting associated with the Appalachian orogenies.

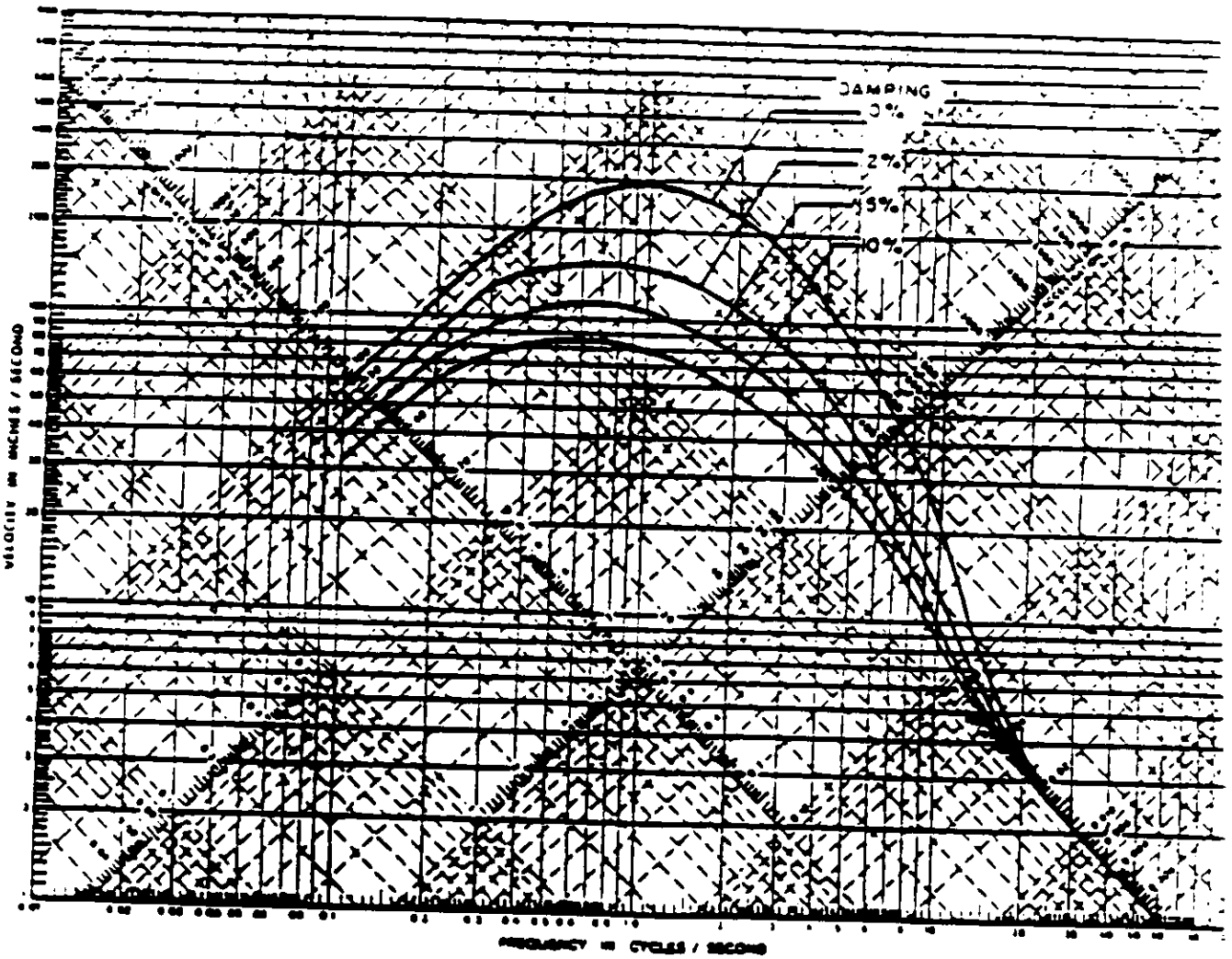

FIGURE 2-43. Response Spectra Normalized to 1 g Peak Ground Acceleration

The second category is faulting of late Triassic and Jurassic ages associated with crustal extension and separation of the North American and African continents. Late Mesozoic and Cenozoic-age faulting, observed primarily in the buried sediments of the Coastal Plain, make up the third category.

For purposes of seismic evaluation and development of seismic criteria, it is necessary, first, to determine if historic seismicity has been associated with any of the structures in the region, and second, to determine if any faults can be considered capable according to 10 CFR 100, Appendix A. This portion of the Code of Federal Regulations, relating to seismic and geologic siting criteria for nuclear power plants, defines a capable fault as a fault that has exhibited one or more of the following characteristics: (1) movement at or near the ground surface at least once within the past 35,000 years or movement of a recurring nature within the past 500,000 years; (2) macroseismicity instrumentally determined with records of sufficient precision to demonstrate a direct relationship with the fault; (3) a structural relationship to a capable fault according to characteristic (1) or (2) above, such that movement on one could reasonably be expected to be accompanied by movement on the other.

It has been concluded, in agreement with the findings of prior studies for nuclear power plants and other nuclear facilities in the region within 200 miles of the site, that there is no known genetic relationship between historic seismicity and well-identified faults or other geologic structures and that no faults in the region are known to be capable (URS/Blume and Assoc. Engineers, 1982). Current seismic work indicates that subsurface faults associated with current seismicity may be delineated (Talwani, 1982). The postulated Millett and Statesboro faults have been studied in detail and found to be not capable, and in fact may not exist.

2.3.1 Paleozoic Faulting

Major faults and fault zones, as well as lesser faults, are widespread in the Appalachian Mountain region (Figure 2-17). The most plausible hypothesis explaining the tectonic regime of the southern Appalachian Mountains includes a great decollement passing beneath the mountain range from which listric thrust faults splay upwards, placing older material above younger (Figure 2-16). The possible seismotectonic significance of the decollement is uncertain and under investigation.

The major thrust faults under the southern Appalachians are of Paleozoic age and were active during the orogenic episodes of that period. The great compressional episodes, which have been explained by plate tectonic theories, ceased near the close of the Paleozoic, and there is no geologic evidence that the mountain-building Paleozoic thrust faults have undergone similar thrust movement since then. Likewise, there is no known source of large compressional forces, which would be required to cause movement and crustal shortening on these faults.

Some Paleozoic faults may have been reactivated in Mesozoic or Cenozoic time (Seever and Armbruster, 1981) but with a different, nonorogenic style of tectonism.

The Paleozoic-age thrust faults (except any that may have been reactivated such as the decollement,) are considered to be inactive and to have no impact on seismic hazard evaluation.

2.3.2 Jurassic-Triassic Extensional Faulting

Jurassic-Triassic extensional faulting along the eastern seaboard is associated with separation of the North American and African continents. Tensional faulting resulting from crustal extension created basins due to fault block rotation or graben formation along the eastern seaboard; some of these are well-known and have been referred to as the Triassic basins, but they are now more accurately called the Jurassic-Triassic rift basins. The basins have been filled with basalt flows and reddish sandstones and shales, which are Triassic and Jurassic in age. Following basin formation and filling, the entire region was peneplained by erosion, creating a smooth surface across both the basins and the surrounding Paleozoic rocks.

The faults and basins elongate northeasterly. Figure 2-10 shows several Triassic basins, two of which are situated in the exposed Paleozoic rocks west of the Fall Line; the remainder are buried beneath the Coastal Plain sediments. The Dunbarton Jurassic-Triassic Rift Basin comprises a portion of the basement rock beneath the SRS (Figure 2-44).

The large basin extending from the Gulf Coast to the Atlantic Coast and including Charleston, called the South Carolina-Georgia Basin, is probably more significant than any of the others because of its great size and because the Paleozoic rocks bounding opposite sides of the basin are distinctively different with respect to stratigraphy, metamorphism, and fossil assemblage. It was suggested that a Paleozoic suture zone is situated between Georgia and Florida coincident with the South Carolina-Georgia Basin. It was commented as follows:

> This suture follows the regional trend of the southwest and southeast Georgia embayments and a continental extension of the East Coast magnetic anomaly. During the Mesozoic opening of the Atlantic, the suture zone was reactivated and controlled the development of an extensive rift system. Recent geophysical work in the Charleston, South Carolina area defines the northeastern boundary of the rift system; however, it does not support the hypothetical northwesterly extension of the Blake Spur Fracture Zone into the continent (Figure 2-44).

Since this was written, studies by Talwani (1985) suggest that there is a northwesterly-trending seismogenic fault near Summerville in approximate alignment with the Blake Spur fracture zone. Future work will no doubt help resolve this problem.

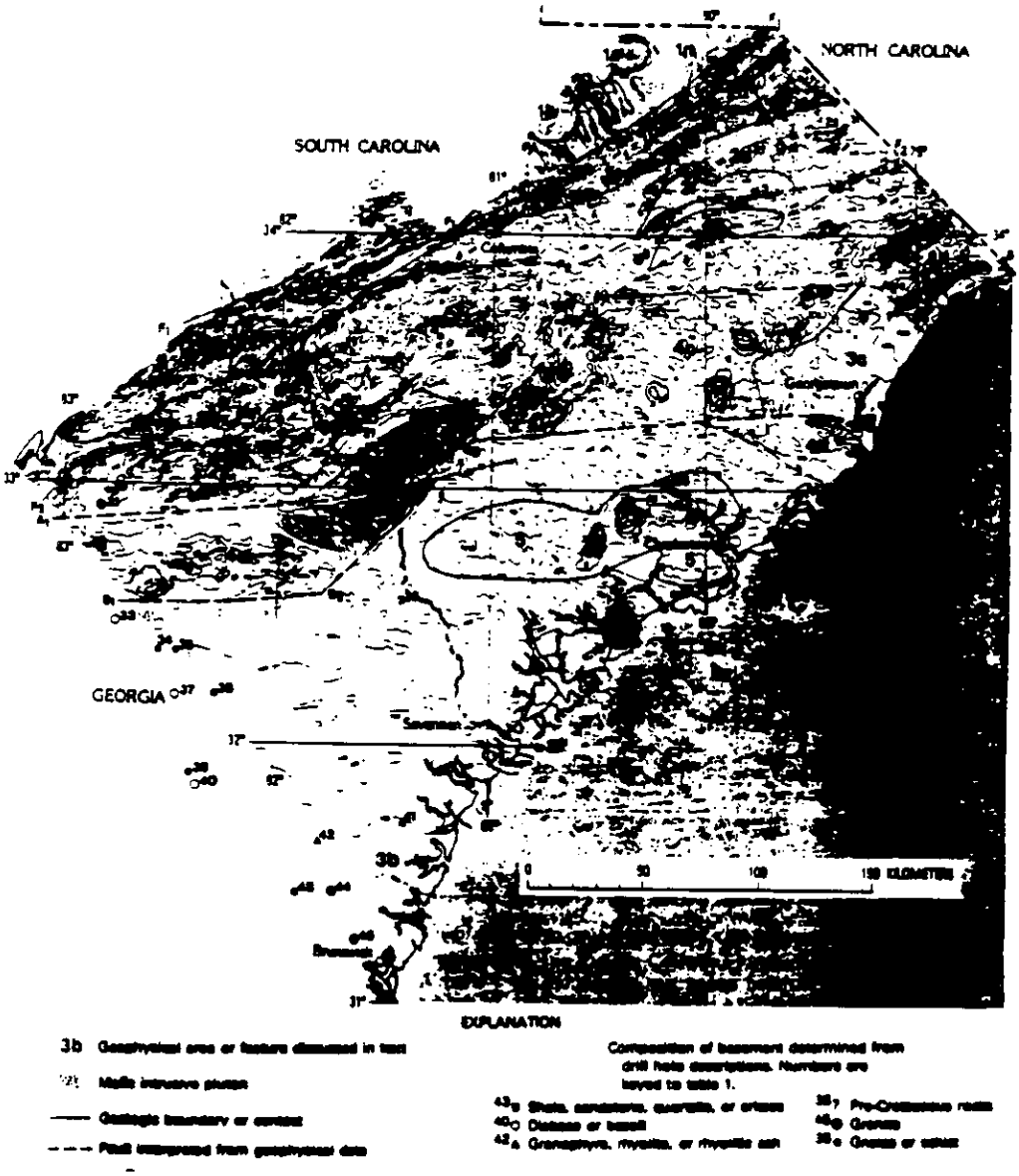

FIGURE 2-44. Magnetic Anomaly Map of the Southeastern United States

It appears that the South Carolina-Georgia Basin may be of tectonic significance because of the numerous normal faults apparently associated with it, some of which may have been reactivated, or because of a major crustal discontinuity consisting of a suture or rift zone within it. There are no known active faults within the basin.

The suture zone, as well as the Blake Spur fracture zone, cannot be considered to be faults in the usual sense. They are both crustal features that could be associated with faulting and seismicity.

Not all lithologic correlations and age determinations of rocks in the South Carolina-Georgia Basin are consistent in confirming its Triassic-Jurassic age. The age of rocks in the Dunbarton Basin is undetermined. However, the distinctive tectonic style and lithology lead to general agreement that the rocks and enclosing basin are probably of Jurassic and Triassic age.

The late Triassic and early Jurassic faulting responsible for formation of the basins was due to extensional stress, which has not recurred as far as is known. Normal movement on the faults appears to have ceased in early Jurassic. None of these faults is known to be capable, and there is no known association of historic seismicity with any of them.

2.3.3 Cenozoic Faulting

The faulting described in this section began after the Triassic basins were filled and eroded to a peneplain. In some instances, the faults were formed or (more likely) reactivated in Cretaceous time, and movement recurred on some of them in Cenozoic time. Where Cenozoic formations are offset, the faults are here called Cenozoic faults, following the usage of Wentworth and Mergner-Keefer (1983).

In contrast to the great Paleozoic faults of the Appalachian Mountains, which have been studied for many decades, Cenozoic faulting is not well developed in the southeast and has been studied primarily within the past decade. The Cenozoic faults known to date within the region of the SRS are primarily within the Coastal Plain. This may be due at least in part to the fact that Cenozoic faults in the Appalachian region are difficult, if not impossible, to identify, because the rocks are nearly all Paleozoic or older in age. Known Cenozoic faults are few in number and small in length and displacement. They lack topographic expression, as far as is known, and their rate of movement has apparently been slow.

Coastal Plain sedimentary rocks are not well suited to recognition of faults at the surface because of their poorly consolidated nature, which results in deep soil profiles and sparse outcrops. However, with careful study, taking advantage of exposures in quarries and road cuts, some faulting has been observed at the surface. These occurrences have been in the upper Coastal Plain region, where the older rocks belonging to the lower portion of the Coastal Plain sedimentary sequence are exposed. In

the lower Coastal Plain, as at Charleston, no faults have been identified at the surface, but they have been detected in the subsurface by use of seismic reflection and refraction, drilling, and analysis of earthquake seismograms.

A number of Cenozoic faults within the study region have been described, one of them being the Belair fault zone, located near Augusta, Georgia (Wentworth and Mergner-Keefer, 1981)(Figure 2-17). Several northeast-trending reverse faults with lengths of about one to three miles and offsets of 16 to 96 feet down to the west were documented by mapping, shallow drilling, and trenching. The Belair fault has been studied in detail and found to be inactive or not capable. The faults form a northeast-trending zone about 14 miles long. Seismic profiling has revealed the Cooke fault near Charleston, which trends east-northeast and is about 5.5 miles long. The fault offsets the base of the Coastal Plain section about 160 feet to the southeast and shows decreasing offset upward through younger formations. This fault is located close to the area of contemporary seismicity.

Seismic profiling has delineated the Helena Banks fault, offshore of Charleston, which trends east-northeast over about 21 miles and is probably about 40 miles in total length. Called an "apparent high-angle reverse fault," it offsets the base of the sedimentary section about 64 feet to the southeast and shows decreasing offset upward (Behrendt et al., 1981). The uppermost formations where deformation is recognized were not broken but warped.

Movement on the Belair fault zone took place from late Cretaceous through at least Eocene time, from about 100 mybp to about 37 mybp. Movement on the Cooke fault began before late Cretaceous time and continued through at least the Paleocene (more than 100 mybp through 53 mybp). Initial movements on the Helena Banks fault took place before upper Cretaceous time (approximately 100 mybp) and continued through the Miocene or Pliocene (Behrendt et al., 1983). The Millett and Statesboro faults, recently postulated near the SRS, have been found to be noncapable and may not exist.

For Cenozoic faults in general, most recent fault movement is Pliocene or about two to five mybp (Wenworth and Mergner-Keefer, 1983). These authors state that the average rate of movement on the faults was about three feet/million years. It is possible that more recent movement may have occurred during this period without leaving detectable indications near the surface. If this has happened, the amount of slip must have been small, and the resulting earthquake probably had a magnitude of less than six. Alternatively, nonseismic creep could have taken place at depth without reaching the surface; such movement could be considered plausible in view of the very low strain rate.

Other investigations of faulting in the Coastal Plain region of interest are described by Cramer and Arden (1978) as follows:

> Faulting dominates the interpretations of isopach and structure contour maps of Oligocene rocks from the Georgia Coastal Plain. The data are from more than 250 wells and an extensive coring program. The faults are: (a) a prominent fault, east-side downthrown several tens of feet, trending southeast from the Macon County area through Coffee County into and probably through Charleston County; (b) less prominent ones parallel to (a) in the northern part of the Coastal Plain, forming horsts and grabens; (c) a pronounced graben, up to 20 miles wide, trending northeastward from Decatur and Grady counties through northern Coffee County to probably the Savannah River and beyond; the throw is several hundred feet; it transects (a) and (b); with thicker Oligocene and Miocene rocks in the graben; (d) faults parallel with (c), some down to the sea, with Oligocene rocks thin or absent on the upthrown sides of some; and (e) smaller faults with a N-S orientation. The faults are consistent with a tensional pattern to be expected on the trailing margin of a continent.

Other more isolated instances of Cenozoic faulting in the Coastal Plain region have also been described (Howell and Zupan, 1974; Wenworth and Mergner-Keefer, 1981; Inden and Zupan, 1975).

Wentworth and Mergner-Keefer (1981) and Wenworth and Mergner-Keefer (1983) have studied the results of investigations in the Charleston meizoseismal area. In addition, they have considered faulting along the Atlantic seaboard as far northeast as New Jersey, which they consider to be related to those faults near the epicentral region of the Charleston earthquake. These authors have summarized their conclusions as follows:

> The available geologic and seismologic evidence leads us to the following hypothesis. An Atlantic coast domain of northwest-southeast compression extends from Georgia to Canada between the Appalachian Mountains and the edge of the continent. Within this domain, movement on scattered northeast-trending reverse faults has been underway for at least 100 million years, but in that time has accumulated offsets on individual faults of no more than about 100 meters. Movement of these faults is a reasonable source of seismicity in the domain. Such faults exist in the Charleston meizoseismal area, and are a likely source of the 1886 earthquake. The reverse faults tend to reuse pre-existing faults and other discontinuities, particularly the normal faults formed during Early Mesozoic rifting. This association and earthquake focal mechanism solutions permit extrapolation of the domain beyond the presently recognized extent of Cenozoic reverse faulting in the southeast. Given the inferred extent of the domain and occurrence of the 1886 earthquake on a northeast-trending reverse fault near Charleston, Charleston-type earthquakes should be possible in most parts of the Atlantic seaboard.

Geophysical data and conclusions appear to contradict the above views (Zoback et al., 1987). On the basis of in-situ stress measurements, test wells, auger holes, and geologic information, these writers identified at least one northwest-trending normal fault in the meizoseismal area of the Charleston earthquake. The writers interpreted the results to suggest

that normal faults in the Coastal Plain sediments near Charleston are active and that the direction of relative horizontal extension appears to be northeast to southwest. Structure contour mapping in the meizoseismal area of the Charleston earthquake identified two normal faults, one appearing to trend northwest and one whose trace approximately follows the east-trending reach of the Stono River (Higgins et al., 1978). Again, these data are difficult to reconcile with a domain of northeast-trending reverse faults.

Wentworth's and Mergner-Keefer's (1983) hypothesis is not entirely compatible with the basic data. It fails to explain the fault mechanisms of Talwani (1982), and it is not a good explanation of faulting within the Coastal Plain in general. High-angle reverse faults, such as the Helena Banks fault, are more indicative of vertical than horizontal movement; low-angle thrust faulting (not common in the Coastal Plain) would substantiate horizontal movement of the crust.

Stress measurements interpreted by Zoback and Zoback (1980) as indicative of regional northwest to southeast compression and used to support Wentworth and Mergner-Keefer's (1983) hypothesis are not convincing. The crystalline rocks of the Appalachian orogen have undergone regional northwest to southeast compression during the Paleozoic era and would surely be left with an imprint of residual stress. It is not clear how residual stress has been taken into account by Zoback and Zoback (1980) in evaluating the contemporary stress field. The horizontal compression hypothesis also lacks a substantiated explanation for the source of horizontal stress.

A hypothesis to explain the seismotectonics of the Coastal Plain should be based on the geologic history of that region. The dominant crustal movement during Cenozoic time has been subsidence and superimposed local differential vertical movement. Vertical movement that has caused the steep faulting is probably due to differential thermal contraction or mineral transformations in the crust. The effect of cooling in the crust since continental separation also explains the diminishing rate of movement through the Cenozoic. This idea addresses only the Coastal Plain and is not considered applicable to the Appalachian Mountains.

Seismic studies indicate two active seismic zones near Summerville, South Carolina, one trending northwest and the other northeast, which are probably fault zones as well (Talwani, 1982).

2.3.4 Capable Faults

In summary, it is first noted that none of the faults showing evidence of Cenozoic displacement have been demonstrated to be capable according to the definition of 10 CFR 100, Appendix A. Further, it appears that the data available at the present time relating to style of faulting and stress regime in the Coastal Plain are not consistent and have led to a variety of interpretations. One view is that the region is being subjected to a northwest to southeast compressional stress due to

back-sliding on the decollement (Seever and Armbruster, 1981). Another is that the region is subject to northwest-to-southeast compressional stress due to crustal spreading at the Mid-Atlantic Ridge (Seever and Armbruster, 1981).

Others suggest that the area is subject to tensional stress resulting in normal faulting (Cramer and Arden, 1978). The views of various investigators are for the most part presented as hypotheses, and there does not appear to be sufficient basis at this time for selection of a most plausible hypothesis.

2.4 STABILITY OF SUBSURFACE MATERIALS AND FOUNDATIONS

A subsurface investigation was performed in 1980 for a proposed facility called the New Production Reactor (NPR). The data were collected at the proposed NPR site, which is about 3 miles north of the reactor sites. The foundation analyses consisted of bearing capacity, settlement, elevation of ground water, presence of subsurface voids and the liquefaction potential. Conclusions and recommendations were:

- The subsoils at the proposed NPR site are complexly interbedded clayey sand, sand, and stiff sandy clay. The clayey soils are usually heavily preconsolidated to stresses above anticipated foundation loads. Low preconsolidation stresses may occur in a silty clay layer encountered at the contact of the Barnwell and McBean formations. Undisturbed samples of that clay should be retrieved in subsurface investigations made from final design and tested to confirm the clay's preconsolidation.

- The subsurface conditions are similar to H and S areas. Therefore, the soil properties, foundation design parameters, and liquefaction criteria from previous investigations are applicable to the proposed site.

- The average ground water table averages 285 feet above msl or approximately 40 feet below the surface, in the area of Plant Coordinates N60,000 and E60,000.

- There is some evidence of leaching of calcareous sand. Voids or leached zones of limited lateral extent were defined between 80 and 90 feet above msl in one area of the site, and other zones may be present.

- Comparison of data from the 1980 subsurface investigation and liquefaction failure criteria developed during a previous investigation in S Area indicates the soils on the SRS are not susceptible to liquefaction from seismic shocks.

2.4.1 Geologic Features

The geologic formations at the proposed NPR site are similar to those at production reactor sites at the SRS. The soil properties at the reactors are very similar to those at the DWPF.

Geologic and engineering foundation investigations conducted in 1950 for the production reactors revealed that the sites are underlain by a thick series of uncemented sediments composed of clays, sands, and gravels in varying proportions. About 100 feet below the surface, a zone of sandy marl and calcareous sand was found. The removal of calcium carbonate from this zone by solution resulted in numerous small cavities. Subsidence has caused sinks or shallow depressions on the surface. Explorations have found openings beneath areas where no surface sinks exist, suggesting that although the surface has not collapsed, it may be in a state of unstable equilibrium.

Because of the sinks, a test program was performed to determine the need for, and feasibility of, grouting beneath principal structures. It was determined that the foundations beneath all 105-, 190-, 221-, and 241-type structures would be grouted where necessary.

It was determined that the grout holes would be drilled by "fishtail" borings. A fishtail boring is one in which a hole is made in the ground by rotating and advancing a cutting bit designed for jetting. Water is pumped through the drill rods and out the end of the bit. The combined action of the jetting and cutting action of the bit loosens the soil, which is floated to the surface by the jetting water. The fishtail borings were made rapidly with rotary, truck-mounted drilling equipment. It was determined that grouting would be performed through the fishtail borings wherever abnormalities were observed during the drilling operations. These abnormalities included sudden dropping of the drill rods without jetting or rotation and sudden or excessive loss of water and drilling mud. The fishtail exploration-grout holes were located on 50-foot centers on lines spaced 25 feet apart. The holes on adjacent lines were staggered and extended approximately 30 feet or more beyond the building line. All drillings, including split-spoon, undisturbed, and fishtail, were utilized in determining the depths at which abnormalities occurred. The depths to the top of the calcareous zone were greater than 100 feet and the average thickness varied from about 10 to 40 feet.

A total of 1724 boreholes were drilled in the building areas for the entire production reactor sites and 1013, or 59%, indicated the presence of calcareous material. Of these a total of 362, or 21%, were grouted. A total of 990 bore holes were drilled in the production reactor areas, of these only 246, or 25%, were grouted. Table 2-4 shows the number of borings made at the P, L, and K production reactor areas, the number of holes that were grouted, and the amount of grout that was pumped into the boreholes.

The grout consisted of 1-1/2 bags of portland cement, eight cubic feet of sand (loose measure), 1/4 bag of bentonite, and six cubic feet of water. The volume per batch varied between 10.5 and 11.3 cubic feet, depending on the physical properties of the sand. In general, a grout pipe was set in those fishtail borings where abnormalities were noted during drilling. Grout was pumped into the hole under a pressure of 25 to 40 pounds per square inch (psi) measured at the top of the grout pipe at the surface. Pumping was continued until refusal. The boring was then flushed with water and grouted again.

During the operations, it was noted that the grout was traveling extensively. This was evidenced by the venting of grout from fishtail borings near the hole being grouted. The venting of an otherwise satisfactory hole was considered indicative of the presence of small channels which were plugged during the drilling of the hole by small pieces of soil and drilling mud. As a result, all fishtail borings that were found to have any venting were grouted. Instead of grouting the hole which vented, an offset hole adjacent to the vented hole was drilled and grouted. Before grouting was begun, the hole was tested with water under a pressure of about 60 psi. When the loss under this pressure was appreciable the grout line was attached and grout pumped into the hole. This ensured that the entire hole would be filled with grout and would be forced into any cavities or soft spots regardless of their depth. In general, it was found that vented holes took very small quantities of grout.

2.4.2 Properties of Subsurface Materials

Index properties were determined for disturbed and undisturbed samples obtained during the field exploration program. These are discussed individually in the following sections.

2.4.2.1 Natural Water Content

The natural water content, American Society of Testing and Materials (ASTM) D 2216, was determined for all tested split-barrel and undisturbed samples. These data, together with the Atterberg limits, provide a qualitative measure of the consistency of subsurface soils. Although most samples had about 25% water contents, some differed considerably. Silty sands having water contents of this magnitude are usually loose to medium dense.

2.4.2.2 Grain-Size Distribution

Grain-size analyses were conducted on both disturbed and undisturbed samples. These tests were performed in accordance with ASTM D 422, and results are shown in Figures 2-45 and 2-46. The results are grouped by geologic formation. Note that Barnwell Formation is equivalent to Dry Branch and Tobacco Road and McBean Formation is equivalent to Santee and

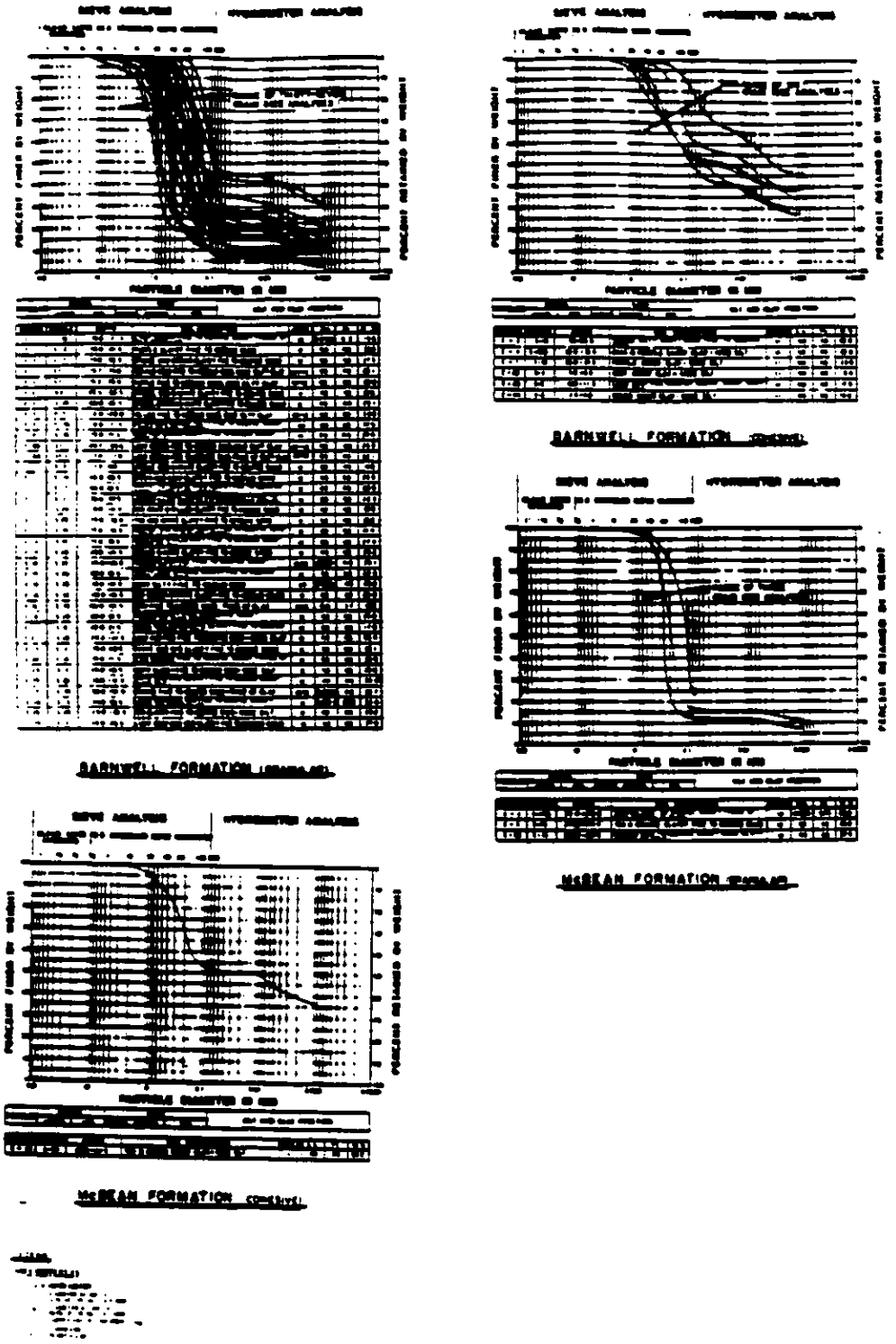

FIGURE 2-45. Subsurface Investigation Laboratory Data Sheet 1

perhaps part of Dry Branch Formations current usage. A total of 52 grain-size analyses were conducted, of which 34 included a determination of the No. 200 sieve size distribution using the hydrometer method. In addition, 80 analyses were conducted using ASTM D 1140 to ascertain the percentage of fines passing a No. 200 sieve for classification using the Unified Soil Classification System (USCS).

The general groupings of grain-size analyses show that the soil consists mostly of sand, silt, and clay-sized particles. The predominant soil may be described by the USCS symbols SM and SC, indicating that the site is underlain mostly by silty to clayey fine to medium sand. For this soil, the percentage by weight passing a No. 200 sieve typically ranges from 5% to 40%, with an average of about 25%. In general, the soil of the Barnwell Formation has smaller percentages of fine-grained material than does the soil of the other formations.

2.4.2.3 Atterberg Limits

The liquid and plastic limits (ASTM D 423 and D 424), together with the resulting plasticity index, were determined for selected cohesive soil samples. A total of 28 tests were conducted on samples taken from 13 different borings to determine the Atterberg limits and classification of cohesive soil. These data are grouped by boring and geologic formation. The plasticity charts are shown in Figure 2-46. The samples tested displayed a wide range of plasticity characteristics. In general, the plasticity index was less than 40%, while the liquid limit, with two exceptions, was less than 80%.

The liquidity index had limited application in measuring the degree of over-consolidating. In general, the liquidity index for the cohesive soil was low, indicating apparent over-consolidation, presumably due to soil desiccation. This is reflected in the consolidation test results for this soil, which show over-consolidation ratios (OCR) ranging from two to five, with an average of about three.

2.4.2.4 Specific Gravity

Specific gravity tests were conducted on seven samples taken from four borings. The specific gravities ranged from 2.67 to 2.77. On the basis of these data, a representative value of 2.70 was derived.

2.4.2.5 Unit Weight

All undisturbed tube samples that were tested during the laboratory program were carefully trimmed and accurately measured and weighed to determine the in-situ total unit weight of the sample.

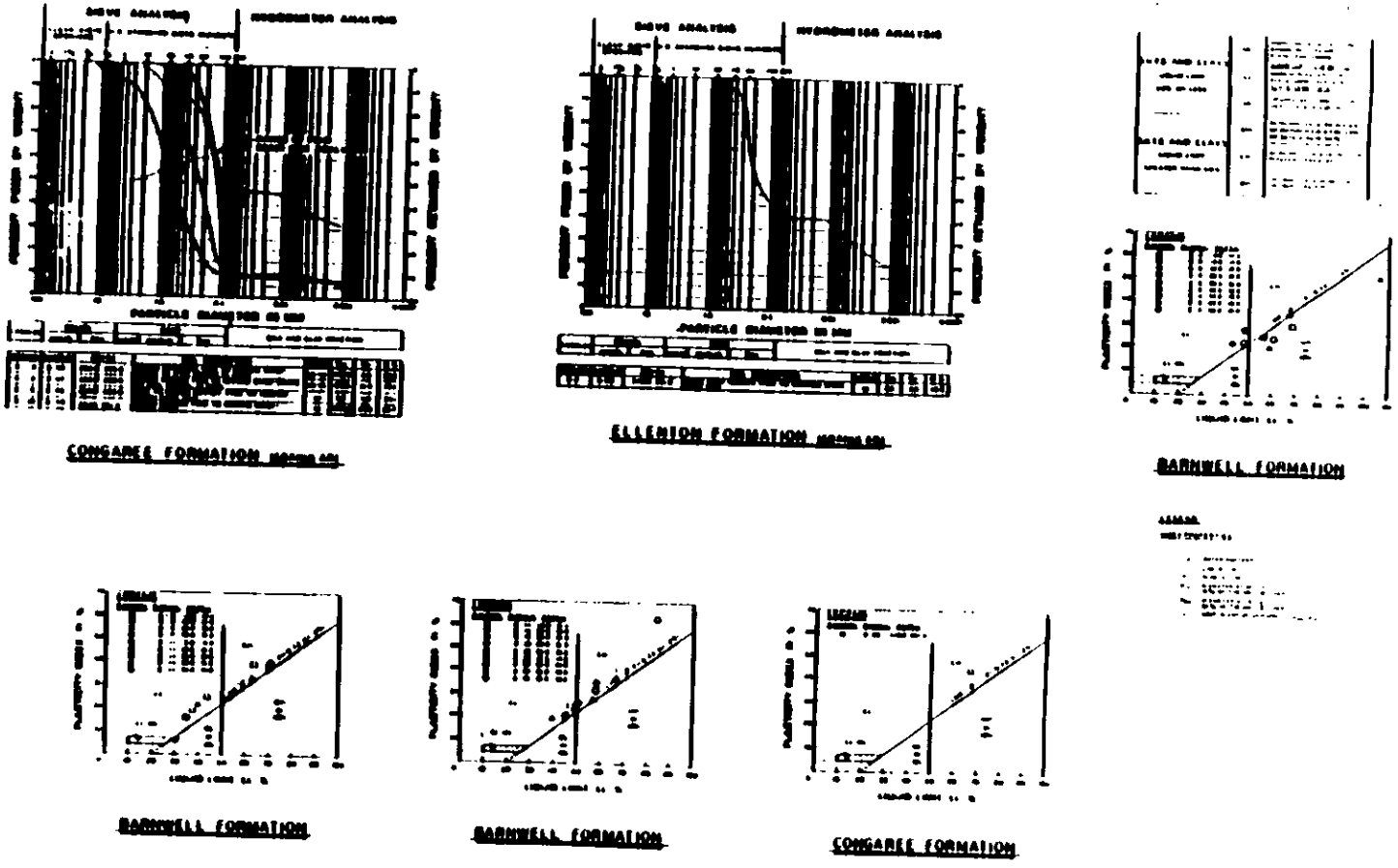

Figure 2-46. Subsurface Investigation Laboaratory Data Sheet 2

2.4.2.6 Consolidation Tests

A total of six consolidation tests (ASTM D 2435-70) were conducted on undisturbed samples of sandy clay recovered from five borings. Summaries of the test results are presented in Table 2-4. Void ratio (e) versus log pressure curves for these tests are shown on Figures 2-47 and 2-48.

The consolidation tests show a wide range of compressibilities, which may be correlated with the consistency, gradation, and plasticity exhibited by these soils. As shown in Table 2-5, the value of the compression index (C_c) ranges from 0.92 to 0.14. In all cases, the value of C_c was determined using the Schmertmann construction procedure to estimate the in-situ field performance. The recompression index (C_{cr}) was generally found to equal approximately one-tenth of the compression index value. The over-consolidation ratio (OCR) ranges from 2.0 to 5.2. The apparently higher values of OCR may result from sample disturbance rather than from actual precompression.

2.4.3 Exploration

A field exploration program, including drilling, sampling, geophysical testing, and in-situ testing was conducted at the proposed NPR reference site from September 10 through November 21, 1978. The information reported in the following sections was extracted from Corps of Engineers, 1952.

2.4.3.1 Drilling, Sampling, and In-Situ Testing

All drilling, sampling, in-situ testing, and piezometer installations were performed in accordance with a Quality Assurance Program developed for subsurface exploration.

Soil sampling, piezometer installation, and in-situ field testing were performed under the direct control of field engineers, geologists, and supervisory personnel. Appropriate onsite modifications of the field drilling and sampling procedures were made to suit the subsurface conditions.

2.4.3.2 Drilling

A total of 46 borings, including cross-hole and piezometer borings, were drilled for the two-phase field investigation. Phase I consisted of drilling borings E-1 through E-9 on a rectangular grid encompassing the site to develop a preliminary view of subsurface conditions and for stratigraphic control for further borings. The Phase II borings, E-10 through E-35, were drilled to provide detailed information at the locations of the structures. The boring locations are shown in plan on Figure 2-49 along with existing site contours and the locations where subsurface stratigraphic cross-sections have been constructed.

TABLE 2-4

Production Reactors Grouting Program

Building	Number of Fishtail Boring Holes	Number of Splitspoon Holes	Number of Holes Grouted	Total Grout Pumped (cubic yards)
105-P	320	3	65	6,469
190-P	27	1	12	1,412
105-L	266	3	67	4,840
190-L	38	1	27	3,429
105-K	289	3	76	4,869
190-K	38	1	10	951
Total	978	12	246	21,970

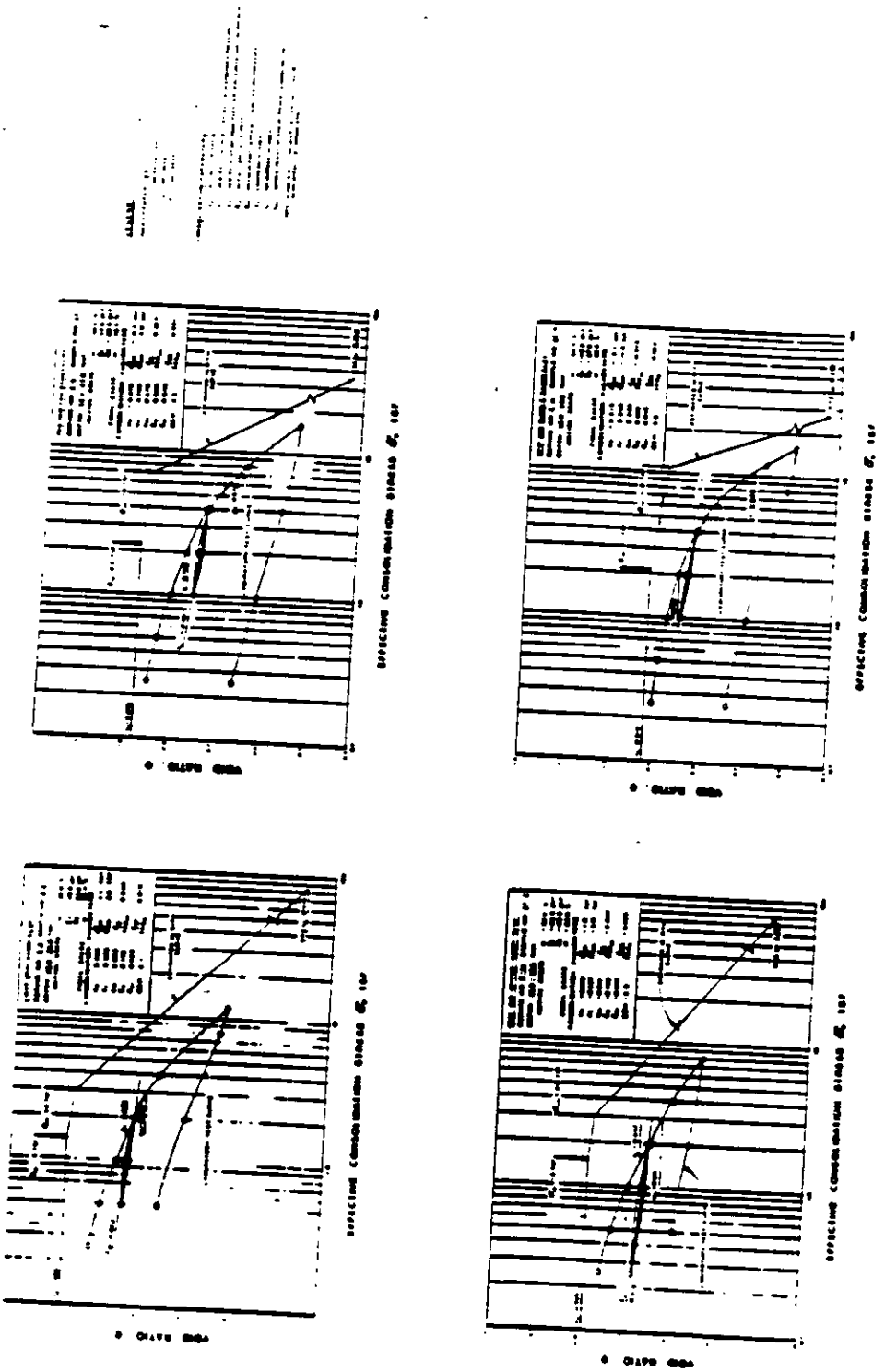

Figure 2-47. Subsurface Investigation Laborabory Data Sheet 3

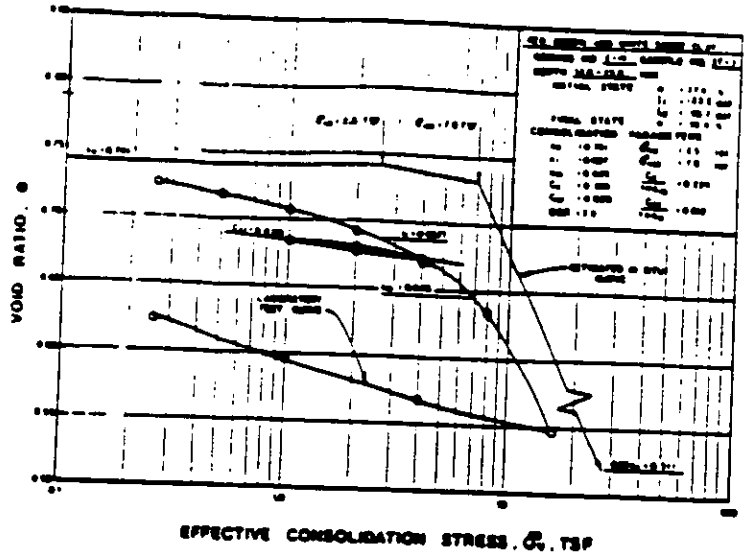

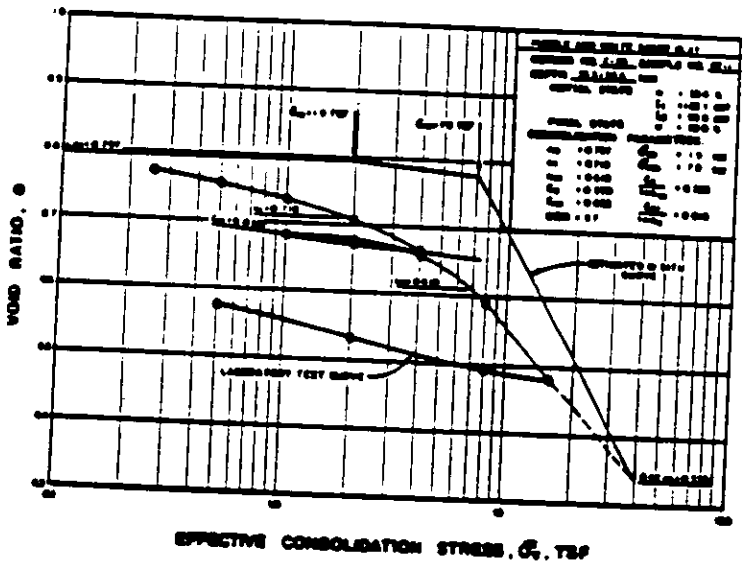

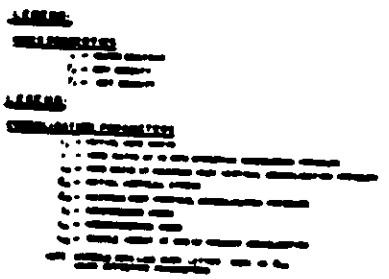

Figure 2-48. Subsurface Investigation Laborabory Data Sheet 4

TABLE 2-5

Summary of Consolidation Test Results

Boring, Sample, and Depth	Description	OCR	Compression Index, C_r	Recompression Index, C_{cr}	Initial Void Ratio
E-3, P-3 22.0'-24.0'	Light gray sandy clay	2.1	0.17	0.02	0.986
E-4, ST-1 42.0'-44.0'	Red and tan sandy clay	3.2	0.61	0.04	0.878
E-11, O-2 25.0'-27.0'	Gray and orange sandy clay	2.0	0.14	0.01	0.595
E-11, O-4 42.0'-44.0'	Gray and purple sandy clay	5.2	0.92	0.05	0.919
E-14, ST-3 53.0'-55.0'	Red, brown, and white sandy clay	2.8	0.37	0.02	0.741
E-30, ST-1 36.5'-38.5'	Purple and white sandy clay	3.7	0.59	0.03	0.797

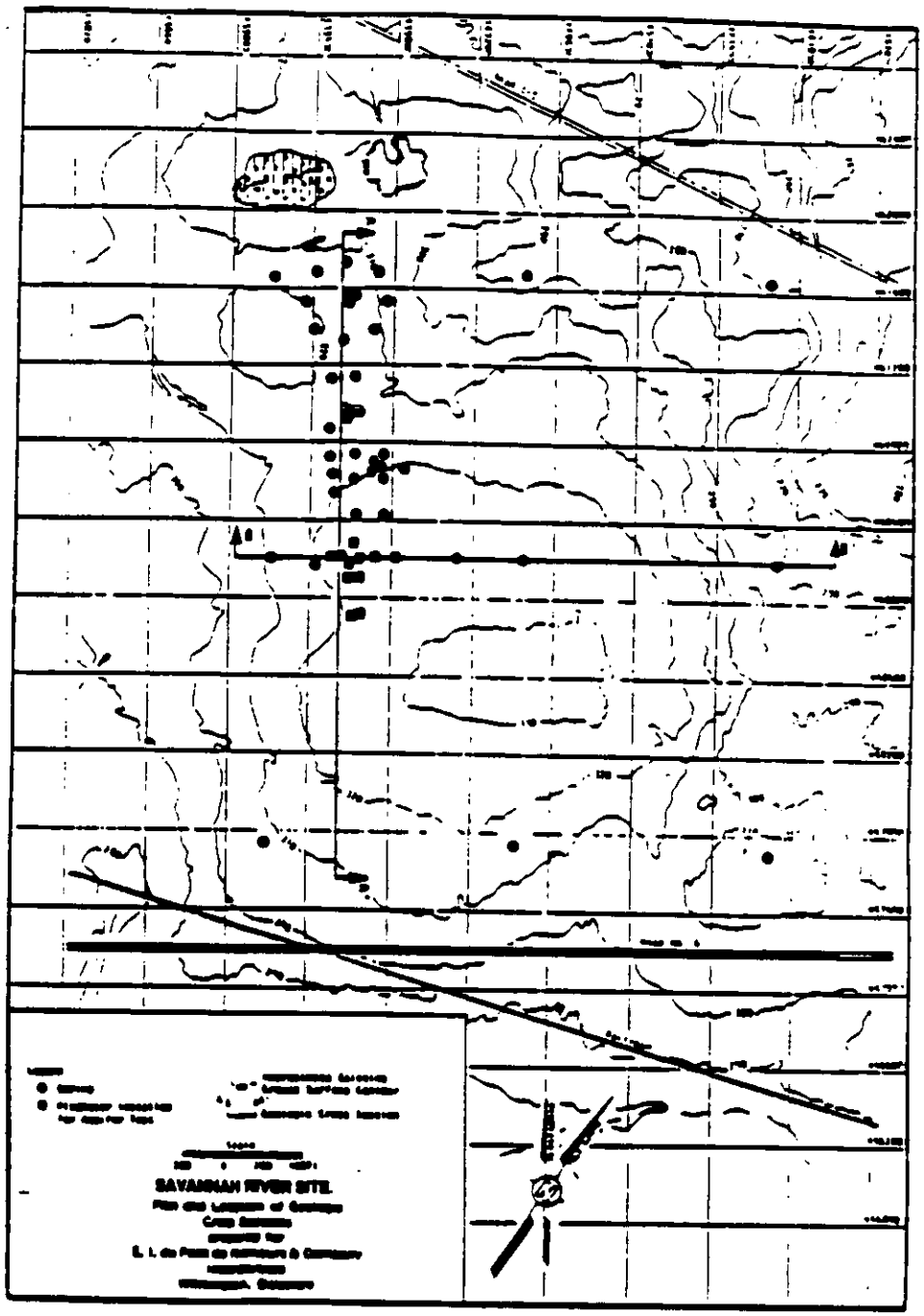

FIGURE 2-49. Plan and Location of Geologic Cross Section

2.4.3.3 Standard Penetration Testing

Standard Penetration Testing (SPT) was performed in accordance with ASTM designation D 1586, entitled "Standard Penetration Test and Split-Barrel Sampling of Soils." As specified in ASTM D 1586, the disturbed samples were obtained using a 2-inch-outside diameter, split-barrel sampler, equipped with a ball check valve at the top, driven 18 inches into the undisturbed soil by repetitive blows from a 140-pound hammer falling freely for 30 inches. The blow counts for the last two, six-inch increments were added to obtain the SPT value for the sample (i.e., number of blows for 12 inches of penetration). For each boring, the SPTs were generally performed at 2.5-foot intervals from the ground surface to a depth of 15 feet, at 5-foot intervals between 15 and 150 feet, at 10-foot intervals from 150 to 300 feet, and also as necessary to define changes in the soil strata.

2.4.3.4 Sampling

The thin-walled tube has dimensions in accordance with ASTM D 1587, "Thin-Walled Tube Sampling of Soils," and is advanced into the soil by hydraulic pressure. The Pitcher barrel sampler is lined with a thin-walled tube and is spring-loaded to provide for the automatic adjustment of the distance by which the cutting edge of the barrel leads the coring bit. The Osterberg piston sampler is a modification of the thin-walled stationary piston sampler. Sampling is accomplished by introducing fluid pressure on top of the actuating piston, thus forcing the sampling tube into the soil.

2.4.3.5 Piezometer Installation

Thirty-two piezometers were installed at the locations of some of the borings. Sensitivity testing was conducted on all piezometers after the heads had stabilized. Results of these tests indicated that all of the installed piezometers responded to applied changes in heads, and thus functioned properly.

2.4.3.6 Pressuremeter Testing

Pressuremeter tests, which are generally used to determine the elastic modulus for foundation analyses, were conducted at two boring locations. The pressuremeter test is conducted at various elevations in a boring by expanding a cylindrical probe under fluid pressure. The volumetric deformation and the applied pressure are recorded.

2.4.4 Geophysical Surveys

Several geophysical surveys were undertaken to obtain subsurface data. These geophysical activities included a seismic reflection survey, three cross-hole seismic surveys, three down-hole seismic surveys, and extensive borehole logging. These activities are described in the following sections.

2.4.4.1 Seismic Reflection Survey

A seismic reflection survey was conducted to provide subsurface data to complement those collected during the drilling and sampling program.

A plan view of seismic coverage of the site is presented on Figure 2-50. Total linear coverage is approximately 13,000 feet. Line B-1 runs north-south and Lines B-2, B-3, and B-4 run east-west and tie with Line B-1.

The reflection survey lines produced good resolution on three reflectors in the subsurface. The lowermost reflectors is the crystalline bedrock surface at 800 to 860 feet below msl. The intermediate-depth reflectors is a Cretaceous sedimentary interface at from 660 to 690 feet below msl, and the uppermost is a similar interface varying from about 600 to 630 feet below msl. Some discontinuities on the crystalline bedrock surface can be observed in the profiles that could be interpreted as fault displacements, but none of these features propagate upward to displace the sedimentary beds (Figures 2-51 through 2-54).

It can be concluded that all faults that may have offset the bedrock could not have moved since about mid-Cretaceous time or over 75 million years ago, and therefore such faults are not capable and do not constitute a seismic hazard.

2.4.4.2 Cross-Hole Seismic Survey

Cross-hole seismic surveys were conducted near the reactor sites to determine in-situ seismic compressional (P) and shear (S) wave velocities in the subsurface soils. The intent of these surveys is to provide detailed seismic velocity information on relatively thin layers (approximately 5 feet thick) from the surface to a depth of 300 feet. Knowledge of the S- and P-wave velocities is essential to the determination of the elastic parameters of the site subsurface materials, which are, in turn, essential for evaluation of structure and foundation behavior under seismic excitation. Results of the cross-hole measurements are shown in Figures 2-55 through 2-57.

2.4.4.3 Down-Hole Seismic Survey

A down-hole survey was performed as a supplement to the cross-hole survey to determine if any vertical anisotropy exists in the dynamic elastic properties of the materials at the test locations. The survey was performed at the same boring locations as the cross-hole survey.

The down-hole survey is similar to the cross-hole survey in that the ultimate result is the vertical description of shear wave velocity as a function of depth. A down-hole survey utilizes a source of shear wave energy located at ground surface very near a single listening boring, in contrast to the previously described cross-hole survey. The down-hole

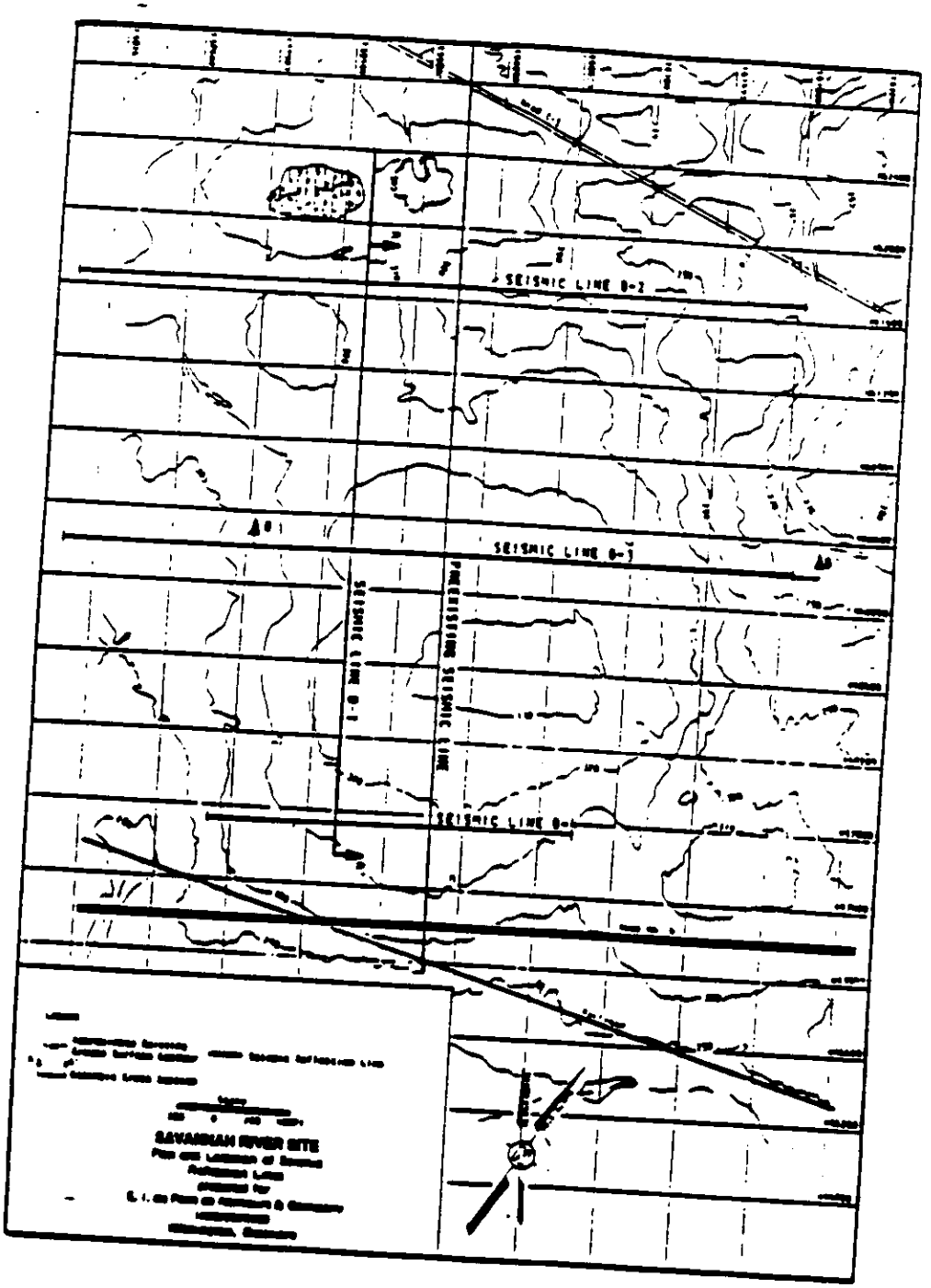

FIGURE 2-50. Plan and Location of Seismic Reflection Lines

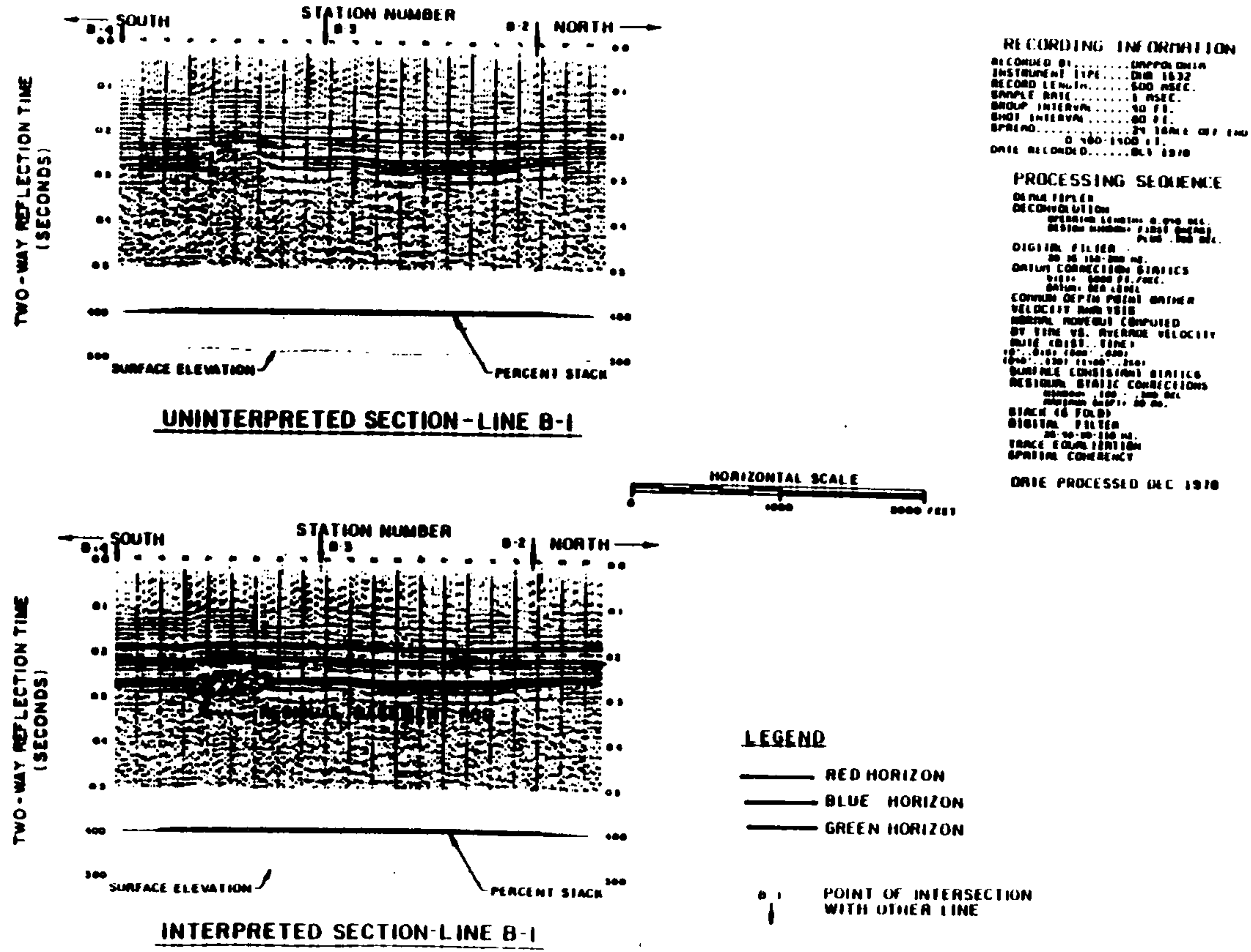

FIGURE 2-51. Seismic Reflection Section Line B-1

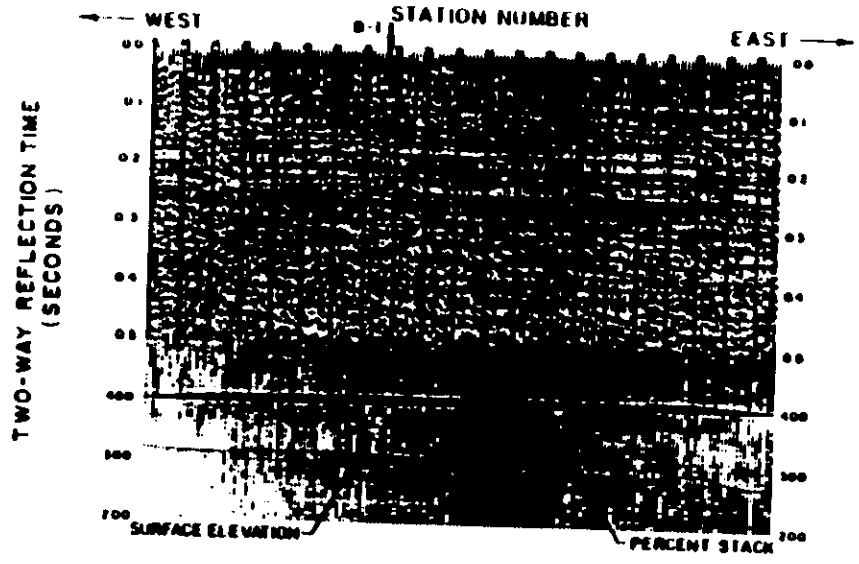

UNINTERPRETED SECTION - LINE B-2

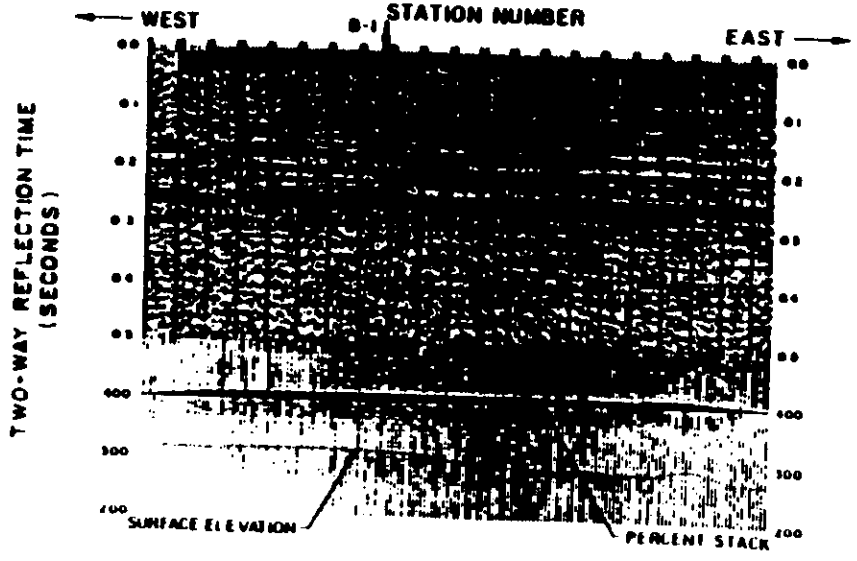

INTERPRETED SECTION - LINE B-2

RECORDING INFORMATION

PROCESSING SEQUENCE

DEMULTIPLEX
DECONVOLUTION
DIGITAL FILTER
ONLINE CORRECTION STATICS
COMMON DEPTH POINT GATHER
VELOCITY ANALYSIS
NORMAL MOVEOUT COMPUTED
BY TIME VS. AVERAGE VELOCITY
RATIO (DIST. TIME)
SURFACE CONSISTENT STATICS
RESIDUAL STATIC CORRECTIONS
STACK (6 FOLD)
DIGITAL FILTER
TRACE EQUALIZATION
SPATIAL COHERENCY

DATE PROCESSED DEC 1978

LEGEND

RED HORIZON
BLUE HORIZON
GREEN HORIZON

B-1 POINT OF INTERSECTION WITH OTHER LINE

HORIZONTAL SCALE

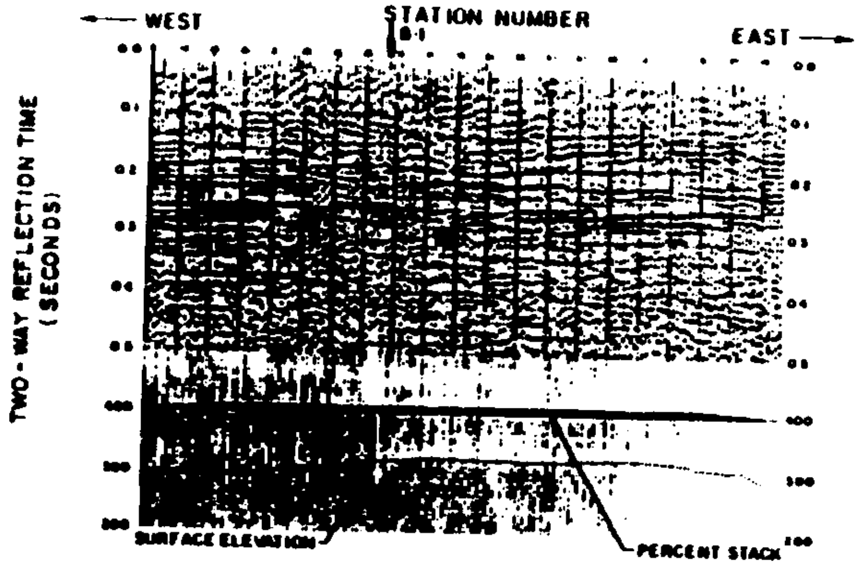

UNINTERPRETED SECTION-LINE B-3

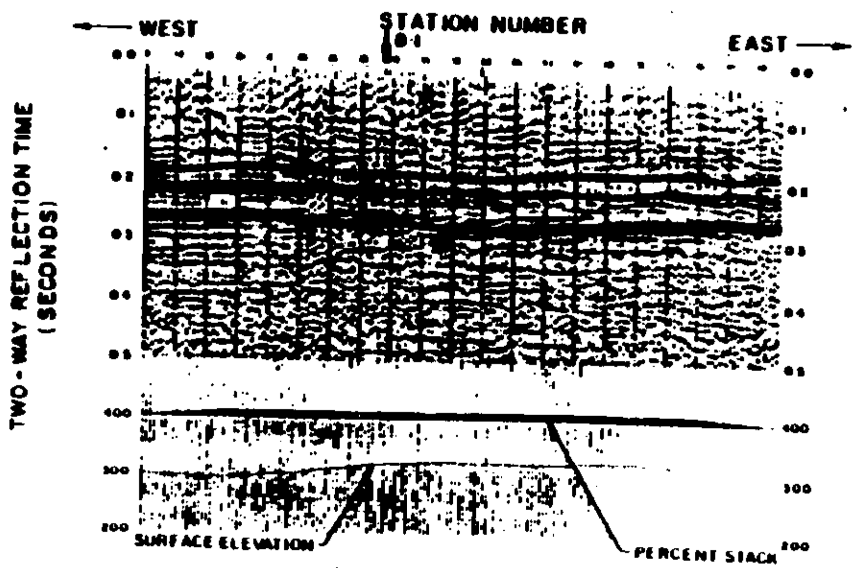

INTERPRETED SECTION-LINE B-3

RECORDING INFORMATION

RECORDED BY.......... [illegible]
INSTRUMENT TYPE..... [illegible] 1632
RECORD LENGTH....... 500 MSEC.
SAMPLE RATE.......... 1 MSEC.
GROUP INTERVAL...... 10 FT.
SHOT INTERVAL....... 80 FT.
SPREAD................ 24 TRACE OFF END
0 400 1100 FT.
DATE RECORDED...... OCT 1978

PROCESSING SEQUENCE

DEMULTIPLEX
DECONVOLUTION
[illegible]
DIGITAL FILTER
[illegible]
DATUM CORRECTION STATICS
[illegible]
COMMON DEPTH POINT GATHER
VELOCITY ANALYSIS
NORMAL MOVEOUT COMPUTED
BY TIME VS. AVERAGE VELOCITY
[illegible]
SURFACE CONSISTANT STATICS
RESIDUAL STATIC CORRECTIONS
[illegible]
STACK (6 FOLD)
DIGITAL FILTER
[illegible]
TRACE EQUALIZATION
SPATIAL COHERENCY

DATE PROCESSED DEC 1978

LEGEND

RED HORIZON
BLUE HORIZON
GREEN HORIZON

B-1 POINT OF INTERSECTION WITH OTHER LINE

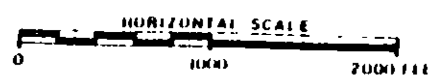

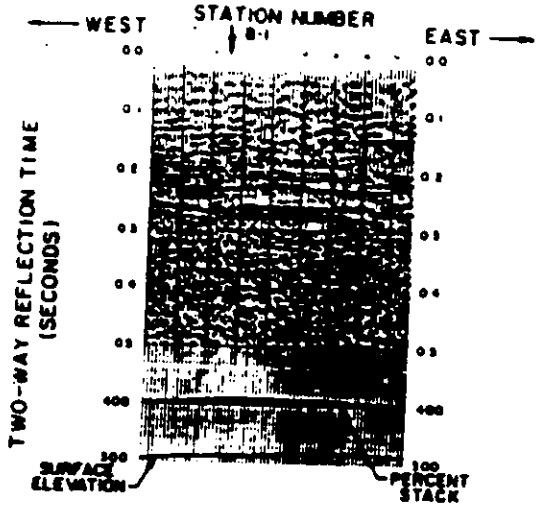

UNINTERPRETED SECTION - LINE B-4

RECORDING INFORMAT

RECORDED BY.....DAPPOLONIA
INSTRUMENT TYPE.....DFS-IV32
RECORD LENGTH.....500 MSEC.
SAMPLE RATE.....1 MSEC.
GROUP INTERVAL.....40 FT.
SHOT INTERVAL.....80 FT.
SPREAD.....24 TRACE OF
0-100-1900 FT.
DATE RECORDED.....OCT 1978

PROCESSING SEQUENC

DEMULTIPLES
DECONVOLUTION
DIGITAL FILTER
DATUM CORRECTION STATICS
COMMON DEPTH POINT GATHER
VELOCITY ANALYSIS
NORMAL MOVEOUT COMPUTED
SURFACE CONSISTANT STATICS
RESIDUAL STATIC CORRECTIONS
STACK (6 FOLD)
DIGITAL FILTER
TRACE EQUALIZATION
SPATIAL COHERENCY

DATE PROCESSED DEC 19

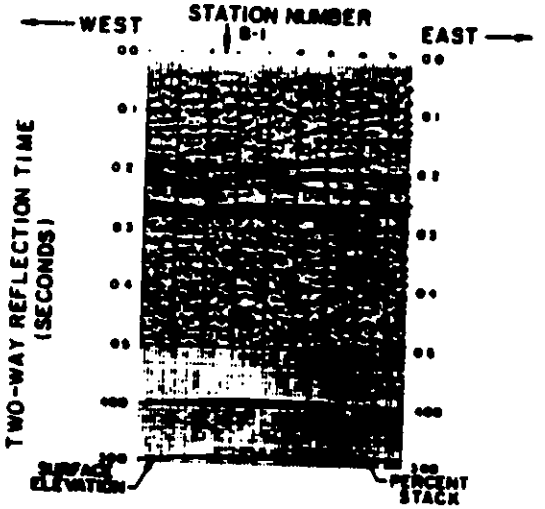

INTERPRETED SECTION - LINE B-4

LEGEND

RED HORIZON
BLUE HORIZON
GREEN HORIZON
POSSIBLE FAULT
B-1 POINT OF INTERSECTION WITH OTHER LINE

HORIZONTAL SCALE
0 1000 2000 FEET

FIGURE 2-54. Seismic Reflection Section Line B-4

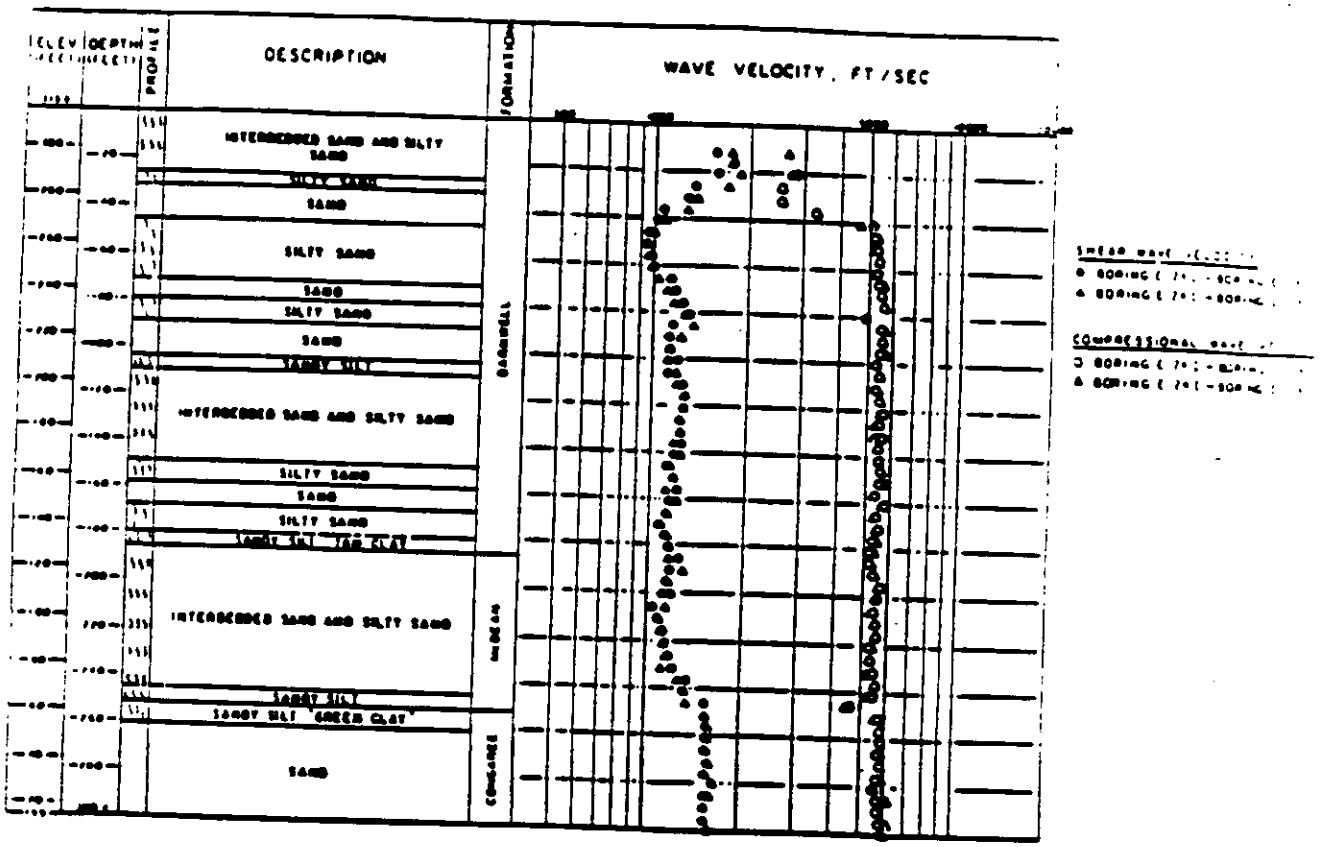

FIGURE 2-55. Compressional and Shear Wave Velocities Versus Depth at Cross-Hole Location E-24

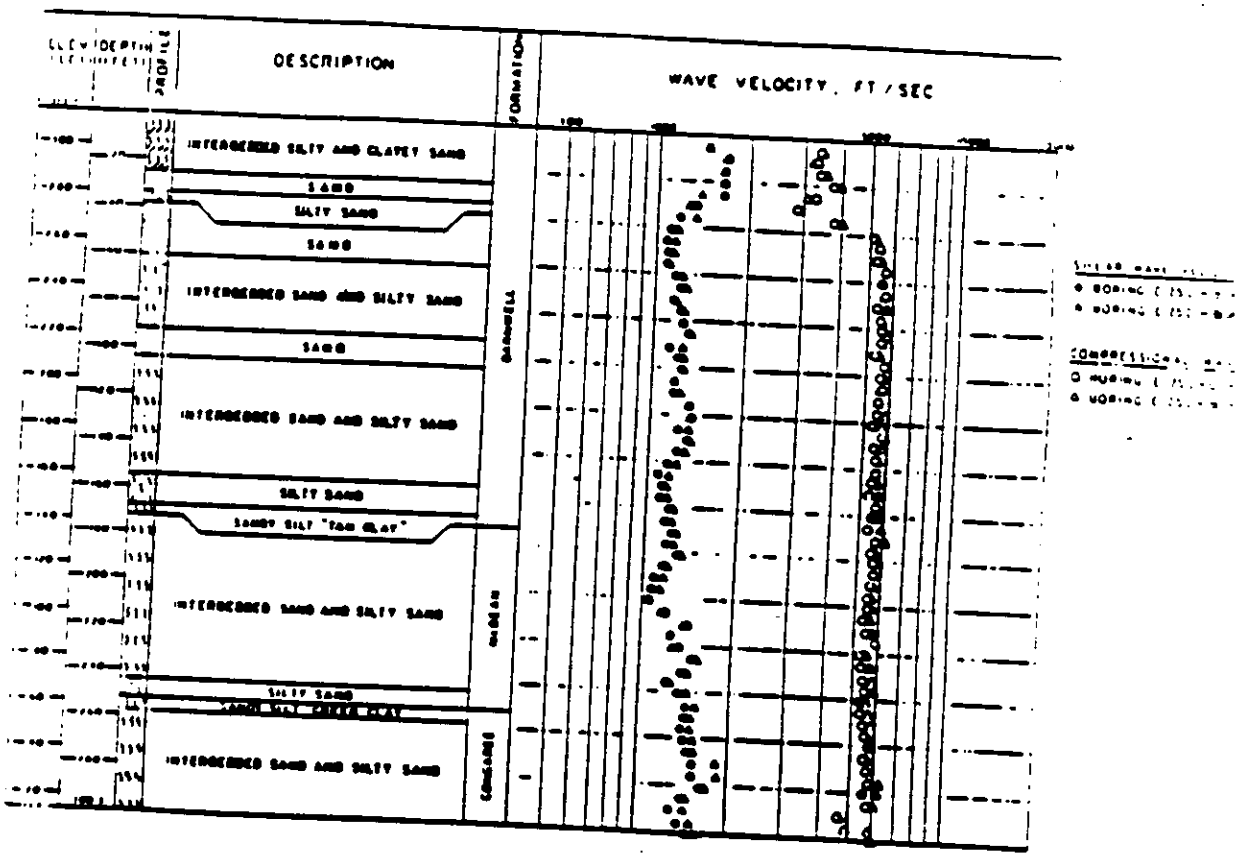

FIGURE 2-56. Compressional and Shear Wave Velocities Versus Depth at Cross-Hole Location E-25

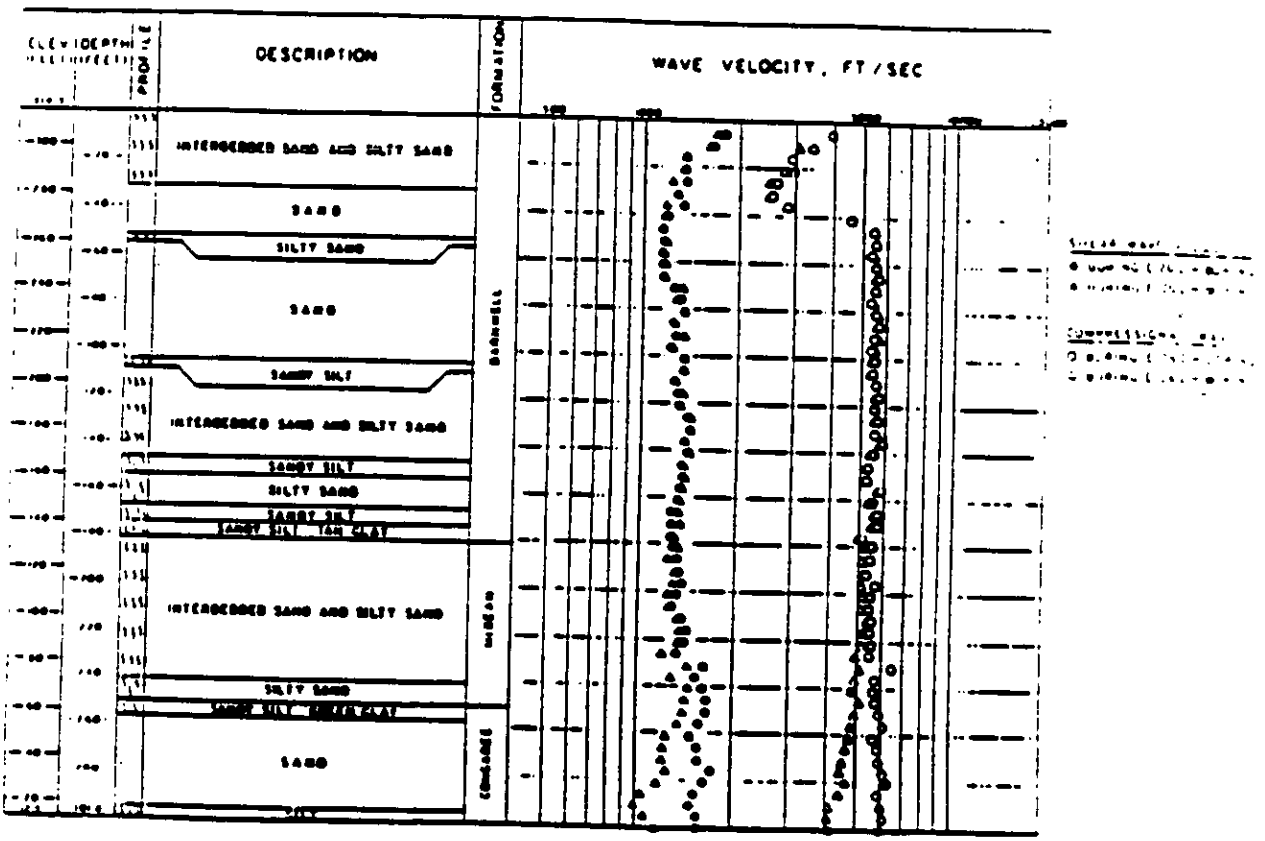

FIGURE 2-57. Compressional and Shear Wave Velocities Versus Depth Cross-Hole Location E-26

survey does not have the inherent precision of the cross-hole technique, but it can be performed in existing borings without drilling additional listening borings and does not require a drill rig on site for performance of the test. Because the path of the shear wave is vertical for a down-hole test, in contrast to the cross-hole test, where it is horizontal, the vertical anisotropy of the soil can be determined from a comparison of the results of the two tests.

Results of down-hole measurements are shown on Figures 2-58 through 2-60.

The shear wave velocities measured are compatible with those at other SRS locations and with those that would be expected in general for soil having similar composition and density. No low velocity zones, indicative of unusually loose or soft soil, were encountered.

The measured compressional wave velocities are in a range of values appropriate for soil of this type and are comparable to dynamic properties at other SRS locations.

2.4.5 Excavations and Backfill

The original plans for the excavation for the 105 reactor buildings specified a one-and-one-half horizontal to one vertical slope. The cubic yardage of excavation and backfill was considerably reduced by excavating on a one-to-one slope with three 5-foot benches, making an overall slope of one-and-one-half to one.

The following quantities of materials were used on the construction of the production reactors:

Area	Excavation, cubic yards	Concrete, cubic yards	Rebar, tons
100 P	2,325,000	200,000	18,175
100 L	2,051,000	165,700	14,100
100 K	2,145,000	166,750	14,300

When the clay spoil from the excavation did not reach the required compaction, sand was used for backfilling under the 100 Area buildings.

2.4.6 Ground Water Conditions

Ground water conditions are discussed in Section 3.

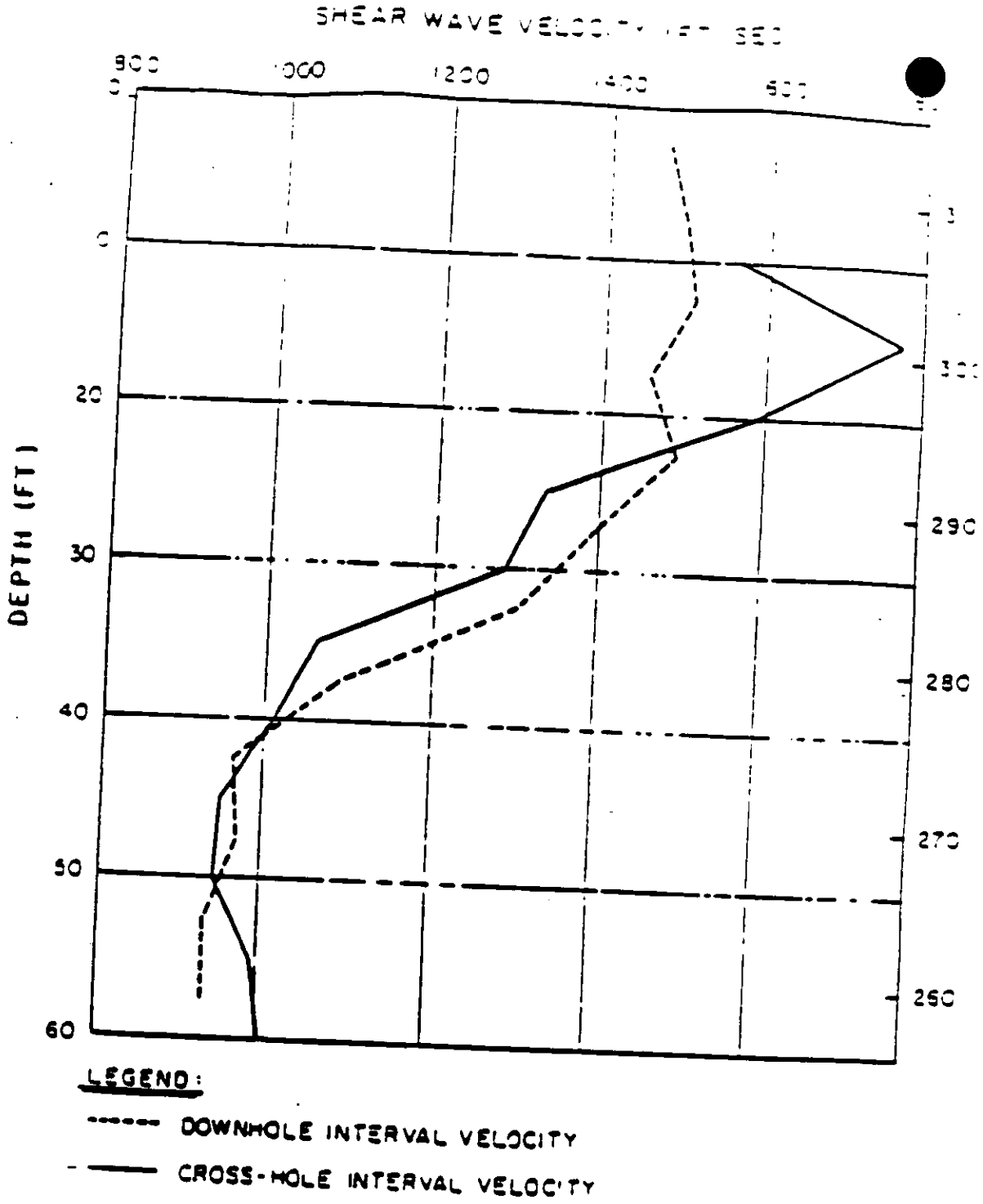

FIGURE 2-58. Comparison of Cross-hole and Down-Hole Interval Shear Velocity for Boring E-24

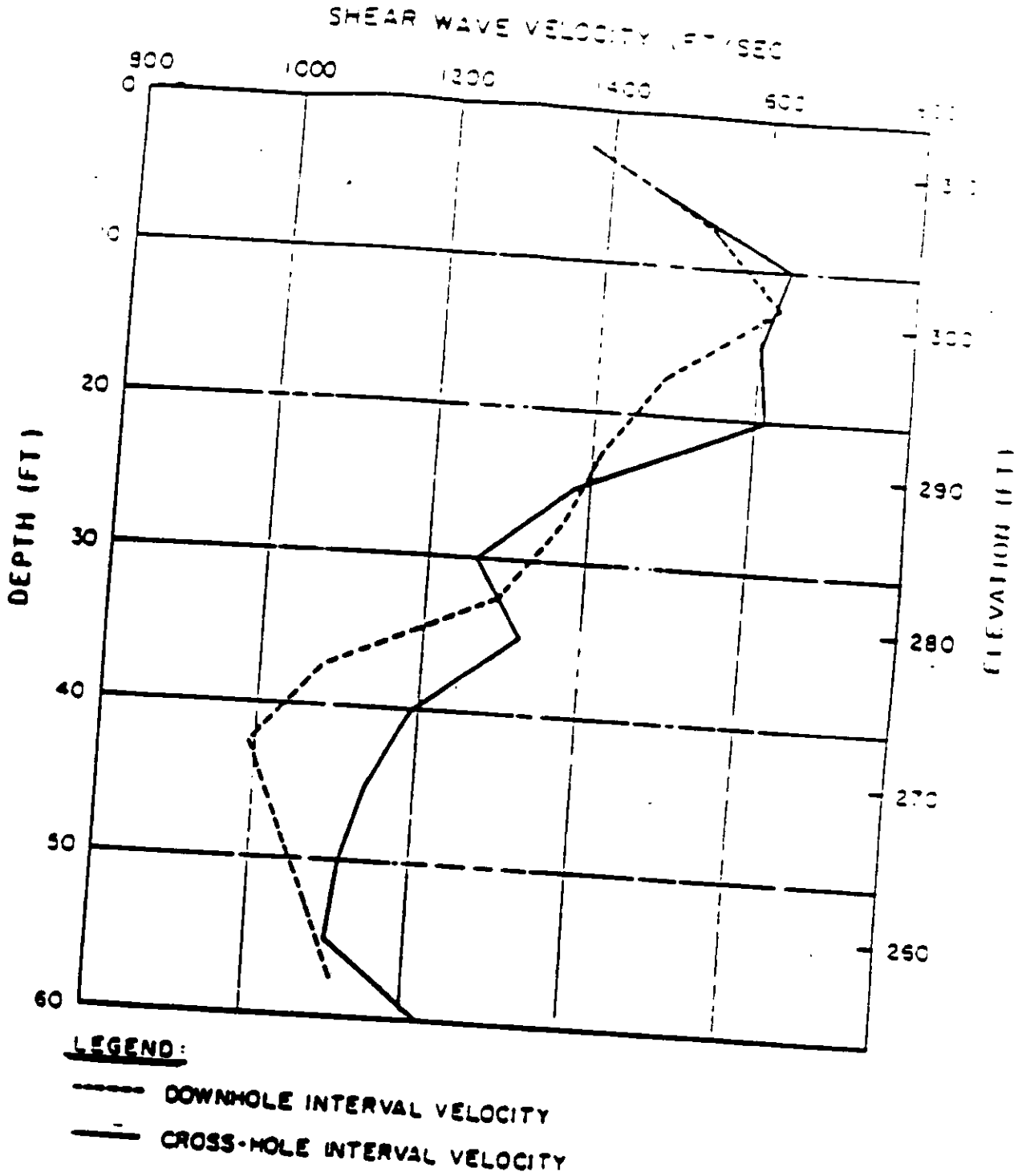

FIGURE 2-59. Comparison of Cross-Hole and Down-Hole Interval Shear Velocity for Boring E-25

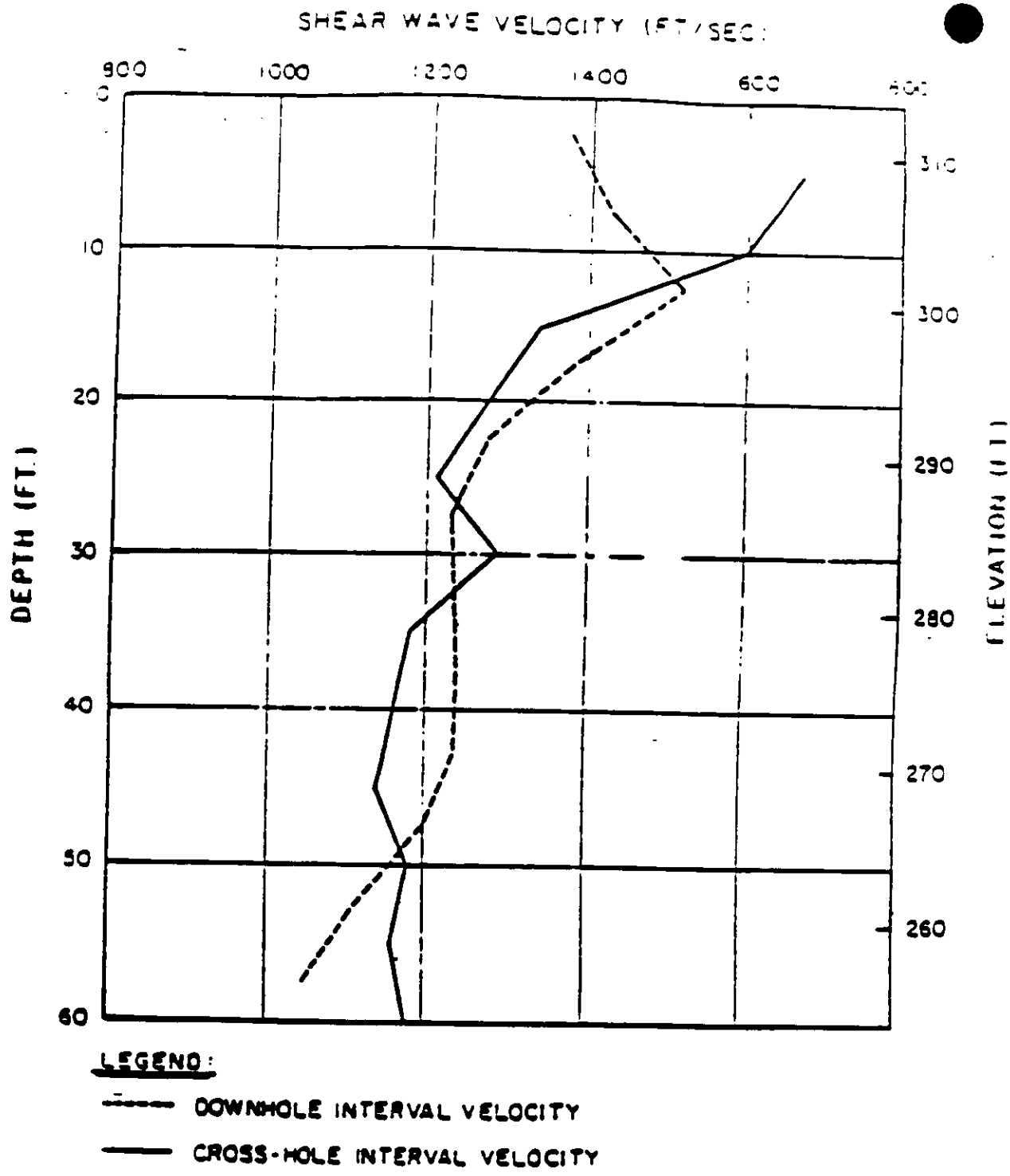

FIGURE 2-60. Comparison of Cross-Hole and Down-Hole Interval Shear Velocity for Boring E-26

2.4.7 Response of Soil and Rock to Dynamic Loading

Liquefaction of saturated sand has been defined as the phenomenon by which the sand undergoes such a substantial reduction in shear strength that the mass of soil actually flows, spreading out until the shear stresses acting on the mass become so small that they are compatible with its reduced shear strength. The term liquefaction has been used for "cyclic mobility," "cyclic liquefaction," and "initial liquefaction," all of which are terms referring to the buildup of pore water pressure and shear strain under cyclic loading. It is the phenomenon of cyclic liquefaction, which may occur even for dense sands under cyclic loading, that is of concern here. One of the widely accepted laboratory investigations of cyclic liquefaction is the constant-volume cyclic triaxial test. In this test, a cyclic deviator stress (o_d) of equal magnitude in compression and tension is applied (undrained loading) to a specimen of saturated sand consolidated to an effective confining pressure, o_o. The constant frequency, constant amplitude cyclic deviator stress is intended to simulate the stress conditions induced in the field (Hazel et al., 1977).

To obtain the strength characteristics of the soil against cyclic liquefaction, cyclic triaxial test were performed (Figure 2-61). The stress-controlled dynamic cyclic triaxial test was performed.

The data relating to possible soil liquefaction includes results of dynamic soil testing as well as soil composition and grain size distribution, standard penetration test (SPT) results, over-consolidation, shear wave velocities, and age of the materials.

A general review of these data based upon criteria recommended by URS/Blume, 1982) indicates that earthquake-induced liquefaction is not a potential problem at the SRS.

2.4.8 Liquefaction Potential

Geotechnical Engineers, Inc. (GEI) (1983) made an in-depth study of the liquefaction potential of soils in S Area near the reactor sites titled "Liquefaction and Cyclic Mobility Potential". This study developed ground failure criteria for three classifications of sands differentiated by the percent by weight passing the No. 200 sieve. Soil conditions at the nearby proposed NPR site and S Area were compared and found to be similar, justifying use of these accepted criteria.

The ground failure criteria presented by GEI are the minimum SPT resistance the soil must have to be immune to liquefaction. The minimum SPT varies with elevation. GEI developed separate criteria for sands with greater than 10%, 7-to-10% and less than 7%, by weight, passing the No. 200 sieve.

The GEI criteria transposed to the reactor sites are shown on Figure 2-62. Figure 2-62 shows the minimum required SPT resistance versus elevation compared to actual SPT values measured in borings. The differences in percent of fine-grained particles is represented by the United Soils

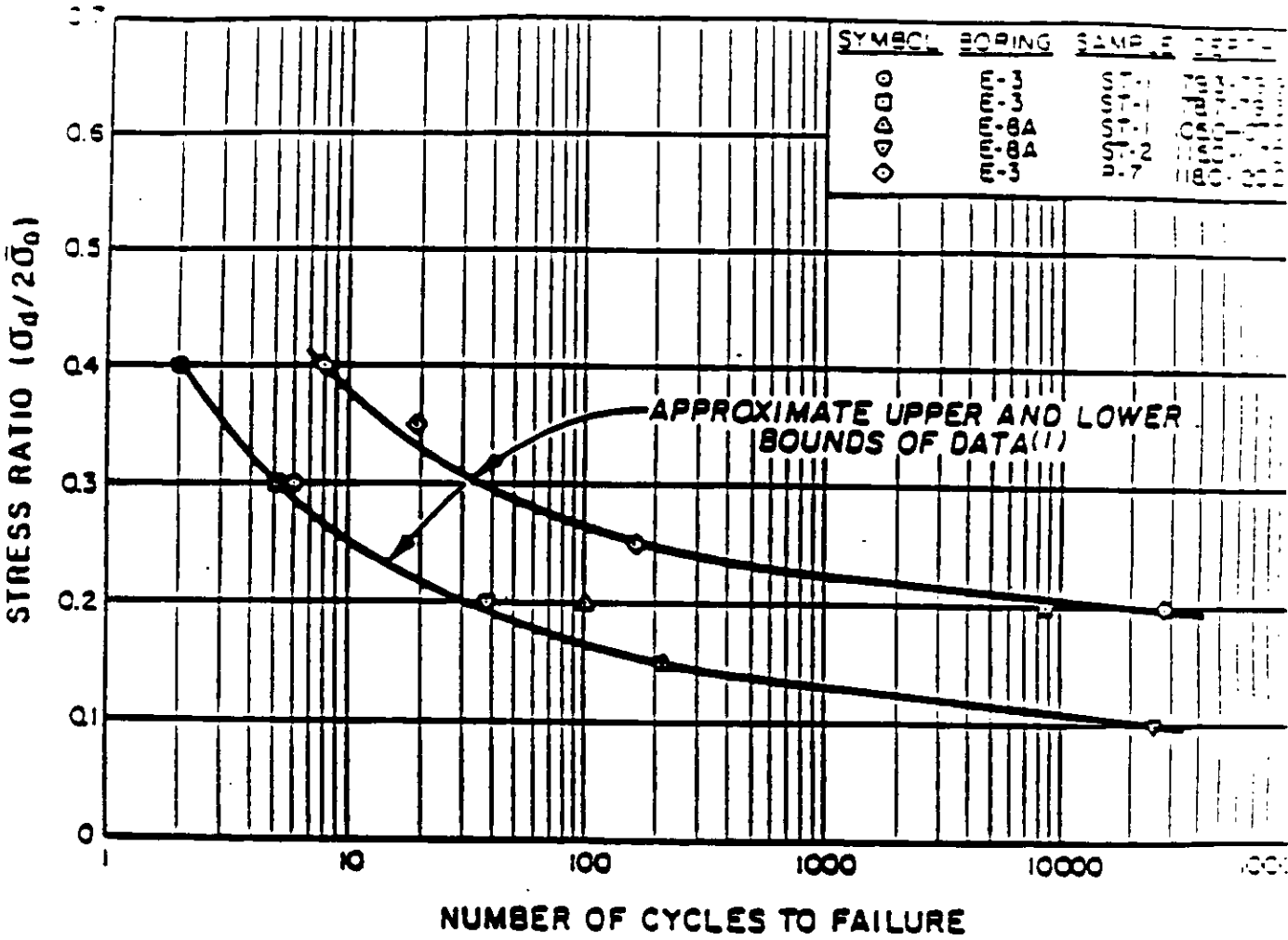

(1) LABORATORY DATA NOT CORRECTED FOR MEMBRANE PENETRATION.

FIGURE 2-61. Undrained Cyclic Triaxial Test Results

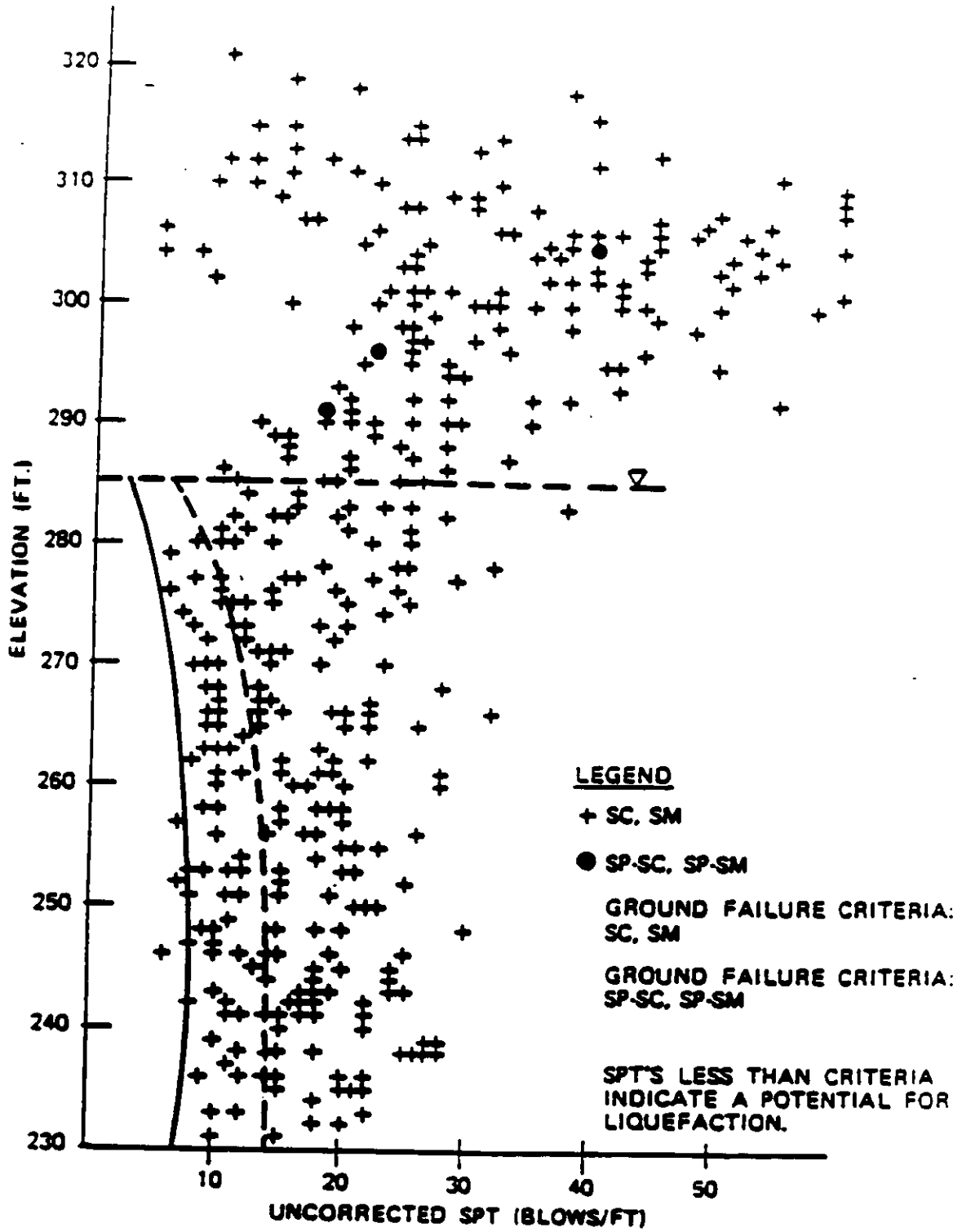

Figure 2-62. Liquefaction Failure Criteria at SRS Site

Classification System (USCS) group symbols. The boring logs assign each sample with greater than 10% passing the No. 200 sieve, and SP-SC and SP-SM correspond to sands with 7-to-10%. The ground failure criterion for Groups SP and SW, corresponding to less than 7% passing the No. 200 sieve, is not shown since these soils were not encountered beyond 230 feet above msl at the nearby proposed NPR site. This is significant because the SP and SW group of soils is the most susceptible to liquefaction.

The comparison of minimum required SPT values with measured values shown on Figure 2-62 and the lack of clean sands, group SP and SW, demonstrates that there is no potential for liquefaction within the area of the reactor sites.

2.5 STABILITY OF SLOPES

Because all of the safety-related structures are located on relatively flat land and were constructed more than 35 years ago, this section does not apply.

The only slopes near the production reactor sites, that might affect any of the sites, are the embankments for PAR Pond and L Lake which are discussed in Section 2.6. A discussion of the excavation and backfill for the safety-related facilities is given in Section 2.4.5.

2.6 EMBANKMENTS AND DAMS

The SRS does not require dams for flood protection. Failure of PAR Pond or L-Lake dams will not jeopardize reactor safety.

The cooling water for P Reactor is normally supplied from PAR Pond. Failure of the PAR Pond dam would temporarily interrupt reactor operation, but safe shutdown could be maintained without the dam. Cooling water from the reactor cooling basin (186 Basin) would, with partial recirculation, provide adequate cooling for safe shutdown. It takes less than one hour to change the status of pumps and valves to switch fully from Par Pond to river water for secondary cooling purposes. Such action may require shutdown of other reactors to maintain adequate river water pressure.

The L Lake serves as a cooling pond for the L-Reactor cooling water effluent. Failure of the L-Lake dam will have no effect on the safety of reactor operation. The principal hazard at this location would be a rapid failure of the dam and release of the impounded water. Failure when the lake is at the crest of the dam would produce a 14-meter-high flood wave. The wave would probably destroy the Seaboard Coastline Railroad (CSX Distribution Services) bridge and South Carolina Highway 125. The wave would break and scatter through the swamp, uprooting trees and vegetation. The effect on the Savannah River is expected to be minor.

REFERENCES FOR CHAPTER 2

Ackermman, H. D. "Seismic-Refraction Study in the Area of the Charleston, South Carolina, 1886 Earthquake," U.S. Geological Survey Professional Paper 1313 (1983).

Amick, D., and Talwani, P. Earthquake Recurrence Rates and Probability Estimates for the Occurrence of Significant Seismic Activity in the Charleston Area: The Next 30 Years, Proceedings of the Third U.S. National Conference on Earthquake Engineering, Vol. I, Earthquake Engineering Research Institute (1986).

Bechtel Corporation. Studies of postulated Millett Fault: Report prepared for Georgia Power Company with Southern Company Services (1982).

Becthel Corporation. Barnwell Nuclear Fuel Plant Safety Analysis Report, San Francisco, CA (1968)

Behrendt, J. C., Hamilton, R. M., Ackerman, H. D., Henry, V. J., and Bayer, K. C. "Marine multichannel seismic-reflection evidence for Cenozoic faulting and deep crustal structure near Charleston, South Carolina," in Gohn, G. S., ed., Studies related to the Charleston, South Carolina earthquake of 1886--Tectonics and seismicity: U.S. Geological Survey Professional Paper 1313 (1983) .

Behrendt, J. C., Hamilton, R. M., Ackerman, H. D., and Henry, V. J. "Cenozoic faulting in the vicinity of the Charleston, South Carolina, 1886 earthquake," Geology, Vol. 9. (1981)

Behrendt, J. C. Interpretations from Multichannel Seismic-Reflection Profiles of the Deep Crush Crossing South Carolina and Georgia from the Appalachian Mountains to the Atlantic Coast, U.S. Geological Survey U.S. Misc. Field Studies, Map MF-1656 (1985).

Bell, J. S. and Gough, D. I. "Northeast-Southwest Compressive Stress in Alberta, Evidence From Oil Wells," Earth and Planetary Science Letters, Vol. 45 (1979).

Bollinger, G. A. "Reinterpretation of the Intensity Data for the 1886 Charleston, South Carolina Earthquake," in Rankin (1977).

Bollinger, G. A. "Seismicity of the Southeastern United States," Bulletin of the Seismological Society of America 63, No. 5 (1973).

Bollinger, G. A., Johnston, A. C., Talwani, P., Long, L. T., Shedlock, K. M., Sibol, M. S., and Chapman, M. C. "Seismicity of the Southeastern U.S. - 1698-1986," Decade of North American Geology (1987).

Bollinger, G. A., and Wheeler, R. L. The Giles County, Virginia Seismogenic Zone - Seismological Results and Geological Interpretations, U.S. Geological Survey Open File Report 82-585 (1982).

Bollinger, G. A., Langer, C. J., and Harding, S. T. "The Eastern Tennessee Earthquake Sequence of October Through December 1973," Bulletin of the Seismological Society of America.

Bonini, W. E. and Woolard, G. P. "Subsurface Geology of North Carolina-South Carolina Coastal Plain from Seismic Data," American Association of Petroleum Geologists Bulletin, Vol. 44 (1960).

Bourland, W. C. and Rigby, J. K. "Sponge Spicules from Early Paleozoic Rocks of the Carolina Slate Belt," Geological Society of America Special Paper 191 (1982).

Bramlett, K. W. "Geology of the Johnston-Edgefield Area, South Carolina, and its Regional Implications," (M. S. Thesis), Columbia University of South Carolina (1980).

Bryant, B. and Reed, Jr., J. C. "Geology of the Grandfather Mountain Window and Vicinity, North Carolina and Tennessee," U.S. Geological Survey Professional Paper 615 (1970).

Butler, J. R. "The Carolina Slate Belt in North Carolina and Northeastern South Carolina," Geologic Notes, Division of Geology, South Carolina State Development Board 15 (1979).

Butler, J. R. and Fullagar, P. D. "Petrochemical and Geochronological Studies of Plutonic Rocks in the Southern Appalachians: III. Leucocratic Adamellites of the Charlotte Belt Near Salisbury, North Carolina," Geological Society of America Bulletin, Vol. 89 (1978).

Butler, J. R. and Ragland, P. C. "A Petrochemical Survey of Plutonic Intrusions in the Piedmont, Southeastern Appalachians, U.S.A.," Contributions to Mineralogy and Petrology, Vol. 24 (1969).

Carpenter, R. H. "Slate Belt of Georgia and the Carolinas: Geology, Stratigraphy, Structure and Exploration Potential," Geological Society of America Special Paper 191 (1982).

Carpenter, R. H. "Investigation of the Stress-Concentration Mechanisms for Intraplate Earthquakes, Geophysical Research Letters (1978).

Carter, J. G. Ed. Biostratigraphy Newsletter, Gulf and Atlantic Coasts of North America, Chapel Hill, NC (1983).

Chapman, W. L., and DiStefano. Savannah River Plant Seismic Survey, 1987-1988 Reserch Report, Conoco, Inc. (1989)

Chowns, T. M., and Williams, C. T. "Pre-Cretaceous Rocks Beneath the Georgia Coastal Plain - Regional Implications," In Gohn (1983).

Christopher, R. A., and Owens, J. P. "Late Cretaceous Palynomorphs From the Cape Fear Formation of North Carolina," Southeastern Geology, Vol. 20 (1979).

Conley, J. F. and Bain, G. L. "Geology of the Carolina Slate Belt West of the Deep River-Wadesboro Triassic Basin, North Carolina," Southeastern Geology, Vol. 6 (1965).

Colquhoun, D. J., Woolen, I. D., Van Nieuwenhuise, D. S., Padgett, G. G., Oldham, R. W., Boylan, D. C., Bishop, J. W., and Howell, P. D. Surface and subsurface stratigraphy, structure, and aquifers of the South Carolina Coastal Plain, Report from Department of Health and Environmental Control, Ground Water Protection Division, published through the Office of the Governor, State of South Carolina, Columbia (1983).

Colquhoun, D. J., Johnson, H. S. "Tertiary Sea-Level Fluctuation in South Carolina," Paleogeography, Paleoclimatology, Paleoecology, 5, 105-126 (1968).

Cooke, C. W. "Carolina Bays, and the Shapes of Eddies," U.S. Geological Survey Professional Paper 254-I (1954).

Cooke, C. W. "Elliptical Bays," Journal of Geology 51 (1943).

Cooke, C. W. "Geology of the Coastal Plain of South Carolina," U.S. Geological Survey Bulletin 867 (1936).

Cramer, H. R., Arden, Jr., D. D. Faults in Oligocene Rocks of the Georgia Coastal Plain, Geological Society America Abstracts with Programs, Southeast Section (1978).

Dallmeyer, R. D., Wright T. E., Secor, D. T., Jr., and Snokes, A. W. "Character of the Alleghenian Orogeny in the Southern Appalachians: Part II. Geochronological Constraints on the Tectonothermal Evolutions of the Eastern Piedmont in South Carolina," Geological Society of America Bulletin, Vol. 9 (1986).

Dallmeyer, R. D. $^{40}Ar/^{39}Ar$ Incremental-Release Ages of Hornblende and Biotite Across the Georgia Inner Piedmont: Their Bearing on Late Paleozoic-Early Mesozoic Tectonothermal History, Geological Society America Abstracts with Programs, Southeast, Section 9 (1977).

Daniels, D. L., Zietz, I., and Popenoe, P. Distribution of Subsurface Lower Mesozoic Rocks in the Southeastern United States, as Interpreted from Regional Aeormagnetic and Gravity Maps, in Ref 83 (1983).

Daniels, D. L. Geologic Interpretation of Geophysical Maps, Central Savannah River Area, South Carolina and Georgia, U.S. Geological Survey, Geophysical Investigation Map GP-893 (1974).

Daniels, R. B., and Wheeler, W. H. "The Goldsboro Ridge, an Enigma," Southeastern Geology, Vol. 12 (1971).

Davis, G. L., Tilton, G. R., and Wetherill, G. W. "Mineral Ages from the Appalachian Province of North Carolina and Tennessee," Journal of Geophysical Research 67 (1962).

De Boer, J. "Paleomagnetic-Tectonic Study of Mesozoic Dike Swarms in the Appalachians," Journal of Geophysical Research, 67 (1967).

Dewey, J. W. A Review of Recent Research on the Seismotectonics of the Southeastern Seaboard and an Evaluation of Hypotheses on the Source of the 1886 Charleston, South Carolina, Earthquake, U.S. Nuclear Regulatory Report, NUREG/CR-4339 (1985).

Dietrich, R. V., Fullager, P. D., and Bottino, M. L. "K/Ar and Rb/Sr Dating of Events of the Appalachians of Southwestern Virginia," Geological Society America Bulletin, 80 (1969).

Doering, J. A. "Quaternary Surface Formations of Southern Part of Atlantic Coastal Plain," Journal of Geology, Vol. 68 (1960).

Dooley, R. E. and Wampler, J. M. Potassium-Argon Relations in Diabase Dikes of Georgia - the Influence of Excess ^{40}Ar on the Geochronology of Early Mesozoic Igneous and Tectonic Events (1983).

Duffield, G. M., Russ, D. R., Root, R. W., Hughes, S. S., Mercer, J. W. Characterization of Groundwater Flow and Transport in the General Separations Areas, report prepared for E. I. du Pont de Nemours and Company, Savannah River Laboratory, Aiken, SC (1986).

Edleman, S. H., Liu, A., and Hatcher, R. D., Jr. "The Brevard Zone in South Carolina and Adjacent Areas: An Alleghenian Orogen Scale Dextral Shear Zone Reactivated as a Thrust Fault," Journal of Geology, Vol. 95 (1987).

Faye, R. E., and Prowell, D. C. Effects of Late Cretaceous and Ceneozoic Faulting on the Geology and Hydrology of the Coastal Plain near the Savannah River, Georgia and South Carolina, U. S. Geological Survey Open-File Report 82-156 (1982).

Froelich, A. J. and Olsen, P. E. "Network Supergroup, a Revision of the Newark Group in Eastern North America," Proceedings of the Second U.S. Geological Survey Workshop on the Early Mesozoic Basins of the Eastern U.S., U.S.G.S. Survey Circular 946 (1985).

Fullagar, P. D. "Summary of Rb-Sr Whole Rock Ages for South Carolina," South Carolina Geology, Vol. 25 (1981).

Fullagar P. D. and Butler, J. R. "325 to 265 Million Year Old Granitic Plutons in the Piedmont of the Southeastern Appalachians," American Journal of Science, Vol. 279 (1979).

Fullagar, P. D. "Age and Origin of Plutonic Intrusions in the Piedmont of the Southeastern Appalachians," Geological Society of America Bulletin, Vol. 82 (1971).

Gamble, E. E., Daniels, R. B., and Wheeler, W. H. Primary and Secondary Rims of Carolina Bays," Southeastern Geology, Vol. 18 (1977).

Geotechnial Engineers, Inc. Assessment of Seismic Stability of S-Area, Savannah River Plant, Aiken, SC, report submitted to E. I. du Pont de Nemours and Co., Inc., Aiken, SC (1983).

Gephart, J. W., and Forsythe, D. D. "On the State of Stress in New England as Determined From Earthquake Focal Mechanisms," Geology, Vol. 13 (1985).

Gibson, G. G., Teeter, S. A., and Fedonkin, M. A. "Ediacarian Fossils from the Carolina Slate Belt, Stanley County, North Carolina," Geology, Vol. 12 (1984).

Gilbert, N. J., Brown, H. S., and Schaeffer, M. F. "Structure and Geologic History of a Part of the Charlotte Belt, South Carolina Piedmont," Southeastern Geology, Vol. 23 (1982).

Glenn, L. C. Some Notes on Farlington Bays, Science, 2 (1985).

Glover, L., III, Poland, F. B., Tucker, R. D., and Bourland, W. C. Diachronous Paleozoic Mylonites and Structural Heredity of Triassic-Jurassic Basins in Virginia, Geological Society of America Abstracts with Programs, Vol. 12 (1980).

Glover, L., III, Mose, D. G., Poland, F. B., Bobyarchick, A. R., and Bourland, W. C. Greenville Basement in the Eastern Piedmont of Virginia: Implications for Orogenic Models, Geological Society of American Abstracts with Programs, Vol. 10 (1978).

Glover, L., III, Sinha, A. K., Higging, M. W., and Kirk, W. S. U-Pb Dating of Carolina Slate Belt and Charlotte Belt Rocks, Virginia District, Virginia and North Carolina, Geological Society of America Abstracts with Programs, Southeast Section 3 (1971).

Gohn, G. S., Ed. "Studies Related to the Charleston, South Carolina, Earthquake of 1886 - Tectonics and Seismicity," U. S. Geological Survey Professional Paper 1313 (1983) .

Gohn, G. S., Gottfried, D., Lanphere, M. A., and Higgins, B. B. "Regional Implications of Traissic or Jurassic Age for Basalt and Sedimentary Reds Beds in the South Carolina Coastal Plain," Science (n.s.), V. 202 (1978a).

Gohn, G. S., Bybell, L. M., Smith, C. C., and Owens, J. P. Preliminary Stratigraphic Cross Sections of Atlantic Coastal Plain Sediments of the Southeastern United States--Cretaceous Sediments Along the South Carolina Coastal Margin, U. S. Geological Survey Misc. Field Studies Map MF-15-A (1978b).

Gohn, G. S., Higgins, B. B., Smith, C. C., and Owens, J. P. Lithostratigraphy of the Deep Corehole (Clubhouse Crossroads 1) Near Charleston, South Carolina, in Rankin (1977).

Griffin, V. S., Jr. "Analysis of the Piedmont in Northwest South Carolina," Geological Society of America Bulletin, Vol. 83 (1974).

Griffin, V. S., Jr. "The Inner Piedmont Belt of the Southern Crystalline Appalachians," Geological Society of America Bulletin, Vol. 83 (1971).

Griffin, V. W., Jr. Migmatitic Inner Piedmont Belt of Northwestern South Carolina, Geologic Notes, Division of Geology, South Carolina State Development Board 13 (1969).

Haimson, B. C. Hydrofracturing Stress Measurements, Bad Creek Pumped Storage Project, Unpublished data submitted to Duke Power Company (1975).

Hatcher, R. D., Jr. "Tectonics of the Southern and Central Appalachian Internides," Annual Reviews of Earth and Planetary Science, Vol. 15 (1987).

Hatcher, R. D., Jr., Hopson, J. L., Edelman, S. H., Liu, A., McClellan, E. A., and Stieve, A. L. "Detailed geologic map of the Appalachian Ultradeep Core Hole (ADCHO) Region: New Constraints on the Structure of the Southern Appalachian Internides," Geological Society of American Abstracts with Programs, V. 18 (1986).

Hatcher, R. D., Jr., and Zietz, I. Tectonic Implications of Regional Aeromagnetic and Gravity Data from the Southern Appalachians, Proceedings, I. G. C. O. Project 27; the Caldonide Oregon 1979 Meeting Blacksburg, VA (1980).

Hatcher, R. D., Jr., Howell, D. E., and Talwani, P. Eastern Piedmont Fault System: Speculations on Its Extent, Geology, V. 5 (1977).

Hatcher, R. D., Jr. "Developmental Model for the Southern Appalachians," Geological Society of America Bulletin, 80 (1972).

Hatcher, R. D., Jr. "Structural, Petrologic, and Stratigraphic Evidence Favoring a Thrust Solution to the Brevard Problems," American Journal of Science, 210 (1971).

Hatcher, R. D., Jr. "Stratigraphy of the Brevard Zone and Poor Mountain Area, Northwestern South Carolina," Geological Society of America Bulletin, Vol. 81 (1970).

Hazel, J. R., Bybell, L. M., Christopher, R. A., Frederiksen, N. O., May, F. E., McLean, D. M., Poore, R. Z., Smith, C. C., Sohl, N. F., Valentine, P. C., and Witmer, R. J. Biostratigraphy of the Deep Corehole (Clubhouse Crossroads Corehole 1) near Charleston, South Carolina, in Rankin, D. W., ed., Studies related to the Charleston, South Carolina, earthquake of 1886--A preliminary report: U. S. Geological Survey Professional Paper 1028 (1977).

Heron, S. D., Jr., Johnson, H. S., and Pooser, K. S. "Clastic Dikes in the Western Coastal Plain of South Carolina," Abs., Geological Society of America Spec. Paper, 87 (1965).

Higgins, B. B., Gohn, G. S., Bybell, L. M. Subsurface Geologic Evidence for Normal Faults in the South Carolina Coastal Plain Near Charleston, Geological Society of America Abstracts with Programs, Southeast Section 10.

Hills, F. A., and Butler, J. R. "Rubidium-Strontium Dates from Some Rhyolites from the Carolina Slate Belt of the North Carolina Piedmont," Geological Society of America Abstracts for 1968, Special Paper 121 (1969).

Horton, J. W., Jr. "Geologic Map of the Kings Mountain Belt Between Gaffney, South Carolina, and Lincolnton, North Carolina," in Horton et al. (1981).

Horton, J. W., Jr. "Alleghanian Deformation, Metamorphism and Granite Emplacement in the Central Piedmont of the Southern Appalachians," American Journal of Science, Vol. 287 (1987).

Horton, J. W., Jr., Buller, J. R., Schaeffer, M. F., Murphy, C. F., Conner, J. M., Milton, D. J., and Sharp, W. E. Field Guide to the Geology of the Kings Mountain Belt Between Gaffney, South Carolina and Lincolnton, North Carolina (1981).

Howell, D. E., and Zupan, A. W. "Evidence for Post-Cretaceous Tectonic Activity in the Westfield Creek Area, North of Cheraw, South Carolina," Geologic Notes, Division of Geology, South Carolina State Development Board, 18 (1974).

Huddlestun, P. F., Hetrick, J. H. "Upper Eocene Stratigraphy of Central and Eastern Georgia," Georgia Geologic Survey Bulletin, 95 (1985).

Inden, R. F., and Zupan, A. W. Normal Faulting of Upper Coastal Plain Sediments, Ideal Kaolin Mine, Langley, South Carolina, Geologic Notes, Division of Geology, South Carolina State Development Board 19 (1975).

Johnson, H. S., Jr., and Heron, S. D., Jr. Slump Features in the McBean Formation and Younger Beds, Riley Cut, Calhoun County, South Carolina, Geologic Notes, Division of Geology, South Carolina Development Board, Vol. 9.

Johnson, D. W. The Origin of the Carolina Bays, Columbia University Press, New York (1942).

Karner, G. D. and Watts, A. B. "Gravity Anomalies and Flexure of the Lithosphere," J. Geophys. Res., Vol. 88, p 10449 (1983).

Kerns, F. L., Katrina, M. P., Lawrence, D. P., and Chalcraft, R. G. Paleoenvironmental Interpretation of a Portion of the Carolina Slate Belt, Saluda County, South Carolina, Geological Society of America Abstracts with Programs, Vol. 13 (1981).

King, P. B. "Systematic Pattern of Triassic Dikes in the Appalachian Region-Second Report," U.S. Geological Survey Professional Paper 759-D (1971).

Kish, P. B., Butler, J. R., and Fullagar, P. D. The Timing of Metamorphism and Deformation in the Central and Eastern Piedmont of North Carolina, Geological Society of America Abstracts with Program, Vol. 11 (1979).

Klitgord, K. D., Behrendt, J. C. Basin Structure of the U.S. Atlantic Margin, Geological and Geophysical Investigations of Constructual Margins, American Association of Petroleum Geologists Memoirs 29 (1979).

LeHuray, A. P. "U-Pb and Th-Pb Whole-Rock Isochrons of the Carolina Slate Belt," Geological Society of America Bulletin, Vol. 99 (1987).

Lindholm, R. C. Triassic - "Triassic Faulting in Eastern North America - A Model Based on Pre-Triassic Structures," Geology, Vol. 6 (1978).

Long, L. T., Zilt, K H., Liow, Propes, R., Shand J., Reinbold, D., and Schecter, B. "The North Georgia Earthquake of October 9, 1984," Earthquake Notes, Vol. 57 (1986).

Long, L. T., and Lowell, R. P. "Thermal Model for Some Continental Margin Sedimentary Basins and Uplift Zones," Geology Vol. 1 (1973).

Maher, H. D., Jr. "Kinematic History of Mylonitic Rocks from the Augusta Fault Zone, South Carolina and Georgia," American Journal of Science, Vol. 287 (1987).

Maher, H. D., Jr. Stratigraphy and Structure of the Belair and Kiokee Belts Near Augusta, Georgia (1978).

Manspeizer, W., Puffer, J. H., and Cousminer, H. L. "Separation of Morocco and Eastern North America: A Triassic-Liassic Stratigraphic Record," Geological Society of America Bulletin, Vol. 89 (1978).

Marine, I. W. Structural Model of the Buried Dunbarton Triassic Basin in South Carolina and Georgia, Geological Society of America Abstracts with Programs, Northeast/Southeast Section 8 (1976).

Marine, I. W., and Sipple, G. E. "Buried Triassic Basin in the Central Savannah River Area, South Carolina and Georgia," Geological Society of America Bulletin, 85 (1974).

Marine, I. W. "Geohydrology of a Buried Triassic Basin at Savannah River Plant, South Carolina," American Association of Petroleum Geological Bulletin, 55 (1974).

Mauk, F. J., Christensen, D., and Henry, S. "The Sharpsburg, Kentucky, Earthquake 27 July 1980: Main Shock Parameters and Isoseismal Maps," Bulletin of the Seismological Society of America, Vol. 72 (1982).

McBride, J. H., Nelson, K. D., and Brown, L. D. Early Mesozoic Basin Structure and Tectonics of the Southeastern United States as Revealed from COCORP Reflection Data and Its Relation to Atlantic Rifting (1988).

McGarr, A., and Gay, N. C. "State of Stress in the Earth's Crust," Annual Review of Earth and Planetary Science, Vol. 6 (1978).

Melton, F. A. "The Origin of the Supposed Meteorite Scars, A Reply," Journal of Geology, Vol. 42 (1934).

Melton, F. A., and Schriever, W. "The Carolina 'Bays'--Are They Meteorite Scars?" Journal Geology, Vol. 41 (1933).

Milton, C., and Grasty, R. "Basement Rocks of Florida and Georgia," American Association of Petroleum Geological Bulletin, 53 (1969).

Milton, C., and Hurst, Vol. J. "Subsurface Basement Rocks of Georgia, Georgia," Geological Survey Bulletin, 76 (1965).

Mixon, R. B., and Pilkey, O. H. "Reconnaissance Geology of the Submerged and Emerged Coastal Plain Province, Cape Lookout Area, North Carolina," Geological Survey Professional Paper 859 (1976).

Munsey, J. W., Bollinger, G. A. "Focal Mechanism Analyses for Virginia Earthquakes (1978-1984)," Bulletin of the Seismological Society of America, Vol. 75 (1985).

Murphy, J. R., and O'Brien, L. J. "The Correction of Peak Ground Acceleration Amplitude with Seismic Intensity and Other Physical Parameters," Seismological Society of America Bulletin, Vol. 67, No. 3 (1977).

Muthanna, A., Talwani, P., Colquohoun, D. J. Preliminary Results from Integration of Stratigraphic and Geophysical Observations in the Central South Carolina Coastal Plain, Eastern Section Seismological Society of America, 59th Annual Meeting (1987).

Nelson, K. D., and Talwani, P. "Reanalysis of Focal Mechanism Data for the Central Virginia Seismogenic Zone, Earthquake Notes, Vol. 56 (1985).

Nelson, K. D., Arnow, J. A., McBride, J. H., Willemin, J. H., Huang, J., Zheng, L., Oliver, J. E., Brown, L. D., and Kaufman, S. "New COCORP Profiling in the Southeastern United States. Part I: Late Paleozoic Sutre and Mesozoic Rift Basin," Geology, V. 13 (1985).

Noel, J. R., Spariousu, D. J., and Dallmeyer, R. D. "Paleomagnetism and $^{40}Ar/^{39}Ar$ Ages from the Carolina Slate Belt, Albermarle, North Carolina: Implications from Terrane Amalgamation with North America," Geology, Vol. 16 (1988).

Nystrom, P. G., Jr., Willoughby, R. H., and Kite, L. E. Cretaceous-Tertiary Stratigraphy of the Upper Edge of the Coastal Plain Between North Augusta and Lexington, South Carolina, Carolina Geological Society Field Trip Guidebook, 9186, South Carolina Geological Survey (1986).

Nystrom, P. G., Jr., and Willoughby, R. H. Geological Investigations Related to the Stratigraphy in the Kaolin Mining District, Aiken County, South Carolina, Carolina Geological Society Field Trip Guidebook 1982, South Carolina Geological Survey, Columbia, South Carolina (1982).

Odom, A. L., and Brown, J. F. Was Florida a Part of North America in the Lower Paleozoic? Geological Society of America Abstracts with Programs, Northeast/Southeast, Section 8 (1976).

Odom A. L., and Fullagar, P. D. Geochronologic and Tectonic Relationships Between the Inner Piedmont, Brevard Zone, and Blue Ridge Belts, North Carolina (1973).

Odom, A. L., Kish, S. A., and Leggo, P. J. Extension of 'Grenville Basement' to the Southern Extremity of the Appalachians: U-Pb Ages of Zircons, Geological Society of America Abstracts with Programs, Southeast Section 5 (1973).

Odom, A. L., and Fullagar, P. D. Isotopic Evidence for Late Devonian Movement Along the Brevard Zone, Geological Society of America Abstracts with Programs, Northeast/Southeast Section 8 (1970).

Overstreet W. C., and Bell, H., II The Crystalline Rocks of South Carolina, U.S. Geological Survey Bulletin 1183 (1965).

Peterson, T. A., Brown, L. D., Cook, F. A., Kaufman, S., and Oliver, J. E. "Structure of the Riddleville Basin from COCORP Seismic Data and Implications for Reactivation Tectonics," Journal of Geology, Vol. 92 (1984).

Phillips, J. D. "Magnetic Basement Near Charleston, South Carolina--A Preliminary Report, U.S. Geological Survey Professional Paper 28 (1977).

Pojecta, J., Jr., Kriz, J., and Berdan, J. M. "Silurian-Devonian Pelecypods and Paleozoic Stratigraphy of Subsurface Rocks in Florida and Georgia and Related Silurian Pelecypods from Bolivia and Turkey," U.S. Geological Survey Professional Paper 879 (1976).

Popenoe, P., and Zietz, I. The Nature of the Geophysical Basement Beneath the Coastal Plain of South Carolina and Northeastern Georgia, in Rankin, 1977 (1977).

Preston, C. D., and Brown, C. Q. "Geologic Section Along a Carolina Bay, Sumter County, South Carolina, Southern Geology, Vol. 6 (1964).

Prouty, W. F. Carolina Bays and Their Origin, Geological Society of America Bulletin 63 (1952).

Prowell, D. C., Christopher, R. A., Edwards, L. E., Bybell, L. M., and Gill, H. E. "Geological Section of the Updip Coastal Plain from Central Georgia to Western South Carolina," U.S. Geological Survey, Text with Map MF-1737 (1985a).

Prowell, D. C., Edwards, L. E., and Frederiksen, N. O. The Ellenton Formation in South Carolina--A Revised Age Designation From Cretaceous to Paleocene, U.S. Geological Survey Bulletin 1605-A (1985b).

Prowell, D. C., and O'Conner, B. J. "Belair Fault Zone: Evidence of Tertiary Fault Displacement in Eastern Georgia, Geology, Vol. 6 (1978).

Rankin, D. W. "Studies Related to the Charleston, South Carolina Earthquake of 1886." U.S. Geological Survey Professional Paper 1028 (1977).

Rankin, D. W. Stratigraphy and Structure of Precambrian Rocks in Northwestern North Carolina, Interscience Publishers, New York (1970).

Rankin, D. W., Stern, T. W., Reed, J. C., Jr., and Newell, M. F. "Zircon Ages of Felsic Volcanic Rocks in the Upper Precambrain of the Blue Ridge, Appalachian Mountains," Science, 166 (1969).

Rastogi, B. K., and Talwani, P. Reservoir Induced Seismicity at Lake Jocassee in South Carolina USE (1981).

Ratcliffe, N. M. "The Ramapo Fault System in New York and Adjacent Northern New Jersey: A Case of Tectonic Heredity," Geological Society of America Bulletin, Vol. 82 (1971).

Rawlins, J. Seismotectonics of the Newberry, South Carolina Earthquakes, (M. S. Thesis) Columbia, University of South Carolina (1986).

Renfro, H. B., and Feray, D. E. Geological Highway Map of the Mid-Atlantic Region United States Geological Highway Map, Vol. 4, American Association of Petroleum Geologists (1970).

Rogers, J. The Tectronics of the Appalachians, New York, Wiley-Interscience (1970).

Rogers, J. Criteria for Recognizing Environments of Formation of Volcanic Suites: Application of these Criteria to Volcanic Sites in the Carolina Slate Belt (1982).

Sacks, P. E., and Dennis, A. J. The Modoc Zone-D_2 (Early Alleghanian) in the Eastern Appalachian Piedmont, South Carolina and Georgia (1987).

Salisbury, R. D. The Physical Geography of New Jersey, In New Jersey Geological Survey Final Report of State Geologist, Vol. 4 (1898).

Schaeffer, M. E., Steffens R. E., and Hatcher, R. D., Jr. In Situ Stress and its Relationship to Joint Formation in the Toxaway Gneiss, Northwestern South Carolina, South-Eastern Geology, Vol. 20 (1979).

Schwab, F. L. "Upper Precambrian-Lower Paleozoic Clastic Sequences, Blue Ridge and Adjacent Areas, Virginia and North Carolina: Initial Rifting and Continental Margin Development, Appalachian Orogen in Society of Economic Paleontologists and Mineralogists (SEPM) Field Guide," Textoris, D. A. (ed.), Third Annual Mid-Year Meeting, Raleigh, NC (1986).

Secor, D. T., Jr., Snoke, A. W., Bramlett, K. W., Costello, O. P., and Kimbrell, O. P. "Character of the Alleghanian orogeny in the Southern Appalachians: Part I. Alleghanian deformation in the eastern Piedmont of South Carolina," Geological Society of America Bulletin, Vol. 97 (1986).

Secor, D. T., Jr. Regional Overview (1987).

Secor, D. T., Jr., Peck, L.S., Pitcher, D. M., Prowell, D. C., Simpson, D. H., Smith, W. A., and Snoke, A. W. "Geology of the Area of Induced Seismic Activity at Monticello Reservoir, South Carolina," Journal of Geophysical Research, Vol. 87 (1982).

Secor, D. T., Jr., Samson, L. S., Snoke, A. W., and Palmer, A. R. "Confirmation of Carolina Slate Belt as an Exotic Terrance," Science, Vol. 221 (1983).

Secor, D. T., Jr., Peck, L. S., Pitcher, D. M., Prowell, D. C., Simpson, D. H., Smith, W. A., and Snoke, A. W. "Geology of the Area of Induced Seismic Activity at Monticello Reservoir, South Carolina," Journal of Geophysical Research, V. 87. No. B8 (1982).

Secor, D. T., Jr., and Snoke, A. W. "Stratigraphy, Structure and Plutonium in he Central South Carolina Piedmont," Carolina Geological Society Field Trip Guidebook for 1978, South Carolina Geological Survey (1978).

Secor, D. T., Jr., and Wagener, H. D. "Stratigraphy Structure Petrology of the Piedmont in Central South Carolina, South Carolina Geological Survey Geologic Notes, Vol. 12 (1968).

Seever, L., and Armbruster, J. G. "The 1886 Charleston, South Carolina Earthquake and the Appalachian Detachment," Journal of Geological Research, Vol. 86 (1981).

Seiders, V. M. "A Chemical Bimodal Calc-Alkalic Suite of Volcanic Rocks, Carolina Volcanic Slate Belt, Central North Carolina," Southeastern Geology, Vol. 19 (1978).

Shar, M. L., and Sykes, L. R. "Contemporary Compressive Stress and Seismicity in Eastern North America: An example of Intraplate Tectronics," Geological Society of America Bulletin, 84 (No. 6) (1973).

Shimer, J. A. Field Guide to Landforms in the United States (1972).

Sinha A. K., and Zietz, I. "Geophysical and Geochemical Evidence for a Hercynian Magmatic Are, Maryland to Georgia, Geology, Vol. 10 (1982).

Siple, G. E. "Geology and Ground Water of the Savannah River Plant and Vicinity, South Carolina," U.S. Geological Survey Water Supply Paper 1841 (1967).

Sloan, E. "Catalog of the Mineral Localities of South Carolina, South Carolina Geological Survey Bulletin 2 (1908).

Smith, W. A., Jr., Talwani, P., and Colquhoun, D. J. "The Seismotectonics of the Bowman Seismic Zone, South Carolina," Geological Society of America Bulletin (1988).

Smith, W. A., Jr. and Talwani, P. "Results of a Refraction Survey in the Bowman Seismogenic Zone, South Carolina," South Carolina Geology (1987).

Smith, W. A., Jr. An Integrated Study of the Seismotechtonics of the Bowman Seismic Zone, South Carolina, (Ph.D. Thesis) Columbia, University of South Carolina (1987).

Smith, L. L. "Solution Depressions in Sandy Sediments of the Coastal Plain in South Carolina," Journal of Geology, Vol. 39 (1931).

Snipes, D. S., Fallaw, W. C., and Price, V. The Pen Branch Fault: Documentation of Cretaceous and Tertiary Faulting in the Coastal Plain of South Carolina, Draft of manuscript (DP-MS-88-219) to be submitted to Geological Society of America Bulleting (1988).

Snoke, A. W., Kish, S. A., and Secor, D. T., Jr. Deformed Hercynian Granitic Rocks from the Piedmont of South Carolina, American Journal of Science, Vol. 280 (1980).

South Carolian Water Resources Commission Report. Water Use Report for the US Department of Energy - Savannah River Plant. 1st Quarter, 1989 (1989).

Steele, K. E., and Colquhoun, D. J. "Subsurface Evidence of the Triassic Newark Supergroup in the South Carolina Coastal Plain," South Carolina Geology, Vol. 28 (1985).

Stephenson, D. E., and Chapman, W.L. "Structure Associated with the Buried Dunbarton Basin, S. C. from Recent Seismic Data," Geological Society of America Abstracts with Programs, V. 20 (1988).

Stromquist, A. A., and Sundelius, H. W. Stratigraphy of the Albemarle Group of the Carolina Slate Belt in Central North Carolina, U.S. Geological Survey Bulletin, 1274-B (1969).

Swift, D. J. P., and Heron, S. D., Jr. "Stratigraphy of the Carolina Cretaceous," Southeastern Geology, Vol. 10 (1969).

Taber, S. "The South Carolina Earthquake of January 1, 1913," Bulletin of the Seismological Society of America, Vol. 3 (1913).

Talwani, P. "Current Thoughts on the Cause of the Charleston, South Carolina Earthquakes, South Carolina Geology," Vol. 29, No. 2 (1985).

Talwani, P., and Cox, J. "Paleoseimic Evidence for Recurrence of Earthquakes Near Charleston, South Carolina," Science, Vol. 229 (1985).

Talwani, P., Rawlins, J., and Stephenson, D. "The Savannah River Plant, South Carolina Earthquake of June 9, 1985, and Its Tectonic Setting, Earthquake Notes, Vol. 56 (1985).

Talwani, P. An Internally Consistent Pattern of Seismicity Near Charleston, South Carolina, Geology (1982).

Tarr, A. C. "Recent Seismicity Near Charleston, South Carolina, and Its Relationship to the August 31, 1886 Earthquake," In Rankin (1977).

Thom, B. G. Carolina Bays in Horry and Marion Counties, South Carolina, Geological Society of America Bulletin, Vol. 81 (1970).

Thornberry, W. D. Principles of Geomorphology, John Wiley and Sons, Inc., New York (1954).

Tschudy, R. H. and Patterson, S. H. "Palynological Evidence for Late Cretaceous, Paleocene, and Early and Middle Eocene Ages for Strata in the Kaolin Belt, Central Georgia," Jour. Res. U.S. Geol. Survey, 3 (1975).

URS/Blume, J. A., and Assoc. Engineers. Update of Seismic Criteria for the Savannah River Plant. Vol. 1 of 2., Geotechnical, DPE-3699, E. I. du Pont de Nemours and Co., Savannah River Laboratory, Aiken, S.C (1982).

Vick, H. K., Channel, J. E. T., and Opdyke, N. D. "Ordovicain Docking of the Carolina Slate Belt: Paleomagnetic Data, Tectonics, Vol. 6 (1987).

Wampler, J. M., Netherly, J. L., and Bentley, R. D. Age Relations in the Alabama Piedmont, Geology of the BAUARD Fault Zone and Related Rocks of the Innter Piedmont of Alabama. Alabama Geological Society Field Trip Guideline (1970).

Weisenfluh, G. A., Snoke, A. W. "An Epizonal Trondhjemite-Quartz Keratophyre Complex near Calhoun Falls, South Carolina," South Carolina Geologic Notes, Vol. 22 (1978).

Wentworth, C. M., and Mergner-Keefer, M. Regenerate Faults of Small Cenozoic Offset-Probable Earthquake Sources in the Southeastern United States, in Glover (1983) (1983).

Wentworth, C. M., and Mergner-Keefer, M. Reverse Faulting Along the Eastern Seaboard and the Potential for Large Earthquakes, Earthquakes and Earthquake Engineering - Eastern United States, Ann Arbor Science Publishers (1983).

Whitney, J. A., Paris, T. A., Carpenter, R. H., and Hartley, M. E., III. "Volcanic Evolution of the Southern Slate Belt of Georgia and South Carolina: A Primitive Oceanic Island Arc," Journal of Geology, Vol. 86 (1978).

Winker, C. D., and Howard, J. D. "Correlation of Tectonically Deformed Shorelines on the Southern Atlantic Coastal Plain, Geology, Vol. 5 (1977).

Wright, J. E., Seides, V. W. "Age of Zircon from Volcanic Rocks of the Central North Carolina Piedmont and Textonic Implications for the Carolina Volcanic Slate Belt," Geological Society of America Bulletin, Vol. 91 (1980).

Zoback, M. D., Nishenko, S. P., Richardson, R. M., Haseqawa, H. S., and Zoback, M. D. Mid-Plate Stress, Deformation and Seismicity, the Geology of North America, Vol. M, the Western Atlantic Region (1987).

Zoback, M. D. Interplate Earthquake, Crustal Deformation, and In Situ Stress, U.S. Geological Survey Open File Report 83-843 (1983).

Zoback, M. L., and Zoback, M. D. "State of Stress in the Conterminous United States," Journal of Geophysical Research, Vol. 85 (1980).

Zupan, A. W., and Abbot, W. H. "Clastic Dikes: Evidence for Post-Eocene Tectonics in the Upper Coastal Plain of South Carolina, Geologic Notes, Division of Geology, South Carolina State Development Board 19 (1975).

3.0 SUBSURFACE HYDROLOGY

In this section, the hydrostratigraphy, groundwater flow, quality, and use are discussed. Also, the impact of releases of constituents to the subsurface environment is discussed.

3.1 HYDROSTRATIGRAPHIC UNITS

On a regional basis (approximately 2.0E+08 km^2) there are essentially three main hydrostratigraphic units in the subsurface water system at the Savannah River Site. The Cape Fear stratigraphic unit (Figures 2-35 and 3-1) is a dense clay that acts as an aquitard at the base of the system. On top of the Cape Fear, is the regional cretaceous-age aquifer (aquifer 1). This unit is composed of unconsolidated sediments from the Middendorf, Black Creek, and Steel Creek stratigraphic units (Figure 3-1). The cretaceous age aquifer is an excellent source of high quality water and can sustain yields of up to four cubic meters per minute. On average, the top 20 feet of the Steel Creek Formation is a dense silty/clay of low permeability. The top 20 feet of the Steel Creek and the Ellenton stratigraphic together constitute a leaky aquitard. Although the Ellenton Formation does contain some coarse sands, the strings and lenses of clays throughout the unit makes it an effective aquitard (Figure 3-1). Above the Ellenton, is a tertiary-age aquifer (aquifer 2) comprised of the Snapp, Four Mile, and Congaree stratigraphic units. This unit is not nearly as prolific as the Cretaceous age aquifer, but can yield water up to 0.4 cubic meters per minute. The Santee Formation acts as an aquitard above aquifer 2. This unit is often called the "green clay" because of the interbedded glauconite which is greenish. However, the Santee is actually mostly fine silty material with interbedded clays. Above the "green clay" is the water table which is not by strict hydrologic definition an aquifer because it is not a capable water source. Several wells screened in the water table at SRS cannot even produce 0.004 cubic meters per minute for a substantial period. Nevertheless, it is a distinct hydrologic feature.

In some areas of the site, it is necessary to modify the hydrologic units to include local features. For example, at the northern part of the site in order to effectively describe the hydrology, it is necessary to add a leaky aquitard into the water table. This aquitard has been called the "tan clay" (Duffield et al., 1986). At the K-, L-, and P-reactor vicinity, evidence from core descriptions and geophysical logs indicate that the tan clay is very sporadic and thin in these areas and is not a capable aquitard.

The elevations of the aquifers and aquitards relative to mean sea level are given in Figures 3-2 through 3-6 for most of the SRS. The Pen Branch Fault (Section 2.1.2.6 and Figure 2-36) is also shown in each of these figures. This fault causes an offset in the hydrogeologic formations that can be quantified by extrapolating up to the fault from both sides. These elevations were used to develop a ground water model for the SRS. Thicknesses of the hydrologic units were determined by difference.

Hydrogeologic Unit	Stratigraphic Unit (s)
Water Table	Upland. Tobacco Road Dry Branch Clinchfield
"Green Clay" Aquitard	Santee
Aquifer 2 or Tertiary Age	Congaree Four Mile Snapp
"Ellenton" Aquitard	Ellenton and 6 meters of Steel Creek
Aquifer 1 or Cretaceous Age	Steel Creek Black Creek Middendorf
Base Aquitard	Cape Fear

FIGURE 3-1. Hydrostratigraphic and Geologic Stratigraphic Units

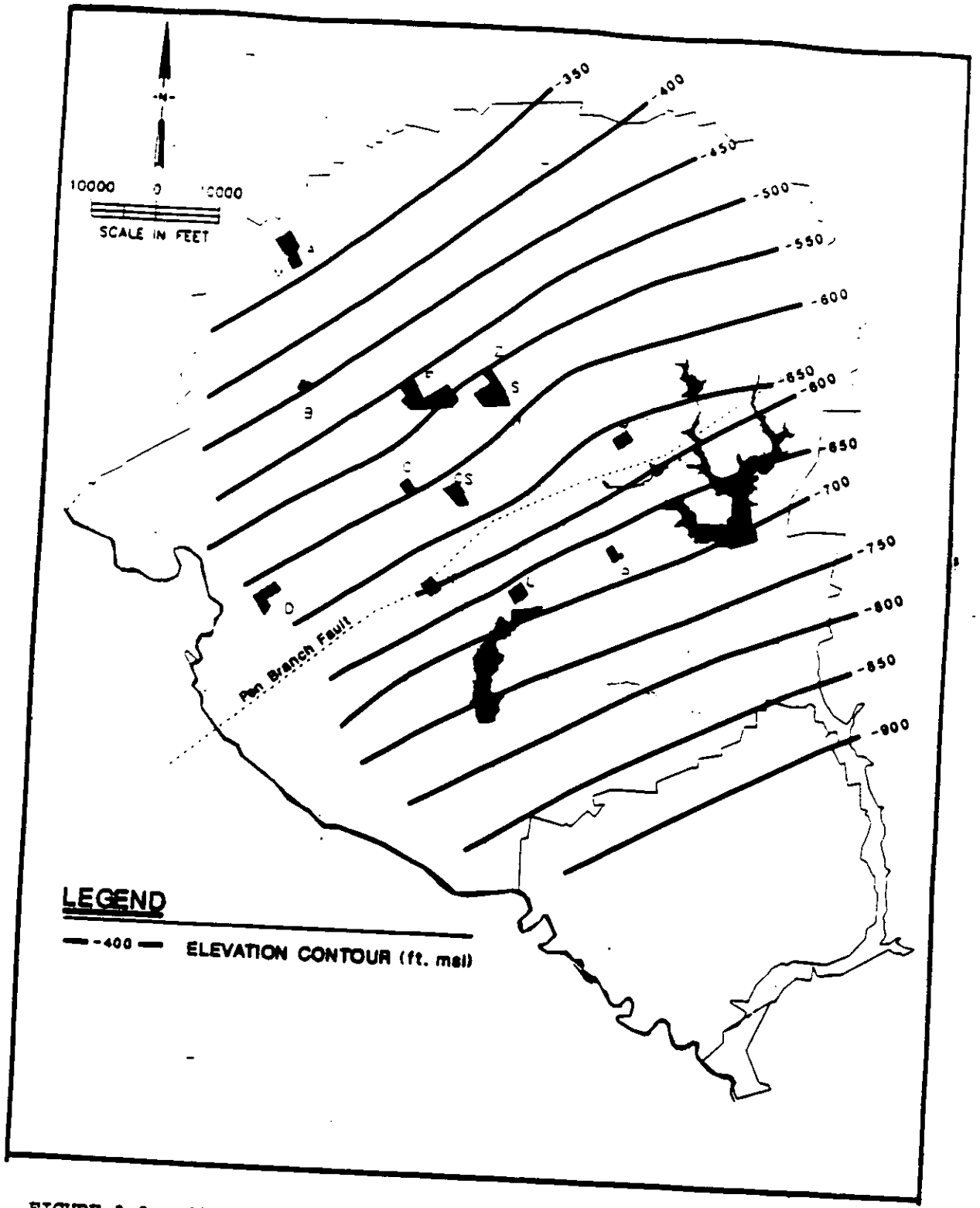

FIGURE 3-2. Elevations of the Base Aquitard (Cape Fear) (ft msl)

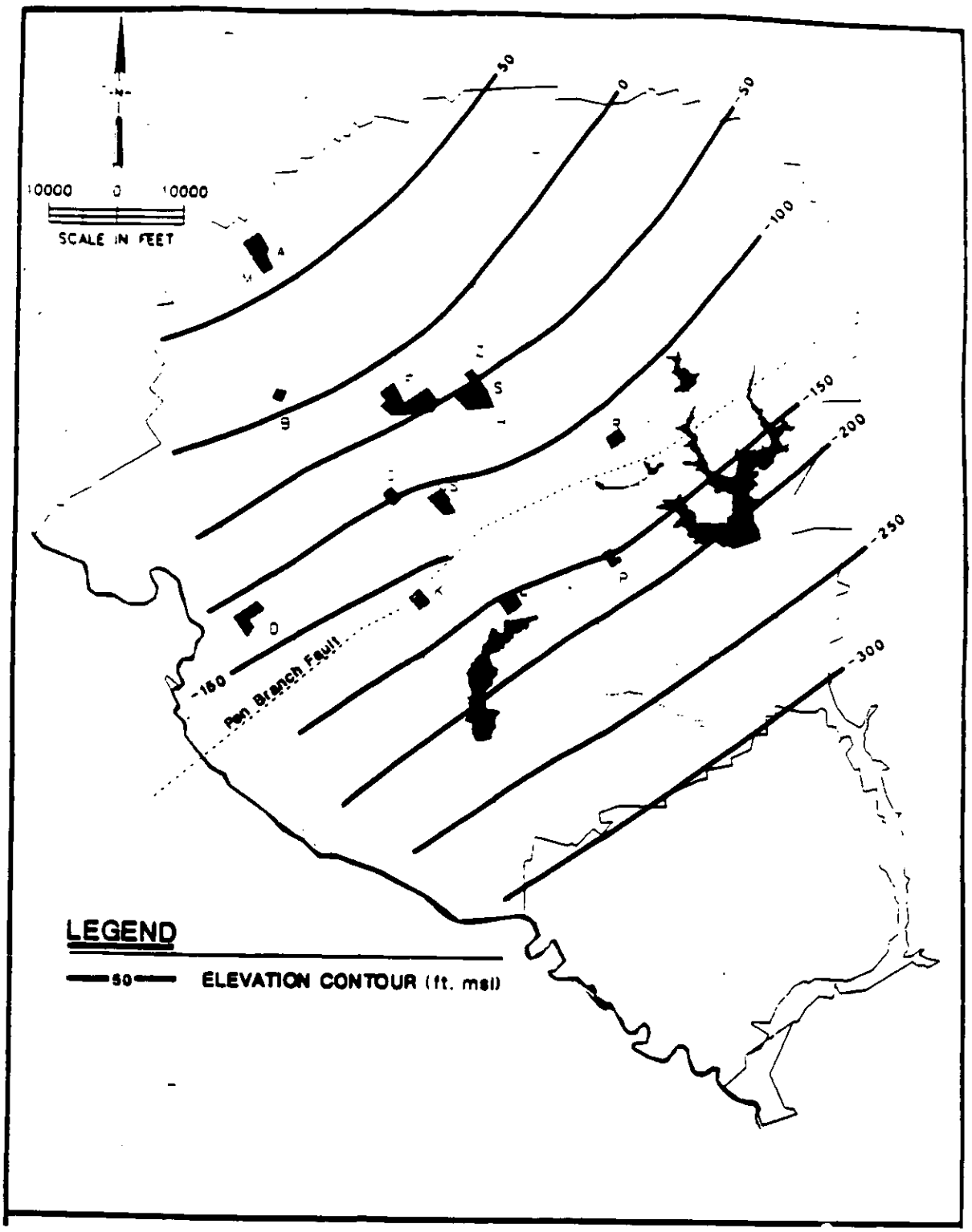

FIGURE 3-3. Elevations of the Top of Aquifer 1 (ft msl)

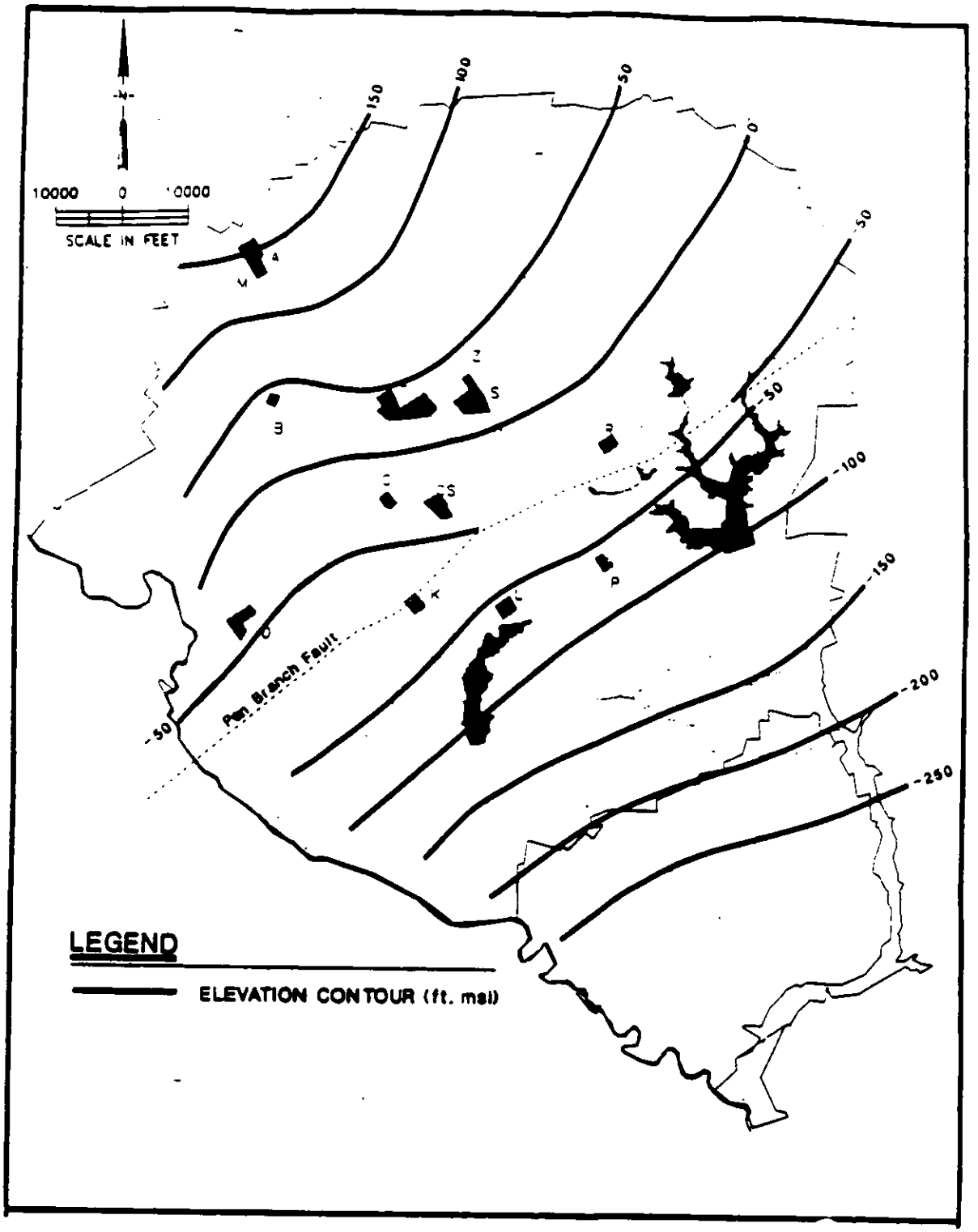

FIGURE 3-4. Elevations of the Top of the "Ellenton" Aquitard (ft msl)

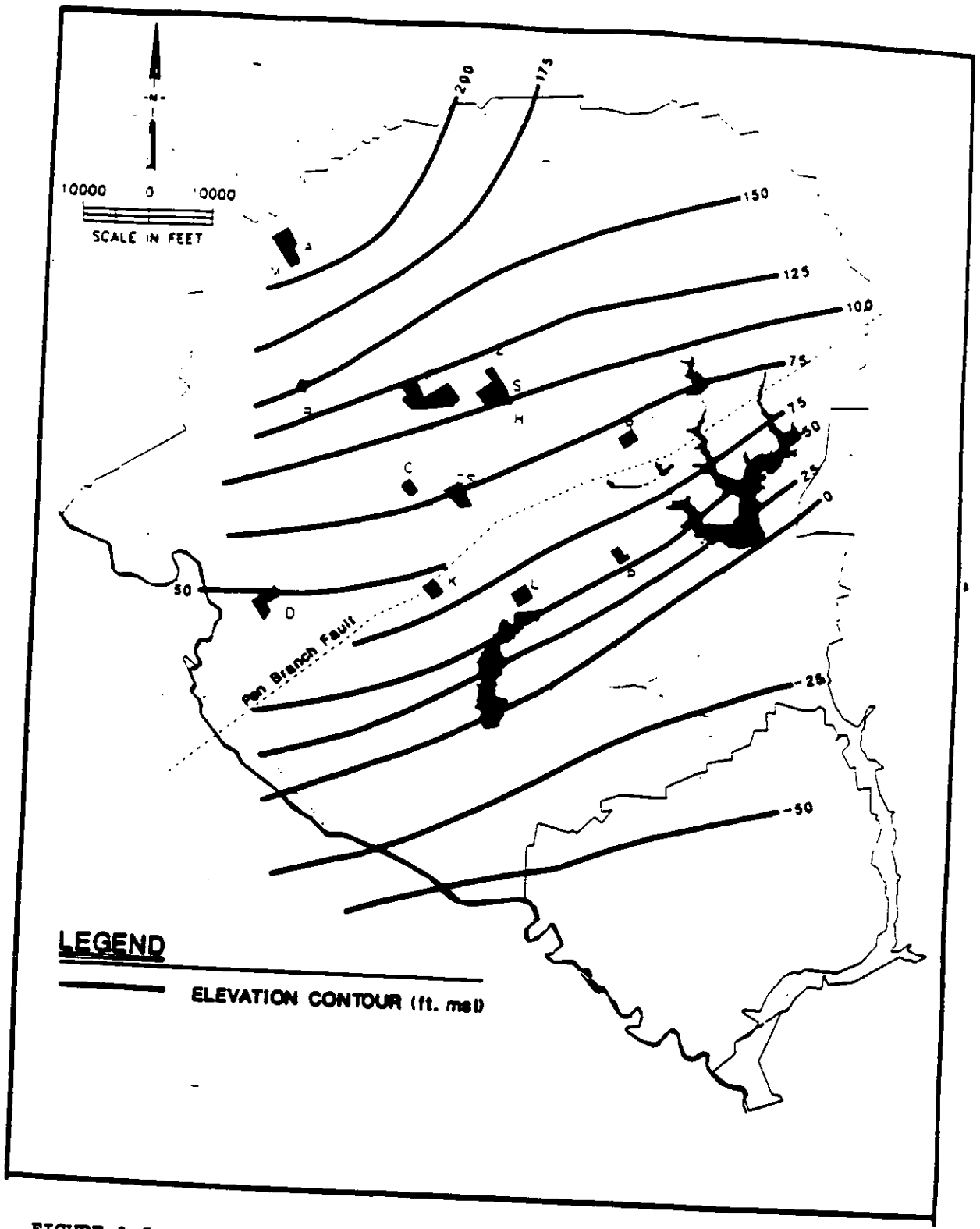

FIGURE 3-5. Elevations of the Top of Aquifer 2 (ft msl)

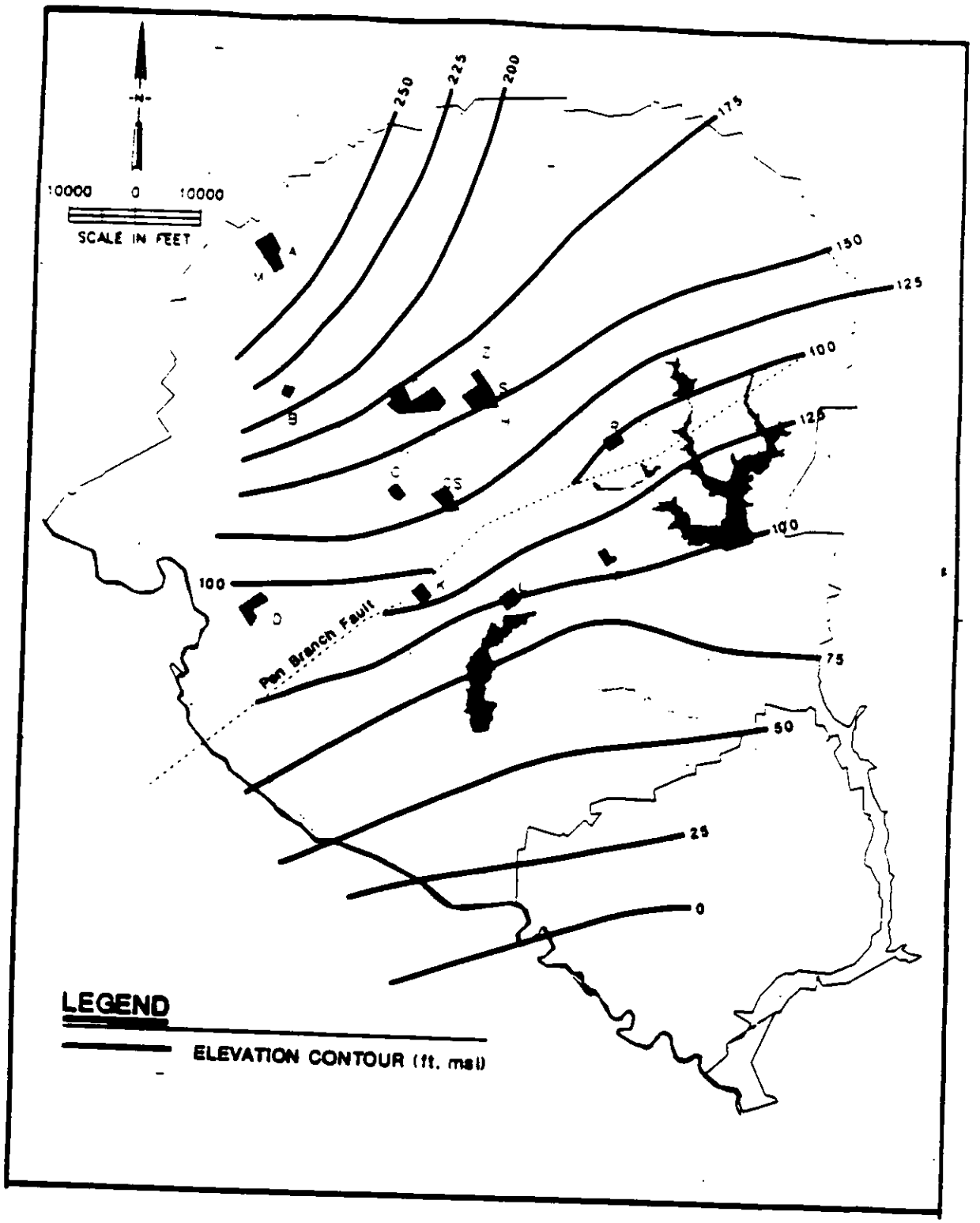

FIGURE 3-6. Elevations of the Top of the "Santee" Aquitard (ft msl)

3.2 GROUNDWATER MOVEMENT

The direction of groundwater flow in a hydrogeologic system is governed by the hydraulic gradients of the system. Potentiometric maps for the regional units (aquifer 1 and 2) at the SRS are shown in Figures 3-7 through 3-9. Local water table elevation maps at the reactors are given in Figures 3-11 through 3-13.

Figures 3-7 and 3-8 are potentiometric maps of the observed hydraulic heads for the lower and upper portions of aquifer 1 (cretaceous age), respectively. In the northern sector of the site, flow in the upper and lower portions coincides and is directly towards the Savannah River. Closer towards the river, the flow in the lower portion becomes westerly and diverges in direction from the upper portion. This occurs because of the complex hydrologic interaction with discharge boundaries. Nevertheless, all water in the cretaceous age aquifer ultimately discharges at the Savannah River, but water in the lower portion of the cretaceous age aquifer takes a different path near the river.

Figure 3-9 is a potentiometric map of observed hydraulic heads for aquifer 2 (tertiary age). In the northwestern section of the site, the flow is towards Upper Three Runs Creek as exemplified by the equipotential lines bending around this feature. This is expected because Upper Three Runs Creek incises aquifer 2. In the southeastern and central sections of the site, flow is towards the Savannah River.

Figure 3-10 is a potential difference map between the upper portion of aquifer 1 and aquifer 2. In some areas of the site, the gradient is from the aquifer 1 up to aquifer 2. This is called "head reversal" and prevents water in aquifer 2 from entering aquifer 1 in those areas. As illustrated, there is no head reversal directly below the K, L, and P reactors. However, just south of the reactors there is a head reversal that would force water back towards aquifer 2.

Figures 3-11, 3-12, and 3-13 are simulated water table elevations at the K, L, and P areas (reactor areas), respectively. Local water table maps instead of regional maps are given because they are largely (but not exclusively) a function of the surface topography. As a result, regional trends that emerge for the lower hydrologic units are not apparent for the water table.

As illustrated in Figure 3-11, water in the water table at the K Reactor flows to the east and discharges at the Pen Branch Creek and to the west where it discharges at Indian Grave Branch Creek. Indian Grave Branch Creek merges with Pen Branch Creek which flows towards the mouth of Steel Creek which discharges at the Savannah River.

As illustrated in Figure 3-12, water in the water table at the L Reactor flows to the southeast towards L Lake and to the west towards Pen Branch Creek. L Lake is a man-made produced by damming Steel Creek.

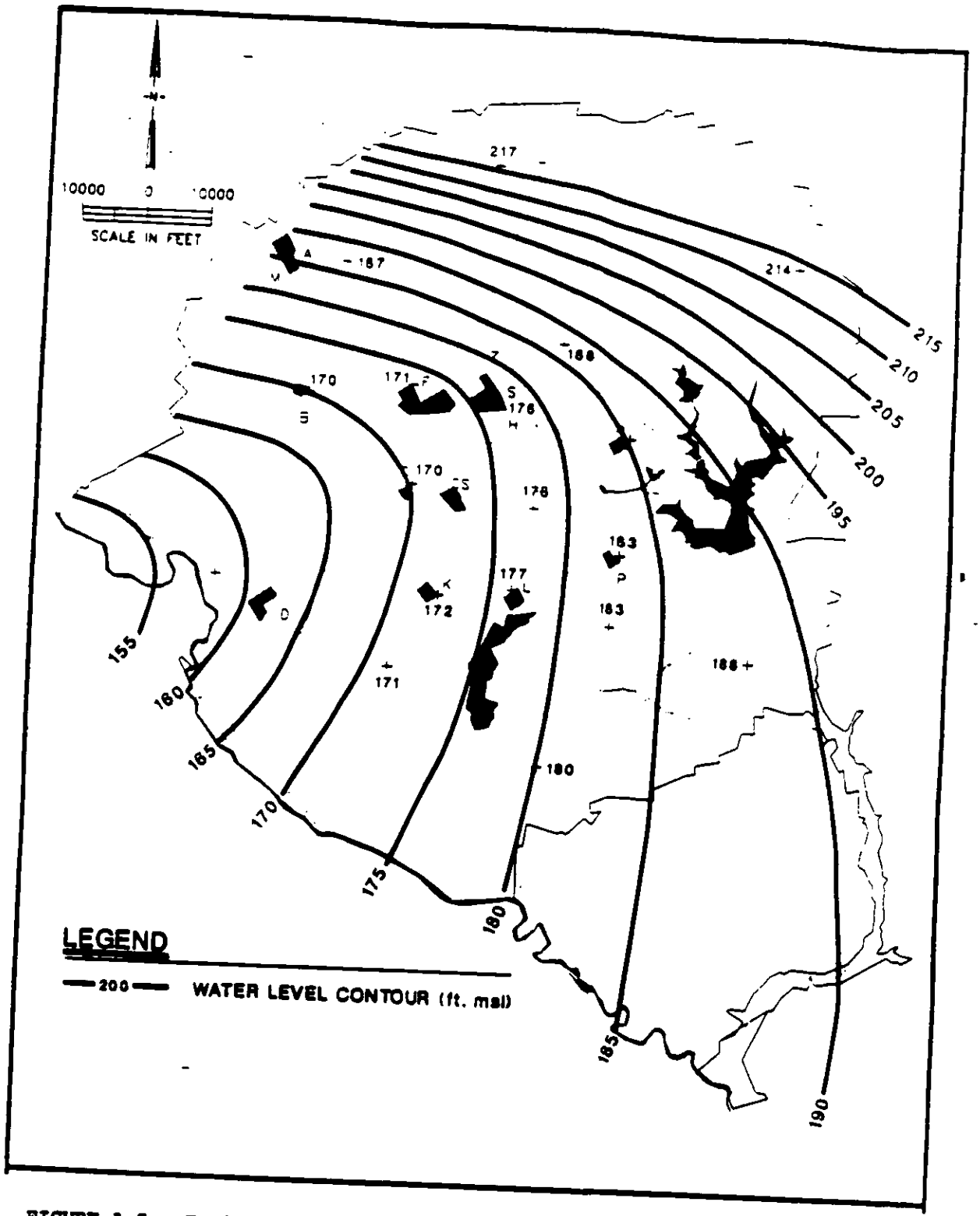

FIGURE 3-7. Equipotential Curves for Lower Portion of Aquifer 1

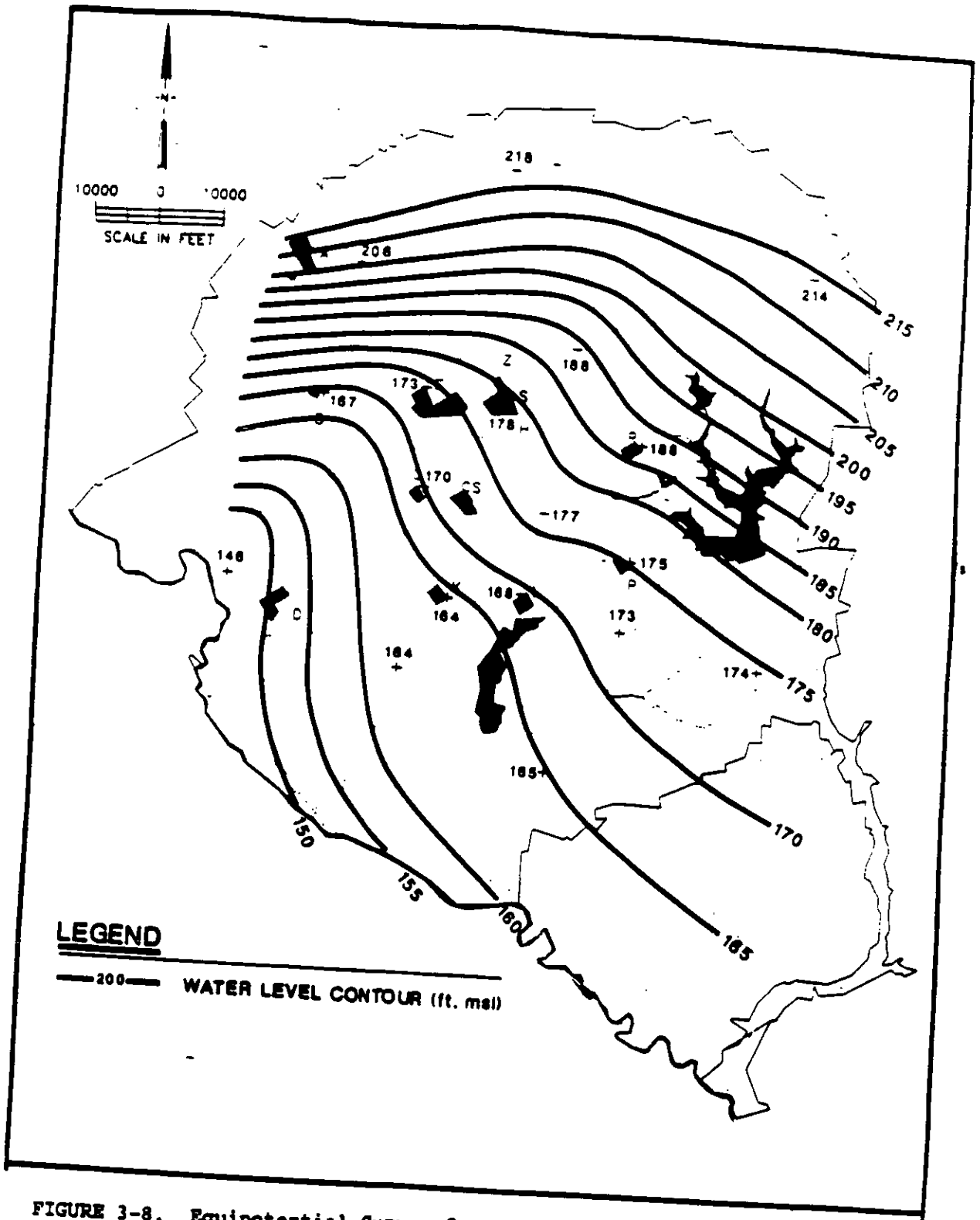

FIGURE 3-8. Equipotential Curves for Upper Portion of Aquifer 1

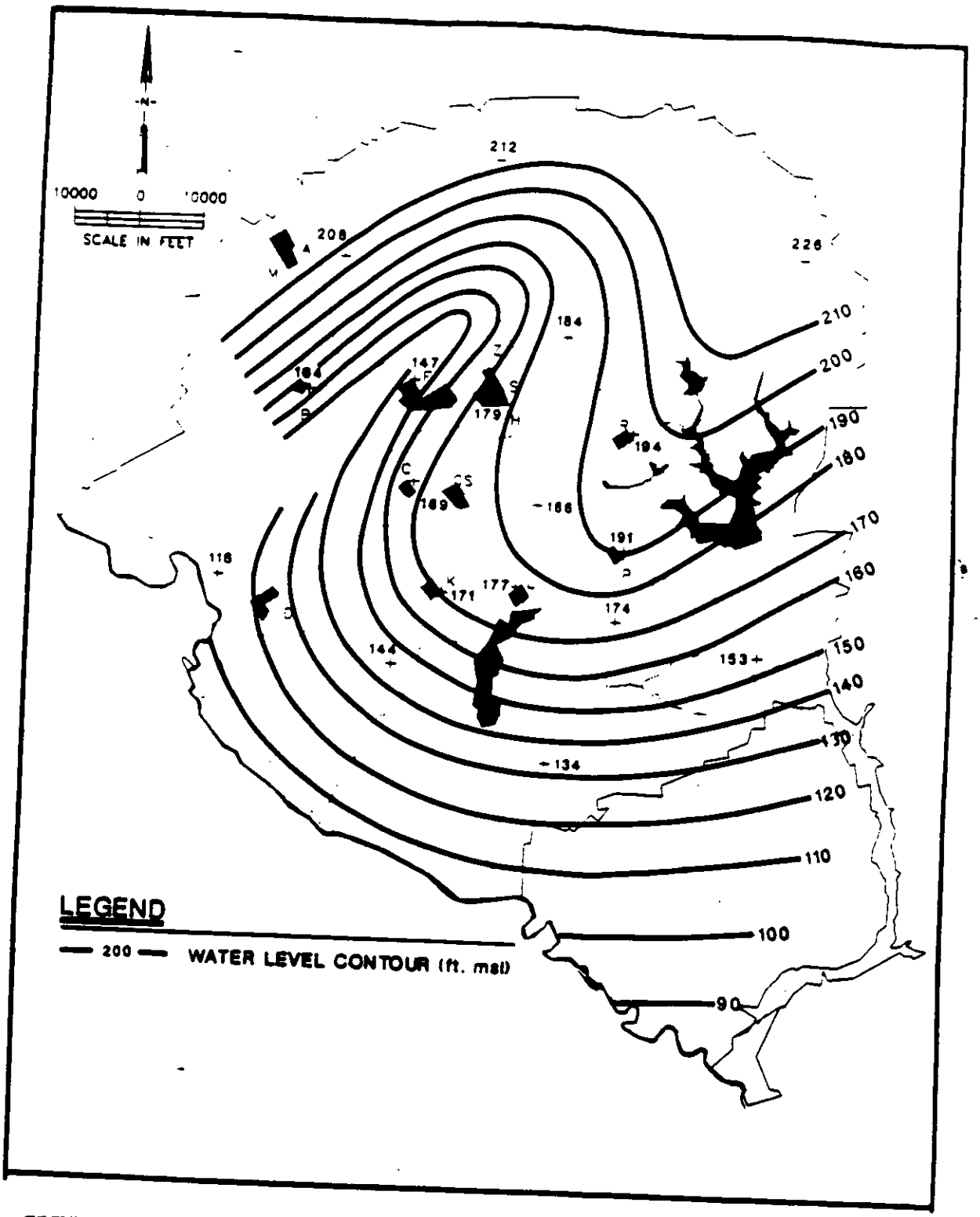

FIGURE 3-9. Equipotential Curves for Aquifer 2

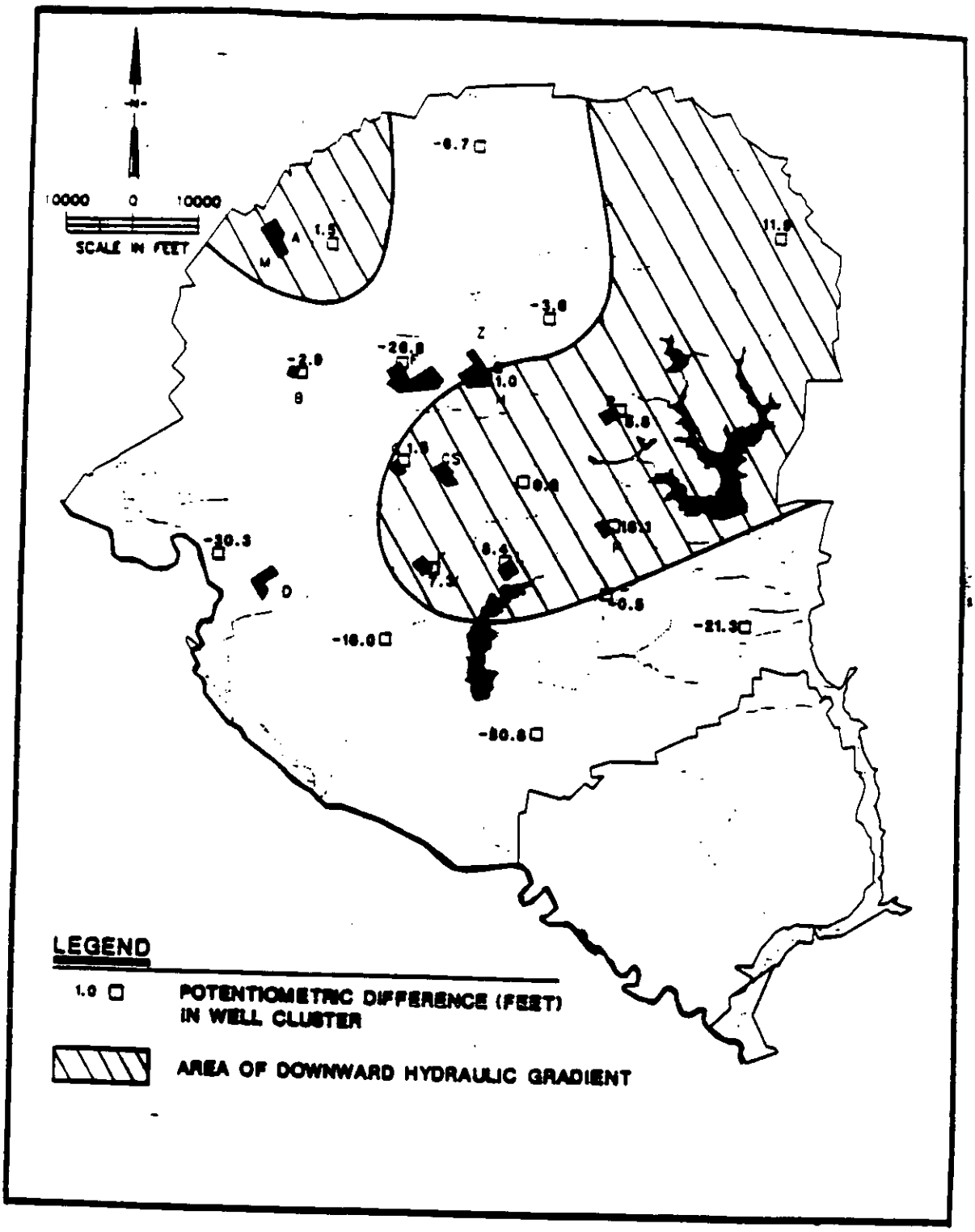

FIGURE 3-10. Potential Difference Map Between the Upper Portion of Aquifer 1 and Aquifer 2

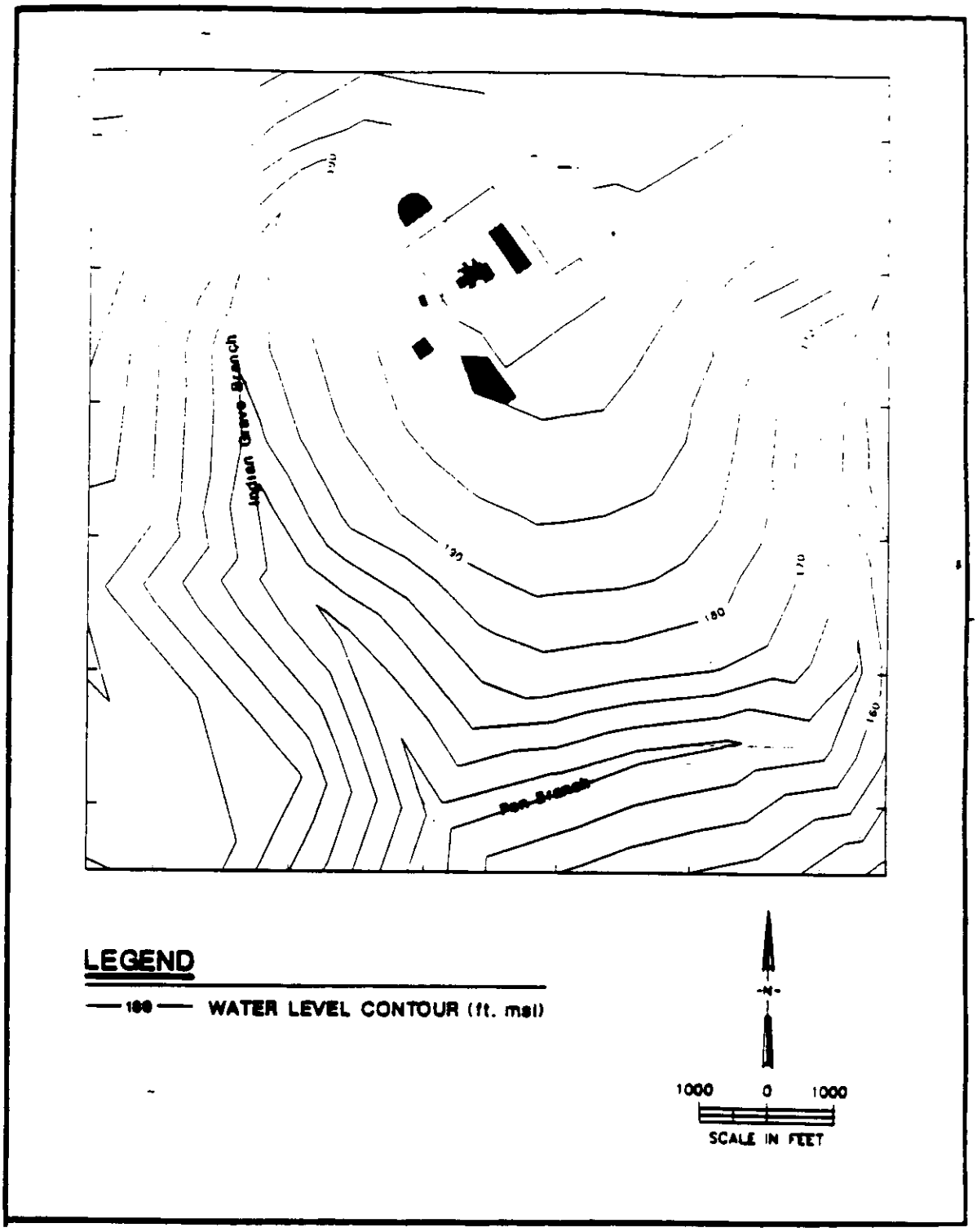

FIGURE 3-11. Water Table Elevations at K Reactor

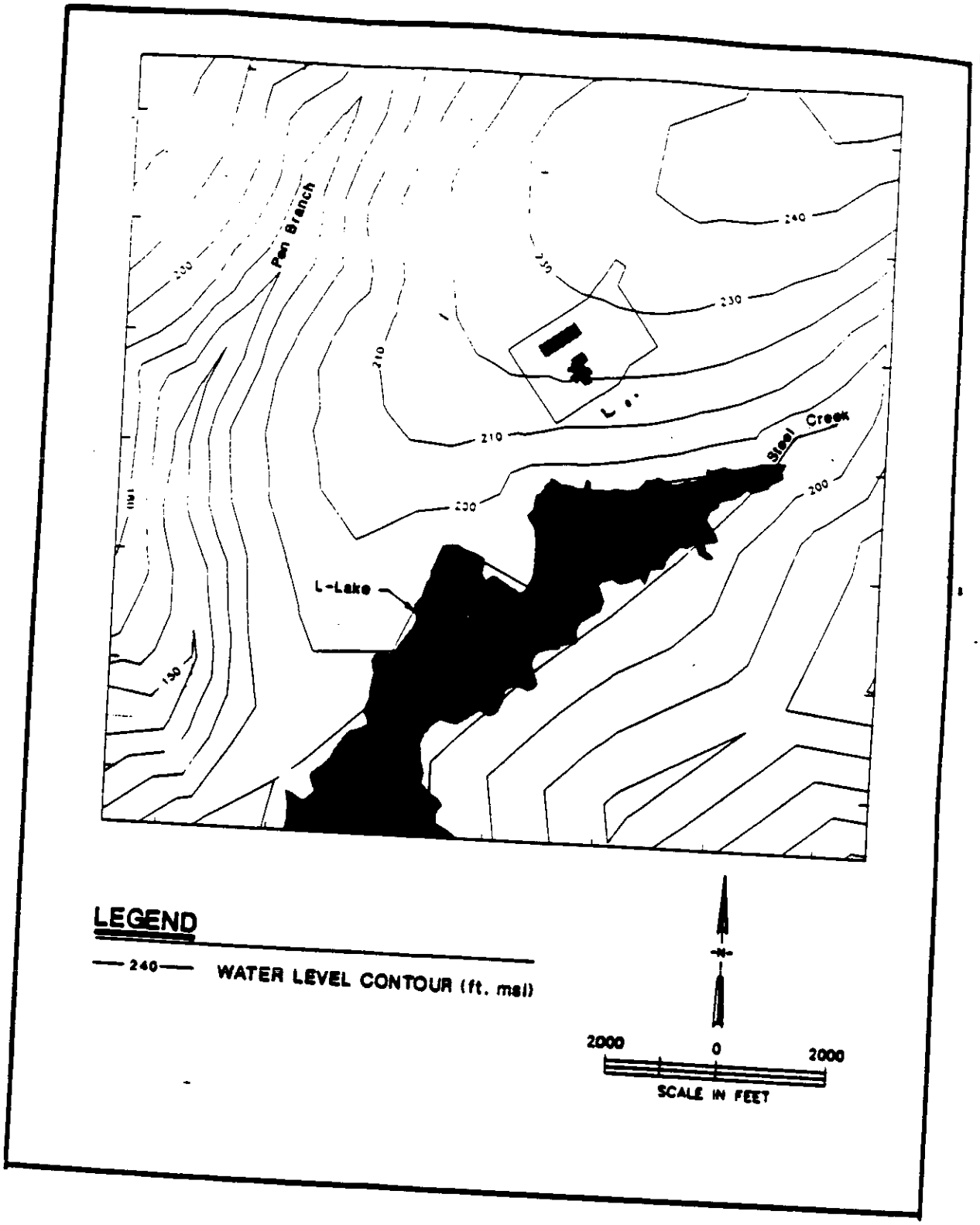

FIGURE 3-12. Water Table Elevations at L Reactor

As illustrated in Figure 3-13, P Reactor lies on top of a water table "mound." Therefore water discharges in all directions from the P Reactor. Likely discharge points are Steel Creek, Par Pond, and Meyers Branch Creek.

The depths to the water table directly beneath the K, L, and P reactors are approximately 15 meters, six meters, and seven meters, respectively. Of course, these values vary temporally with the amount of precipitation.

In summary, water released to the subsurface in the reactor areas flows to the water table. Once in the water table, it can either flow downward to deeper aquifers or a relatively short distance to surface waters. Most water discharges into surface waters from the water table because flow into deeper aquifers is impeded by the "green clay" or Santee aquitard. All surface water at the SRS eventually reaches the Savannah River. Results of an analysis of transport of materials in the subsurface are reported in Section 3.6.

3.3 GROUND WATER QUALITY

For the purpose of discussing the general ground water quality underlying the SRS, the geology of the site can be broken down into three main systems. From deep to shallow, these systems are: (1) the buried crystalline metamorphic basement rock where water occurs in small fractures; (2) a buried depositional basin consisting of consolidated clastic sediments of Triassic age, where water occurs in the intergranular pore space and is characterized by extremely low permeability; and (3) the Coastal Plain sediments of Cretaceous and Tertiary age where water occurs in porous, unconsolidated to semiconsolidated sands, clays, and occasional limestone deposits. Of the three systems, only the Coastal Plain sediments are capable of providing ground water of sufficient quantity or quality.

Waters found in both the crystalline basement and the Triassic age sediments are characterized by high total dissolved solids. Typically water from the crystalline basement has a total dissolved solids content of around 6,000 mg/L, consisting mainly of calcium (500 mg/L), sodium (1,300 mg/L), sulfate (2,500 mg/L), and chloride (1,100 mg/L) (Table 3-1). Waters from Triassic sediments have values for total dissolved solids ranging from around 12,000 to 18,000 mg/L, mainly sodium chloride (Table 3-1).

Water from the aquifer units found within the formations of Cretaceous age can be characterized as mainly sodium bicarbonate in nature, although sodium chloride type water is also common. The water is generally acidic, soft, and low in dissolved solids and iron content (Table 3-1). Because of the soft and acidic nature, the water has a tendency to corrode most metal surfaces. This is especially true where the water contains appreciable amounts of dissolved oxygen and carbon dioxide.

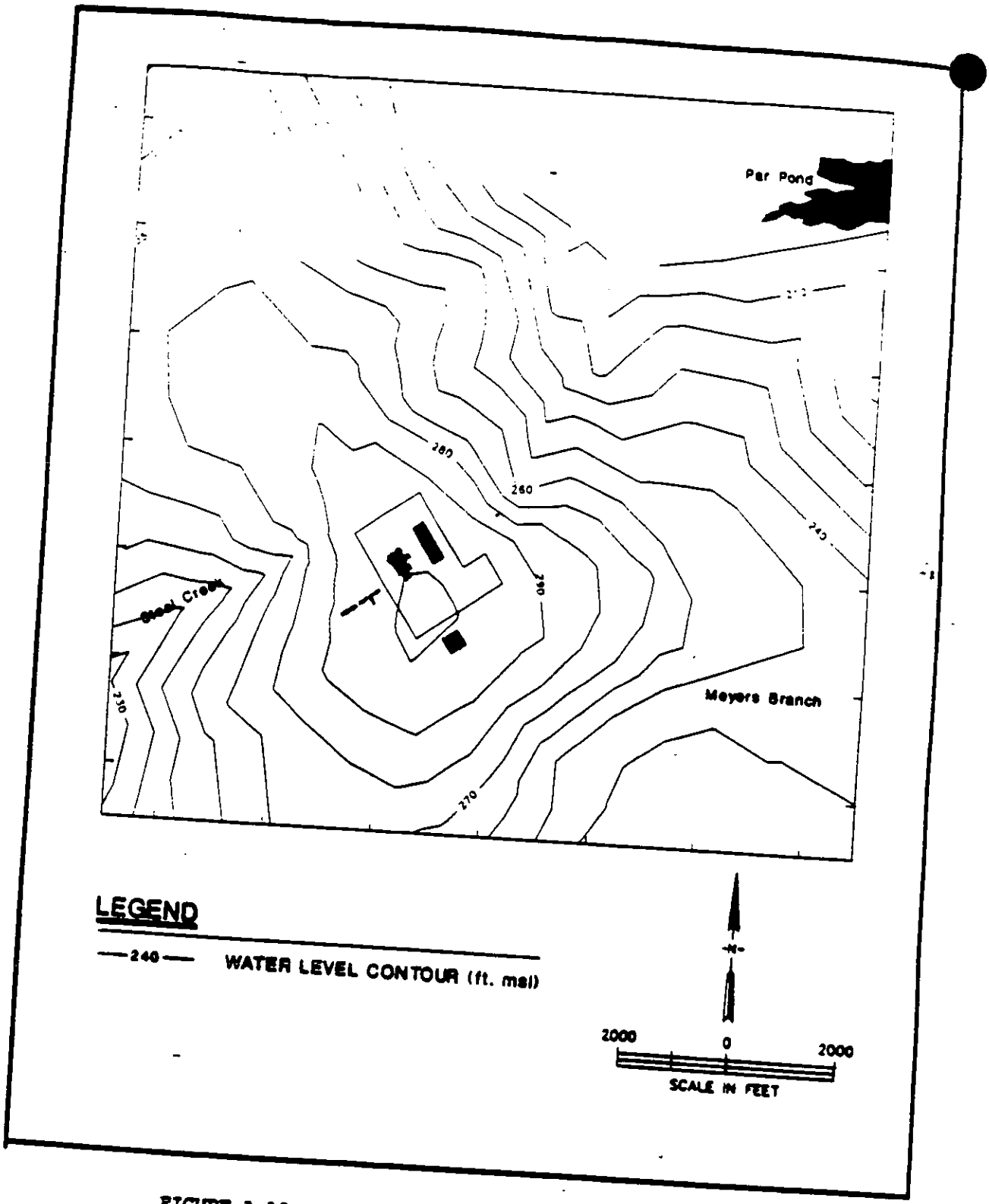

FIGURE 3-13. Water Table Elevations at P Reactor

TABLE 3-1

Chemical Analyses of Water from Metamorphic and Triassic Rock at SRS

Formation	Boring No.	Chemical Constituents (mg/L)									Total Dissolved Solids (mg/L)
		SiO_2	Fe	Ca	Mg	Na	K	HCO_3	SO_4	Cl	
Crystalline rock	DRB8	7.6	0.03	467	15	1,200	16	18	2,590	900	5,660
Triassic	DRB9	1.0	0.00	518	83	1,120	30	72	420	2,620	5,950
Crystalline rock	DRB9	6.1	0.09	461	38	1,440	11	29	2,460	1,260	5,990
Triassic	P12R	-	0.05	22	7.6	262	9.3	157	<1	330	800
Triassic	DRB11	-	<1	3,845	8.5	2,710	22.1	~1	~1	11,600	18,500
Triassic	DRB10	3.5	0.04	1,990	53	2,100	44	85	110	6,720	11,900

Although not a significant aquifer unit, discontinuous sands within the Ellenton Formation is capable of supplying significant quantities of water to wells. A small number of wells are completed in these sands. Water from this unit is typically of the calcium sulfate type. The water is characterized by moderate total dissolved solids, low hardness, and high iron and sulfate contents (Table 3-2).

Water from the sand units of Tertiary Age above the Ellenton Formation is generally a calcium bicarbonate type. The water is acidic and low in total dissolved solids with occasional slightly elevated levels of iron, as compared to other aquifer units. Samples of waters from the Tertiary Age limestone units are typically calcium bicarbonate in nature with a pH of around seven. The water is moderately hard to hard and higher in total dissolved solids than the Tertiary Age sand units (Table 3-2). Most of the increase in dissolved solids is from calcium and bicarbonate ions, which is attributed to the higher calcium carbonate content of the sediments.

3.4 GROUND WATER USE FOR REACTOR AREAS

Table 3-3 lists the groundwater produced for the K-, L-, and P-reactor areas as well as the production well identifications. All of these production wells are screened in aquifer 1. The amount of water produced at K Area has been significantly reduced. In the past, two wells were operated full time and excess water was discharged. Now only one well is operated to meet the reactor needs. This should slightly reduce the downward gradient in K Area.

3.5 RELATIONSHIP OF GROUND WATER USE TO WATER LEVELS

The aquifer that the production wells are screened in can easily produce four cubic meters per minute (Siple, 1967). Reactor use is well below this value. As a result, the change in water levels resulting from water production cannot be distinguished from normal seasonal variations. Simulations of water production at the reactors verify this (Camp, Dresser, and McKee, 1989).

3.6 ENVIRONMENTAL CONSEQUENCES

This section is a discussion of the subsurface environmental impacts due to the release of radionuclides to the reactor seepage basins during normal reactor operations. Also included is a discussion of the potential subsurface environmental impacts due to accidents occurring at the K, L, and P reactor sites.

To analyze the subsurface environmental impacts of normal seepage basin discharges, a groundwater flow and contaminant transport model was developed, calibrated, and used to simulate the movement of radionuclides

TABLE 3-2

pH and Composition of Water from Four Major Sources in the Vicinity of SRS*

Source of Water	Number of Analyses	Range and Median	pH	Chemical Constituents (mg/L) Fe	Ca^{2+}	Mg^{2+}	$Na^{+}+K^{+}$	CO_3^{2-}	SO_4^{2-}	Cl^{-}	F^{-}	NO_3^{-}	Total Dissolved Solids**	Hardness†
Aquifer I	13	Maximum	6.9	0.77	1.4	0.9	6.7	17	4.8	4.0	0.1	8.8	28	7
		Minimum	4.4	0.00	0.3	0.0	0.9	0	0.5	0.8	0.00	0.0	14	2
		Median	5.4	0.16	0.9	0.5	2.1	3	1.4	2.2	0.0	0.6	19	5
"Ellenton" aquitard	16	Maximum	6.8	4.1	8.7	1.3	4.2	23	27	6.0	0.2	0.9	54	30
		Minimum	4.4	0.10	3.9	0.4	1.5	4	7.4	1.5	0.0	0.0	36	10
		Median	5.9	1.1	6.4	1.0	2.7	12	11	2.1	0.1	0.0	41	19
Tertiary limestone	15	Maximum	7.6	1.0	47	9.4	19	17.1	14	4.5	0.5	6.2	192	132
		Minimum	6.8	0.00	17	0.3	0.4	5.5	0.8	0.4	0.0	0.0	75	50
		Median	7.1	0.25	27	2.0	1.7	9.4	4.3	2.8	0.1	0.2	95	72
Tertiary sand	9	Maximum	6.1	1.84	8.7	4.2	2.4	17	9.3	4.0	0.3	2.3	29	15
		Minimum	4.2	0.04	0.5	0.3	0.4	1	0.8	1.5	0.00	0	20	4
		Median	5.5	0.16	1.5	0.7	2.1	5.5	1.9	2.7	0.1	1.3	21	8

* From Siple (1967)

** Residue after evaporation at 180°C in mg/L

† As $CaCO_3$

TABLE 3-3

Ground Water Usage at K, L, and P Areas

Location	Wells	Plant Coordinates North	Plant Coordinates East	1st Quarter 1989 Production (m^3/min)
K Area	905-94K	53170	41500	0.75
	905-95K	53230	41300	
L Area	905-104L	47128	51250	0.94
	905-105L	46690	51250	
P Area	905-92P	42950	65700	1.35
	905-93P	43150	65650	

Note: Total pumping is distributed among the wells.

Source: S.C. Water Resources Commission Report (1989)

after they enter the groundwater system through the seepage basins. The groundwater flow and transport model codes used in the analysis were the DYNFLOW (DYNamic groundwater FLOW simulation) and DYNTRACK (DYNamic particle TRACKing) computer programs developed by Camp Dresser & McKee Inc. (CDM) in 1982. These codes have been peer reviewed and validated by the International Ground Water Modeling Center at the Holcomb Research Institute, and have been accepted by the U.S. Environmental Protection Agency (USEPA) for use on Superfund sites.

DYNFLOW uses a Galerkin finite element formulation to solve the partial differential equation that describes the transient, three-dimensional flow of a homogeneous incompressible fluid through a heterogeneous, anisotropic medium. The program uses linear finite elements, and incorporates induced infiltration from streams, artificial and natural recharge or discharge, and heterogeneous and anisotropic hydraulic properties. The program handles both linear (confined) and nonlinear (unconfined) aquifer flow conditions, and has special routines to handle a change in status from a confined to unconfined situation. The program also has a "rising water" scheme to allow drainage to local streams if the potentiometric head in a phreatic aquifer rises to the elevation of the stream bed or land surface.

DYNTRACK is a computer program that simulates three-dimensional contaminant transport in the saturated zone of an aquifer, and uses the same three-dimensional finite element grid discretization used for DYNFLOW. DYNTRACK uses the random walk method to solve the contaminant transport equation and can model contaminant movement for conservative constituents with dispersion, as well as constituents subject to first-order decay or adsorption. Thus, DYNTRACK permits the evaluation of complicated contaminant transport problems. It should be noted that the mass of the particles is the important factor not the number of particles when interpreting simulated plumes because of radioactive decay.

The finite element grid used in this analysis is shown superimposed on a basemap of the SRS in Figure 3-14. The grid was developed such that significant physical features such as streams, lakes, the Savannah River, the Pen Branch Fault, wells, and the three reactor areas could be adequately represented. The grid consists of 701 nodes and 1349 elements. A variable size grid system is used so that aquifer impacts could be evaluated over a large area while still maintaining sufficient detail within the reactor areas. The grid network is most dense around the reactor areas where radionuclides are released. A dense element network in these areas allows the head distribution to be calculated at a degree of resolution that is suitable for simulating the movement of radionuclides from the seepage basins.

The vertical grid consists of seven levels of nodes that define six layers and five hydrostratigraphic units (one hydrostratigraphic unit is divided in half for better discretization). The seven node levels represent the following hydrostratigraphic unit boundaries:

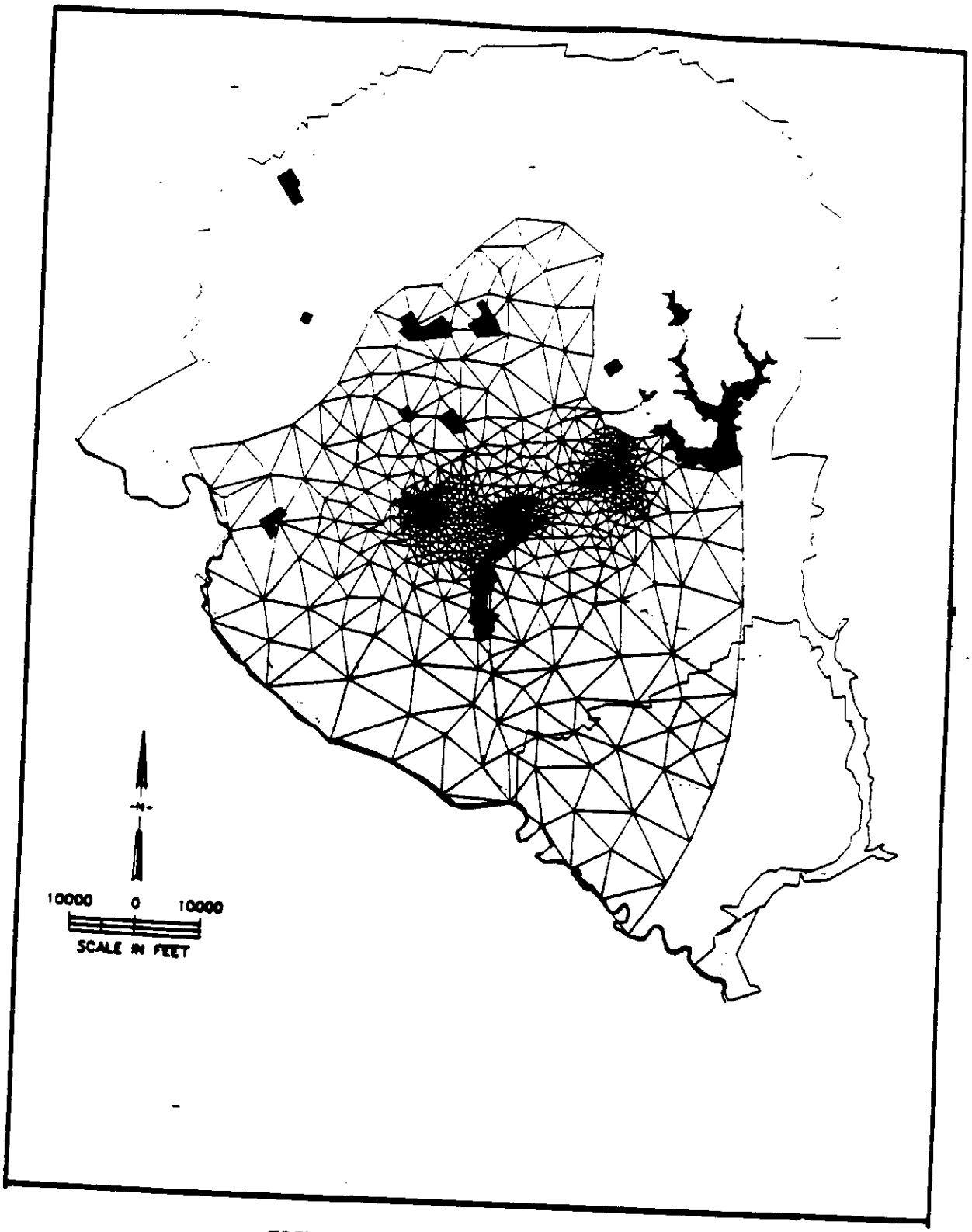

FIGURE 3-14. Finite Element Grid

- Level 1 - Top of the Base Aquitard (Cape Fear)
- Level 2 - Middle of the Aquifer 1 (Cretaceous Aquifer)
- Level 3 - Top of Aquifer 1 (Cretaceous Aquifer)
- Level 4 - Top of the "Ellenton" Aquitard
- Level 5 - Top of Aquifer 2 (Congaree Aquifer)
- Level 6 - Top of the "Santee" Aquitard
- Level 7 - Land Surface

The hydrostratigraphic elevations input to the model were presented previously in Figures 3-2 through 3-6. Cross-sectional views of the hydrostratigraphic units are shown in Figures 3-15 and 3-16. The locations of these cross-sections are shown in Figure 3-17.

The size of the model area was selected based on the prevailing boundary conditions. Ideally, model boundaries are chosen so that they coincide with stable hydrologic boundaries. Since only a few truly stable hydrologic boundaries exist at the SRS (i.e., the Savannah River and Upper Three Runs Creek), the other model boundaries are located far enough from the reactor sites so that conditions imposed on the boundaries do not significantly alter simulation results within the areas of interest, as long as the conditions imposed are realistic.

Boundary conditions imposed along the borders of the model vary between a specified head condition and a "no flow" condition, which ever is more representative of observed groundwater flow condition in each aquifer and aquitard. The distribution of specified heads along the model borders was estimated based on available, current (1986-1989), observation well water level data (see Figures 3-7 through 3-9), as well as surface water measurements taken along the Savannah River and other surface water features at the SRS. At the bottom of the model (Level 1), a vertical "no flow" condition is specified at every node in the model, thus preventing any leakage in or out of the model through the base aquitard. Streams and swampy areas located in the interior of the model grid are represented through a "rising" head boundary condition. In these areas, the water table is allowed to rise to land surface, but not above it. If the water table is driven above the land surface, a discharge flux sufficient to keep the water table at land surface is introduced. This discharge flux represents a surface discharge of water which is lost from the groundwater system as surface flow. The final boundary condition imposed in the model is for L Lake which is modeled as a specified head condition at the top of the groundwater system (Level 7).

Two forms of aquifer stress are incorporated in the model: rainfall recharge and aquifer pumpage. Based on previous studies performed at the SRS, rainfall recharge is estimated to be 38 centimeters per year. This recharge is applied uniformly over the model area. Aquifer pumping rates use at the SRS.

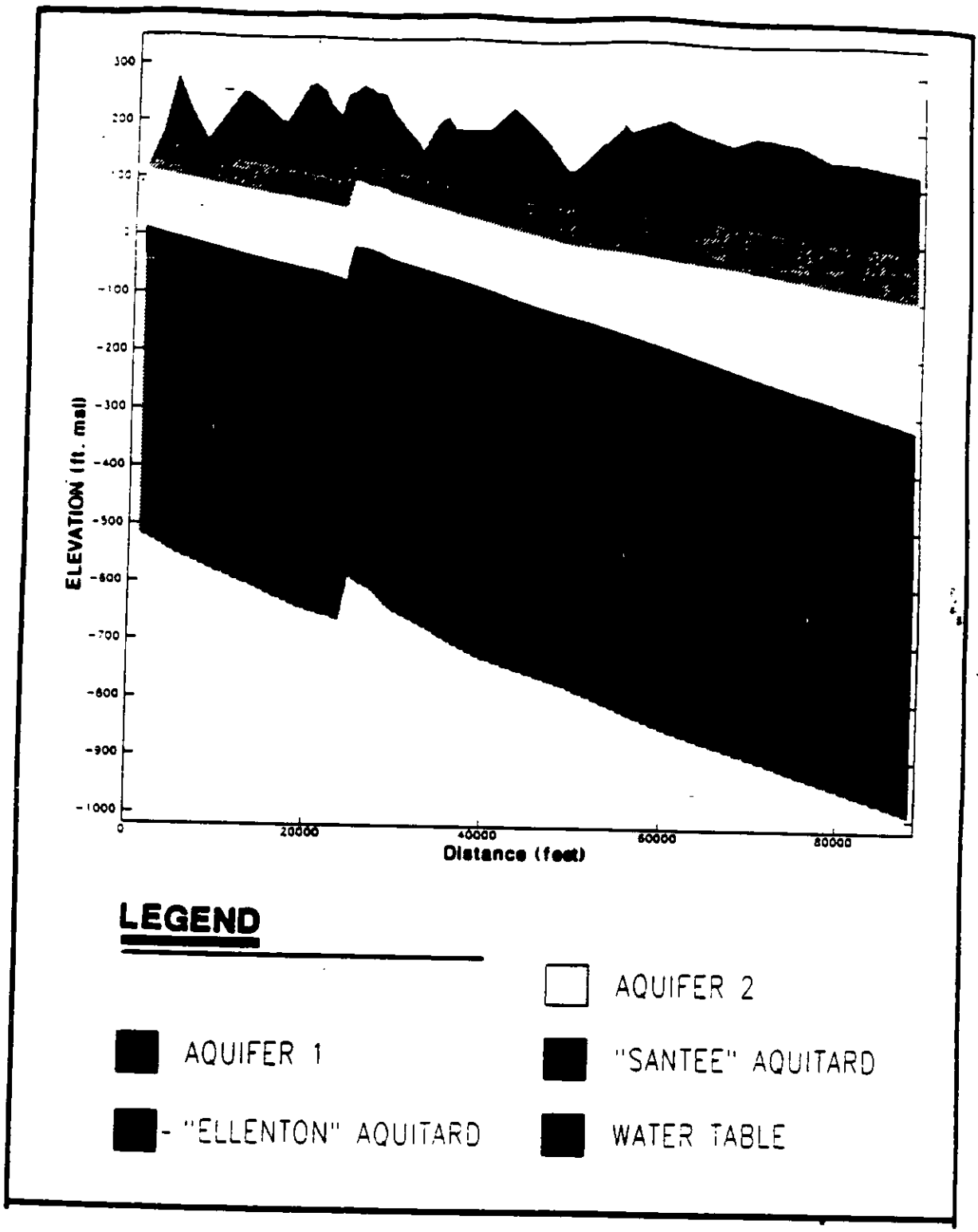

FIGURE 3-15. NW - SE Model Hydrostratigraphic Cross-Section

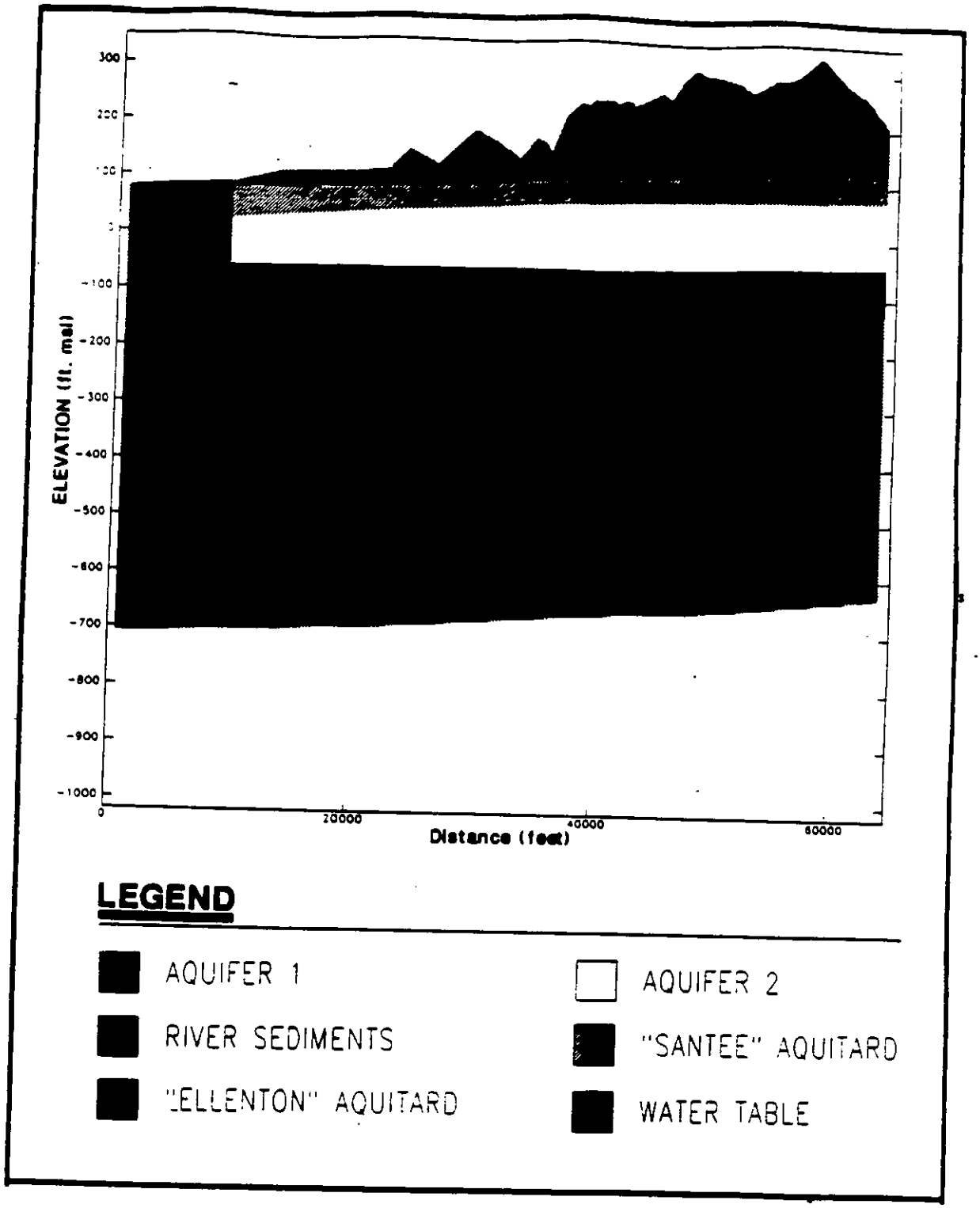

FIGURE 3-16. NE - SE Model Hydrostratigraphic Cross-Section

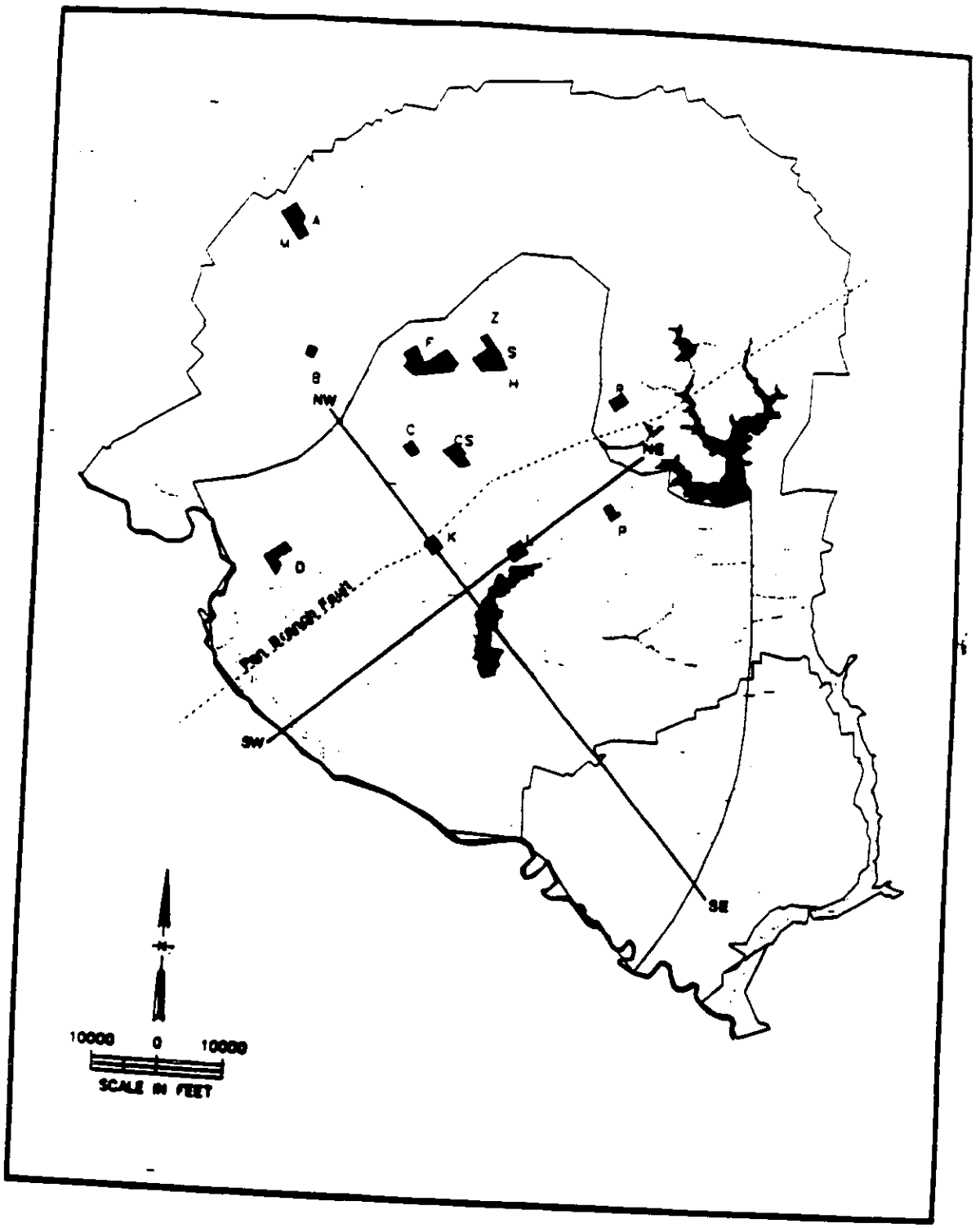

FIGURE 3-17. Model Cross Section Locations

applied in the model are shown in Table 3-4. These rates applied in the model are shown in Table 3-4. These rates are based on well production flows measured during the first quarter of 1989 and on anticipated future The flow model was calibrated under steady-state conditions using average water levels measured in observation wells located throughout the SRS. Model-generated aquifer water levels were compared to observed aquifer water levels, and a sequence of adjustments in hydraulic conductivities was made so that the predicted water levels more closely reproduced observed water levels. During this process, however, the value of individual hydraulic conductivities was kept within realistic limits. The ranges of hydraulic conductivity values shown in Table 3-5 were established prior to calibration based on previous studies performed at the SRS, and model hydraulic conductivity values were kept within these ranges during the calibration process. The final calibration hydraulic conductivity values are presented in Table 3-6. The property zones corresponding to the calibrated hydraulic conductivity values are shown in Figures 3-18 through 3-22. Simulated water level contour maps for Aquifer 2, the top of Aquifer 1, and the bottom of Aquifer 1 are presented in Figures 3-23 through 3-25, respectively. Simulated water level contour maps for the water table at the K, L, and P reactor sites were presented previously in Figures 3-11 through 3-13, respectively.

Due to the lack of observed contaminant transport data, calibration of the contaminant transport model was not possible. Instead, best estimates of the contaminant transport properties as identified by Looney, et al., (1987), were used to develop the model. The estimated contaminant transport property values for the radionuclides of concern in this analysis are presented in Table 3-7.

For further details on development and calibration of the groundwater flow and contaminant transport model used in this analysis, refer to the document titled "Numerical Simulation of Groundwater Flow and Contaminant Transport at the K, L, and P Areas at the Savannah River Site, Aiken, South Carolina" (Camp Dresser & McKee, 1989).

3.6.1 Groundwater Quality

The average annual mass loading rate and half-life of each radionuclide released to the reactor seepage basins are presented in Table 3-8. The mass loading rates were calculated based on records of releases at the C, K, and P seepage basins for the years 1984-1986 because the reactors are essentially equivalent. To narrow down the number of radionuclides to be analyzed with the contaminant transport model, radionuclides with a half-life less than 0.5 years were eliminated from further consideration, which reduced the number of radionuclides of concern to nine. These nine radionuclides are presented in Table 3-9 along with the average mass loading rates and concentrations of the radionuclides in the water discharged to each seepage basin. The concentrations were calculated based on the mass loading rates and an average discharge of 2×10^7 liters/year. Also included in Table 3-9 are the nine radionuclide concentrations that the USEPA allows in drinking water. USEPA standard

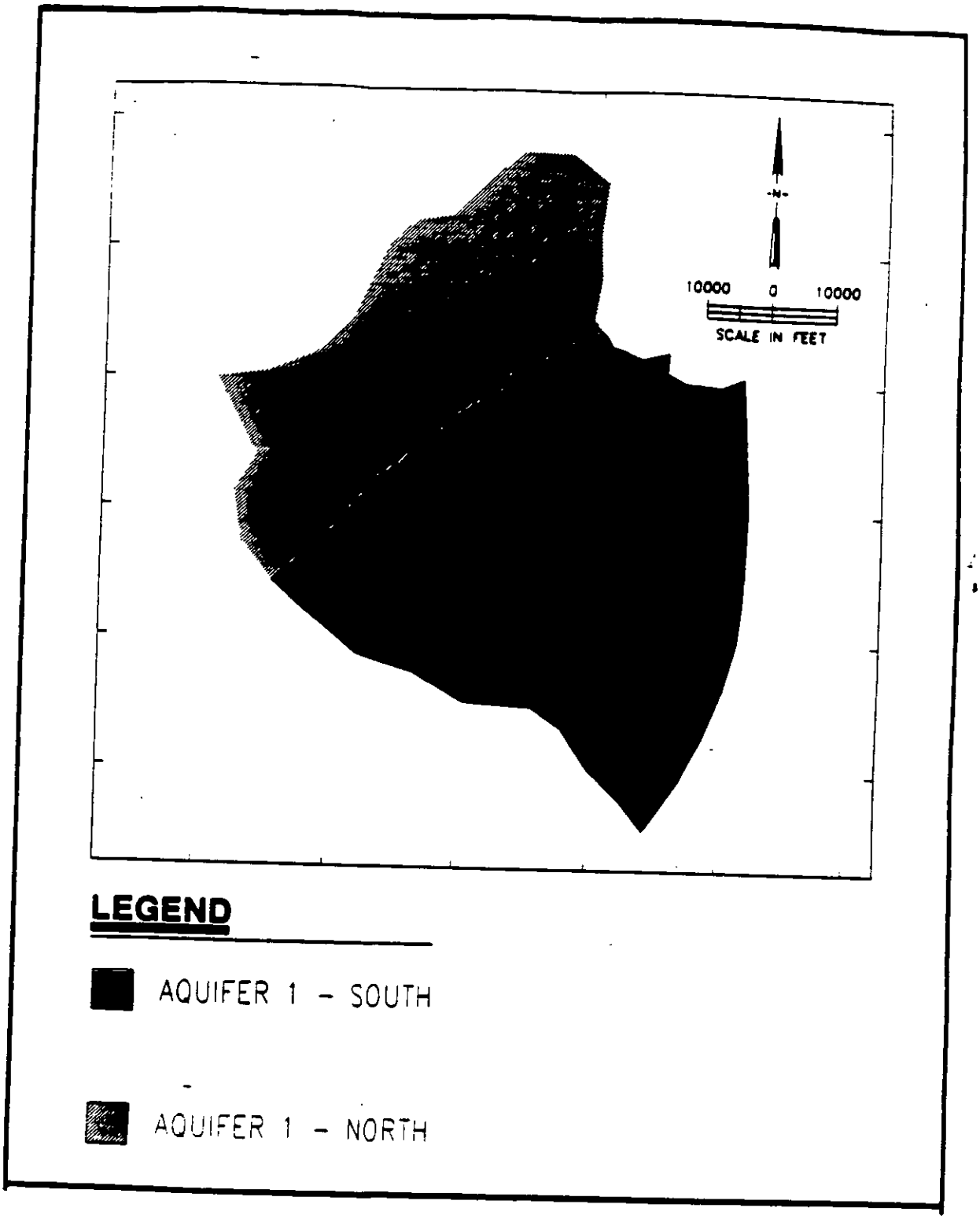

FIGURE 3-18. Model Property Zones for Aquifer 1

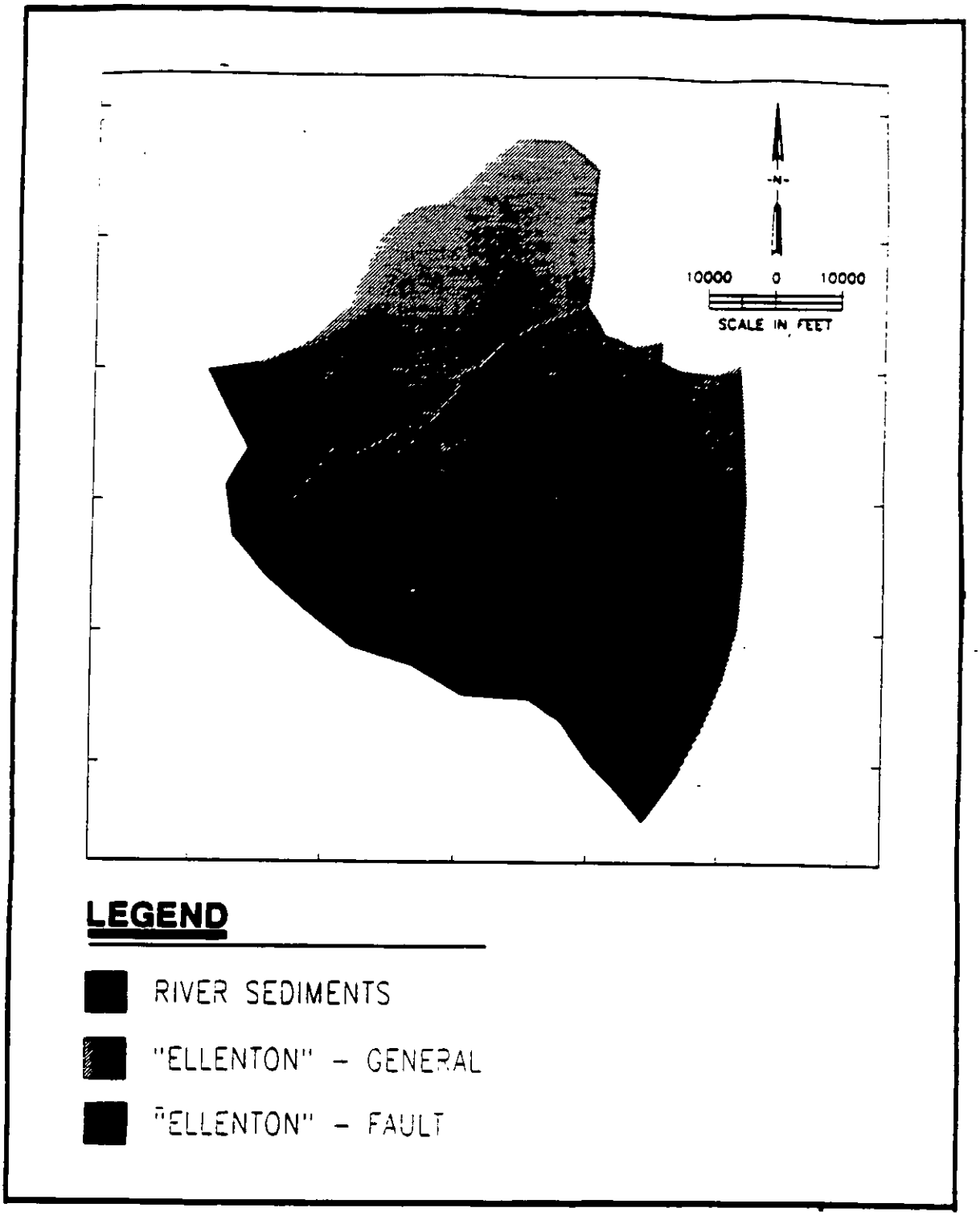

FIGURE 3-19. Model Property Zones for "Ellenton" Aquitard

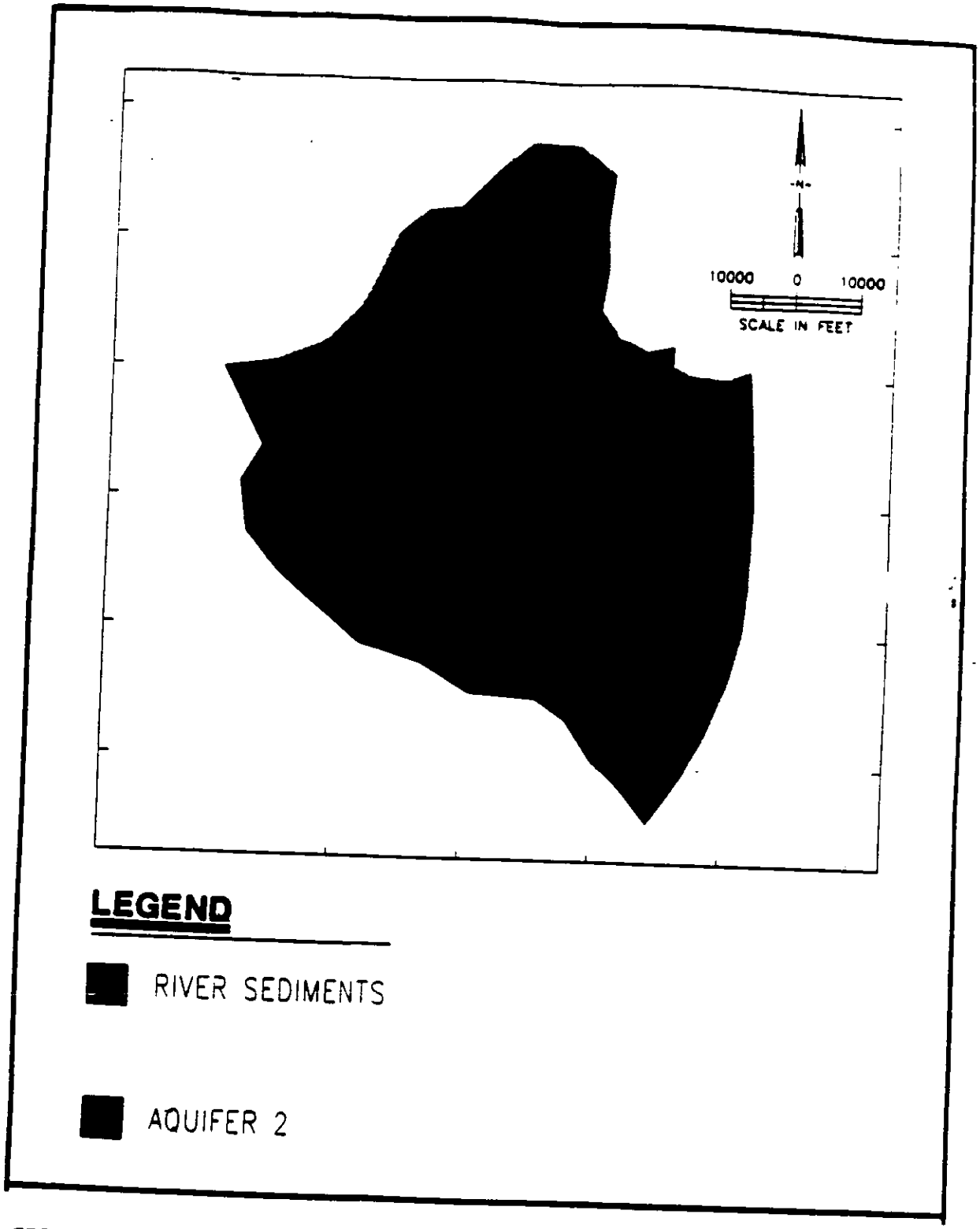

FIGURE 3-20. Model Property Zones for Aquifer 2

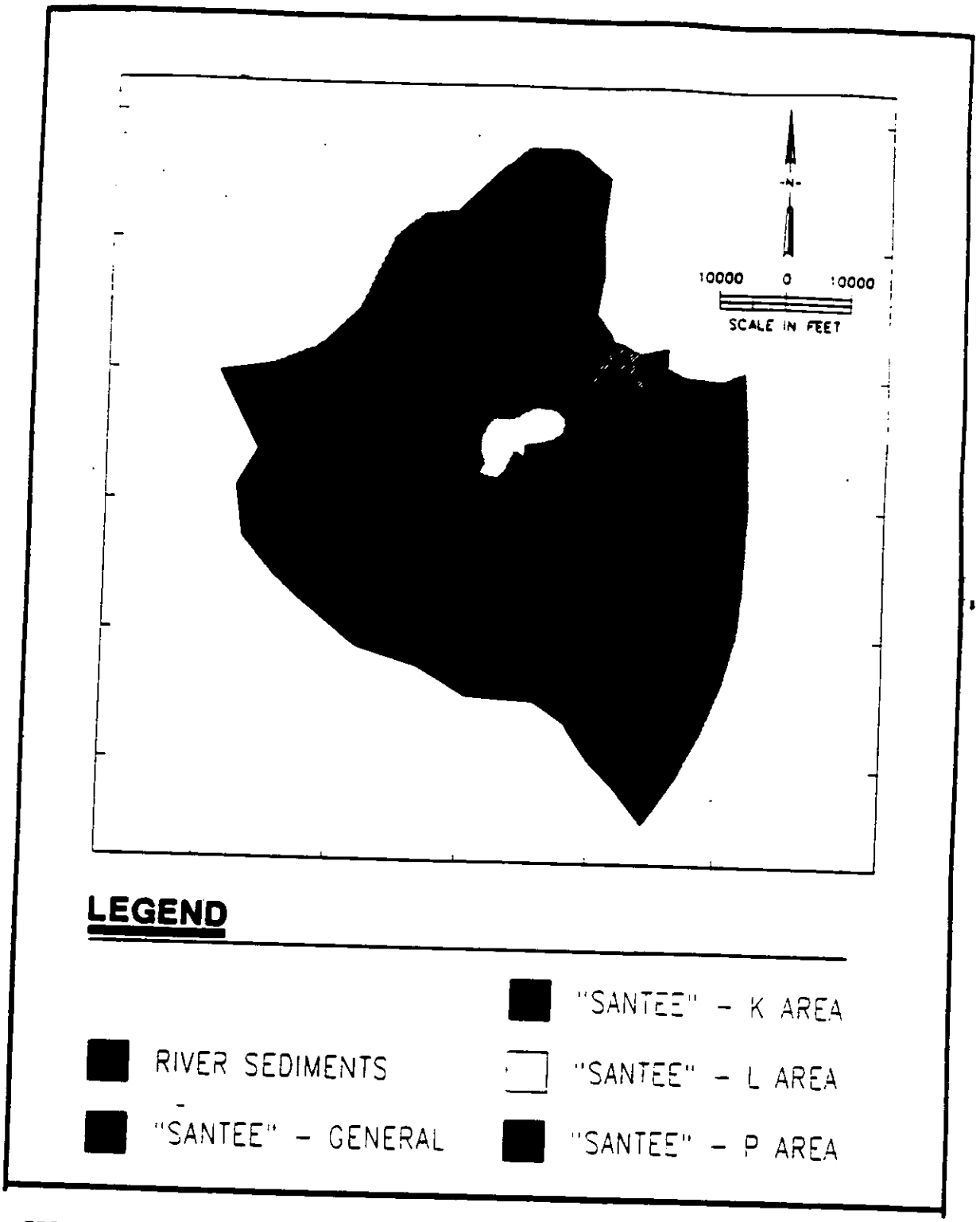

FIGURE 3-21. Model Property Zones for "Santee" Aquitard

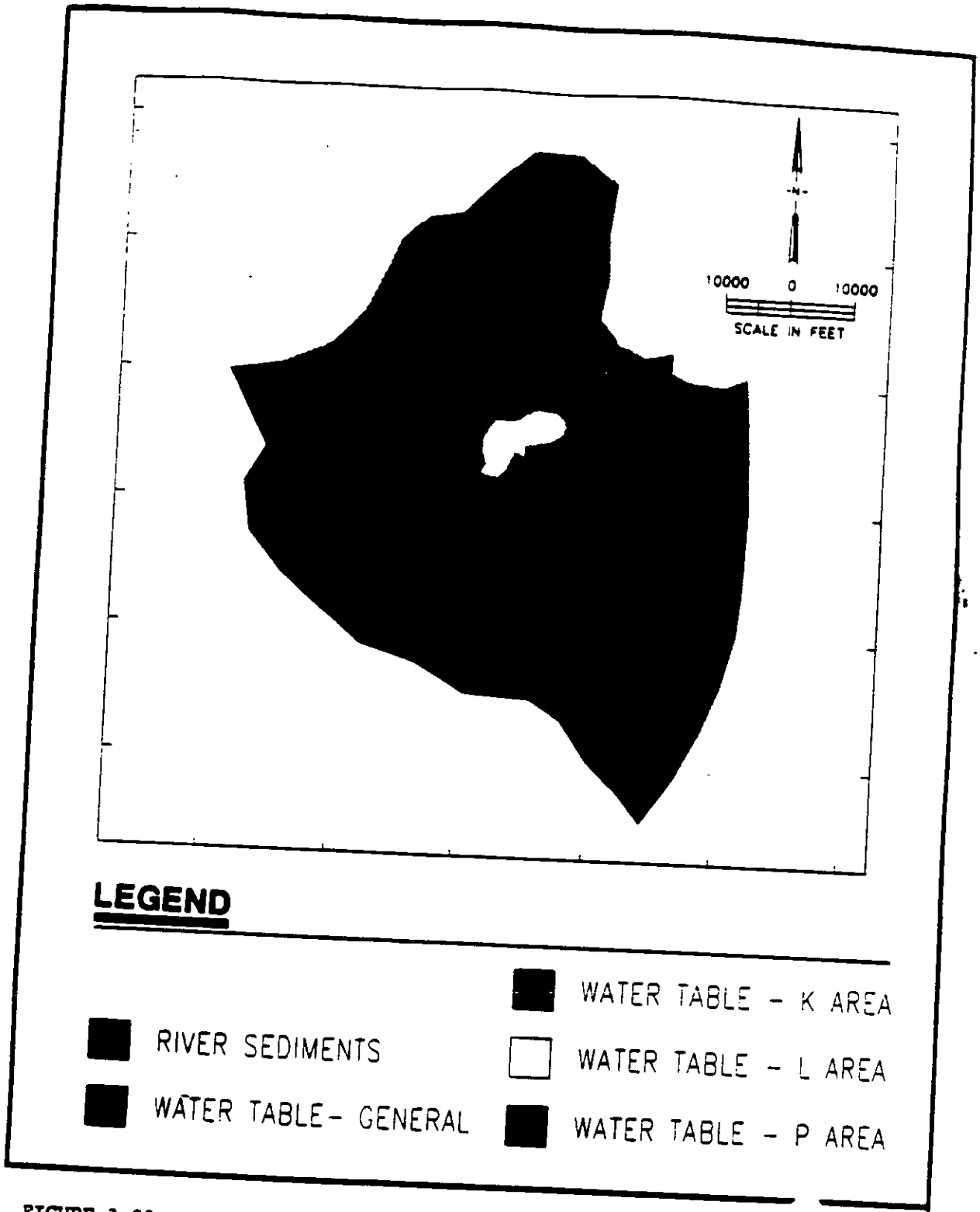

FIGURE 3-22. Model Property Zones for Water Table Unit

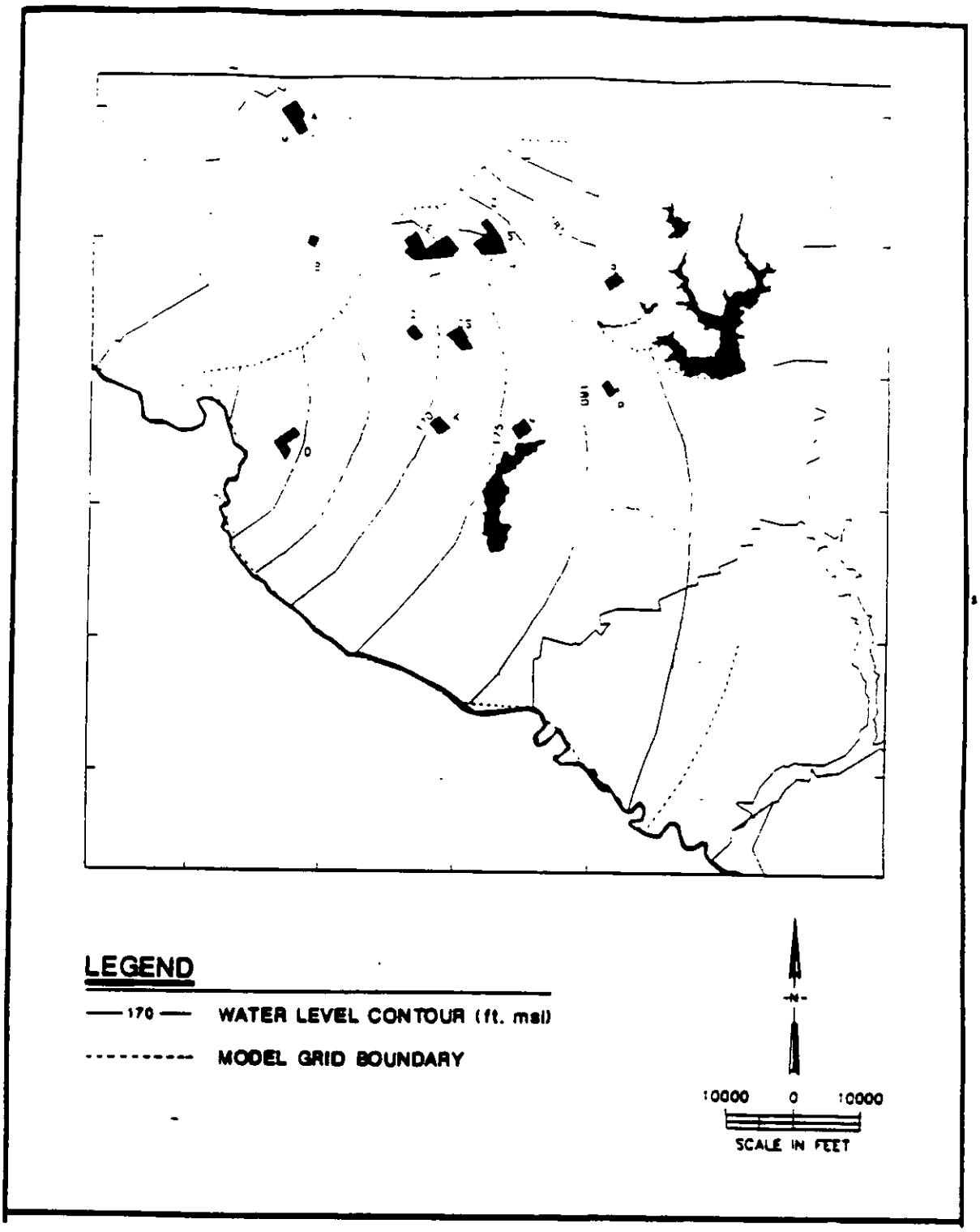

FIGURE 3-23. Simulated Equipotential Curves for Bottom Aquifer 1

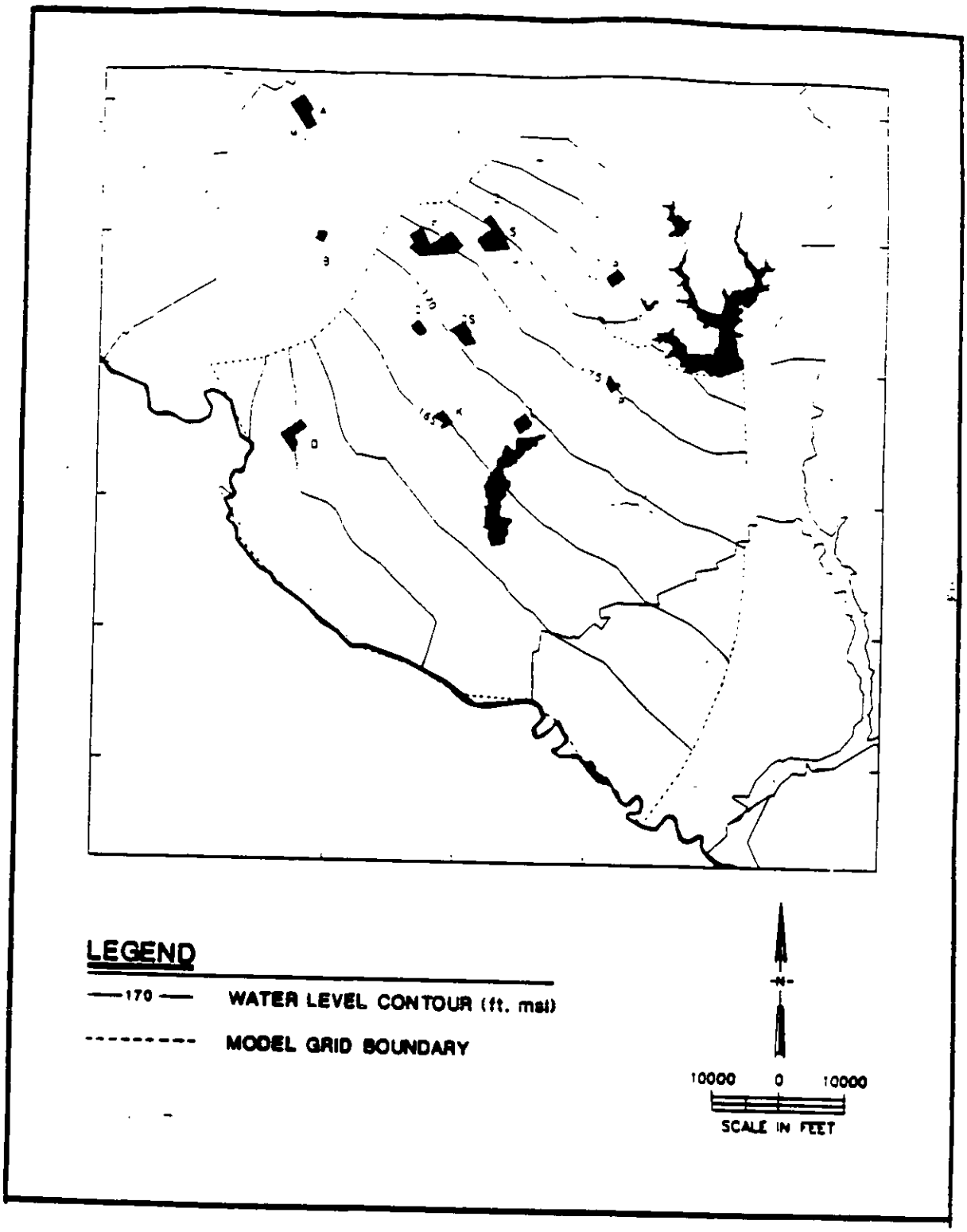

FIGURE 3-24. Simulated Equipotential Curves for Top Aquifer 1

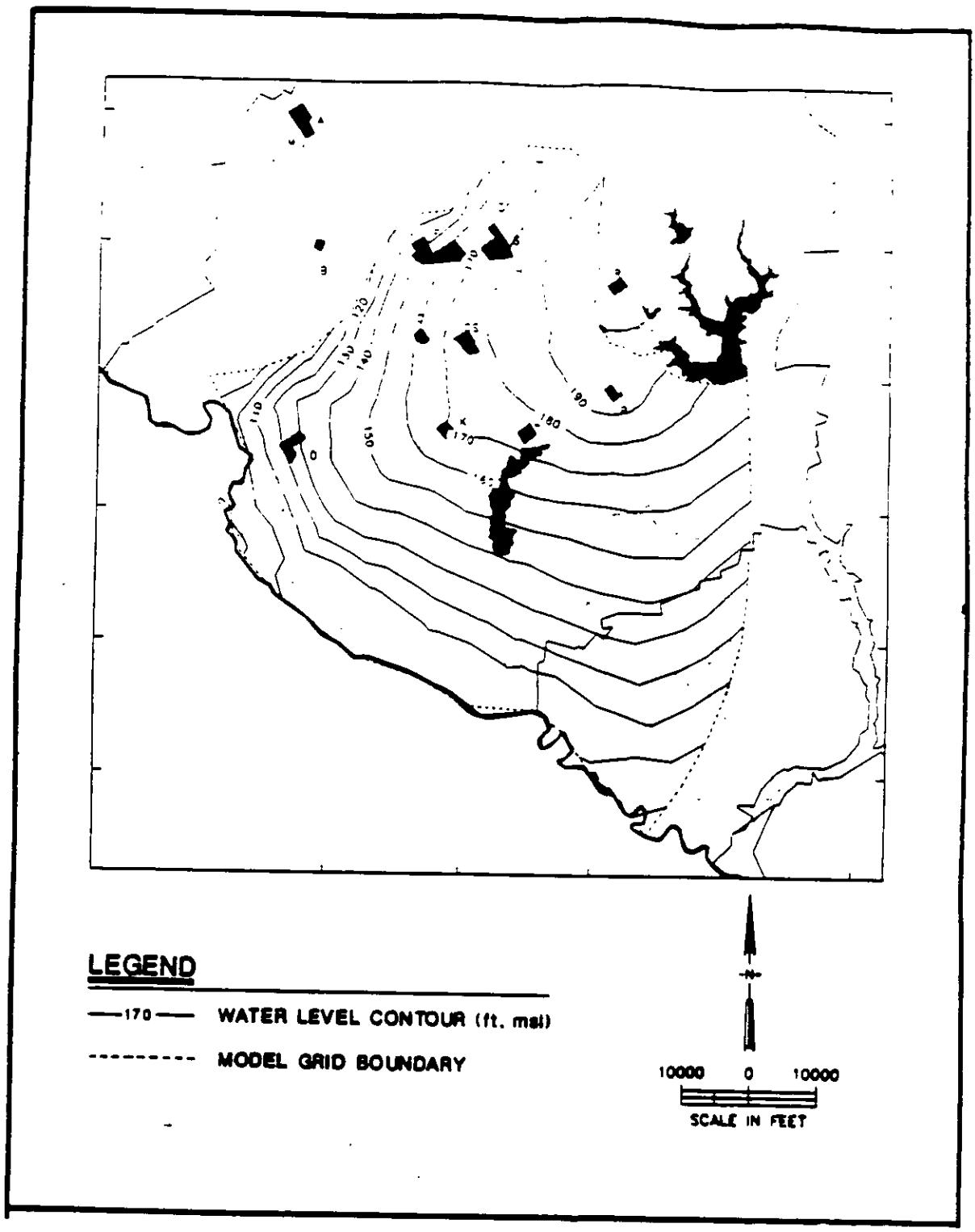

FIGURE 3-25. Simulated Equipotential Curves for Aquifer 2

40 CFR 141.16 specifies that drinking water may contain no concentration of radionuclides that yields a radiation dose over 4 millirem/year. Note that the concentration standards presented in Table 3-9 are those concentrations of the radionuclides which yield a radiation dose of 4 millirem/year on an individual basis. If more than one radionuclide is present in the drinking water, the concentration of each must be less than the standard such that the total radiation dose exposure is less than 4 millirem/year.

Based on the contaminant transport properties, source concentrations, and EPA drinking water standards presented in Tables 3-7 and 3-9 for the nine radionuclides of concern, the number of radionuclides to be further analyzed with the contaminant transport model was narrowed down to three: tritium, strontium-90, and cesium-137. Four of the radionuclides (cobalt-60, ruthenium-106, antimony-125, and polonium-147) were not considered further because they are released at concentrations at least two times below drinking water standards, and they are significantly retarded as they move through the soil. The two other radionuclides (cesium-134 and cerium-144) were not considered further because comparison of the contaminant transport properties and source strengths of these two radionuclides with that of cesium-137 indicates that the subsurface environmental impacts from cesium-137 will in all regards be greater. Both cesium-137 and cerium-144 have shorter half-lives than cesium-137, and are released at lower concentrations relative to their EPA drinking water standards. In addition, the retardation factor for cerium-144 is greater than that of cesium-137, while the retardation factor for cesium-134 is equivalent to that of cesium-137. Analysis of the subsurface impacts of tritium, strontium-90, and cesium-137 provides a worst case environmental consequences evaluation since they represent the more mobile, persistent, and strongest (concentration) of the nine radionuclides of concern. The impact of the six other radionuclides will be less than that of the three selected radionuclides.

To further provide a worst case impacts analysis, the contaminant transport model simulations included a steady source loading rate at each of the seepage basins with radionuclides being released directly in to the groundwater system. No allowance was made for decay and retardation as the radionuclides move through the unsaturated zone. The model was run until a steady-state plume for concentrations above 1/100 of the drinking water standard were reached. Steady-state plume simulations were achievable due to the loss of contamination through surface water discharge and radioactive decay. The simulated steady-state plumes for the three radionuclides analyzed are shown in Figures 3-26 through 3-36.

The worst subsurface environmental impacts occur by far with the release of tritium. In fact, tritium is the only radionuclide for which groundwater concentrations above the drinking water standard are simulated at a distance of more than a few hundred feet from each of the seepage basins. In addition, tritium is the only radionuclide for which the simulated steady-state plume for 1/100 of the drinking water standard intercepts a surface water body and also moves down into Aquifer 2. Retardation of

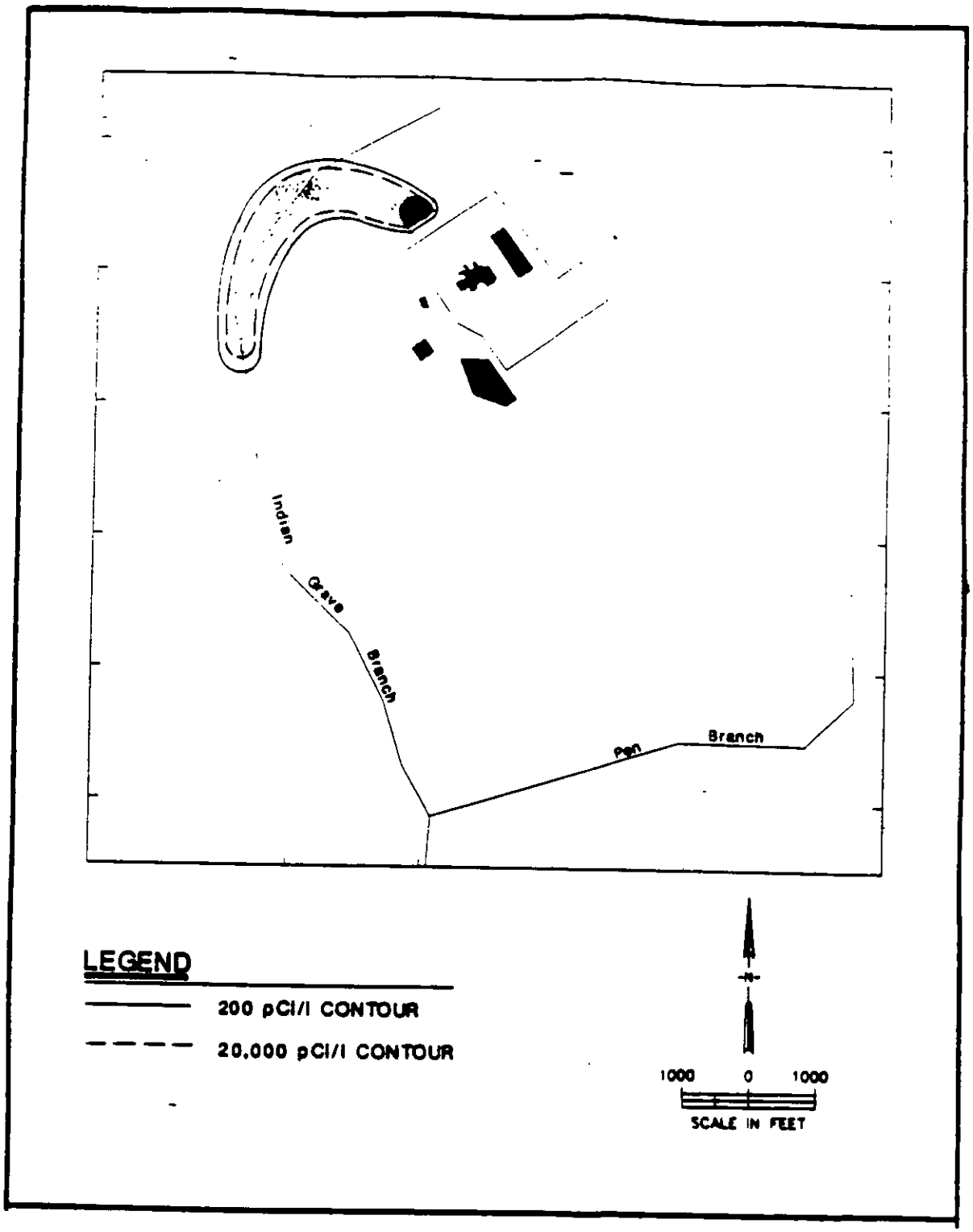

FIGURE 3-26. Water Table Tritium Plume at K-Reactor

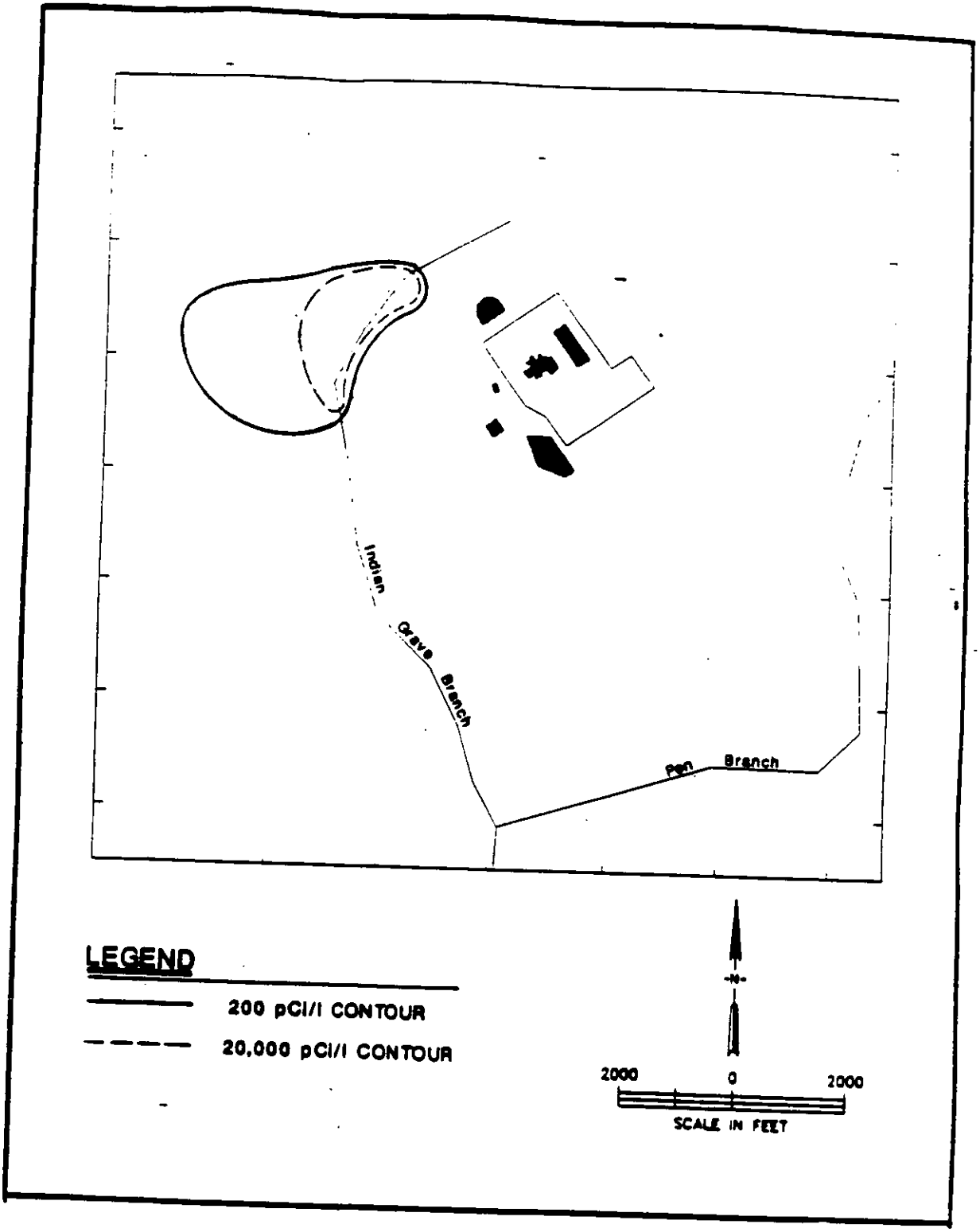

FIGURE 3-27. Aquifer 2 Tritium Plume at K-Reactor

W8907038

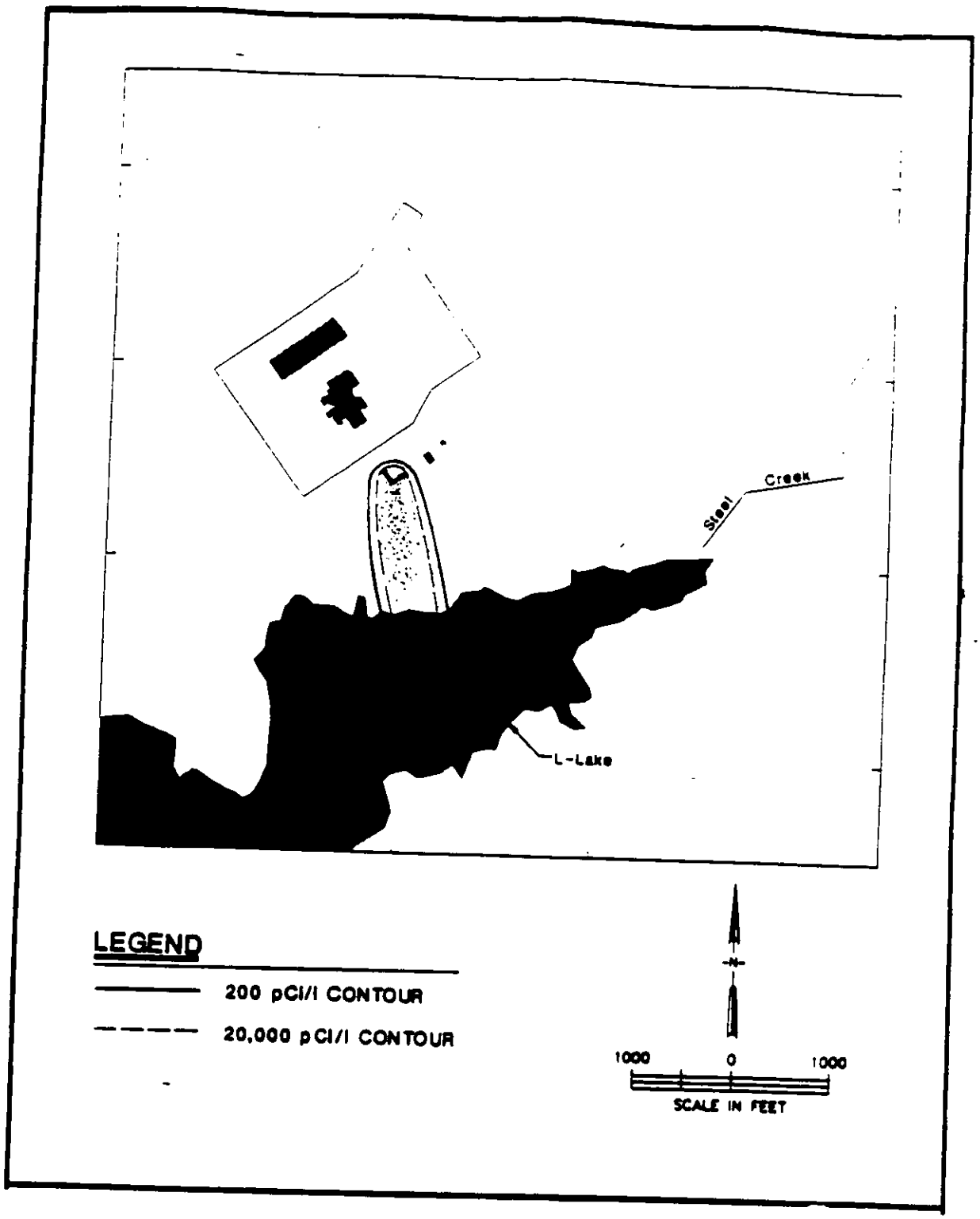

FIGURE 3-28. Water Table Tritium Plume at L-Reactor

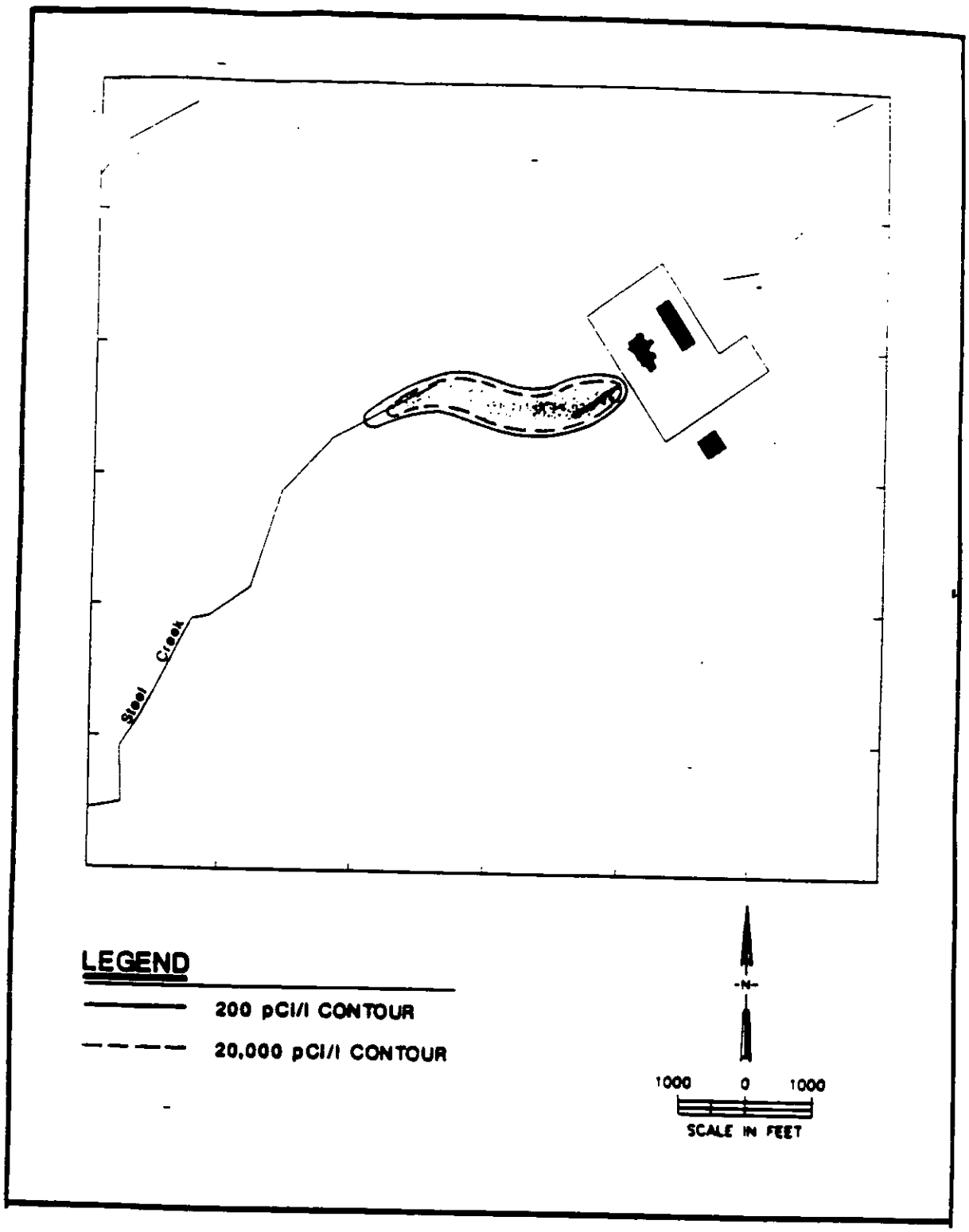

FIGURE 3-29. Water Table Tritium Plume at P-Reactor

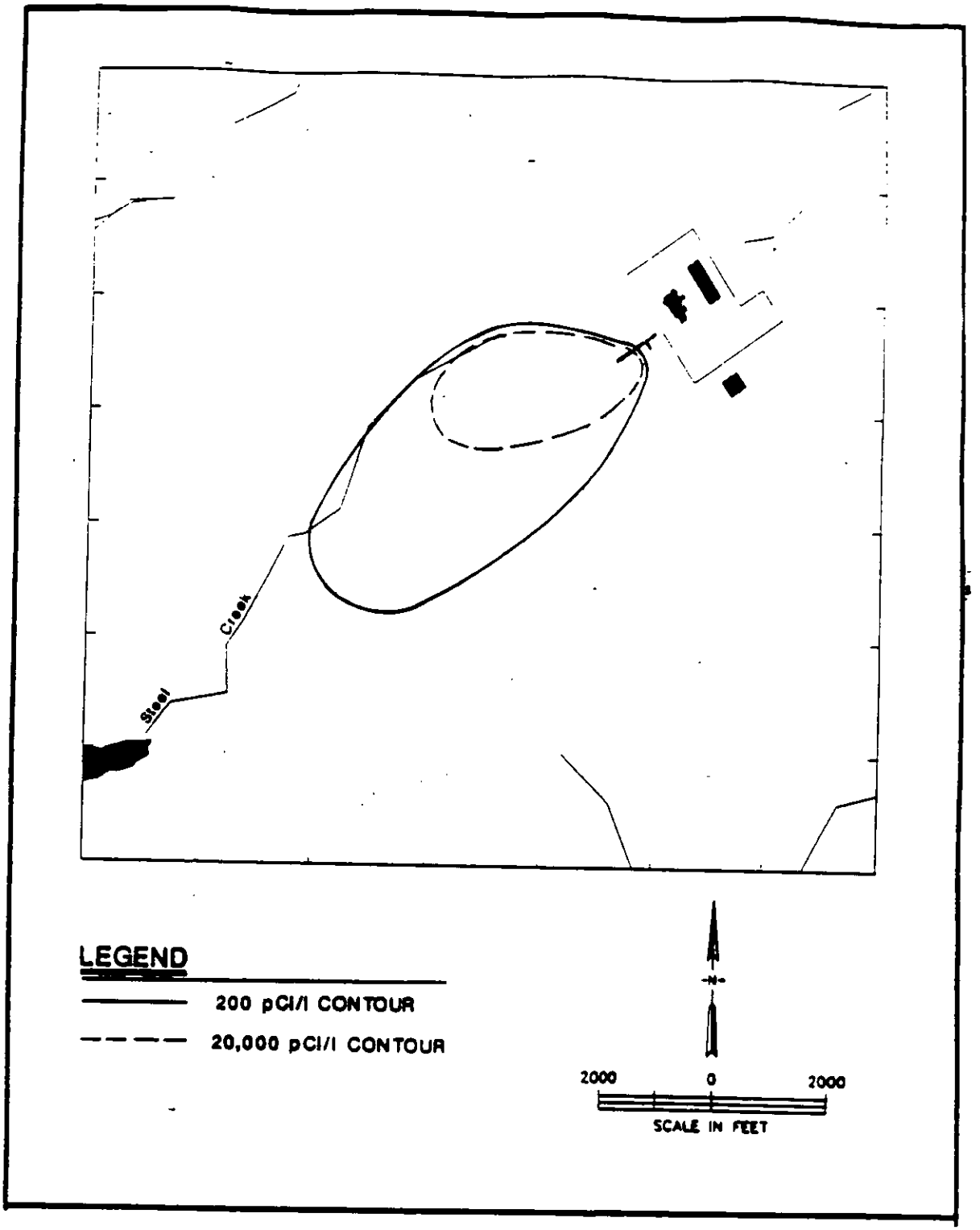

FIGURE 3-30. Aquifer 2 Tritium Plume at P-Reactor

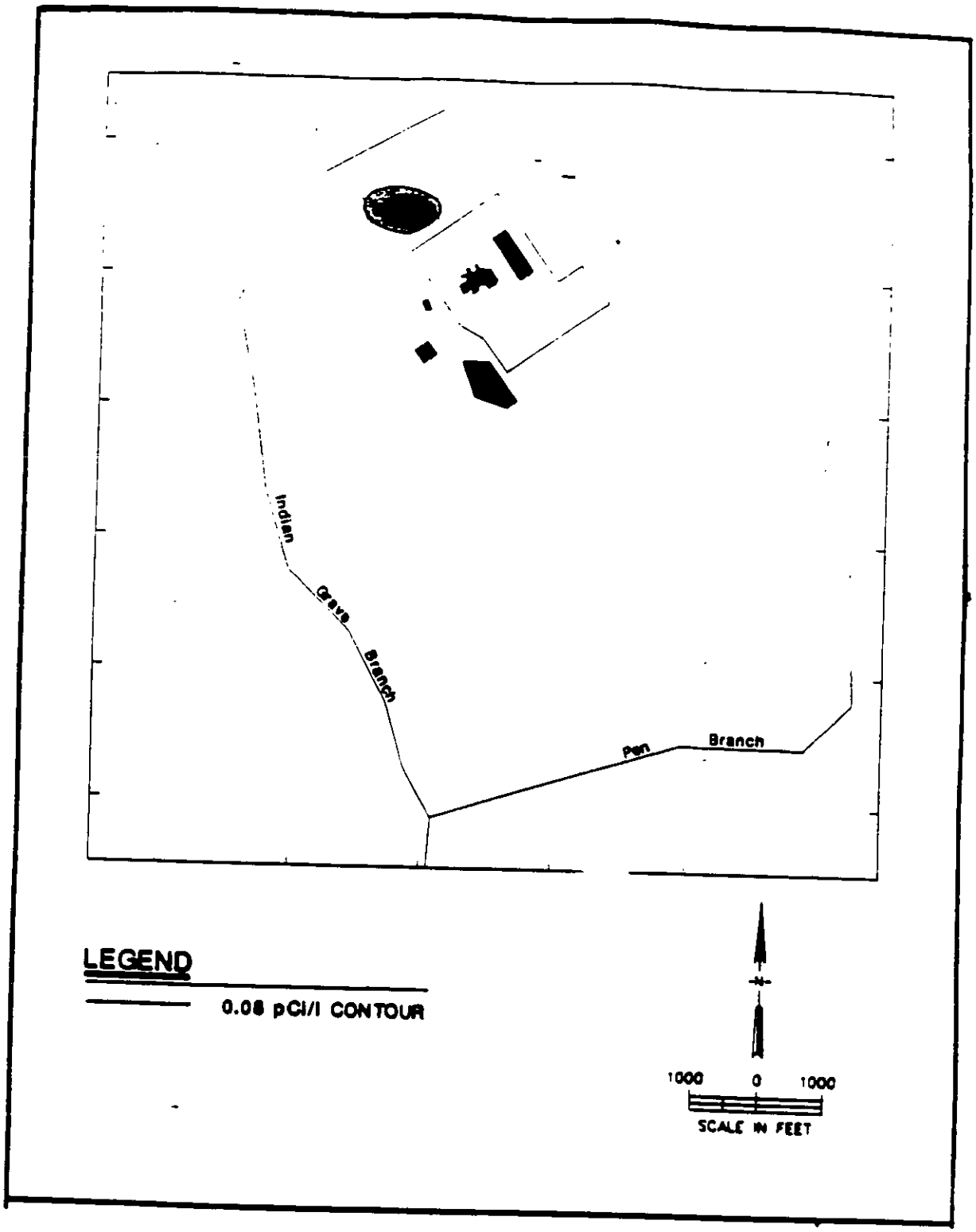

FIGURE 3-31. Water Table Strontium-90 Plume at K-Reactor

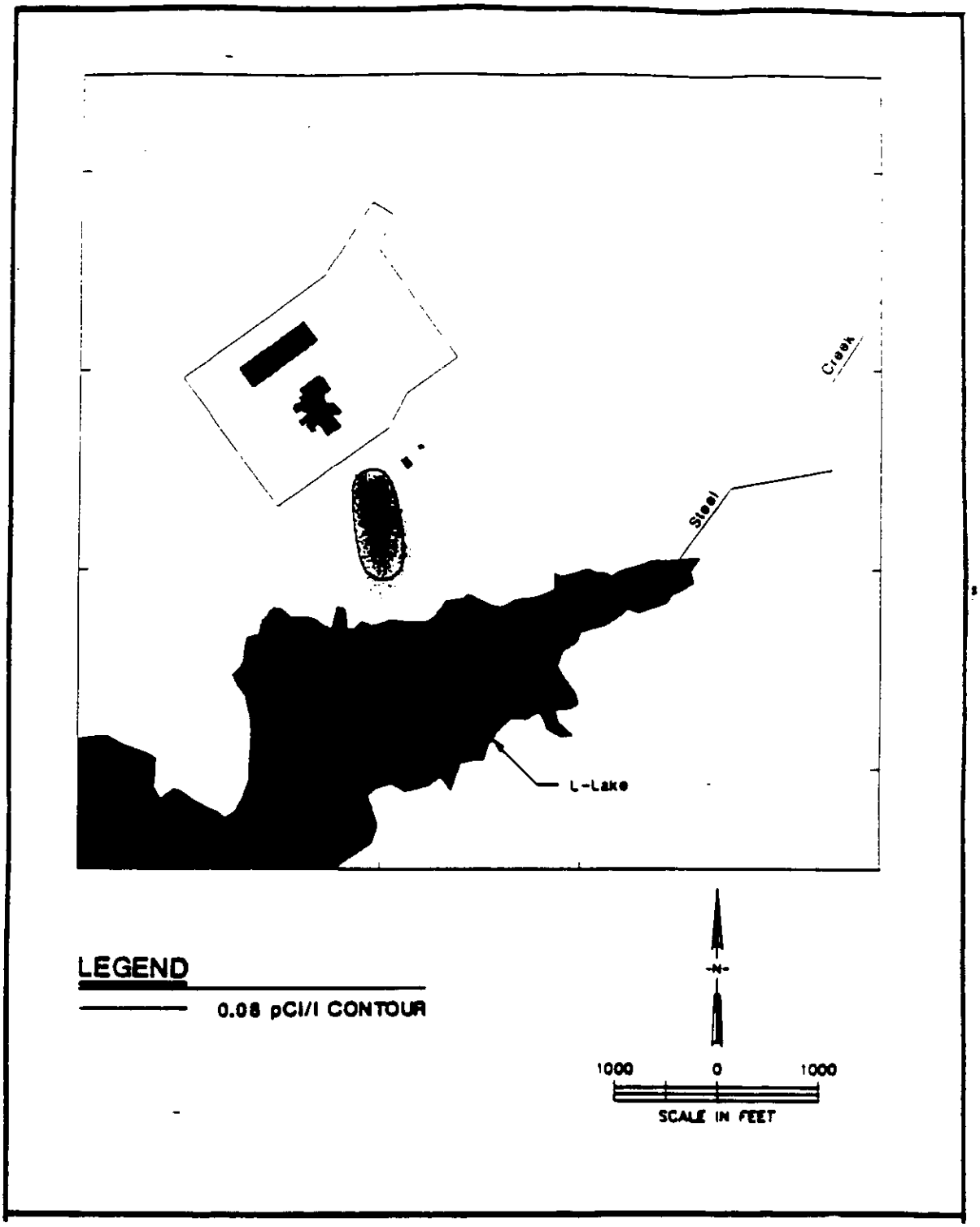

FIGURE 3-32. Water Table Strontium-90 Plume at L-Reactor

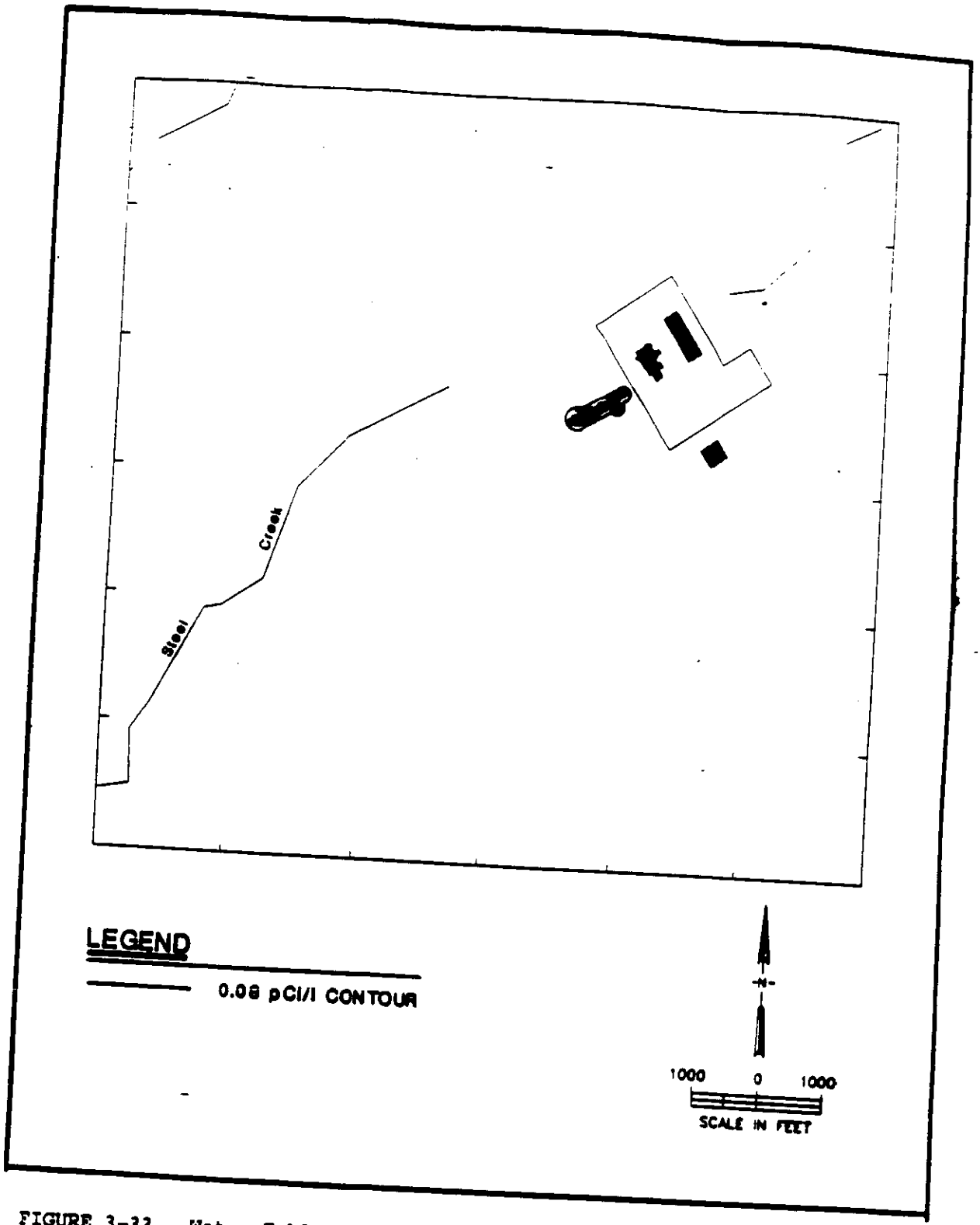

FIGURE 3-33. Water Table Strontium-90 Plume at P-Reactor

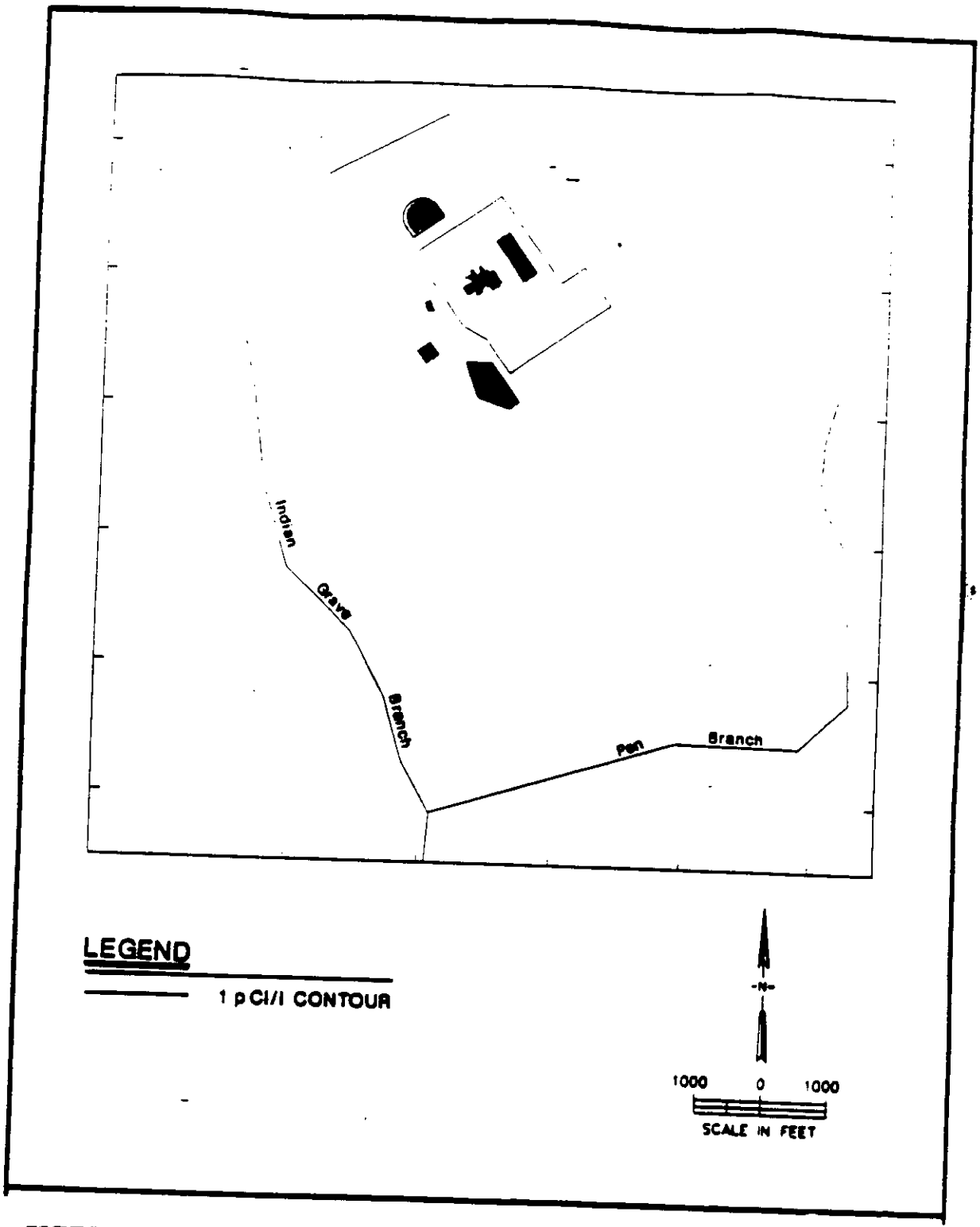

FIGURE 3-34. Water Table Cesium-137 Plume at K-Reactor

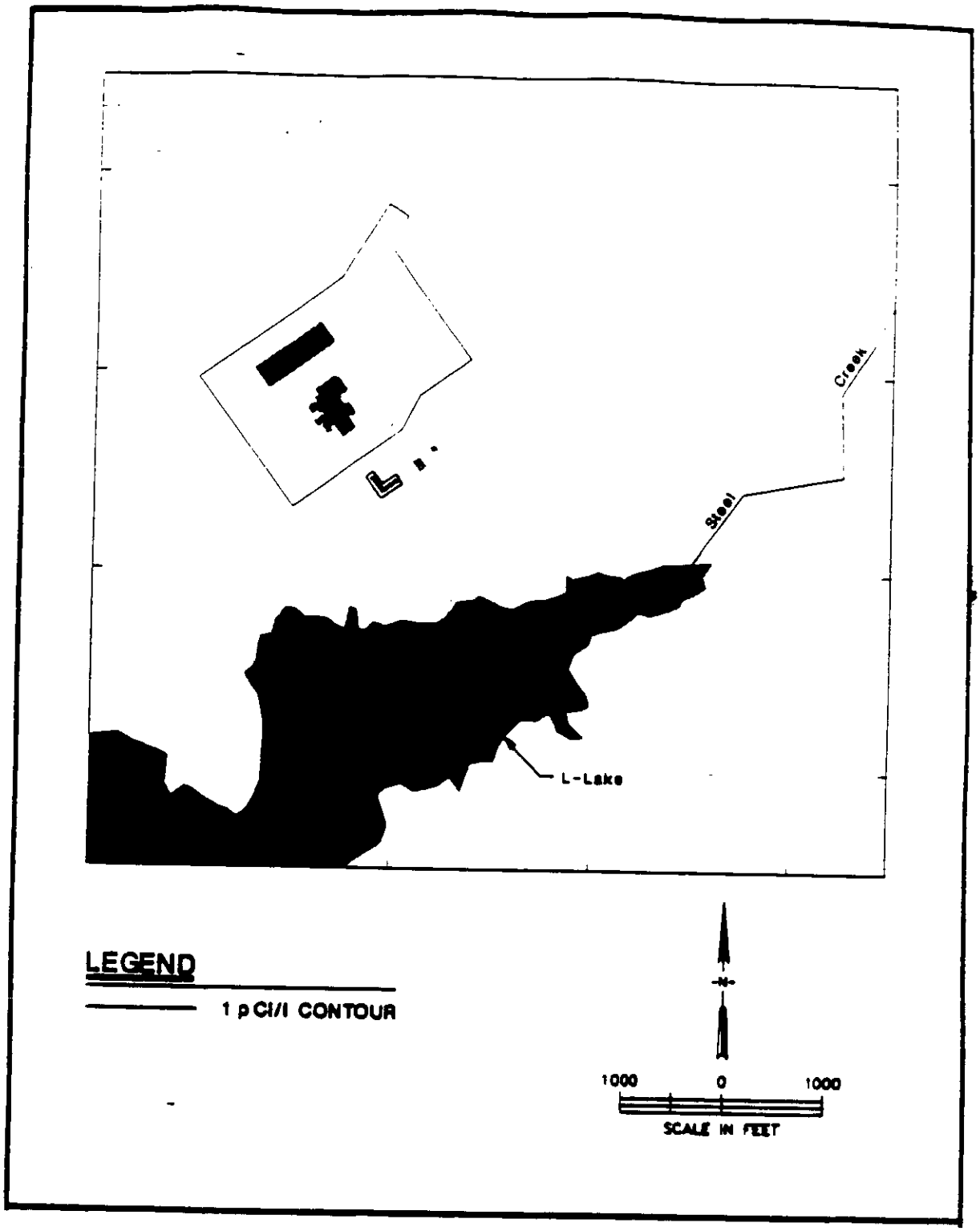

FIGURE 3-35. Water Table Cesium-137 Plume at L-Reactor

W8907038

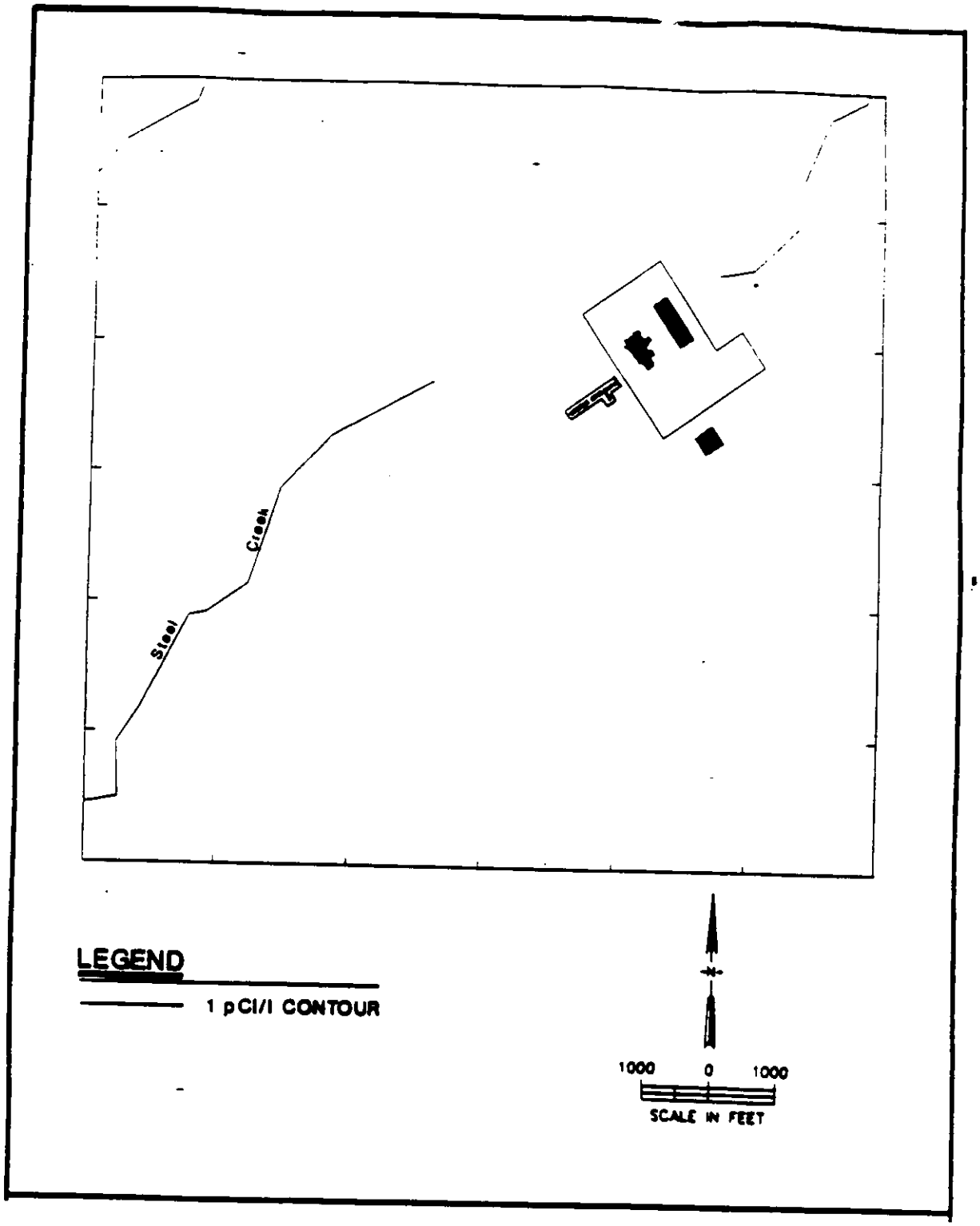

FIGURE 3-36. Water Table Cesium-137 Plume at P-Reactor

the other two radionuclides, especially cesium-137, prevents them from moving very fast so that before they can move very far they have decayed to low concentrations relative to the drinking water standards. At the K Reactor, while both the 200 pCi/l and 20,000 pCi/l tritium contours extend to Indian Grave Branch Creek in the Water Table, and beyond the creek in Aquifer 2, the 0.08 pCi/l strontium-90 contour extends only about half the distance to Indian Grave Branch Creek, and the 1 pCi/l cesium-137 contour extends less than a few hundred feet from the seepage basin. At the L Reactor, while both the 200 pCi/l and 20,000 pCi/l tritium contours extend far enough from the seepage basin (in the Water Table only) to be intercepted by L Lake, the 0.08 pCi/l strontium-90 contour extends only about two-thirds the distance to L Lake, and the 1 pCi/l cesium-137 contour extends less than a few hundred feet from the seepage basin. At the P Reactor, while both the 200 pCi/l and 20,000 pCi/l tritium contours extend to Steel Creek in the Water Table, and further downgradient in Aquifer 2, both the 0.08 pCi/l strontium-90 and the 1 pCi/l cesium-137 contours extend less than a few hundred feet from the seepage basin. Therefore, because the subsurface impacts from strontium-90 and cesium-137 releases are not nearly as extensive as the impacts from tritium releases, the rest of the subsurface environmental impacts analysis concentrated on evaluating the impacts of tritium release.

Cross-sections of the tritium plumes are shown in Figures 3-37 through 3-39. These cross-sections were taken along the main axes of the plumes. At the L-Reactor site, migration of tritium is limited to the water table unit, while at the K- and P-Reactor sites, tritium migrates downward into Aquifer 2 (Congaree). At none of the three sites, however, does tritium migrate down any further than Aquifer 2 at concentrations above 1/100 of the drinking water standard.

3.6.2 Groundwater Quantity

The simulated steady-state tritium plume volumes are presented in Table 3-10. The plume volumes presented were calculated based on the three dimensional shape of the plume and an assumed effective porosity of 0.20. The greatest volume of contaminated groundwater is at the P reactor site, while the smallest volume of contaminated groundwater is at the L-Reactor site. This variation in plume volumes is to be expected since most of the tritium at the L Area leaves the groundwater system relatively quickly through surface water discharge, while very little of the tritium leaves the P Area through surface water discharge (see Section 3.6.3). Thus, although the tritium moves more slowly at the P reactor site, at steady-state, tritium contamination covers a much larger area and volume of groundwater.

3.6.3 Groundwater - Surface Water Interactions

The simulated steady-state tritium mass fluxes are presented in Table 3-11. Also presented in Table 3-10 are the groundwater discharges to surface water along the reaches where tritium is discharged and the

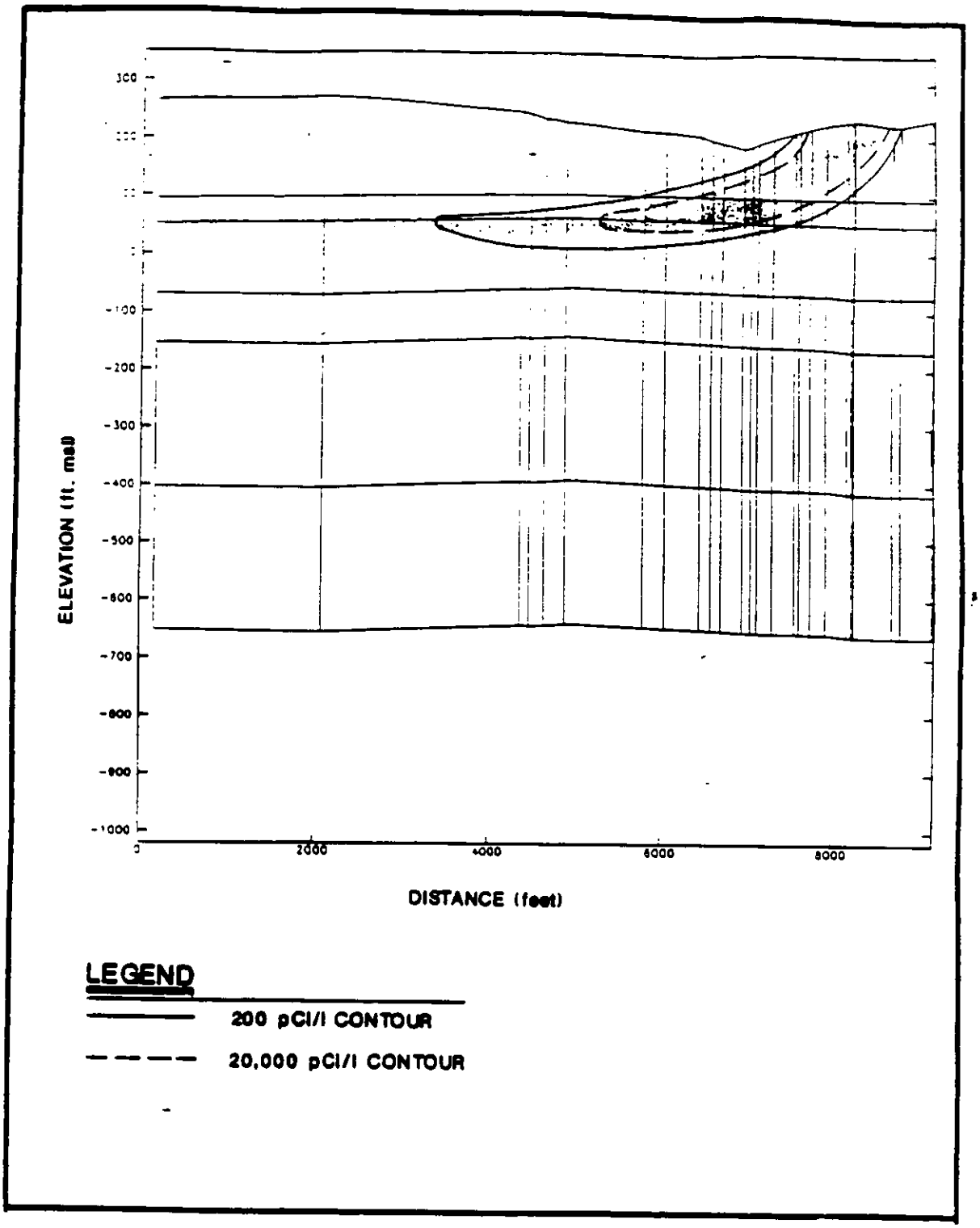

FIGURE 3-37. Tritium Plume Cross Section at K-Reactor

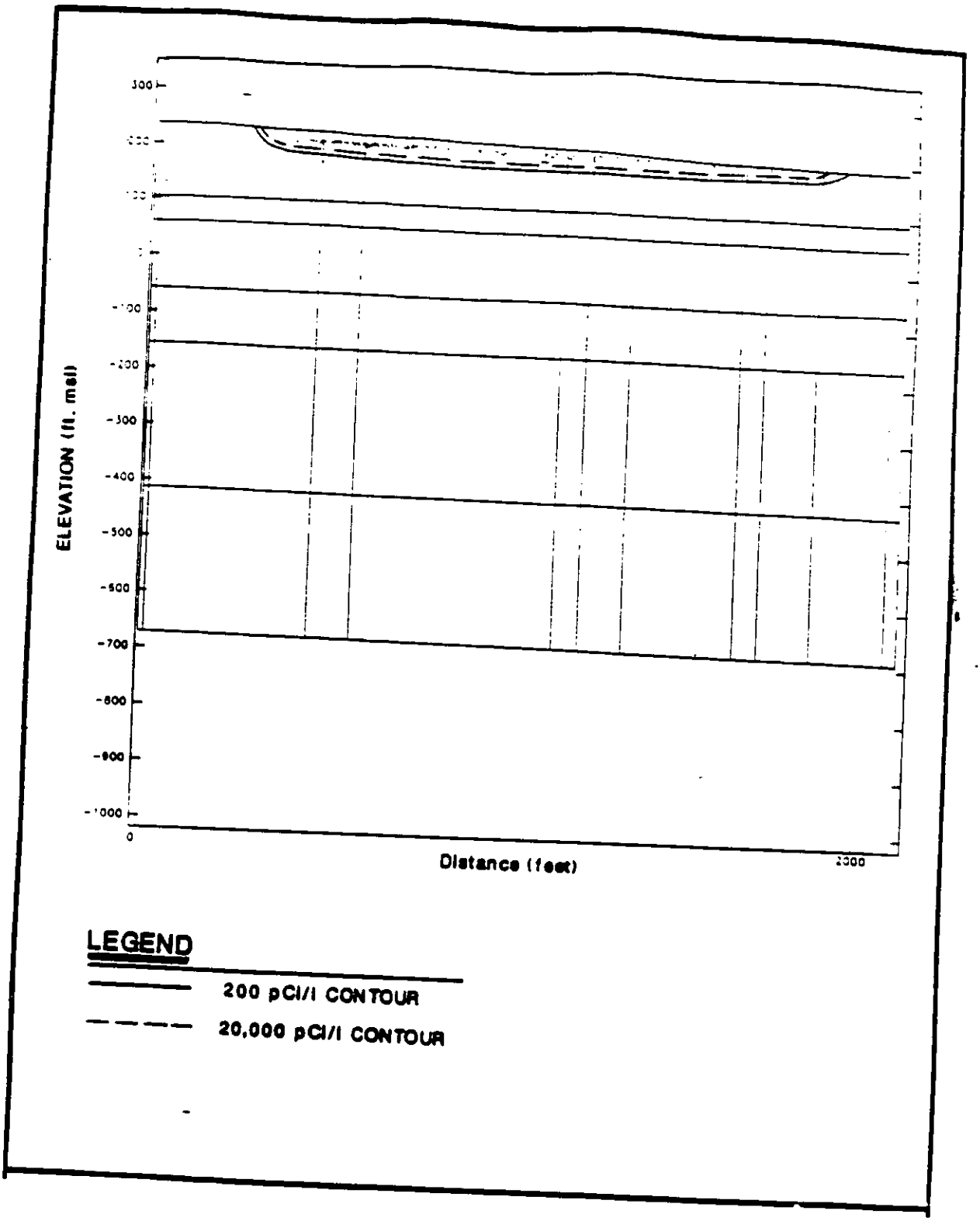

FIGURE 3-38. Tritium Plume Cross Section at L-Reactor

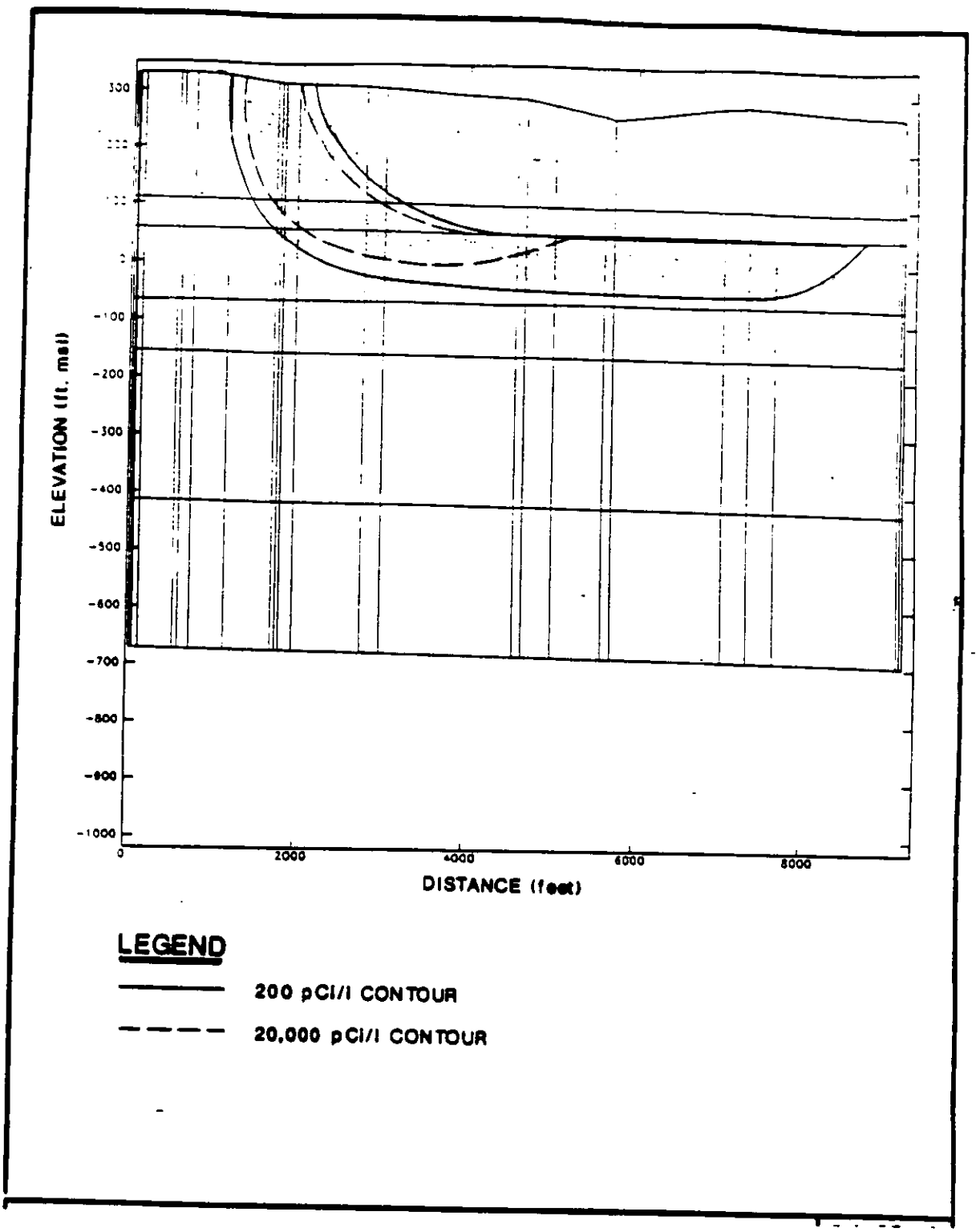

FIGURE 3-39. Tritium Plume Cross Section at P-Reactor

average groundwater discharge concentration of tritium at the three reactor sites. At the L-Reactor site, most of the tritium (67%) eventually leaves the groundwater system through surface water discharge to L Lake. Model simulations indicate that tritium reaches L Lake within 5 years after release to the L-Reactor seepage basin. The remaining tritium (33%) leaves the system through radioactive decay. At the K reactor site, some of the tritium (38%) eventually leaves the groundwater system through surface water discharge to Indian Grave Branch Creek, but most of the tritium (62%) is lost through radioactive decay. Model simulations indicate that tritium reaches Indian Grave Branch Creek within 6 years after release to the K-Reactor seepage basin. At the P-Reactor site, very little tritium (0.2%) is lost through surface water discharge to Steel Creek, while the majority (99.8%) is eventually lost through radioactive decay. Model simulations indicate that what little tritium does discharge into Steel Creek reaches the creek within 30 years after discharge to the P-Reactor seepage basin. The primary reason most of the tritium eventually leaves the groundwater system through radioactive decay instead of surface water discharge at the K- and P-Reactor sites, is because most of the tritium migrates down vertically before it moves horizontally to a surface water discharge feature at these sites. At the L-Reactor site, however, horizontal groundwater velocities are greater than at the K- and P-Reactor sites, and the surface water discharge feature (L Lake) is closer to the seepage basin, thus allowing more tritium to exit the groundwater system through surface water discharge.

The proceeding evaluations were for full power reactor operation; for less than full power operation, less radionuclides and the same volume of water
would be discharged to the reactor seepage basins. As a result, the initial concentration of radionuclides reaching the groundwater would be reduced correspondingly. Therefore, the environmental impact to the groundwater will always be less for less than full power reactor operation.

3.6.4 Accidents

Design Base accidents that could result in a liquid discharge of radionuclides to the environment at the K, L, P reactors are a loss of coolant accident, a loss of circulation accident, or a discharge mishap. A loss of coolant accident or circulation accident might result in a partial core meltdown (only in the event of backup system failures) and a subsequent discharge of radioactive water if tanks installed to receive the emergency cooling water overflow. A discharge mishap would occur when an irradiated component dropped on the reactor room floor and the reactor room spray system water subsequently overflows a confinement tank.

An Emergency Coolant System (ECS) is deployed in the event of a loss of coolant or circulation accident. The ECS maintains coolant or circulation in a reactor by adding water at a maximum rate of 14,000 gallons per minute. With full ECS flow, no core melting would occur, but for postulated accidents in which only one water-addition system operates, it has

TABLE 3-4

Model Groundwater Pumping Rates

Location	Wells	Plant Coordinates North	Plant Coordinates East	Pumping Rate (m^3/min)
K Area	905-94K	53170	41500	0.75
	905-95K	53230	41300	
L Area	905-104L	47128	51250	0.94
	905-105L	46690	51250	
P Area	905-92P	42950	65700	1.35
	905-93P	43150	65650	
C Area	905-90C	66730	46720	1.21
	905-91C	66730	46520	
CS Area	905-71G	62134	52404	0.30
	905-83G	61394	52202	
F Area	905-79F	78045	54220	6.11
	905-100F	76430	53950	
	905-101F	77980	54598	
	905-102F	77280	54250	
H Area	905-66H	72115	62202	5.44
	905-80H	71664	62641	
	905-87H	70775	62228	
	905-88H	71405	63150	
	905-108H	70552	63189	

Reference: SC Water Resources Commission Report, 1989.

Note: Total pumpage for each location is applied at one node centrally located between the wells.

TABLE 3-5

SRS Hydraulic Conductivity Ranges

Hydrostratigraphic Unit	Horizontal Hydraulic Conductivity (m/day)	Vertical Hydraulic Conductivity (m/day)
Aquifer 1 (Cretaceous)	10 - 75	0.00003 - 0.03
"Ellenton" Aquitard	0.03 - 15	0.000003 - 0.003
Aquifer 2 (Congaree)	0.3 - 45	0.0003 - 0.03
"Santee" Aquitard	0.003 - 0.3	0.000003 - 0.003
Water Table	0.03 - 3	0.0003 - 0.03
Savannah River Section	0.03 - 15	0.0003 - 0.03

TABLE 3-6

Calibrated Hydraulic Conductivities

Hydrostratigraphic Unit	Horizontal Hydraulic Conductivity (m/day)	Vertical Hydraulic Conductivity (m/day)
Aquifer 1 (Cretaceous) Northern Section	20	0.03
Aquifer 1 (Cretaceous) Southern Section	75	0.00003
"Ellenton" Aquitard General	0.88	0.000049
"Ellenton" Aquitard Fault Zone	0.88	0.0024
Aquifer 2 (Congaree)	4.6	0.003
"Santee" Aquitard - General	0.12	0.00011
"Santee" Aquitard - K Area	0.0076	0.00021
"Santee" Aquitard - L Area	0.034	0.000003
"Santee" Aquitard - P Area	0.012	0.00043
Water Table - General	3.0	0.0012
Water Table - K Area	1.7	0.03
Water Table - L Area	2.3	0.0061
Water Table - P Area	0.7	0.0018
Savannah River Section	8.8	0.0024

TABLE 3-7

Estimated Contaminant Transport Properties

Parameter	H-3	CO-60	SR-90	RU-106	SB-125
Longitudinal Dispersivity (m)	15	15	15	15	15
Transverse Dispersivity (m)	1.5	1.5	1.5	1.5	1.5
Vertical Dispersion Anisotropy Ratio	0.1	0.1	0.1	0.1	0.1
Effective Porosity	0.2	0.2	0.2	0.2	0.2
Retardation Factor	1	81	65	1300	32000
Half-Life (years)	12.3	5.25	28.6	1.01	2.77

Parameter	CS-134	CS-137	CE-144	PM-147
Longitudinal Dispersivity (m)	15	15	15	15
Transverse Dispersivity (m)	1.5	1.5	1.5	1.5
Vertical Dispersion Anisotropy Ratio	0.1	0.1	0.1	0.1
Effective Porosity	0.2	0.2	0.2	0.2
Retardation Factor	4000	4000	8000	3200
Half-Life (years)	2.06	30.1	0.78	2.50

TABLE 3-8

Radionuclide Releases to Seepage Basins

Radionuclide	Average Seepage Basin Loading Rate (Ci/yr)	Half-Life (years)
Tritium	4030	12.3
Phosphorus-32	0.00041	0.04
Sulfur-35	0.00943	0.24
Chromium-51	0.07300	0.08
Cobalt-58	0.00171	0.20
Cobalt-60		5.25
Strontium-89	0.00054	0.14
Strontium-90	0.00034	28.6
Zirconium-95	0.01793	0.18
Niobium-95		0.18
Ruthenium-103	0.00096	0.11
Ruthenium-106		1.01
Antimony-124	0.00227	0.16
Antimony-125		2.77
Iodine-131	0.00880	0.02
Cesium-134	0.00312	2.06
Cesium-137	0.03183	30.1
Cesium-141	0.01373	0.09
Cesium-144		0.78
Promethium-147	0.00293	2.50
Beta	0.13300	NA
Alpha	0.00153	NA

TABLE 3-9

Radionuclide Source Parameters

Radionuclide	Average Seepage Basin Loading Rate (Ci/yr)	Average Seepage Basin Discharge Concentration (pCi/L)	USEPA Drinking Water Guideline (pCi/L)
Tritium	4030	200,000,000	20,000
Cobalt-60	0.00171	86	200
Strontium-90	0.00034	17	8
Ruthenium-106	0.00096	48	300
Antimony-125	0.00227	114	4000
Cesium-134	0.00312	156	80
Cesium-137	0.03183	1590	100
Cesium-144	0.01373	685	80
Promethium-147	0.00293	146	1600

Guideline calculated as 4 mrem/yr exposure with each radionuclide based on an average daily consumption of 2 liters of water.

TABLE 3-10

Simulated Tritium Plume Volumes

Location	Unit	20,000 pCi/L Plume Volume (m^3)	200 pCi/L Plume Volume (m^3)
K Area	Water Table[a]	420,000	1,100,000
	Aquifer 2[b]	230,000	3,900,000
	Total	650,000	5,000,000
L Area	Water Table	20,000	95,000
P Area	Water Table[a]	360,000	1,000,000
	Aquifer 2[b]	1,560,000	30,000,000
	Total	1,920,000	31,000,000

[a] Includes the Water Table unit and the upper half of the "Santee" Unit

[b] Includes Aquifer 2 and the lower half of the "Santee" unit

TABLE 3-11

Simulated Steady-State Tritium Fluxes

Flux	K Area	L Area	P Area
Mass Inflow to Seepage Basin (Ci/year)	4030	4030	4030
Radioactive Decay (Ci/year)	2490	1320	4020
Mass Outflow to Surface Water (Ci/year)	1540	2710	10
Affected Groundwater Discharge to Surface Water (m^3/day)	1940	270	850
Average Groundwater Discharge Concentration of Tritium (pCi/ml)	2200	28,000	32

been calculated that up to 1 percent of the core could melt (Chapter 2, SID). If partial core melting does occur, radionuclides would be transported by cooling water from the reactor room through drains or sumps. The water from the drains or sumps would first fill a 60,000 gallon underground tank, then a 500,000 gallon tank, and then discharge to an unlined earthen basin. The tanks are designed to minimize the mixing of overflow water with the tank contents. Therefore, any radionuclides released to the earthen basin in the event of a partial core meltdown would be extremely diluted.

In the event of a discharge mishap, cooling water would be sprayed into the reactor room at a rate of at least 2000 gallons per minute. For this scenario, partial melting might occur if the irradiated component is shielded from spray water, if the spray is not uniform, or if the component is of a geometry that is not conducive to cooling. This type of accident might result in a internal release of 0.2 percent of the core inventory of fission products (DPST-76-408). In this event, the cooling water and radionuclides would flow through the reactor drains to the 60,000 and 500,000 gallon confinement tanks and eventually to the earthen basin. Discharge to the earthen basic would occur if spray continues for over 4.5 hours. The potential consequences of this release are even less than the already nominal radionuclide release to the earthen basin for a loss of coolant or circulation accident.

Because any potential radioactive constituents discharged to the earthen basin would be extremely diluted, the environmental consequences of the postulated accident scenarious were not considered. However, in the unlikely event of a significant release of radionuclides to the earthen basins, a remediation system could be easily designed, because of the length of time for constituents to be reach surface waters once discharged to the basins.

REFERENCES FOR CHAPTER 3

Duffield, G. M., D. R. Buss, R. W. Root, S. S. Hughes, and J. W. Mercer. Characterization of Groundwater Flow and Transport in the General Separations Areas, report prepared for E. I. du Pont de Nemours and Company, Savannah River Laboratory Aiken, SC (1986).

Haslow, J. S. and M. D. Taylor. Numerical Simulation of Flow and Contaminant Transport at the K, L, and P AreaS of the Savannah River Site, WSRC-RP-89-1198 (1989).

South Carolina Water Resources Commission Report, 1st Quarter, 1989. Water Use Report for the U.S. Department of Energy - Savannah River Plant (1989).